The effect of suction and blowing on the spreading of a thin fluid film: a Lie point symmetry analysis

Doctor of Philosophy

Naeemah Modhien

Supervisor: Professor D.P. Mason

A thesis submitted to the Faculty of Science, University of the Witwatersrand in fulfillment of the requirements for the degree of Doctor of Philosophy

Declaration

I declare that this dissertation is my own unaided work except where references have been made. It is being submitted for the degree of Doctor of Philosophy at the University of the Witwatersrand, Johannesburg. It has not been submitted before for any degree or examination at any other university.

Naeemah Modhien

3rd day of April 2017

Dedication

I dedicate this thesis to my daughters, Aadilah and Zaakirah Desai.

Acknowledgements

Alhamdulillah, All praises are due to Allah who has guided me towards the completion of this degree.

I would like to thank my supervisor, Prof Mason for his unwavering support and guidance in preparation of this thesis. I would like to thank him for his patience, compassion, time, understanding and valuable criticism.

I would like to thank Prof Momoniat for believing and supporting me during my studies. I appreciate the discussions and advice from Rhameez.

I would like to offer my gratitude to the group of members I work with, namely, Dr Kevin Pereira, Mrs Karin Hunt and Mrs Natalia Gildin for their encouragement and being there for me and for having faith in me and for giving me the time and space to pursue this degree.

Lastly I would like to thank my family for always keeping me in their prayers and their belief in my abilities. A special thanks to Fazel Desai for giving me every reason to complete this degree and for standing by me. More importantly a huge thanks to my children for continuously loving me despite all the sacrifices we have had to make throughout my studies. This is for you.

Abstract

The effect of suction and blowing at the base on the horizontal spreading under gravity of a two-dimensional thin fluid film and an axisymmetric liquid drop is investigated. The velocity v_n which describes the suction/injection of fluid at the base is not specified initially. The height of the thin film satisfies a nonlinear diffusion equation with v_n as a source term. The Lie group method for the solution of partial differential equations is used to reduce the partial differential equations to ordinary differential equations and to construct group invariant solutions. For a group invariant solution to exist, v_n must satisfy a first order linear partial differential equation. The two-dimensional spreading of a thin fluid film is first investigated. Two models for v_n which give analytical solutions are analysed. In the first model v_n is proportional to the height of the thin film at that point. The constant of proportionality is β ($-\infty < \beta < \infty$). The half-width always increases to infinity as time increases even for suction at the base. The range of β for the thin fluid film approximation to be valid is determined. For all values of suction and a small range of blowing the maximum height of the film tends to zero as time $t \to \infty$. There is a value of β corresponding to blowing for which the maximum height remains constant with the blowing balancing the effect of gravity. For stronger blowing the maximum height tends to infinity algebraically, there is a value of β for which the maximum height tends to infinity exponentially and for stronger blowing, still in the range for which the thin film approximation is valid, the maximum height tends to infinity in a finite time. For blowing the location of a stagnation point on the centre line is determined by solving a cubic equation approximately by a singular perturbation method and then exactly using a trigonometric solution. A dividing streamline passes through the stagnation point which separates the flow into two regions, an upper region consisting of fluid descending due to gravity and a lower region consisting of fluid rising due to blowing. For sufficiently strong blowing the lower region fills the whole of the film. In the second model v_n is proportional to the spatial gradient of the height with constant of proportionality β^* ($-\infty < \beta^* < \infty$). The maximum height always decreases to zero as time increases even for blowing. The range of β^* for the thin fluid film approximation to be valid is determined. The half-width tends to infinity algebraically for all blowing and a small range of weak suction. There is a value of β^* corresponding to suction for which the half-width remains constant with the suction balancing the spreading due to gravity. For stronger suction the half-width tends to zero as $t \to \infty$. For even stronger suction there is a value of β^* for which the half-width tends to zero exponentially and a range of β^* for which it tends to zero in a finite time but these values lie outside the range for which the thin fluid film approximation is valid. For blowing there is a stagnation point on the centre line at the base. Two dividing streamlines passes through the stagnation point which separate fluid descending due to gravity from fluid rising due to blowing. An approximate analytical solution is derived for the two dividing streamlines. A similar analysis is performed for the axisymmetric spreading of a liquid drop and the results are compared with the two-dimensional spreading of a thin fluid film. Since the two models for v_n are still quite general it can be expected that general results found will apply to other models. These include the existence of a dividing streamline separating descending and rising fluid for blowing, the existence of a strength of blowing which balances the effect of gravity so the maximum height remains constant and the existence of a strength of suction which balances spreading due to gravity so that the half-width/radius remains constant.

Contents

List of Figures

List of Tables

Chapter 1

Introduction

Thin fluid films occur almost everywhere in nature and they have many applications [32]. They play a role in many technological processes. For example in coating applications and the spreading of paints. There are applications of thin films in the lung [11] and the eye [37]. A practical application would be that of ice skating where a thin layer of water between the blade and the ice lubricates the motion of the skate.

Thin film flows usually occur under the action of gravity, surface tension or on a rotating substrate [23, 26]. Thin film flows on solid substrates as well as the moving contact line problem have been considered by O'Brien and Schwartz [30] and Hocking [15]. Davis and Hocking [7, 8] have considered the spreading of a liquid drop on a porous base while Sherman [34] studied the spreading on a non-porous substrate. Hele-Shaw flow can be used to model the flow of fluid in a porous medium and where gravity can be neglected Hele-Shaw flow obeys Darcy's law which provides a relation between the pressure and the velocity [31]. Steady state models of two-dimensional droplets have been studied [31].

A nonlinear diffusion equation arises in the study of thin flows and exact solutions have been found to be similarity solutions [13, 14]. The application of the Lie group method which is employed in this thesis has been successful in solving problems in thin film theory [22, 25, 27].

Draining in the thin film equation has been investigated by Van der Berg et al. [36]. The spreading of an axisymmetric liquid drop with fluid injection/suction on a porous base has been investigated by Mason and Momoniat [20]. The injection/suction velocity was determined from the symmetry properties of the free surface. This work is commented on further in Chapter 7. They extended their work to include surface tension [24].

In [28] the authors investigated the effect of slot injection/suction on the spreading of a thin film where surface tension and gravity effects were included. They also investigated the behaviour of the streamlines and how they evolve with suction/blowing. They discovered that there is a breakup of streamlines as a consequence of injection/suction. The velocity profile of the fluid was obtained from [33] where it had been used to stabilise the flow around an obstacle.

An investigation was undertaken by Mason and Chung [19] on the spreading of a liquid drop with slip but there was no injection of fluid. With the aid of streamlines they were able to show how the liquid spreads. It was found that vortices can occur at the base or close to the axis.

1.1 Aims and outline of the thesis

This thesis is concerned with investigating the effects of fluid extraction (suction) and fluid injection (blowing) at the base on the horizontal spreading under gravity of a two-dimensional thin fluid film and an axisymmetric liquid drop. The equation for the surface profile is a nonlinear diffusion equation with a source term. The source term is the suction/blowing velocity which is modelled as an arbitrary function v_n of the time and spatial coordinate. The velocity v_n is kept unspecified as long as possible in order to investigate the general effects of fluid extraction or injection on the spreading of a thin fluid film. To begin with the only conditions placed on v_n are that an invariant solution can be derived using Lie group analysis for differential equations and that it satisfies the balance law for fluid volume. Later two general forms for v_n will be specified to close the system of equations and derive analytical solution. A significant feature of the investigation will be the analysis of the streamlines inside the two-dimensional thin film and liquid drop. The streamlines helped us to understand how the thin fluid film and liquid drop spread.

An outline of the dissertation is as follows:

- In Chapter 2, mathematical preliminaries covering the basic operations, definitions and theory are discussed.
- In Chapter 3, the mathematical model for the spreading of a two-dimensional thin fluid film is developed.
- In Chapter 4, Lie group analysis is applied to reduce the nonlinear partial differential equation for the spreading of a two-dimensional thin fluid film to an ordinary differential equation.
- In Chapter 5, we derive the analytical solution and analyse the results for the case in which the suction/blowing velocity at the base is proportional to the height of the thin film in a two-dimensional thin fluid film. The velocity on the centre line using exact and perturbation techniques and the streamlines within the thin fluid film are investigated.
- In Chapter 6, we derive the analytical solution and analyse the results for the case in which the suction/blowing velocity at the base is proportional to the spatial gradient of the height of a two-dimensional thin fluid film. The streamlines are investigated.

- In Chapter 7, we derive the mathematical model for the axisymmetric spreading of a liquid drop.
- In Chapter 8, we derive the analytical solutions and analyse the results for the case in which the suction/blowing velocity at the base is proportional to the height of the liquid drop. The zeros of the fluid velocity on the axis of symmetry using exact and perturbation techniques and the streamlines are investigated.
- In Chapter 9, we derive the analytical solution and analyse the results for the case in which the suction/blowing velocity at the base is proportional to the spatial gradient of the height of the liquid drop. The streamlines are investigated.
- In Chapter 10, a comparison of the results for the spreading of a two-dimensional thin fluid film and an axisymmetric liquid drop is presented.
- In Chapter 11, the conclusions are stated.

Chapter 2

Mathematical Preliminaries

2.1 Introduction

In this chapter we discuss the theory of thin fluid film flows that will used in the derivation of the mathematical model for the two-dimensional fluid film in Chapter 3 and the axisymmetric liquid drop in Chapter 7. We also present results from Lie group analysis that will be used to solve the nonlinear partial differential equation in Chapter 4 and in Chapter 7.

2.2 Thin fluid film theory

A thin film free flow consists of the spreading of an incompressible fluid with a free surface where the fluid is usually exposed to another fluid such as air. Thin film flow is governed by the Navier-Stokes and conservation of mass equations for an incompressible fluid, [1]

$$\rho\left(\frac{\partial \underline{v}}{\partial t} + (\underline{v}\cdot\underline{\nabla})\underline{v}\right) = -\underline{\nabla}p + \rho\underline{F} + \mu\nabla^2\underline{v}, \tag{2.2.1}$$

$$\nabla\cdot\underline{v} = 0, \tag{2.2.2}$$

where ∇^2 is the Laplace operator. Equation (2.2.2) is also called the continuity equation.

The free surface of the fluid is usually unknown and must be obtained as part of the solution. Generally the characteristic thickness, H, in one direction is much smaller than the characteristic length scale,L, in the other direction. The flow takes place typically in the direction of the longer dimension under the action of either gravity, surface tension or rotation. If we let U denote a typical flow speed of the fluid, we form a dimensionless quantity

$$Re = \frac{UL}{\nu}, \tag{2.2.3}$$

which is known as the Reynolds number, where $\nu = {}^{\mu}/_{\rho}$ is the kinematic viscosity. The non-dimensional *aspect ratio* of the flow is defined by

$$\epsilon = \frac{H}{L} \ll 1. \tag{2.2.4}$$

Since ϵ is very small, the film is long and thin. The second assumption in thin fluid film theory is

$$\epsilon^2 Re \ll 1. \tag{2.2.5}$$

Since $H \ll L$,we do not require $Re \ll 1$ to satisfy (2.2.5).

We will derive the thin film equations both in terms of Cartesian coordinates and cylindrical polar coordinates from the Navier-Stokes equation (2.2.1) and the conservation of mass equation (2.2.2).

2.2.1 Thin film flow in Cartesian coordinates

We consider an incompressible viscous fluid. The $x-$ and $y-$ axes are horizontal and the z-axis is vertically upwards. The fluid variables are

$$v_x = v_x(t,x,y,z), \quad v_y = v_y(t,x,y,z), \quad v_z = v_z(t,x,y,z), \quad p = p(t,x,y,z). \tag{2.2.6}$$

We introduce characteristic quantities and dimensionless variables and write the Navier-Stokes equation (2.2.1) in dimensionless form where ∇^2 is given by

$$\nabla^2 = \frac{\partial^2}{\partial x^2} + \frac{\partial^2}{\partial y^2} + \frac{\partial^2}{\partial z^2}. \tag{2.2.7}$$

Let the characteristic length in x and y directions be L, the characteristic length in the z direction be H, the characteristic body force per unit mass be F_0 and the characteristic flow speed in the x and y directions be U. Then the characteristic flow speed in the z direction is $V = \frac{H}{L}U$, the characteristic fluid pressure is $P = \mu({}^{L}/_{H^2})U$ and the characteristic time is $T = L/U$.

We now justify the definitions of V, P and T. Consider first the characteristic velocity in the z-direction: From the continuity equation (2.2.2)

$$\frac{\partial v_x}{\partial x} + \frac{\partial v_y}{\partial y} + \frac{\partial v_z}{\partial z} = 0, \tag{2.2.8}$$

and therefore

$$\bigcirc\left(\frac{U}{L}\right) + \bigcirc\left(\frac{U}{L}\right) + \bigcirc\left(\frac{V}{H}\right) = 0. \tag{2.2.9}$$

Thus

$$V = \left(\frac{H}{L}U\right). \tag{2.2.10}$$

Consider next the characteristic pressure P: It is not an independent quantity that can be set in an experiment and therefore it is related to the other parameters in the problem. Since viscous effects dominate, an estimate of the magnitude of P is not ρU^2 which is used when viscous forces are not dominant. To obtain P, we balance the pressure gradient in the x-direction with the viscous forces in the x-direction:

$$\frac{\partial p}{\partial x} \sim \mu \left(\frac{\partial^2 v_x}{\partial x^2} + \frac{\partial^2 v_x}{\partial y^2} + \frac{\partial^2 v_x}{\partial z^2}\right), \tag{2.2.11}$$

$$\frac{\partial p}{\partial x} \sim \mu \frac{\partial^2 v_x}{\partial z^2} \qquad \left(\frac{\partial^2 v_x}{\partial z^2} \gg \frac{\partial^2 v_x}{\partial x^2} + \frac{\partial^2 v_x}{\partial y^2}\right), \tag{2.2.12}$$

$$\frac{P}{L} = \mu \frac{U}{H^2}, \tag{2.2.13}$$

$$P = \mu \frac{L}{H^2}U. \tag{2.2.14}$$

Introduce dimensionless variables

$$\overline{t} = \frac{U}{L}t, \qquad \overline{x} = \frac{x}{L}, \qquad \overline{y} = \frac{y}{L}, \qquad \overline{z} = \frac{z}{H}, \qquad \overline{F} = \frac{F}{F_0}, \tag{2.2.15}$$

$$\overline{v}_x = \frac{v_x}{U}, \qquad \overline{v}_y = \frac{v_y}{U}, \qquad \overline{v}_z = \frac{L}{H\,U}\,v_z, \qquad \overline{p} = \frac{p}{P} = \frac{H^2\,p}{\mu\,L\,U}. \tag{2.2.16}$$

Write the components of the Navier-Stokes equation (2.2.1) in dimensionless form using (2.2.15) and (2.2.16) [1]:

x-component:

$$\begin{aligned} &\rho\left(\frac{\partial v_x}{\partial t} + v_x\frac{\partial v_x}{\partial x} + v_y\frac{\partial v_x}{\partial y} + v_z\frac{\partial v_x}{\partial z}\right) \\ &= -\frac{\partial p}{\partial x} + \rho\,F_x + \mu\left(\frac{\partial^2 v_x}{\partial x^2} + \frac{\partial^2 v_x}{\partial y^2} + \frac{\partial^2 v_x}{\partial z^2}\right), \end{aligned} \tag{2.2.17}$$

which when expressed in dimensionless form may be written as

$$\begin{aligned} &Re\left(\frac{H}{L}\right)^2\left(\frac{\partial \overline{v}_x}{\partial \overline{t}} + \overline{v}_x\frac{\partial \overline{v}_x}{\partial \overline{x}} + \overline{v}_y\frac{\partial \overline{v}_x}{\partial \overline{y}} + \overline{v}_z\frac{\partial \overline{v}_x}{\partial \overline{z}}\right) \\ &= -\frac{\partial \overline{p}}{\partial \overline{x}} + \frac{F_0\,H^2}{\nu U}\,\overline{F}_x + \left(\frac{H}{L}\right)^2\frac{\partial^2 \overline{v}_x}{\partial \overline{x}^2} + \left(\frac{H}{L}\right)^2\frac{\partial^2 \overline{v}_x}{\partial \overline{y}^2} + \frac{\partial^2 \overline{v}_x}{\partial \overline{z}^2}. \end{aligned} \tag{2.2.18}$$

y-component:

$$\begin{aligned} &\rho\left(\frac{\partial v_y}{\partial t} + v_x\frac{\partial v_y}{\partial x} + v_y\frac{\partial v_y}{\partial y} + v_z\frac{\partial v_y}{\partial z}\right) \\ &= -\frac{\partial p}{\partial y} + \rho\,F_y + \mu\left(\frac{\partial^2 v_y}{\partial x^2} + \frac{\partial^2 v_y}{\partial y^2} + \frac{\partial^2 v_y}{\partial z^2}\right), \end{aligned} \tag{2.2.19}$$

which in dimensionless form is

$$\begin{aligned} &Re\left(\frac{H}{L}\right)^2\left(\frac{\partial \overline{v}_y}{\partial \overline{t}} + \overline{v}_x\frac{\partial \overline{v}_y}{\partial \overline{x}} + \overline{v}_y\frac{\partial \overline{v}_y}{\partial \overline{y}} + \overline{v}_z\frac{\partial \overline{v}_y}{\partial \overline{z}}\right) \\ &= -\frac{\partial \overline{p}}{\partial \overline{y}} + \frac{F_0\,H^2}{\nu U}\,\overline{F}_y + \left(\frac{H}{L}\right)^2\frac{\partial^2 \overline{v}_y}{\partial \overline{x}^2} + \left(\frac{H}{L}\right)^2\frac{\partial^2 \overline{v}_y}{\partial \overline{y}^2} + \frac{\partial^2 \overline{v}_y}{\partial \overline{z}^2}. \end{aligned} \tag{2.2.20}$$

z-component:

$$\begin{aligned} &\rho\left(\frac{\partial v_z}{\partial t} + v_x\frac{\partial v_z}{\partial x} + v_y\frac{\partial v_z}{\partial y} + v_z\frac{\partial v_z}{\partial z}\right) \\ &= -\frac{\partial p}{\partial z} + \rho\,F_z + \mu\left(\frac{\partial^2 v_z}{\partial x^2} + \frac{\partial^2 v_z}{\partial y^2} + \frac{\partial^2 v_z}{\partial z^2}\right), \end{aligned} \tag{2.2.21}$$

which in dimensionless form is

$$\begin{aligned} &Re\left(\frac{H}{L}\right)^4\left(\frac{\partial \overline{v}_z}{\partial \overline{t}} + \overline{v}_x\frac{\partial \overline{v}_z}{\partial \overline{x}} + \overline{v}_y\frac{\partial \overline{v}_z}{\partial \overline{y}} + \overline{v}_z\frac{\partial \overline{v}_z}{\partial \overline{z}}\right) \\ &= -\frac{\partial \overline{p}}{\partial \overline{z}} + \frac{F_0\,H^3}{\nu\,U\,L}\overline{F}_z + \left(\frac{H}{L}\right)^4\frac{\partial^2 \overline{v}_z}{\partial \overline{x}^2} + \left(\frac{H}{L}\right)^4\frac{\partial^2 \overline{v}_z}{\partial \overline{y}^2} + \left(\frac{H}{L}\right)^2\frac{\partial^2 \overline{v}_z}{\partial \overline{z}^2}. \end{aligned} \tag{2.2.22}$$

Continuity equation (2.2.2):

$$\frac{\partial v_x}{\partial x} + \frac{\partial v_y}{\partial y} + \frac{\partial v_z}{\partial z} = 0, \tag{2.2.23}$$

which becomes in dimensionless form

$$\frac{\partial \overline{v}_x}{\partial \overline{x}} + \frac{\partial \overline{v}_y}{\partial \overline{y}} + \frac{\partial \overline{v}_z}{\partial \overline{z}} = 0. \tag{2.2.24}$$

By imposing the thin film approximation (2.2.4) and (2.2.5), equations (2.2.18), (2.2.20), (2.2.22) and (2.2.24) reduce to

$$0 = -\frac{\partial \overline{p}}{\partial \overline{x}} + \frac{F_0\, H^2}{\nu\, U}\, \overline{F}_x + \frac{\partial^2 \overline{v}_x}{\partial \overline{z}^2}, \tag{2.2.25}$$

$$0 = -\frac{\partial \overline{p}}{\partial \overline{y}} + \frac{F_0\, H^2}{\nu\, U}\, \overline{F}_y + \frac{\partial^2 \overline{v}_y}{\partial \overline{z}^2}, \tag{2.2.26}$$

$$0 = -\frac{\partial \overline{p}}{\partial \overline{z}} + \frac{F_0\, H^3}{\nu\, U\, L}\, \overline{F}_z, \tag{2.2.27}$$

$$\frac{\partial \overline{v}_x}{\partial \overline{x}} + \frac{\partial \overline{v}_y}{\partial \overline{y}} + \frac{\partial \overline{v}_z}{\partial \overline{z}} = 0. \tag{2.2.28}$$

Expressed in terms of the original variables, (2.2.25)-(2.2.28) are

$$\frac{\partial p}{\partial x} = \rho F_x + \mu\, \frac{\partial^2 v_x}{\partial z^2}, \tag{2.2.29}$$

$$\frac{\partial p}{\partial y} = \rho F_y + \mu\, \frac{\partial^2 v_y}{\partial z^2}, \tag{2.2.30}$$

$$\frac{\partial p}{\partial z} = \rho F_z, \tag{2.2.31}$$

$$\frac{\partial v_x}{\partial x} + \frac{\partial v_y}{\partial y} + \frac{\partial v_z}{\partial z} = 0. \tag{2.2.32}$$

Consider next the Cauchy stress tensor. The Navier-Poisson law is

$$\tau_{ik} = \left(-p + \lambda\left(\underline{\nabla} \cdot \underline{v}\right)\right) \delta_{ik} + 2\mu\, d_{ik}, \tag{2.2.33}$$

$$= -p\, \delta_{ik} + \mu \left(v_{i,k} + v_{k,i}\right), \tag{2.2.34}$$

since $(\underline{\nabla} \cdot \underline{v}) = 0$. The characteristic stress is the same as the characteristic pressure P:

$$\text{characteristic stress} \quad P = \frac{\mu\, L}{H^2}\, U. \tag{2.2.35}$$

Rewrite the components τ_{ik} in dimensionless form:

$$\tau_{xx} = -p + 2\mu \frac{\partial v_x}{\partial x}, \qquad \overline{\tau}_{xx} = -\overline{p} + 2\left(\frac{H}{L}\right)^2 \frac{\partial \overline{v}_x}{\partial \overline{x}}, \tag{2.2.36}$$

(2.2.37)

$$\tau_{xy} = \mu\left(\frac{\partial v_x}{\partial y} + \frac{\partial v_y}{\partial x}\right), \qquad \overline{\tau}_{xy} = \left(\frac{H}{L}\right)^2 \left(\frac{\partial \overline{v}_x}{\partial \overline{y}} + \frac{\partial \overline{v}_y}{\partial \overline{x}}\right), \tag{2.2.38}$$

(2.2.39)

$$\tau_{xz} = \mu\left(\frac{\partial v_x}{\partial z} + \frac{\partial v_z}{\partial x}\right), \qquad \overline{\tau}_{xz} = \frac{H}{L}\frac{\partial \overline{v}_x}{\partial \overline{z}} + \left(\frac{H}{L}\right)^3 \frac{\partial \overline{v}_z}{\partial \overline{x}}, \tag{2.2.40}$$

(2.2.41)

$$\tau_{yy} = -p + 2\mu \frac{\partial v_y}{\partial y}, \qquad \overline{\tau}_{yy} = -\overline{p} + 2\left(\frac{H}{L}\right)^2 \frac{\partial \overline{v}_y}{\partial \overline{y}}, \tag{2.2.42}$$

(2.2.43)

$$\tau_{yz} = \mu\left(\frac{\partial v_y}{\partial z} + \frac{\partial v_z}{\partial y}\right), \qquad \overline{\tau}_{yz} = \frac{H}{L}\frac{\partial \overline{v}_y}{\partial \overline{z}} + \left(\frac{H}{L}\right)^3 \frac{\partial \overline{v}_z}{\partial \overline{y}}, \tag{2.2.44}$$

(2.2.45)

$$\tau_{zz} = -p + 2\mu \frac{\partial v_z}{\partial z}, \qquad \overline{\tau}_{zz} = -\overline{p} + 2\left(\frac{H}{L}\right)^2 \frac{\partial \overline{v}_z}{\partial \overline{z}}. \tag{2.2.46}$$

To zero order in H/L,

$$\overline{\tau}_{ik} = -\overline{p}\,\delta_{ik}, \tag{2.2.47}$$

and therefore

$$\tau_{ik} = -p\,\delta_{ik}. \tag{2.2.48}$$

We use (2.2.48) when imposing boundary conditions on the normal components of stress at the boundary. When imposing boundary conditions on the tangential components of stress, terms of order H/L are retained. Thus in the thin-film approximation, the stress tensor is given as

$$\tau_{xx} = -p, \quad \tau_{yy} = -p, \quad \tau_{zz} = -p, \quad \tau_{xy} = 0, \quad \tau_{xz} = \mu\frac{\partial v_x}{\partial z}, \quad \tau_{yz} = 0. \tag{2.2.49}$$

2.2.2 Axisymmetric flow in cylindrical polar coordinates

We consider a viscous and incompressible fluid. The flow is axisymmetric, hence $\frac{\partial}{\partial\theta} = 0$ with no flow in the θ-direction thus, $v_\theta = 0$. The initial radius of the thin film is a and the initial height at $r = 0$ is h_0. The fluid variables are

$$v_r = v_r(t, r, z), \quad v_\theta = 0, \quad v_z = v_z(t, r, z), \quad p = p(t, r, z). \tag{2.2.50}$$

We introduce characteristic quantities and dimensionless variables and write the Navier-Stokes equation (2.2.1) in dimensionless form where

$$(\underline{v} \cdot \underline{\nabla}) = v_r \frac{\partial}{\partial r} + \frac{v_\theta}{r}\frac{\partial}{\partial\theta} + v_z \frac{\partial}{\partial z}, \tag{2.2.51}$$

$$\nabla^2 = \frac{1}{r}\frac{\partial}{\partial r}\left(r\frac{\partial}{\partial r}\right) + \frac{1}{r^2}\frac{\partial^2}{\partial\theta^2} + \frac{\partial^2}{\partial z^2}. \tag{2.2.52}$$

Let the characteristic length in the r direction be a and the characteristic length in the z direction be h_0, the characteristic body force per unit mass be F_0 and the characteristic velocity in the r direction be U. Then the characteristic velocity in the z direction is $V = \frac{h_0}{a}U$, the characteristic fluid pressure is $P = \mu\frac{aU}{h_0^2}$ and the characteristic time is $T = a/U$.

We now justify the definitions of V and P. Consider first the characteristic velocity in the z-direction. From the continuity equation (2.2.2) with $v_\theta = 0$

$$\frac{\partial v_r}{\partial r} + \frac{v_r}{r} + \frac{\partial v_z}{\partial z} = 0, \tag{2.2.53}$$

and therefore

$$\bigcirc\left(\frac{U}{a}\right) + \bigcirc\left(\frac{U}{a}\right) + \bigcirc\left(\frac{v_z}{h_0}\right) = 0. \tag{2.2.54}$$

Thus

$$V = \left(\frac{h_0}{a}U\right). \tag{2.2.55}$$

To obtain P, we consider the r-component of (2.2.1) and we balance the pressure gradient in the r-direction with the viscous forces in the r-direction

$$\frac{\partial p}{\partial r} \sim \mu\left(\frac{\partial^2 v_r}{\partial r^2} + \frac{1}{r}\frac{\partial v_r}{\partial r} + \frac{\partial^2 v_r}{\partial z^2} - \frac{v_r}{r^2}\right), \tag{2.2.56}$$

$$\begin{aligned} \frac{P}{a} &\sim \mu \left(\frac{U}{a^2} + \frac{U}{a^2} + \frac{U}{h_0^2} - \frac{U}{a^2}\right), && (2.2.57) \\ &\sim \mu \frac{U}{h_0^2}\left(1 + \bigcirc\left(\frac{h_0}{a}\right)^2\right), && (2.2.58) \\ P &= \mu \frac{a\,U}{h_0^2}. && (2.2.59) \end{aligned}$$

Introduce dimensionless variables

$$\overline{t} = \frac{U}{a}t, \qquad \overline{r} = \frac{r}{a}, \qquad \overline{z} = \frac{z}{h_0}, \qquad \overline{F} = \frac{F}{F_0}, \tag{2.2.60}$$

$$\overline{v}_r = \frac{v_r}{U}, \qquad \overline{v}_z = \frac{a}{h_0}\frac{v_z}{U}, \qquad \overline{p} = \frac{h_0^2\,p}{\mu\,a\,U}. \tag{2.2.61}$$

Write the components of the Navier-Stokes equation (2.2.1) in dimensionless form using (2.2.60) and (2.2.61). Since the flow is axisymmetric $v_\theta = 0$ and all θ-derivatives vanish [1].

r-component:

$$\begin{aligned} &\rho\left(\frac{\partial v_r}{\partial t} + v_r\frac{\partial v_r}{\partial r} + v_z\frac{\partial v_r}{\partial z}\right) \\ &= -\frac{\partial p}{\partial r} + \rho\,F_r + \mu\left(\frac{\partial^2 v_r}{\partial r^2} + \frac{1}{r}\frac{\partial v_r}{\partial r} + \frac{\partial^2 v_z}{\partial z^2} - \frac{v_r}{r^2}\right), \end{aligned} \tag{2.2.62}$$

which when expressed in dimensionless form may be written as

$$\begin{aligned} &Re\left(\frac{h_0}{a}\right)^2\left(\frac{\partial \overline{v}_r}{\partial \overline{t}} + \overline{v}_r\frac{\partial \overline{v}_r}{\partial \overline{r}} + \overline{v}_z\frac{\partial \overline{v}_r}{\partial \overline{z}}\right) \\ &= -\frac{\partial \overline{p}}{\partial \overline{r}} + \frac{F_0\,h_0^2}{\nu U}\,\overline{F}_r + \left(\frac{h_0}{a}\right)^2\frac{\partial^2 \overline{v}_r}{\partial \overline{r}^2} + \left(\frac{h_0}{a}\right)^2\frac{1}{r}\frac{\partial \overline{v}_r}{\partial \overline{r}} + \frac{\partial^2 \overline{v}_r}{\partial \overline{z}^2} - \left(\frac{h_0}{a}\right)^2\frac{\overline{v}_r}{\overline{r}^2}. \end{aligned} \tag{2.2.63}$$

θ-component:

$$F_\theta = 0. \tag{2.2.64}$$

z-component:

$$\begin{aligned} &\rho\left(\frac{\partial v_z}{\partial t} + v_r\frac{\partial v_z}{\partial r} + v_z\frac{\partial v_z}{\partial z}\right) \\ &= -\frac{\partial p}{\partial z} + \rho\,F_z + \mu\left(\frac{\partial^2 v_z}{\partial r^2} + \frac{1}{r}\frac{\partial v_z}{\partial r} + \frac{\partial^2 v_z}{\partial z^2}\right), \end{aligned} \tag{2.2.65}$$

which in dimensionless form is

$$
\begin{aligned}
&Re\left(\frac{h_0}{a}\right)^4\left(\frac{\partial \overline{v}_z}{\partial \overline{t}}+\overline{v}_r\frac{\partial \overline{v}_z}{\partial \overline{r}}+\overline{v}_z\frac{\partial \overline{v}_z}{\partial \overline{z}}\right)\\
&=-\frac{\partial \overline{p}}{\partial \overline{z}}+\frac{F_0\,h^3}{\nu\,U\,a}\overline{F}_z+\left(\frac{h_0}{a}\right)^4\frac{\partial^2 \overline{v}_z}{\partial \overline{r}^2}+\left(\frac{h_0}{a}\right)^4\frac{1}{\overline{r}}\frac{\partial \overline{v}_z}{\partial \overline{r}}+\left(\frac{h_0}{a}\right)^2\frac{\partial^2 \overline{v}_z}{\partial \overline{z}^2}.
\end{aligned} \tag{2.2.66}
$$

Continuity equation (2.2.2):

$$
\frac{\partial v_r}{\partial r}+\frac{v_r}{r}+\frac{\partial v_z}{\partial z}=0, \tag{2.2.67}
$$

which becomes in dimensionless form

$$
\frac{\partial \overline{v}_r}{\partial \overline{r}}+\frac{\overline{v}_r}{\overline{r}}+\frac{\partial \overline{v}_z}{\partial \overline{z}}=0. \tag{2.2.68}
$$

By imposing the thin film approximation, (2.2.4) and (2.2.5), equations (2.2.63), (2.2.64), (2.2.66) and (2.2.68) reduce to

$$
0 = -\frac{\partial \overline{p}}{\partial \overline{r}}+\frac{F_0\,h_0^2}{\nu\,U}\,\overline{F}_r+\frac{\partial^2 \overline{v}_r}{\partial \overline{z}^2}, \tag{2.2.69}
$$

$$
0 = \overline{F}_\theta, \tag{2.2.70}
$$

$$
0 = -\frac{\partial \overline{p}}{\partial \overline{z}}+\frac{F_0\,h_0^3}{\nu\,U\,a}\,\overline{F}_z, \tag{2.2.71}
$$

$$
\frac{\partial \overline{v}_r}{\partial \overline{r}}+\frac{\overline{v}_r}{\overline{r}}+\frac{\partial \overline{v}_z}{\partial \overline{z}}=0. \tag{2.2.72}
$$

Expressed in terms of the original variables, (2.2.69)-(2.2.72) are

$$
\frac{\partial p}{\partial r} = \rho F_r+\mu\,\frac{\partial^2 v_r}{\partial z^2}, \tag{2.2.73}
$$

$$
0 = F_\theta, \tag{2.2.74}
$$

$$
\frac{\partial p}{\partial z} = \rho F_z, \tag{2.2.75}
$$

$$
\frac{1}{r}\frac{\partial}{\partial r}\left(r\,v_r\right)+\frac{\partial v_z}{\partial z} = 0. \tag{2.2.76}
$$

Consider now the physical components of the stress tensor. The characteristic stress is the same as the characteristic pressure P,

$$
\text{characteristic stress} \quad P=\frac{\mu\,U\,a}{h_0^2}. \tag{2.2.77}
$$

Rewrite the components τ_{ik} in dimensionless form. We have $\frac{\partial}{\partial\theta} = 0$ and $v_\theta = 0$:

$$\tau_{rr} = -p + 2\mu\frac{\partial v_r}{\partial r}, \qquad \overline{\tau}_{rr} = -\overline{p} + 2\left(\frac{h_0}{a}\right)^2\frac{\partial \overline{v}_r}{\partial \overline{r}}, \tag{2.2.78}$$

$$\tag{2.2.79}$$

$$\tau_{r\theta} = \mu\left(\frac{1}{r}\frac{\partial v_r}{\partial\theta} + \frac{\partial v_\theta}{\partial r} - \frac{v_\theta}{r}\right), \qquad \overline{\tau}_{r\theta} = 0, \tag{2.2.80}$$

$$\tag{2.2.81}$$

$$\tau_{rz} = \mu\left(\frac{\partial v_r}{\partial z} + \frac{\partial v_z}{\partial r}\right), \qquad \overline{\tau}_{rz} = \frac{h_0}{a}\frac{\partial \overline{v}_r}{\partial \overline{z}} + \left(\frac{h_0}{a}\right)^3\frac{\partial \overline{v}_z}{\partial \overline{r}}, \tag{2.2.82}$$

$$\tag{2.2.83}$$

$$\tau_{\theta\theta} = -p + 2\mu\left(\frac{1}{r}\frac{\partial v_\theta}{\partial\theta} + \frac{v_r}{r}\right), \qquad \overline{\tau}_{\theta\theta} = -\overline{p} + 2\left(\frac{h_0}{a}\right)^2\frac{\overline{v}_r}{\overline{r}}, \tag{2.2.84}$$

$$\tag{2.2.85}$$

$$\tau_{\theta z} = \mu\left(\frac{\partial v_\theta}{\partial z} + \frac{1}{r}\frac{\partial v_z}{\partial\theta}\right), \qquad \overline{\tau}_{\theta z} = 0, \tag{2.2.86}$$

$$\tag{2.2.87}$$

$$\tau_{zz} = -p + 2\mu\frac{\partial v_z}{\partial z}, \qquad \overline{\tau}_{zz} = -\overline{p} + 2\left(\frac{h_0}{a}\right)^2\frac{\partial \overline{v}_z}{\partial \overline{z}}. \tag{2.2.88}$$

To zero order in h_0/a,

$$\tau_{rr} = -p, \quad \tau_{\theta\theta} = -p, \quad \tau_{zz} = -p, \quad \tau_{ik} = 0, \quad i \neq k. \tag{2.2.89}$$

As in two-dimensional flow, we use (2.2.89) when imposing boundary conditions on the normal components of stress at a boundary and retain terms of order h_0/a when imposing boundary conditions on the tangential components of stress

$$\tau_{r\theta} = 0, \quad \tau_{rz} = \mu\frac{\partial v_r}{\partial z}, \quad \tau_{\theta z} = 0. \tag{2.2.90}$$

2.3 Lie group theory

Lie group theory is used to determine infinitesimal transformations that leave the model equation form invariant. The order of the model equation can then be reduced or group invariant solutions admitted by the model equation can be found using the generator of the infinitesimal transformations. The following is a summary from [5, 16].

2.3.1 Lie point symmetries

We consider the second order nonlinear partial differential equation of the form

$$F(t, x, h, h_t, h_x, h_{tx}, h_{tt}, h_{xx}) = 0, \tag{2.3.1}$$

where h is the dependent variable and x and t are the independent variables.The subscripts denote partial differentiation. The Lie point symmetry generators admitted by (2.3.1) are of the form

$$X = \xi^1(t, x, h)\frac{\partial}{\partial t} + \xi^2(t, x, h)\frac{\partial}{\partial x} + \eta(t, x, h)\frac{\partial}{\partial h}. \tag{2.3.2}$$

The coefficients $\xi^1(t, x, h), \xi^2(t, x, h)$ and $\eta(t, x, h)$ are related to the infinitesimal transformations

$$\bar{t} \approx t + a\xi^1(t, x, h), \quad \bar{x} \approx x + a\xi^2(t, x, h), \quad \bar{h} \approx h + a\eta(t, x, h), \tag{2.3.3}$$

where $a \ll 1$, that leaves (2.3.1) form invariant. Consequently the transformations (2.3.3) change (2.3.1) into

$$F(\bar{t}, \bar{x}, \bar{h}, \bar{h}_{\bar{t}}, \bar{h}_{\bar{x}}, \bar{h}_{\bar{t}\bar{x}}, \bar{h}_{\bar{t}\bar{t}}, \bar{h}_{\bar{x}\bar{x}}) = 0. \tag{2.3.4}$$

As a result of solving the determining equation

$$X^{[2]}F(t, x, h, h_t, h_x, h_{tx}, h_{tt}, h_{xx})|_{F=0} = 0, \tag{2.3.5}$$

we obtain $\xi^1(t, x, h), \xi^2(t, x, h)$ and $\eta(t, x, h)$. The generator $X^{[2]}$ is called the second prolongation (extension) of the generator X and is given by

$$X^{[2]} = X + \zeta_1\frac{\partial}{\partial h_t} + \zeta_2\frac{\partial}{\partial h_x} + \zeta_{11}\frac{\partial}{\partial h_{tt}} + \zeta_{12}\frac{\partial}{\partial h_{tx}} + \zeta_{22}\frac{\partial}{\partial h_{xx}}, \tag{2.3.6}$$

where

$$\zeta_i = D_i(\eta) - h_k D_i(\xi^k), \quad i = 1, 2, \tag{2.3.7}$$

$$\zeta_{ij} = D_j(\zeta_i) - h_{ik}\, D_j(\xi^k), \quad i = 1, 2, \tag{2.3.8}$$

with summation over the repeated index k from 1 to 2. The total derivatives with respect to the independent variables t and x in (2.3.7) and (2.3.8) are

$$D_1 = D_t = \frac{\partial}{\partial t} + h_t \frac{\partial}{\partial h} + h_{tt} \frac{\partial}{\partial h_t} + h_{xt} \frac{\partial}{\partial h_x} + \ldots, \tag{2.3.9}$$

$$D_2 = D_x = \frac{\partial}{\partial x} + h_x \frac{\partial}{\partial h} + h_{tx} \frac{\partial}{\partial h_t} + h_{xx} \frac{\partial}{\partial h_x} + \ldots, \tag{2.3.10}$$

Due to the fact that we are solving a second order partial differential equation, we need the second prolongation of X. Since $\xi^1(t, x, h), \xi^2(t, x, h)$ and $\eta(t, x, h)$ are functions of t, x and h only and do not depend on the derivatives of h, the determining equation (2.3.5) can be separated according to coefficients of powers and products of the derivatives of h thus resulting in an over-determined linear system of equations for $\xi^1(t, x, h), \xi^2(t, x, h)$ and $\eta(t, x, h)$. One then equates these coefficients to zero which results in expressions for $\xi^1(t, x, h), \xi^2(t, x, h)$ and $\eta(t, x, h)$. The solution of the determining equations can be carried out by hand or by using computer algebra packages such as MathLie [4] and Lie [12, 35].

2.3.2 Group invariant solutions

The symmetry generators obtained are of the form

$$X_i = \xi_i^1(t, x, h)\frac{\partial}{\partial t} + \xi_i^2(t, x, h)\frac{\partial}{\partial x} + \eta_i(t, x, h)\frac{\partial}{\partial h}, \tag{2.3.11}$$

for $i = 1, 2, \ldots, n$ where n is the number of admitted Lie point symmetries. Any linear combination of the Lie point symmetries is also a Lie point symmetry of the partial differential equation. This linear combination may be denoted as X_k where

$$X_k = k_1 X_1 + k_2 X_2 + \ldots + k_n X_n. \tag{2.3.12}$$

The group invariant solution, $h = \Phi(t, x)$, of the nonlinear partial differential equation (2.3.1) is obtained by solving the equation

$$X_k(h - \Phi(t, x))|_{h=\Phi(t,x)} = 0. \tag{2.3.13}$$

By substituting the group invariant solution into the nonlinear partial differential equation, the number of independent variables in the reduced system is fewer than the original system. Thus one can reduce the order of the second order nonlinear partial differential equation (2.3.1) by one resulting in an ordinary differential equation.

2.4 Conclusions

The main approximation in thin fluid film theory is that the inertia term in the Navier-Stokes equation can be neglected. The boundary conditions are also simplified. Lie Group analysis is a systemic way to look for group invariant solutions which could lead to exact analytical solutions of nonlinear partial differential equations.

Chapter 3

Two-dimensional thin film flow

3.1 Introduction

In this chapter we derive the partial differential equation describing the spreading on a horizontal surface of a two-dimensional thin film flow with suction/blowing at the base. To obtain the partial differential equation for the height of the free surface, $h(t, x)$, we use the theory described in Section 2.2. We also discuss the volume of the thin film and its time rate of change because it gives the extra condition needed to solve for $h(t, x)$.

3.2 Mathematical modelling of a two-dimensional thin film with suction/blowing

Consider the two-dimensional spreading of a thin film of viscous incompressible fluid under gravity on a fixed horizontal plane. At the horizontal plane there is suction of fluid from the thin film or blowing of fluid into the thin film. A graphical representation of the model is given in Figure 3.1. The thin film is infinite in the y-direction. The equation of the free surface of the thin film is $z = h(t, x)$. The film is symmetrical about $x = 0$ so that

$$h(t, -x) = h(t, x). \tag{3.2.1}$$

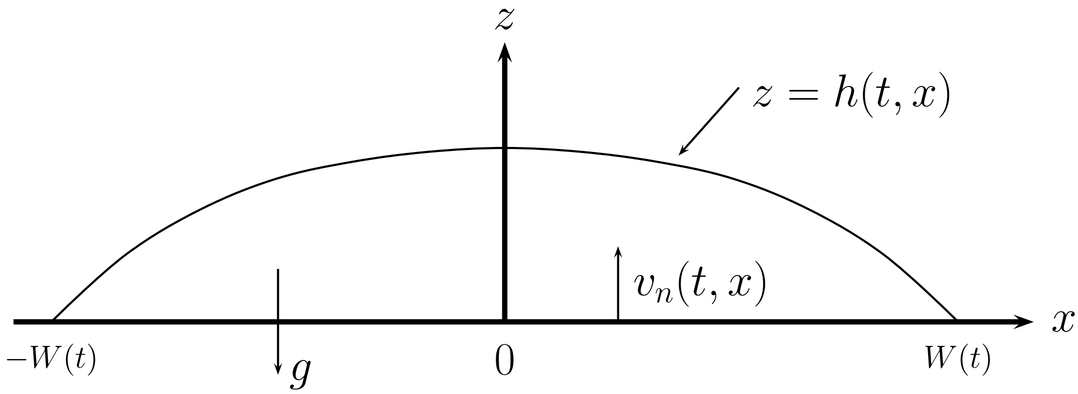

Figure 3.1: Co-ordinate system

At time t the base is

$$-W(t) \leq x \leq W(t). \tag{3.2.2}$$

The flow is two-dimensional:

$$v_x = v_x(t, x, z), \qquad v_y = 0, \qquad v_z = v_z(t, x, z), \qquad p = p(t, x, z). \tag{3.2.3}$$

The body force per unit mass is due to gravity and acts in the $-z$ direction:

$$F_x = 0\ , \qquad F_y = 0\ , \qquad F_z = -g. \tag{3.2.4}$$

From Section 2.2, the dimensional thin film equations are given by equations (2.2.29)-(2.2.32) and the components of the Cauchy stress tensor by (2.2.49). Using (3.2.3) and (3.2.4), the equations become

$$\frac{\partial p}{\partial x} = \mu \frac{\partial^2 v_x}{\partial z^2}, \tag{3.2.5}$$

$$\frac{\partial p}{\partial z} = -\rho\, g, \tag{3.2.6}$$

$$\frac{\partial v_x}{\partial x} + \frac{\partial v_z}{\partial z} = 0. \tag{3.2.7}$$

The Cauchy stress tensor is given by [3, 18]

$$\tau_{xx} = -p, \quad \tau_{yy} = -p, \quad \tau_{zz} = -p, \quad \tau_{xy} = 0, \quad \tau_{xz} = \mu\frac{\partial v_x}{\partial z}, \quad \tau_{yz} = 0. \tag{3.2.8}$$

Consider now the boundary conditions as illustrated in Figure (3.2):

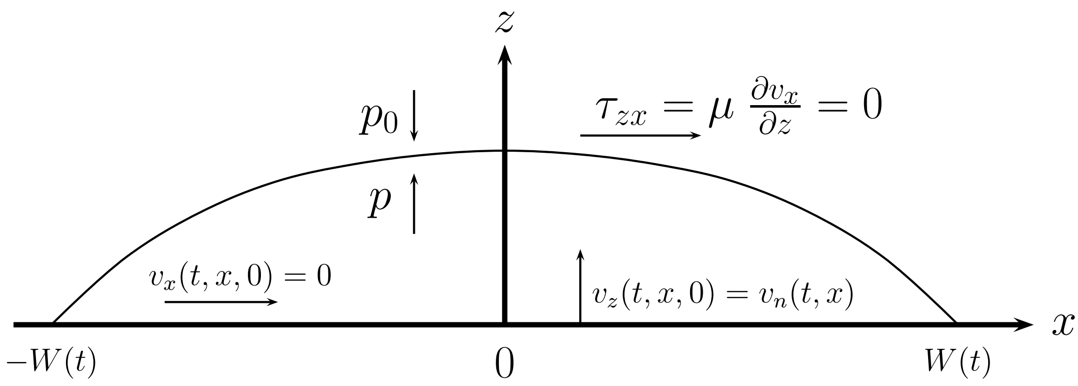

Figure 3.2: Boundary conditions

$z = 0$: No slip boundary condition for a viscous fluid at a solid boundary

$$v_x(t, x, 0) = 0. \tag{3.2.9}$$

$z = 0$: A normal velocity is induced by the fluid injection/suction

$$v_z(t, x, 0) = v_n(t, x), \tag{3.2.10}$$

where if

$$\begin{aligned} v_n(t,x) &> 0 \quad \text{blowing/injection,} \\ v_n(t,x) &< 0 \quad \text{suction.} \end{aligned}$$

$z = h(t, x)$:

$$p(t, x, h) = p_0, \tag{3.2.11}$$

where p_0 is the atmospheric pressure.

$z = h(t,x)$: No tangential stress on the free surface

$$\tau_{zx} = \mu \frac{\partial v_x}{\partial z}(t,x,h) = 0. \tag{3.2.12}$$

$z = h(t,x)$: A fluid particle on the free surface must remain on the free surface as the fluid evolves. Thus

$$\frac{D}{Dt}(z - h(t,x))\bigg|_{z=h(t,x)} = 0, \tag{3.2.13}$$

and therefore

$$\frac{Dz}{Dt}\bigg|_{z=h(t,x)} = \frac{D}{Dt}\, h(t,x)\bigg|_{z=h(t,x)}. \tag{3.2.14}$$

Now since

$$\frac{Dz}{Dt}\bigg|_{z=h(t,x)} = v_z(t,x,h) \quad \text{and} \quad \frac{D}{Dt} = \frac{\partial}{\partial t} + \underline{v}\cdot\underline{\nabla}, \tag{3.2.15}$$

it follows that

$$v_z(t,x,h) = \frac{\partial h}{\partial t} + v_x(t,x,h)\frac{\partial h}{\partial x}, \tag{3.2.16}$$

and therefore

$$\frac{\partial h}{\partial t} + v_x(t,x,h)\frac{\partial h}{\partial x} = v_z(t,x,h). \tag{3.2.17}$$

We now write the equations and boundary conditions in dimensionless form. We list the characteristic quantities and then motivate their choice.

Characteristic length in x-direction: $L = W_0 = W(0)$, initial half-width of the thin film.

Characteristic length in z-direction: $H = h(0,0)$, initial height of the thin film at the center of film.

Characteristic velocity in the x-direction:

$$U = \frac{g\,H^3}{\nu\,W_0}.$$

Characteristic velocity in the z-direction:

$$\frac{H\,U}{W_0} = \frac{g\,H^4}{\nu\,W_0^2}.$$

Characteristic pressure: $P = \rho\,g\,H$.

Characteristic time:

$$T = \frac{W_0}{U} = \frac{\nu\,W_0^2}{g\,H^3}.$$

Justification of the characteristic quantities:

To obtain U we use the two expressions for the characteristic pressure P and equate them. From Chapter 2, the first expression is

$$P = \mu\,\frac{L}{H^2}\,U = \mu\,\frac{W_0}{H^2}\,U. \tag{3.2.18}$$

To obtain the second expression, $P = \rho\,g\,H$ for the characteristic pressure P, we balance the pressure gradient force per unit volume in the z-direction with the force of gravity per unit volume in the z-direction:

$$\frac{\partial p}{\partial z} \sim \rho\,F_z, \tag{3.2.19}$$

therefore

$$\frac{P}{H} = \rho\,g, \tag{3.2.20}$$

thus resulting in

$$P = \rho\,g\,H. \tag{3.2.21}$$

Equating (3.2.18) and (3.2.21) gives

$$U = \frac{g\,H^3}{\nu\,W_0}, \tag{3.2.22}$$

where the kinematic viscosity $\nu = \mu/\rho$.

We define the following dimensionless variables:

$$\overline{x} = \frac{x}{W_0}, \qquad \overline{z} = \frac{z}{H}, \qquad \overline{v}_x = \frac{v_x}{U}, \qquad \overline{v}_z = \frac{W_0\, v_z}{H\, U}, \tag{3.2.23}$$

$$\overline{v}_n = \frac{W_0\, v_n}{H\, U}, \qquad \overline{t} = \frac{t}{T}, \qquad \overline{h} = \frac{h}{H}, \qquad \overline{p} = \frac{p}{P}, \qquad \overline{\tau}_{ik} = \frac{\tau_{ik}}{P}. \tag{3.2.24}$$

Expressed in dimensionless form equations (3.2.5)-(3.2.7) become

$$\frac{\partial \overline{p}}{\partial \overline{x}} = \frac{\partial^2 \overline{v}_x}{\partial \overline{z}^2}, \tag{3.2.25}$$

$$\frac{\partial \overline{p}}{\partial \overline{z}} = -1, \tag{3.2.26}$$

$$\frac{\partial \overline{v}_x}{\partial \overline{x}} + \frac{\partial \overline{v}_z}{\partial \overline{z}} = 0. \tag{3.2.27}$$

The boundary conditions are:

$$\overline{z} = 0: \qquad \overline{v}_x(\overline{t}, \overline{x}, 0) = 0, \tag{3.2.28}$$

$$\overline{z} = 0: \qquad \overline{v}_z(\overline{t}, \overline{x}, 0) = \overline{v}_n(\overline{t}, \overline{x}), \tag{3.2.29}$$

$$\overline{z} = \overline{h}(\overline{t}, \overline{x}): \qquad \overline{p}(\overline{t}, \overline{x}, \overline{h}) = \overline{p}_0, \tag{3.2.30}$$

$$\overline{z} = \overline{h}(\overline{t}, \overline{x}): \qquad \overline{\tau}_{zx}(\overline{t}, \overline{x}, \overline{h}) = \frac{H}{W_0}\frac{\partial \overline{v}_x}{\partial \overline{z}}(\overline{t}, \overline{x}, \overline{h}) = 0, \tag{3.2.31}$$

$$\bar{z} = \bar{h}(\bar{t}, \overline{x}): \qquad \frac{\partial \bar{h}}{\partial \bar{t}} + \overline{v}_x(\overline{t}, \overline{x}, \overline{h})\,\frac{\partial \bar{h}}{\partial \overline{x}} = \overline{v}_z(\overline{t}, \overline{x}, \overline{h}). \tag{3.2.32}$$

Initial conditions:

Since

$$\overline{W}(t) = \frac{W(t)}{W(0)}, \tag{3.2.33}$$

it follows that

$$\overline{W}(0) = \frac{W(0)}{W(0)} = 1. \tag{3.2.34}$$

The overhead bars will be suppressed from equations (3.2.25)-(3.2.34).

3.2.1 Partial differential equation for $h(t, x)$

We first obtain $v_z(t, x, h)$. We integrate the continuity equation (3.2.27) with respect to z from $z = 0$ to $z = h(t, x)$:

$$\int_0^{h(t,x)} \frac{\partial v_z}{\partial z}\, dz = -\int_0^{h(t,x)} \frac{\partial v_x}{\partial x}(t,x,z)\, dz. \tag{3.2.35}$$

However

$$\int_0^{h(t,x)} \frac{\partial v_z}{\partial z}\, dz = [v_z(t,x,z)]_0^{h(t,x)} = v_z(t,x,h) - v_z(t,x,0), \tag{3.2.36}$$

resulting in

$$v_z(t,x,h) - v_z(t,x,0) = -\int_0^{h(t,x)} \frac{\partial v_x(t,x,z)}{\partial x}\, dz. \tag{3.2.37}$$

Using the boundary condition on v_z, (3.2.29), equation (3.2.37) becomes

$$v_z(t,x,h) = v_n(t,x) - \int_0^{h(t,x)} \frac{\partial v_x(t,x,z)}{\partial x}\, dz. \tag{3.2.38}$$

In order to take the derivative outside the integral sign in (3.2.38), we apply Leibniz's rule [10]

$$\frac{d}{dx}\int_{\phi_1(x)}^{\phi_2(x)} f(x,z)\, dz = \int_{\phi_1(x)}^{\phi_2(x)} \frac{\partial f(x,z)}{\partial x}\, dz + f(x,\phi_2(x))\,\phi_2'(x) - f(x,\phi_1(x))\,\phi_1'(x). \tag{3.2.39}$$

Hence we obtain

$$\frac{\partial}{\partial x}\int_0^{h(t,x)} v_x(t,x,z)\, dz = \int_0^{h(t,x)} \frac{\partial v_x(t,x,z)}{\partial x}\, dz + v_x(t,x,h)\,\frac{\partial h}{\partial x}, \tag{3.2.40}$$

and therefore

$$\int_0^{h(t,x)} \frac{\partial v_x(t,x,z)}{\partial x}\, dz = \frac{\partial}{\partial x}\int_0^{h(t,x)} v_x(t,x,z)\, dz - v_x(t,x,h)\,\frac{\partial h}{\partial x}(t,x). \tag{3.2.41}$$

Substituting (3.2.41) into (3.2.38) results in the required expression for $v_z(t,x,h)$:

$$v_z(t,x,h) = v_n(t,x) + v_x(t,x,h)\,\frac{\partial h}{\partial x} - \frac{\partial}{\partial x}\int_0^{h(t,x)} v_x(t,x,z)\, dz. \tag{3.2.42}$$

Substituting (3.2.42) into the boundary condition (3.2.32) results in

$$\frac{\partial h}{\partial t} + \frac{\partial}{\partial x}\int_0^{h(t,x)} v_x(t,x,z)\, dz = v_n(t,x). \tag{3.2.43}$$

Equation (3.2.43) does not depend $v_z(t,x,h)$ which now does not need to be calculated. The left hand side of (3.2.43) is in conserved form. The right hand side of (3.2.43) is in the form of a source term.

We next calculate $v_x(t,x,h)$. To do this $p\,(t,x,h)$ is first obtained by integrating equation (3.2.26) and applying boundary condition (3.2.30):

$$p\,(t,x,z) = -z + p_0 + h(t,x). \tag{3.2.44}$$

Substituting (3.2.44) into (3.2.25) and integrating twice with respect to z results in

$$v_x(t,x,z) = \frac{z^2}{2}\,\frac{\partial h}{\partial x}(t,x) + z\;B(t,x) + C(t,x), \tag{3.2.45}$$

where $B(t,x)$ and $C(t,x)$ are functions of integration. By applying boundary conditions (3.2.28) and (3.2.31), one can solve for the functions of integration and the resulting expression for $v_x(t,x,z)$ is

$$v_x(t,x,z) = \left(\frac{z^2}{2} - z\;h(t,x)\right)\,\frac{\partial h}{\partial x}(t,x). \tag{3.2.46}$$

In order to evaluate (3.2.43), consider

$$\begin{aligned}
\int_0^{h(t,x)} v_x(t,x,z)\;dz &= \frac{\partial h}{\partial x}(t,x)\int_0^{h(t,x)}\left(\frac{z^2}{2} - z\;h(t,x)\right)\;dz, && (3.2.47)\\
&= \frac{\partial h}{\partial x}(t,x)\;\left[\frac{z^3}{6} - \frac{z^2}{2}\;h\right]_0^h, && (3.2.48)\\
&= -\frac{1}{3}\,h^3\,\frac{\partial h}{\partial x}. && (3.2.49)
\end{aligned}$$

Substituting (3.2.49) into (3.2.43) gives the required partial differential equation for $h(t,x)$,

$$\frac{\partial h}{\partial t} = \frac{1}{3}\,\frac{\partial}{\partial x}\,\left(h^3\,\frac{\partial h}{\partial x}\right) + v_n(t,x). \tag{3.2.50}$$

3.3 Total volume of thin film per unit length in y-direction

The total volume does not remain constant because fluid is extracted or injected into the thin film. We use dimensional quantities and then make the equation dimensionless at the end. Let $V(t)$ be the total volume of fluid film per unit length in the y-direction at time t. The half-width of the base at time t is $W(t)$. The volume element with base of width $\delta\, x$ at distance x, per unit length in the y-direction, is

$$\delta\, V = \delta x.1.h(t,x). \tag{3.3.1}$$

Hence

$$V(t) = \int_{-W(t)}^{W(t)} h(t,x)\; dx = 2\int_{0}^{W(t)} h(t,x)\; dx, \tag{3.3.2}$$

where we have used $h(t,x) = h(t,-x)$.

Consider now the rate of change of volume as given in Figure 3.3.

Volume of fluid which flows into base area, width $\delta\, x$, unit length in the y-direction in time $\delta\, t$ is

$$\delta\, x.\, 1.\, v_n(t,x)\; \delta\; t. \tag{3.3.3}$$

Let $\delta\; V$ be the increase in total volume of thin film of unit width in the y-direction in time $\delta\; t$. Then letting $\delta\, x \to 0$,

$$\delta\; V = \delta\; t \int_{-W(t)}^{W(t)} v_n(t,x)\; dx, \tag{3.3.4}$$

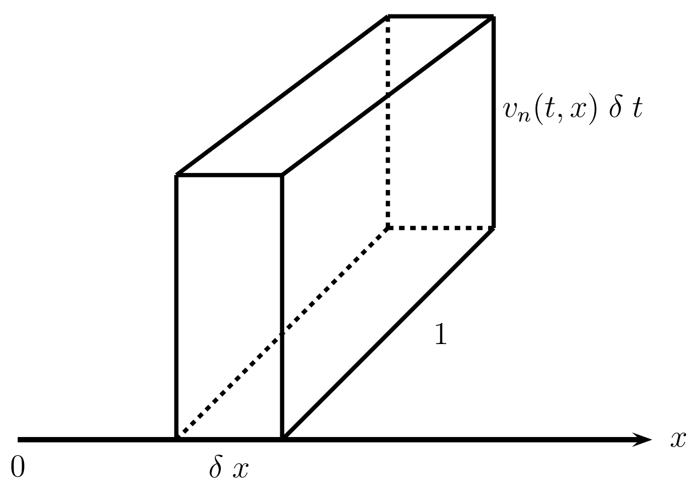

Figure 3.3: Rate of change of volume

and therefore

$$\frac{\delta V}{\delta t} = \int_{-W(t)}^{W(t)} v_n(t,x)\, dx. \tag{3.3.5}$$

Let $\delta t \to 0$,

$$\frac{d V}{d t} = \int_{-W(t)}^{W(t)} v_n(t,x)\, dx. \tag{3.3.6}$$

But we assume that $v_n(t,x) = v_n(t,-x)$, hence

$$\frac{d V}{d t} = 2 \int_{0}^{W(t)} v_n(t,x)\, dx. \tag{3.3.7}$$

We make (3.3.2) and (3.3.7) dimensionless using the following dimensionless variables

$$\overline{V} = \frac{V}{W_0\, H}, \quad \overline{W}(t) = \frac{W(t)}{W_0}, \quad \overline{v}_n = \frac{W_0}{H}\,\frac{v_n}{U}, \quad \overline{t} = \frac{U}{W_0}\, t, \quad \overline{x} = \frac{x}{W_0}. \tag{3.3.8}$$

The motivation for the definition of the characteristic volume being $W_0\ H$ is that the characteristic volume is defined in terms of its characteristic lengths. In non-dimensional form equations (3.3.2) and (3.3.7) are

$$\overline{V}(\overline{t}) = 2 \int_0^{\overline{W}(t)} \overline{h}(\overline{t},\overline{x})\, d\overline{x}, \tag{3.3.9}$$

$$\frac{d\,\overline{V}}{d\,\overline{t}} = 2 \int_0^{\overline{W}(t)} \overline{v}_n(\overline{t},\overline{x})\, d\overline{x}. \tag{3.3.10}$$

We suppress the overhead bars.

3.4 Summary of the mathematical model

A summary of the model that we are solving is presented below: Solve the nonlinear diffusion equation

$$\frac{\partial h}{\partial t} = \frac{1}{3}\,\frac{\partial}{\partial x}\left(h^3\,\frac{\partial h}{\partial x}\right) + v_n(t,x), \tag{3.4.1}$$

subject to the conditions

$$h(t, \pm W(t)) = 0, \tag{3.4.2}$$

$$W(0) = 1, \tag{3.4.3}$$

$$\frac{d\,V}{d\,t} = 2 \int_0^{W(t)} v_n(t,x)\; dx, \tag{3.4.4}$$

where

$$V(t) = 2 \int_0^{W(t)} h(t,x)\; dx. \tag{3.4.5}$$

The blowing/suction velocity, $v_n(t,x)$, is not yet specified. It is chosen later to give a group invariant solution.

3.5 Conclusions

The problem of spreading of a thin two-dimensional film of fluid with suction or blowing at the base has been reduced to the solution of a nonlinear diffusion equation with an unspecified source term. Lie group analysis will be applied in the next chapter to investigate solutions for the height of the thin film and the fluid injection velocity at the base.

Chapter 4

Lie group analysis of two-dimensional thin film

4.1 Introduction

In this chapter we derive the Lie point symmetries for the partial differential equation (3.4.1) obtained in Section 3.2 for the height $h(t,x)$ and the blowing/suction velocity, $v_n(t,x)$, using the techniques discussed in Section 2.3.1. By taking a linear combination of the Lie point symmetries we derive a group invariant solution that reduces the partial differential equation to an ordinary differential equation using the techniques described in Section 2.3.2. We make use of Lie group analysis to derive a first order linear partial differential equation satisfied by $v_n(t,x)$.

4.2 Lie point symmetries

The partial differential equation (3.4.1) is

$$\frac{\partial h}{\partial t} = \frac{1}{3}\frac{\partial}{\partial x}\left(h^3\frac{\partial h}{\partial x}\right) + v_n(t,x), \tag{4.2.1}$$

$$= h^2\left(\frac{\partial h}{\partial x}\right)^2 + \frac{1}{3}h^3\frac{\partial^2 h}{\partial x^2} + v_n(t,x). \tag{4.2.2}$$

It can be written as

$$F(t, x, h, h_t, h_x, h_{xx}) = 0, \tag{4.2.3}$$

where

$$F = h_t - h^2\, h_x^2 - \frac{1}{3}\, h^3\, h_{xx} - v_n(t, x). \tag{4.2.4}$$

The Lie point symmetry generators are of the form given by equation (2.3.2) and obtained by solving the determining equation (2.3.5). The second prolongation $X^{[2]}$ of the generator X is defined by

$$\begin{aligned} X^{[2]} &= \xi^1(t, x, h)\,\frac{\partial}{\partial t} + \xi^2(t, x, h)\,\frac{\partial}{\partial x} + \eta(t, x, h)\,\frac{\partial}{\partial h} + \zeta_1\,\frac{\partial}{\partial h_t} + \zeta_2\,\frac{\partial}{\partial h_x} \\ &+ \zeta_{11}\,\frac{\partial}{\partial h_{tt}} + \zeta_{12}\,\frac{\partial}{\partial h_{tx}} + \zeta_{22}\,\frac{\partial}{\partial h_{xx}}. \end{aligned} \tag{4.2.5}$$

We have to evaluate the determining equation (2.3.5) where F is given in (4.2.4) [16]. Now

$$\begin{aligned} X^{[2]}F = \xi^1\left(-\frac{\partial v_n}{\partial t}\right) + \xi^2\left(-\frac{\partial v_n}{\partial x}\right) + \eta\left(-2hh_x^2 - h^2 h_{xx}\right) + \zeta_1 \\ + \zeta_2(-2h^2 h_x) + \zeta_{22}\left(-\frac{1}{3}h^3\right) = 0. \end{aligned} \tag{4.2.6}$$

We need evaluate only ζ_1, ζ_2 and ζ_{22} because the partial differential equation is independent of h_{tt} and h_{tx}. Expansions for $\zeta_1 = \zeta_t, \zeta_2 = \zeta_x$ and $\zeta_{22} = \zeta_{xx}$ are required:

$$\zeta_t = \frac{\partial \eta}{\partial t} + \left(\frac{\partial \eta}{\partial h} - \frac{\partial \xi^1}{\partial t}\right) h_t - \frac{\partial \xi^2}{\partial t}\, h_x - \frac{\partial \xi^1}{\partial h}\, h_t^2 - \frac{\partial \xi^2}{\partial h}\, h_x\, h_t, \tag{4.2.7}$$

$$\zeta_x = \frac{\partial \eta}{\partial x} + \left(\frac{\partial \eta}{\partial h} - \frac{\partial \xi^2}{\partial x}\right) h_x - \frac{\partial \xi^1}{\partial x}\, h_t - \frac{\partial \xi^2}{\partial h}\, h_x^2 - \frac{\partial \xi^1}{\partial h}\, h_t\, h_x, \tag{4.2.8}$$

$$\begin{aligned} \zeta_{xx} &= \frac{\partial^2 \eta}{\partial x^2} + \left(2\,\frac{\partial^2 \eta}{\partial x \partial h} - \frac{\partial^2 \xi^2}{\partial x^2}\right) h_x - \frac{\partial^2 \xi^1}{\partial x^2}\, h_t + \left(\frac{\partial \eta}{\partial h} - 2\,\frac{\partial \xi^2}{\partial x}\right) h_{xx} \\ &- 2\frac{\partial^2 \xi^1}{\partial x \partial h}\, h_x\, h_t - \frac{\partial^2 \xi^2}{\partial h^2}\, h_x^3 - \frac{\partial^2 \xi^1}{\partial h^2}\, h_t\, h_x^2 - 3\frac{\partial \xi^2}{\partial h}\, h_x\, h_{xx} \\ &- 2\,\frac{\partial \xi^1}{\partial x}\, h_{xt} + \left(\frac{\partial^2 \eta}{\partial h^2} - 2\frac{\partial^2 \xi^2}{\partial h \partial x}\right) h_x^2 - \frac{\partial \xi^1}{\partial h}\, h_t\, h_{xx} \\ &- 2\,\frac{\partial \xi^1}{\partial h}\, h_x\, h_{xt}. \end{aligned} \tag{4.2.9}$$

Using expansions (4.2.7), (4.2.8) and (4.2.9) equation (4.2.6) becomes

$$
\begin{aligned}
X^{[2]}F \;=\;& -\xi^1\frac{\partial v_n}{\partial t}-\xi^2\frac{\partial v_n}{\partial x}+\eta\left(-2hh_x^2-h^2h_{xx}\right)+\frac{\partial \eta}{\partial t}+\left(\frac{\partial \eta}{\partial h}-\frac{\partial \xi^1}{\partial t}\right)h_t\\
-\;& \frac{\partial \xi^2}{\partial t}\,h_x-\frac{\partial \xi^1}{\partial h}\,h_t^2-\frac{\partial \xi^2}{\partial h}\,h_x\,h_t-2\frac{\partial \eta}{\partial x}\,h^2\,h_x-2\left(\frac{\partial \eta}{\partial h}-\frac{\partial \xi^2}{\partial x}\right)h^2\,h_x^2\\
+\;& 2\frac{\partial \xi^1}{\partial x}\,h^2\,h_x\,h_t+2\frac{\partial \xi^2}{\partial h}\,h^2\,h_x^3+2\frac{\partial \xi^1}{\partial h}\,h^2\,h_t\,h_x^2-\frac{1}{3}\frac{\partial^2\eta}{\partial x^2}\,h^3\\
-\;& \frac{1}{3}\left(2\,\frac{\partial^2\eta}{\partial x\partial h}-\frac{\partial^2\xi^2}{\partial x^2}\right)h^3\,h_x+\frac{1}{3}\frac{\partial^2\xi^1}{\partial x^2}\,h^3\,h_t-\frac{1}{3}\left(\frac{\partial \eta}{\partial h}-2\,\frac{\partial \xi^2}{\partial x}\right)h^3\,h_{xx}\\
+\;& \frac{2}{3}\frac{\partial^2\xi^1}{\partial x\partial h}\,h^3\,h_x\,h_t+\frac{1}{3}\frac{\partial^2\xi^2}{\partial h^2}\,h^3\,h_x^3+\frac{1}{3}\frac{\partial^2\xi^1}{\partial h^2}\,h^3\,h_t\,h_x^2\\
+\;& \frac{\partial \xi^2}{\partial h}\,h^3\,h_x\,h_{xx}+\frac{2}{3}\frac{\partial \xi^1}{\partial x}\,h^3\,h_{xt}-\frac{1}{3}\left(\frac{\partial^2\eta}{\partial h^2}-2\frac{\partial^2\xi^2}{\partial h\partial x}\right)h^3\,h_x^2\\
+\;& \frac{1}{3}\frac{\partial \xi^1}{\partial h}\,h^3\,h_t\,h_{xx}+\frac{2}{3}\frac{\partial \xi^1}{\partial h}\,h^3\,h_x\,h_{xt}=0.
\end{aligned}
\tag{4.2.10}
$$

Since we require (4.2.10) to be evaluated at $F=0$, we substitute

$$
h_t=h^2\,h_x^2+\frac{1}{3}\,h^3\,h_{xx}+v_n(t,x) \tag{4.2.11}
$$

in equation (4.2.10):

$$
\begin{aligned}
& X^{[2]}F|_{F=0} \qquad\qquad (4.2.12)\\
=\;& -\xi^1\frac{\partial v_n}{\partial t}-\xi^2\frac{\partial v_n}{\partial x}+\eta\left(-2hh_x^2-h^2h_{xx}\right)+\frac{\partial \eta}{\partial t}\\
+\;& \left(\frac{\partial \eta}{\partial h}-\frac{\partial \xi^1}{\partial t}\right)\left(h^2\,h_x^2+\frac{1}{3}\,h^3\,h_{xx}+v_n(t,x)\right)-\frac{\partial \xi^2}{\partial t}\,h_x\\
-\;& \frac{\partial \xi^1}{\partial h}\left(h^2\,h_x^2+\frac{1}{3}\,h^3\,h_{xx}+v_n(t,x)\right)^2-\frac{\partial \xi^2}{\partial h}\,h_x\left(h^2\,h_x^2+\frac{1}{3}\,h^3\,h_{xx}+v_n(t,x)\right)\\
-\;& 2\frac{\partial \eta}{\partial x}h^2\,h_x-2\left(\frac{\partial \eta}{\partial h}-\frac{\partial \xi^2}{\partial x}\right)h^2\,h_x^2+2\frac{\partial \xi^1}{\partial x}\,h^2\,h_x\left(h^2\,h_x^2+\frac{1}{3}\,h^3\,h_{xx}+v_n(t,x)\right)\\
+\;& 2\frac{\partial \xi^2}{\partial h}\,h^2\,h_x^3+2\frac{\partial \xi^1}{\partial h}h^2h_x^2\left(h^2\,h_x^2+\frac{1}{3}\,h^3\,h_{xx}+v_n(t,x)\right)-\frac{1}{3}\frac{\partial^2\eta}{\partial x^2}\,h^3\\
-\;& \frac{1}{3}\left(2\,\frac{\partial^2\eta}{\partial x\partial h}-\frac{\partial^2\xi^2}{\partial x^2}\right)h^3\,h_x+\frac{1}{3}\left(\frac{\partial^2\xi^1}{\partial x^2}\right)h^3\left(h^2\,h_x^2+\frac{1}{3}\,h^3\,h_{xx}+v_n(t,x)\right)\\
-\;& \frac{1}{3}\left(\frac{\partial \eta}{\partial h}-2\,\frac{\partial \xi^2}{\partial x}\right)h^3\,h_{xx}+\frac{2}{3}\left(\frac{\partial^2\xi^1}{\partial x\partial h}\right)h^3\,h_x\left(h^2\,h_x^2+\frac{1}{3}\,h^3\,h_{xx}+v_n(t,x)\right)\\
+\;& \frac{1}{3}\frac{\partial^2\xi^2}{\partial h^2}\,h^3\,h_x^3+\frac{1}{3}\frac{\partial^2\xi^1}{\partial h^2}\,h^3\,h_x^2\left(h^2\,h_x^2+\frac{1}{3}\,h^3\,h_{xx}+v_n(t,x)\right)
\end{aligned}
$$

$$
\begin{aligned}
&+ \quad \frac{\partial \xi^2}{\partial h} h^3 h_x h_{xx} + \frac{2}{3}\frac{\partial \xi^1}{\partial x} h^3 h_{xt} - \frac{1}{3}\left(\frac{\partial^2 \eta}{\partial h^2} - 2\frac{\partial^2 \xi^2}{\partial h \partial x}\right) h^3 h_x^2 \\
&+ \quad \frac{1}{3}\frac{\partial \xi^1}{\partial h} h^3 h_{xx}\left(h^2 h_x^2 + \frac{1}{3} h^3 h_{xx} + v_n(t,x)\right) + \frac{2}{3}\frac{\partial \xi^1}{\partial h} h^3 h_x h_{xt} = 0. \qquad (4.2.13)
\end{aligned}
$$

Since ξ^1, ξ^2 and η do not depend on the derivatives on h, we may separate (4.2.13) by the coefficients of these derivatives.

$$
\begin{aligned}
h_x h_{xt}: &\qquad \frac{\partial \xi^1}{\partial h} = 0, && (4.2.14)\\
h_{xt}: &\qquad \frac{\partial \xi^1}{\partial x} = 0, && (4.2.15)\\
h_x h_{xx}: &\qquad \frac{\partial \xi^2}{\partial h} + h^2\frac{\partial \xi^1}{\partial x} + \frac{1}{3}h^3\frac{\partial^2 \xi^1}{\partial x \partial h} = 0, && (4.2.16)\\
h_x^2 h_{xx}: &\qquad h\frac{\partial^2 \xi^1}{\partial h^2} + 3\frac{\partial \xi^1}{\partial h} = 0, && (4.2.17)
\end{aligned}
$$

$$
\begin{aligned}
h_{xx}: &\qquad -\eta + \frac{1}{3}h\left(\frac{\partial \eta}{\partial h} - \frac{\partial \xi^1}{\partial t}\right) - \frac{2}{3}v_n h\frac{\partial \xi^1}{\partial h} - \frac{1}{3}h\left(\frac{\partial \eta}{\partial h} - 2\frac{\partial \xi^2}{\partial x}\right)\\
&\qquad +\frac{1}{9}h^4\frac{\partial^2 \xi^1}{\partial x^2} + \frac{1}{3}v_n h\frac{\partial \xi^1}{\partial h} = 0, && (4.2.18)\\
h_x^2: &\qquad -2\eta + h\left(\frac{\partial \eta}{\partial h} - \frac{\partial \xi^1}{\partial t}\right) - 2v_n h\frac{\partial \xi^1}{\partial h} - 2h\left(\frac{\partial \eta}{\partial h} - \frac{\partial \xi^2}{\partial x}\right)\\
&\qquad +2v_n h\frac{\partial \xi^1}{\partial h} + \frac{1}{3}h^4\frac{\partial^2 \xi^1}{\partial x^2} + \frac{1}{3}v_n h^2\frac{\partial^2 \xi^1}{\partial h^2} - \frac{1}{3}h^2\left(\frac{\partial^2 \eta}{\partial h^2} - 2\frac{\partial^2 \xi^2}{\partial h \partial x}\right)\\
&\qquad =0, && (4.2.19)\\
h_x^3: &\qquad \frac{\partial \xi^2}{\partial h} + 2h^2\frac{\partial \xi^1}{\partial x} + \frac{2}{3}h^3\frac{\partial^2 \xi^1}{\partial x \partial h} + \frac{1}{3}h\frac{\partial^2 \xi^2}{\partial h^2} = 0, && (4.2.20)\\
h_x^4: &\qquad \frac{\partial \xi^1}{\partial h} + \frac{1}{3}h\frac{\partial^2 \xi^1}{\partial h^2} = 0, && (4.2.21)\\
h_x: &\qquad -\frac{\partial \xi^2}{\partial t} - v_n\frac{\partial \xi^2}{\partial h} - 2h^2\frac{\partial \eta}{\partial x} + 2v_n h^2\frac{\partial \xi^1}{\partial x} - \frac{1}{3}h^3\left(2\frac{\partial^2 \eta}{\partial x \partial h} - \frac{\partial^2 \xi^2}{\partial x^2}\right)\\
&\qquad +\frac{2}{3}v_n h^3\frac{\partial^2 \xi^1}{\partial x \partial h} = 0, && (4.2.22)
\end{aligned}
$$

remainder:

$$
\begin{aligned}
&- \xi^1\frac{\partial v_n}{\partial t} - \xi^2\frac{\partial v_n}{\partial x} + \frac{\partial \eta}{\partial t} + v_n\left(\frac{\partial \eta}{\partial h} - \frac{\partial \xi^1}{\partial t}\right) - v_n^2\frac{\partial \xi^1}{\partial h}\\
&-\frac{1}{3}h^3\frac{\partial^2 \eta}{\partial x^2} + \frac{1}{3}v_n h^3\frac{\partial^2 \xi^1}{\partial x^2} = 0. \qquad (4.2.23)
\end{aligned}
$$

Equations (4.2.14) and (4.2.15) for the partial derivatives of ξ^1 with respect to x and h give

$$\xi^1 = \xi^1(t). \tag{4.2.24}$$

Substituting (4.2.24) into (4.2.16) gives

$$\xi^2 = \xi^2(t, x). \tag{4.2.25}$$

Using (4.2.24) and (4.2.25), equations (4.2.17), (4.2.20) and (4.2.21) are identically satisfied while equations (4.2.18), (4.2.19), (4.2.22) and (4.2.23) simplify to the following

$$h_{xx}: \qquad -\eta - \frac{1}{3}h\frac{d\xi^1}{dt} + \frac{2}{3}h\frac{\partial \xi^2}{\partial x} = 0, \tag{4.2.26}$$

$$h_x^2: \qquad 2\eta + h\frac{\partial \eta}{\partial h} + h\frac{d\xi^1}{dt} + \frac{1}{3}h^2\frac{\partial^2 \eta}{\partial h^2} = 0, \tag{4.2.27}$$

$$h_x: \qquad -\frac{\partial \xi^2}{\partial t} - 2h^2\frac{\partial \eta}{\partial x} - \frac{2}{3}h^3\frac{\partial^2 \eta}{\partial x \partial h} + \frac{1}{3}h^3\frac{\partial^2 \xi^2}{\partial x^2} = 0, \tag{4.2.28}$$

remainder:

$$-\xi^1\frac{\partial v_n}{\partial t} - \xi^2\frac{\partial v_n}{\partial x} + \frac{\partial \eta}{\partial t} + v_n\left(\frac{\partial \eta}{\partial h} - \frac{d\xi^1}{dt}\right) - \frac{1}{3}h^3\frac{\partial^2 \eta}{\partial x^2} = 0. \tag{4.2.29}$$

From (4.2.26)

$$\eta = \frac{1}{3}h\left(2\frac{\partial \xi^2}{\partial x} - \frac{d\xi^1}{dt}\right). \tag{4.2.30}$$

Calculating ${}^{\partial\eta}/_{\partial h}$ and ${}^{\partial^2\eta}/_{\partial h^2}$ and substituting in (4.2.27) results in (4.2.27) being identically satisfied while calculating ${}^{\partial\eta}/_{\partial x}$ and ${}^{\partial^2\eta}/_{\partial x\partial h}$ and substituting in (4.2.28) gives

$$\frac{\partial \xi^2}{\partial t} + \frac{13}{9}h^3\frac{\partial^2 \xi^2}{\partial x^2} = 0. \tag{4.2.31}$$

Since ξ^2 is independent of h from (4.2.25), we may separate (4.2.31) by powers of h thus giving

$$h^0 \quad : \qquad \frac{\partial \xi^2}{\partial t} = 0, \tag{4.2.32}$$

$$h^3 \quad : \qquad \frac{\partial^2 \xi^2}{\partial x^2} = 0. \tag{4.2.33}$$

Equation (4.2.32) tells us that ξ^2 is independent of t and integrating (4.2.33) twice with respect x gives

$$\xi^2 = b_1\, x + b_2, \tag{4.2.34}$$

where b_1 and b_2 are arbitrary constants. With (4.2.34) for ξ^2, equation (4.2.30) for η reduces to

$$\eta = \frac{1}{3} h \left(2\, b_1 - \frac{d\xi^1}{dt} \right). \tag{4.2.35}$$

Substituting (4.2.34) and (4.2.35) into (4.2.29) gives

$$-\xi^1 \frac{\partial v_n}{\partial t} - (b_1\, x + b_2)\, \frac{\partial v_n}{\partial x} - \frac{1}{3} h \frac{d^2\xi^1}{dt^2} + \frac{1}{3} v_n \left(2\, b_1 - \frac{d\xi^1}{dt} \right) - v_n \frac{d\xi^1}{dt} = 0. \tag{4.2.36}$$

Since ξ^1 is independent of h, separating (4.2.36) by powers of h we obtain

$$h^0 \quad : \qquad \frac{d^2\xi^1}{dt^2} = 0, \tag{4.2.37}$$

$$h \quad : \qquad -\xi^1 \frac{\partial v_n}{\partial t} - (b_1\, x + b_2)\, \frac{\partial v_n}{\partial x} - \frac{4}{3} v_n \frac{d\xi^1}{dt} + \frac{2}{3}\, v_n\, b_1 = 0. \tag{4.2.38}$$

Integrating (4.2.37) twice with respect to t gives

$$\xi^1 = b_3\, t + b_4, \tag{4.2.39}$$

where b_3 and b_4 are arbitrary constants and substituting (4.2.39) into (4.2.35) gives

$$\eta = \frac{1}{3} h \left(2b_1 - b_3 \right). \tag{4.2.40}$$

We rename the constants as

$$b_1 \to c_3, \qquad b_2 \to c_4, \qquad b_3 \to c_2, \qquad b_4 \to c_1, \tag{4.2.41}$$

$$\xi^1(t) = c_1 + c_2\, t, \qquad \xi^2(x) = c_4 + c_3\, x, \qquad \eta(h) = \frac{1}{3} h (2c_3 - c_2). \tag{4.2.42}$$

The Lie point symmetry generators are of the form

$$X = (c_1 + c_2\, t) \frac{\partial}{\partial t} + (c_4 + c_3\, x) \frac{\partial}{\partial x} + \frac{1}{3} h \left(2c_3 - c_2 \right) \frac{\partial}{\partial h}, \tag{4.2.43}$$

$$= c_1\, X_1 + c_2\, X_2 + c_3\, X_3 + c_4\, X_4. \tag{4.2.44}$$

where

$$X_1 = \frac{\partial}{\partial t}, \tag{4.2.45}$$
$$X_2 = t\frac{\partial}{\partial t} - \frac{1}{3}h\frac{\partial}{\partial h}, \tag{4.2.46}$$
$$X_3 = x\frac{\partial}{\partial x} + \frac{2}{3}h\frac{\partial}{\partial h}, \tag{4.2.47}$$
$$X_4 = \frac{\partial}{\partial x}. \tag{4.2.48}$$

The velocity $v_n(t,x)$ cannot be arbitrary for Lie point symmetries to exist. It must satisfy the first order linear partial differential equation (4.2.38),

$$(c_1 + c_2\, t)\frac{\partial v_n}{\partial t} + (c_4 + c_3\, x)\,\frac{\partial v_n}{\partial x} = \frac{2}{3}(c_3 - 2c_2)v_n. \tag{4.2.49}$$

We do not consider the case where the constants are linearly dependent in (4.2.49) as these could lead to special cases. We focus on the general solution where the constants are linearly independent.

4.3 Group invariant solution

Using the method explained in Section 2.3.2 one may obtain the group invariant solution. Now $h = \Phi(t,x)$ is a group invariant solution of the partial differential equation (4.2.1) provided

$$\left((c_1 + c_2 t)\frac{\partial}{\partial t} + (c_4 + c_3 x)\frac{\partial}{\partial x} + \frac{1}{3}h\,(2c_3 - c_2)\,\frac{\partial}{\partial h}\right)(h - \Phi(t,x))|_{h=\Phi} = 0. \tag{4.3.1}$$

Consequently, $\Phi(t,x)$ satisfies the first order linear partial differential equation

$$(c_1 + c_2\, t)\frac{\partial \Phi}{\partial t} + (c_4 + c_3\, x)\frac{\partial \Phi}{\partial x} = \frac{1}{3}\,(2c_3 - c_2)\,\Phi. \tag{4.3.2}$$

Equation (4.3.2) may be solved by the method of characteristics. We consider the general case in which $c_2 \neq 0, c_3 \neq 0$ and $c_2 \neq 2c_3$. The differential equations of the characteristic curves of (4.3.2) are

$$\frac{dt}{(c_1 + c_2 t)} = \frac{dx}{(c_4 + c_3 x)} = \frac{3}{(2c_3 - c_2)}\frac{d\Phi}{\Phi}. \tag{4.3.3}$$

The first pair gives

$$\frac{dt}{(c_1 + c_2 t)} = \frac{dx}{(c_4 + c_3 x)}, \tag{4.3.4}$$

and therefore

$$\frac{c_4 + c_3\, x}{(c_1 + c_2 t)^{\frac{c_3}{c_2}}} = a_1, \tag{4.3.5}$$

where a_1 is a constant, whereas the first and third terms give

$$\frac{dt}{(c_1 + c_2 t)} = \frac{3}{(2c_3 - c_2)} \frac{d\Phi}{\Phi}, \tag{4.3.6}$$

thus

$$\frac{\Phi}{(c_1 + c_2\, t)^{\frac{1}{3}\left(2\frac{c_3}{c_2} - 1\right)}} = a_2, \tag{4.3.7}$$

where a_2 is a constant. Since $\Phi = h(t, x)$, the general solution is

$$h(t, x) = (c_1 + c_2\, t)^{\frac{1}{3}\left(2\frac{c_3}{c_2} - 1\right)} F(\xi), \tag{4.3.8}$$

where

$$\xi = \frac{c_4 + c_3\, x}{(c_1 + c_2 t)^{\frac{c_3}{c_2}}} \tag{4.3.9}$$

and F is an arbitrary function.

Consider equation (4.2.49) for $v_n(t, x)$. We assume further that $c_3 \neq 2c_2$. It may also be solved by the method of characteristics and the differential equations of the characteristic curves of (4.2.49) are

$$\frac{dt}{(c_1 + c_2 t)} = \frac{dx}{(c_4 + c_3 x)} = \frac{dv_n}{\frac{2}{3}(c_3 - 2c_2)\, v_n}. \tag{4.3.10}$$

The first pair is identical to (4.3.4) and gives again the result as in equation (4.3.5) whereas the first and third pair gives

$$\frac{v_n}{(c_1 + c_2\, t)^{\frac{2}{3}\left(\frac{c_3}{c_2} - 2\right)}} = a_3. \tag{4.3.11}$$

The general solution for $v_n(t, x)$ is

$$v_n(t, x) = (c_1 + c_2\, t)^{\frac{2}{3}\left(\frac{c_3}{c_2} - 2\right)} G(\xi), \tag{4.3.12}$$

where the similarity variable ξ is given in (4.3.9) and G is an arbitrary function.

4.3.1 Reduction of the nonlinear diffusion equation to an ordinary differential equation

We reduce the nonlinear diffusion equation (4.2.1) to an ordinary differential equation using the group invariant solution given by equations (4.3.8), (4.3.9) and (4.3.12). We work with ξ and t as variables and eliminate x in terms of ξ and t. With ξ defined in (4.3.9), its partial derivatives are

$$\frac{\partial \xi}{\partial t} = -\frac{c_3\,\xi}{c_1 + c_2\,t}, \qquad \frac{\partial \xi}{\partial x} = \frac{c_3}{(c_1 + c_2\,t)^{\frac{c_3}{c_2}}}. \tag{4.3.13}$$

Using (4.3.8) and (4.3.13) we obtain

$$\frac{\partial h}{\partial t} = c_3\,(c_1 + c_2\,t)^{\frac{2}{3}\left(\frac{c_3}{c_2}-2\right)} \left[\left(\frac{2}{3} - \frac{1}{3}\frac{c_2}{c_3}\right) F(\xi) - \xi \frac{dF}{d\xi}\right] \tag{4.3.14}$$

and

$$\frac{\partial}{\partial x}\left(h^3 \frac{\partial h}{\partial x}\right) = c_3^2\,(c_1 + c_2\,t)^{\frac{2}{3}\left(\frac{c_3}{c_2}-2\right)} \frac{d}{d\xi}\left(F^3 \frac{dF}{d\xi}\right). \tag{4.3.15}$$

Hence, substituting (4.3.14), (4.3.15) and (4.3.12) into (4.2.1) reduces the nonlinear diffusion equation to the ordinary differential equation (ODE)

$$c_3 \frac{d}{d\xi}\left(F^3 \frac{dF}{d\xi}\right) + 3\frac{d}{d\xi}(\xi\,F) + \left(\frac{c_2}{c_3} - 5\right) F + \frac{3}{c_3} G = 0. \tag{4.3.16}$$

The ordinary differential equation (4.3.16) does not depend on constants c_1 and c_4.

4.3.2 Boundary condition at the moving contact line

We need to write the boundary condition, (3.4.2), in terms of the similarity variable ξ defined by (4.3.9). Consider first the moving contact line $x = +W(t)$. Now

$$h(t, W(t)) = 0 \qquad \text{for all} \quad t \geq 0, \tag{4.3.17}$$

therefore using (4.3.8) for $h(t,x)$

$$F\left(\frac{c_4 + c_3\,W(t)}{(c_1 + c_2\,t)^{\frac{c_3}{c_2}}}\right) = 0. \tag{4.3.18}$$

Let

$$\frac{c_4 + c_3\, W(t)}{(c_1 + c_2\, t)^{\frac{c_3}{c_2}}} = A(t), \tag{4.3.19}$$

then

$$F(A(t)) = 0, \qquad t \geq 0. \tag{4.3.20}$$

Differentiating (4.3.20) with respect to t gives

$$\frac{dF}{dA}\frac{dA}{dt} = 0. \tag{4.3.21}$$

But F is not a constant function and therefore $\frac{dF}{dA} \neq 0$. Hence

$$\frac{dA}{dt} = 0, \tag{4.3.22}$$

and A = constant = A_0. Substituting $A(t) = A_0$ into (4.3.19) gives

$$\frac{c_4 + c_3\, W(t)}{(c_1 + c_2\, t)^{\frac{c_3}{c_2}}} = A_0. \tag{4.3.23}$$

Consider next the moving contact line $x = -W(t)$. We have that

$$h(t, -W(t)) = 0 \qquad \text{for all} \quad t \geq 0, \tag{4.3.24}$$

therefore

$$F\left(\frac{c_4 - c_3\, W(t)}{(c_1 + c_2\, t)^{\frac{c_3}{c_2}}}\right) = 0. \tag{4.3.25}$$

Let

$$\frac{c_4 - c_3\, W(t)}{(c_1 + c_2\, t)^{\frac{c_3}{c_2}}} = B(t), \tag{4.3.26}$$

then

$$F(B(t)) = 0, \qquad t \geq 0. \tag{4.3.27}$$

As before it follows that

$$B(t) = B_0, \tag{4.3.28}$$

where B_0 is a constant. Thus

$$\frac{c_4 - c_3\, W(t)}{(c_1 + c_2\, t)^{\frac{c_3}{c_2}}} = B_0. \tag{4.3.29}$$

Adding (4.3.23) and (4.3.29) gives

$$\frac{2\,c_4}{(c_1+c_2\,t)^{\frac{c_3}{c_2}}} = A_0 + B_0, \tag{4.3.30}$$

and differentiating (4.3.30) with respect to t results in

$$2\,c_4\,c_3(c_1+c_2\,t)^{-\frac{c_3}{c_2}-1} = 0. \tag{4.3.31}$$

Thus either $c_3 = 0$ or $c_4 = 0$. We do not want $c_3 = 0$ because then ξ would not depend on x. Thus $c_4 = 0$ and consequently from (4.3.30)

$$B_0 = -A_0. \tag{4.3.32}$$

Also, (4.3.23) becomes

$$\frac{c_3\,W(t)}{(c_1+c_2\,t)^{\frac{c_3}{c_2}}} = A_0 \tag{4.3.33}$$

and therefore

$$W(t) = \frac{A_0}{c_3}\,c_1^{\frac{c_3}{c_2}}\left(1+\frac{c_2}{c_1}\,t\right)^{\frac{c_3}{c_2}}. \tag{4.3.34}$$

But from the initial condition (3.4.3)

$$W(0) = 1. \tag{4.3.35}$$

Thus (4.3.34) yields

$$A_0 = c_3\,c_1^{-\frac{c_3}{c_2}}. \tag{4.3.36}$$

Substituting (4.3.36) for A_0 back into (4.3.34) gives

$$W(t) = \left(1+\frac{c_2}{c_1}\,t\right)^{\frac{c_3}{c_2}}. \tag{4.3.37}$$

From (4.3.32) and (4.3.36) the boundary conditions (4.3.20) and (4.3.27) become

$$F(A_0) = 0, \qquad\qquad F(-A_0) = 0. \tag{4.3.38}$$

$$F\left(c_3\,c_1^{-\frac{c_3}{c_2}}\right) = 0 \qquad F\left(-c_3\,c_1^{-\frac{c_3}{c_2}}\right) = 0. \tag{4.3.39}$$

Also, since $c_4 = 0$, the similarity variable ξ given by (4.3.9) can be written as

$$\xi = c_3\,c_1^{-\frac{c_3}{c_2}}\,\frac{x}{W(t)}. \tag{4.3.40}$$

where $W(t)$ is given by (4.3.37).

4.3.3 Balance law for fluid volume

The volume of the thin film per unit breadth, (3.4.5), and rate of change of volume per unit breadth, (3.4.4), are now written in terms of the similarity variable ξ. Using (4.3.40) for ξ, we have that

$$dx = \frac{W(t)}{c_3}\, c_1^{\frac{c_3}{c_2}}\, d\xi = \frac{c_1^{\frac{c_3}{c_2}}}{c_3}\left(1+\frac{c_2}{c_1}\,t\right)^{\frac{c_3}{c_2}} d\xi, \tag{4.3.41}$$

since $W(t)$ is given in (4.3.37). Substituting (4.3.8), (4.3.40) and (4.3.41) into (3.4.5), the volume becomes

$$V(t) = V_0\left(1+\frac{c_2}{c_1}\,t\right)^{\frac{5}{3}\frac{c_3}{c_2}-\frac{1}{3}}, \tag{4.3.42}$$

where

$$V_0 = \frac{2}{c_3}\, c_1^{\frac{5}{3}\frac{c_3}{c_2}-\frac{1}{3}} \int_0^{c_3\, c_1^{-\frac{c_3}{c_2}}} F(\xi)\, d\xi. \tag{4.3.43}$$

Using (4.3.12) for $v_n(t,x)$, as well as (4.3.40) and (4.3.41), the rate of change of volume (3.4.4) becomes

$$\frac{dV}{dt} = \frac{2}{c_3}\, c_1^{\frac{5}{3}\frac{c_3}{c_2}-\frac{1}{3}}\left(1+\frac{c_2}{c_1}\,t\right)^{\frac{5}{3}\frac{c_3}{c_2}-\frac{4}{3}} \int_0^{c_3\, c_1^{-\frac{c_3}{c_2}}} G(\xi)\, d\xi. \tag{4.3.44}$$

But differentiating (4.3.42) with respect to t gives

$$\frac{dV}{dt} = \left(\frac{5}{3}\frac{c_3}{c_2}-\frac{1}{3}\right)\frac{c_2}{c_1}\, V_0\left(1+\frac{c_2}{c_1}\,t\right)^{\frac{5}{3}\frac{c_3}{c_2}-\frac{1}{3}}. \tag{4.3.45}$$

Thus equating (4.3.44) and (4.3.45), where V_0 is given in (4.3.43), the balance law for fluid volume is

$$c_2\left(\frac{5}{3}\frac{c_3}{c_2}-\frac{1}{3}\right)\int_0^{c_3\, c_1^{-\frac{c_3}{c_2}}} F(\xi)\, d\xi = \int_0^{c_3\, c_1^{-\frac{c_3}{c_2}}} G(\xi)\, d\xi. \tag{4.3.46}$$

4.3.4 Change of variables

To proceed we consider a change of variables. Let

$$\xi = A\,\zeta, \qquad F(\xi) = B\, f(\zeta), \qquad G(\xi) = D\, g(\zeta). \tag{4.3.47}$$

where A, B and C are constants to be determined. Substituting (4.3.47) into (4.3.16), the ordinary differential equation becomes

$$c_3 \frac{B^3}{A^2} \frac{d}{d\zeta} \left(f^3 \frac{df}{d\zeta} \right) + 3 \frac{d}{d\zeta} (\zeta f(\zeta)) + \left(\frac{c_2}{c_3} - 5 \right) f(\zeta) + \frac{3}{c_3} \frac{D}{B} g = 0. \tag{4.3.48}$$

Using (4.3.47), the boundary conditions in (4.3.39) become

$$f\left(\frac{c_3 \, c_1^{-\frac{c_3}{c_2}}}{A} \right) = 0, \qquad f\left(\frac{-c_3 \, c_1^{-\frac{c_3}{c_2}}}{A} \right) = 0 \tag{4.3.49}$$

and the balance law (4.3.46) takes the form

$$\frac{B}{D} c_2 \left(\frac{5}{3} \frac{c_3}{c_2} - \frac{1}{3} \right) \int_0^{\frac{c_3 \, c_1^{-\frac{c_3}{c_2}}}{A}} f(\zeta) \, d\zeta = \int_0^{\frac{c_3 \, c_1^{-\frac{c_3}{c_2}}}{A}} g(\zeta) \, d\zeta. \tag{4.3.50}$$

We choose, from (4.3.48),

$$c_3 \frac{B^3}{A^2} = 1, \qquad \frac{D}{c_3 \, B} = 1, \tag{4.3.51}$$

and from (4.3.49)

$$\frac{c_3 \, c_1^{-\frac{c_3}{c_2}}}{A} = 1. \tag{4.3.52}$$

Then

$$A = c_3 \, c_1^{-\frac{c_3}{c_2}}, \tag{4.3.53}$$

$$B = \left(\frac{A^2}{c_3} \right)^{\frac{1}{3}} = c_3^{\frac{1}{3}} \, c_1^{-\frac{2}{3} \frac{c_3}{c_2}}, \tag{4.3.54}$$

$$D = c_3 \, B = c_3^{\frac{4}{3}} c_1^{-\frac{2}{3} \frac{c_3}{c_2}}. \tag{4.3.55}$$

From (4.3.51) and (4.3.52), the ordinary differential equation simplifies to

$$\frac{d}{d\zeta} \left(f^3 \frac{df}{d\zeta} \right) + 3 \frac{d}{d\zeta} (\zeta f) + \left(\frac{c_2}{c_3} - 5 \right) f(\zeta) + 3 \, g(\zeta) = 0, \tag{4.3.56}$$

the boundary equations (4.3.49) simplify to

$$f(1) = 0, \qquad f(-1) = 0, \tag{4.3.57}$$

and the balance law (4.3.50) becomes

$$\frac{1}{3}\left(5-\frac{c_2}{c_3}\right)\int_0^1 f(\zeta)\,d\zeta = \int_0^1 g(\zeta)\,d\zeta. \tag{4.3.58}$$

The initial volume V_0, given by (4.3.43), expressed in terms of the new variables (4.3.47) is

$$V_0 = 2\,\frac{c_1^{\frac{5}{3}\,\frac{c_3}{c_2}-\frac{1}{3}}}{c_3}\,A\,B\int_0^{\frac{c_3\,c_1^{-\frac{c_3}{c_2}}}{A}} f(\zeta)\,d\zeta, \tag{4.3.59}$$

which, when using (4.3.53) and (4.3.54) for A and B, becomes

$$V_0 = 2\left(\frac{c_3}{c_1}\right)^{\frac{1}{3}}\int_0^1 f(\zeta)\,d\zeta. \tag{4.3.60}$$

The height $h(t,x)$ given by (4.3.8) becomes, using (4.3.47) and (4.3.54) for B,

$$h(t,x) = \left(\frac{c_3}{c_1}\right)^{\frac{1}{3}}\left(1+\frac{c_2}{c_1}\,t\right)^{\frac{2}{3}\left(\frac{c_3}{c_2}-\frac{1}{2}\right)} f(\zeta), \tag{4.3.61}$$

and the suction/blowing velocity $v_n(t,x)$ given by (4.3.12), becomes, using (4.3.47) and (4.3.55) for D

$$v_n(t,x) = \left(\frac{c_3}{c_1}\right)^{\frac{4}{3}}\left(1+\frac{c_2}{c_1}\,t\right)^{\frac{2}{3}\left(\frac{c_3}{c_2}-2\right)} g(\zeta). \tag{4.3.62}$$

From (4.3.47), $\zeta = {}^{\xi}/_{A}$ and by using (4.3.40) for ξ and (4.3.53) for A we obtain

$$\zeta = \frac{x}{W(t)}. \tag{4.3.63}$$

There is one remaining condition to impose and that is on the initial dimensionless height at the central line. From the choice of the characteristic length in the z-direction in Section 3.2, the dimensionless height $h(t,x)$ satisfies $h(0,0)=1$. Using (4.3.61), we obtain

$$h(0,0) = \left(\frac{c_3}{c_1}\right)^{\frac{1}{3}} f(0) \tag{4.3.64}$$

and therefore

$$\frac{c_3}{c_1} = \frac{1}{f^3(0)}. \tag{4.3.65}$$

Now ${}^{c_2}/_{c_3}$ occurs in the ODE (4.3.56) and in the balance law (4.3.58). The ratio ${}^{c_2}/_{c_3}$ is either given or it is determined from the balance law (4.3.58). It therefore remains to determine ${}^{c_2}/_{c_1}$ which occurs in $W(t)$, $h(t,x)$ and $v_n(t,x)$. Now using (4.3.65),

$$\frac{c_2}{c_1} = \frac{c_2}{c_3}\,\frac{c_3}{c_1} = \frac{c_2}{c_3}\,\frac{1}{f^3(0)}\,. \tag{4.3.66}$$

If we let

$$\alpha = \frac{c_3}{c_2}, \tag{4.3.67}$$

then

$$\frac{c_2}{c_1} = \frac{1}{\alpha\, f^3(0)}, \tag{4.3.68}$$

where α still remains to be specified.

We now write the ordinary differential equation, $W(t)$, $V(t)$, V_0, $h(t,x)$ and $v_n(t,x)$, given respectively by (4.3.56), (4.3.37), (4.3.42), (4.3.60), (4.3.61),(4.3.62) and the balance law (4.3.58) and boundary conditions (4.3.57) in terms of the transformed variables and the single parameter α defined by (4.3.67):

$$\frac{d}{d\zeta}\left(f^3\,\frac{df}{d\zeta}\right) + 3\,\frac{d}{d\zeta}\,(\zeta\, f) + \left(\frac{1}{\alpha} - 5\right) f(\zeta) + 3\,g(\zeta) = 0, \tag{4.3.69}$$

$$f(1) = 0, \qquad f(-1) = 0, \tag{4.3.70}$$

$$\int_0^1 g(\zeta)\, d\zeta = \frac{1}{3}\left(5 - \frac{1}{\alpha}\right)\int_0^1 f(\zeta)\, d\zeta., \tag{4.3.71}$$

$$\begin{aligned}
W(t) &= \left(1 + \frac{t}{\alpha\, f^3(0)}\right)^{\alpha}, && (4.3.72)\\
V(t) &= V_0\left(1 + \frac{t}{\alpha\, f^3(0)}\right)^{\frac{5}{3}\alpha - \frac{1}{3}}, && (4.3.73)\\
V_0 &= 2\int_0^1 \frac{f(\zeta)}{f(0)}\, d\zeta, && (4.3.74)\\
h(t,x) &= \frac{f(\zeta)}{f(0)}\left(1 + \frac{t}{\alpha\, f^3(0)}\right)^{\frac{2}{3}\left(\alpha - \frac{1}{2}\right)}, && (4.3.75)
\end{aligned}$$

$$v_n(t,x) \quad = \quad \frac{1}{f^4(0)}\left(1+\frac{t}{\alpha\, f^3(0)}\right)^{\frac{2}{3}(\alpha-2)} g(\zeta), \tag{4.3.76}$$

where

$$\zeta = \frac{x}{W(t)} \tag{4.3.77}$$

The Lie point symmetry is given in (4.2.43) and when divided by c_1 becomes

$$X = \left(1+\frac{t}{\alpha f^3(0)}\right)\frac{\partial}{\partial t} + \frac{x}{f^3(0)}\frac{\partial}{\partial x} + \frac{1}{3\, f^3(0)}\left(2-\frac{1}{\alpha}\right) h\frac{\partial}{\partial h}. \tag{4.3.78}$$

Some assumption has to be made on $g(\zeta)$ to close the system. We will consider two assumptions so as to give two models which we will compare. The simplest assumption is that the velocity $v_n(t,x)$ is proportional to the height $h(t,x)$ and the second assumption is that the velocity $v_n(t,x)$ is proportional to the spatial gradient of the height, ${}^{\partial h(t,x)}/_{\partial x}$.

4.4 Conclusions

The nonlinear diffusion equation with source term admits four Lie point symmetries provided the fluid injection velocity at the base satisfies a first order linear partial differential equation. The general form of the group invariant solution generated by a linear combination of the four Lie point symmetries has been derived. The second order ordinary differential equation in the group invariant solution depends on two unknown functions and one unknown parameter. One further condition is required. In Chapters 5 and 6 two models will be investigated by assuming a relation between the two unknown functions.

Chapter 5

Model I: Leak-off velocity proportional to the height of the thin film

5.1 Introduction

In this chapter we make an assumption on $g(\zeta)$ to close the system so as to enable us to solve the ordinary differential equation (4.3.69). The simplest assumption is to consider the normal fluid velocity $v_n(t,x)$ at the base to be proportional to the height $h(t,x)$. Once the solution has been derived for $h(t,x)$ and $v_n(t,x)$ we examine the velocity on the axis $x = 0$ and with the aid of v_z and v_x we plot the streamlines to describe the flow within the thin film.

5.2 Relation between $g(\zeta)$ and $f(\zeta)$

We consider

$$g(\zeta) = \beta\, f(\zeta), \qquad -\infty < \beta < \infty, \tag{5.2.1}$$

where β is a constant. We can examine the physical significance of (5.2.1) by examining (4.3.76) for $v_n(t,x)$ and (4.3.75) for $h(t,x)$:

$$v_n(t,x) = \frac{1}{f^4(0)}\left(1+\frac{t}{\alpha\, f^3(0)}\right)^{\frac{2}{3}(\alpha-2)} g(\zeta), \tag{5.2.2}$$

$$h(t,x) = \frac{f(\zeta)}{f(0)}\left(1+\frac{t}{\alpha\, f^3(0)}\right)^{\frac{2}{3}\left(\alpha-\frac{1}{2}\right)}. \tag{5.2.3}$$

Thus by substituting (5.2.1) into (5.2.2) we obtain

$$v_n(t,x) = \frac{\beta}{f^3(0)}\left(1+\frac{t}{\alpha\, f^3(0)}\right)^{\frac{2}{3}(\alpha-2)} \frac{f(\zeta)}{f(0)} \tag{5.2.4}$$

and expressing $f(\zeta)$ in terms of $h(t,x)$ using (5.2.3) results in

$$v_n(t,x) = \frac{\beta\, h(t,x)}{f^3(0)}\left(1+\frac{t}{\alpha\, f^3(0)}\right). \tag{5.2.5}$$

Thus $v_n(t,x)$ is proportional to $h(t,x)$. The velocity $v_n(t,x)$ is greatest in the central region where $h(t,x)$ is greatest and vanishes at the moving contact lines $x = \pm W(t)$. Hence if

$\beta > 0$	then	$v_n > 0$:	blowing of fluid into the thin film,	(5.2.6)
$\beta = 0$	then	$v_n = 0$:	no leak-off of fluid, non-porous substrate,	(5.2.7)
$\beta < 0$	then	$v_n < 0$:	suction or leak-off of fluid into porous substrate.	(5.2.8)

5.2.1 Flux boundary condition at $\zeta = 1$

There is no flux of fluid across the moving contact line. The flux of fluid mass in the x-direction per unit length in the y-direction is

$$Q(t,x) = \rho \int_0^h v_x(t,x,z)\, dz. \tag{5.2.9}$$

But from (3.2.49)

$$\int_0^{h(t,x)} v_x(t,x,z)\, dz = -\frac{1}{3}\, h^3\, \frac{\partial h}{\partial x}, \tag{5.2.10}$$

thus

$$Q(t,x) = -\frac{\rho}{3}\, h^3\, \frac{\partial h}{\partial x}. \tag{5.2.11}$$

We express $Q(t, x)$ in terms of the similarity variables:

$$h(t,x) = \left(1+\frac{t}{\alpha\, f^3(0)}\right)^{\frac{2}{3}\left(\alpha-\frac{1}{2}\right)} \frac{f(\zeta)}{f(0)} \sim f(\zeta) \quad \text{as} \quad \zeta \to 1, \tag{5.2.12}$$

$$\frac{\partial h(t,x)}{\partial x} = \left(1+\frac{t}{\alpha\, f^3(0)}\right)^{\frac{2}{3}\left(\alpha-\frac{1}{2}\right)} \frac{1}{f(0)}\frac{df}{d\zeta}\frac{1}{W(t)} \sim \frac{df}{d\zeta} \quad \text{as} \quad \zeta \to 1. \tag{5.2.13}$$

Hence

$$Q(t,x) \sim f^3(\zeta)\,\frac{df}{d\zeta} \quad \text{as} \quad \zeta \to 1. \tag{5.2.14}$$

Since there is no flux across the moving contact line at $\zeta = 1$ and $\zeta = -1$ it follows that

$$f^3(1)\,\frac{df}{d\zeta}(1) = 0, \qquad f^3(-1)\,\frac{df}{d\zeta}(-1) = 0. \tag{5.2.15}$$

These boundary conditions are useful when solving the ordinary differential equation (4.3.69).

5.3 Solution of the ordinary differential equation

By using the balance law (4.3.71) and (5.2.1) we have

$$\left[\beta - \frac{1}{3}\left(5-\frac{1}{\alpha}\right)\right]\int_0^1 f(\zeta)\, d\zeta = 0. \tag{5.3.1}$$

Equation (5.3.1) is satisfied when

$$\beta - \frac{1}{3}\left(5-\frac{1}{\alpha}\right) = 0, \tag{5.3.2}$$

thus

$$\alpha = \frac{1}{5-3\,\beta}, \qquad \beta \neq \frac{5}{3}. \tag{5.3.3}$$

Using this value for α we may solve the ordinary differential equation (4.3.69) for $f(\zeta)$ and obtain $W(t)$, $V(t)$, $h(t,x)$ and $v_n(t,x)$.

Substituting (5.3.3) into (4.3.69) results in an integrable ordinary differential equation

$$\frac{d}{d\zeta}\left(f^3\,\frac{df}{d\zeta}\right) + 3\,\frac{d}{d\zeta}\,(\zeta\, f) = 0. \tag{5.3.4}$$

Integrating (5.3.4) once with respect to ζ and applying boundary condition (5.2.15) and (4.3.70) results in a variable separable ordinary differential equation for f

$$f^2\,\frac{df}{d\zeta} + 3\,\zeta = 0, \tag{5.3.5}$$

which when integrated and applying again (5.2.15) gives

$$f(\zeta) = \left(\frac{9}{2}\right)^{\frac{1}{3}} \left(1-\zeta^2\right)^{\frac{1}{3}}. \tag{5.3.6}$$

The boundary conditions in (5.2.15) and (4.3.70) can be applied at either $\zeta = 1$ or $\zeta = -1$ since the thin film is symmetric about the axis $\zeta = 0$. Substituting (5.3.6) and α given by (5.3.3) into (4.3.72), (4.3.73), (4.3.74), (4.3.75) and (4.3.76) gives

$$W(t) = \left(1 + \frac{2\,(5-3\,\beta)\,t}{9}\right)^{\frac{1}{5-3\,\beta}}, \tag{5.3.7}$$

$$V(t) = V_0 \left(1 + \frac{2\,(5-3\,\beta)\,t}{9}\right)^{\frac{\beta}{5-3\,\beta}}, \tag{5.3.8}$$

$$V_0 = 2\int_0^1 \left(1-\zeta^2\right)^{\frac{1}{3}}\, d\zeta, \tag{5.3.9}$$

$$h(t,x) = \left(1 + \frac{2\,(5-3\,\beta)\,t}{9}\right)^{\frac{\beta-1}{5-3\,\beta}} \left(1-\zeta^2\right)^{\frac{1}{3}}, \tag{5.3.10}$$

$$v_n(t,x) = \frac{2\,\beta}{9}\left(1 + \frac{2\,(5-3\,\beta)\,t}{9}\right)^{\frac{2(2\,\beta-3)}{5-3\,\beta}} \left(1-\zeta^2\right)^{\frac{1}{3}}, \tag{5.3.11}$$

where

$$\zeta = \frac{x}{W(t)}, \qquad -1 \le \zeta \le 1. \tag{5.3.12}$$

For the results (5.3.7)-(5.3.12), $\beta \neq \frac{5}{3}$.

Consider now the limit as $\beta \to \frac{5}{3}$ in (5.3.7). We first rewrite (5.3.7) as

$$W(t) = \exp\left[\frac{1}{3\left(\frac{5}{3}-\beta\right)}\ln\left(1 + \frac{2}{3}\left(\frac{5}{3}-\beta\right)\,t\right)\right]. \tag{5.3.13}$$

Using the expansion [2]

$$\ln(1+\epsilon) = \epsilon - \frac{\epsilon^2}{2} + \frac{\epsilon^3}{3} - \frac{\epsilon^4}{4} + \dots \tag{5.3.14}$$

then (5.3.13) becomes

$$W(t) = \exp\left[\frac{2\,t}{9} + \bigcirc\left(\left(\frac{5}{3} - \beta\right) t^2\right)\right] \quad \text{as} \quad \beta \to \frac{5}{3}, \tag{5.3.15}$$

and therefore

$$\lim_{\beta \to \frac{5}{3}} W(t) = \exp\left[\frac{2\,t}{9}\right]. \tag{5.3.16}$$

As $\beta \to \frac{5}{3}$, (5.3.8)-(5.3.12) tend to

$$W(t) = \exp\left[\frac{2\,t}{9}\right], \tag{5.3.17}$$

$$V(t) = V_0 \exp\left[\frac{10\,t}{27}\right], \tag{5.3.18}$$

$$h(t,x) = \exp\left[\frac{4\,t}{27}\right]\left(1 - \zeta^2\right)^{\frac{1}{3}}, \tag{5.3.19}$$

$$v_n(t,x) = \frac{10}{27}\exp\left[\frac{4\,t}{27}\right]\left(1 - \zeta^2\right)^{\frac{1}{3}}, \tag{5.3.20}$$

where V_0 is given in (5.3.9) and ζ is given in (5.3.12).

We analyse the results and their dependence on β. If we study the equations for the base $W(t)$ given by (5.3.7) and (5.3.17), then we find that $\frac{dW}{dt} > 0$ for $-\infty < \beta < \infty$. This means that the base always expands, even for values of $\beta < 0$ that describe the suction of fluid from the thin film. For $-\infty < \beta < \frac{5}{3}$, $W(t) \to \infty$ algebraically as $t \to \infty$, $W(t) \to \infty$ exponentially as $t \to \infty$ for $\beta = \frac{5}{3}$ and for $\frac{5}{3} < \beta < \infty$, $W(t) \to \infty$ in a finite time

$$t_1 = \frac{3}{2\left(\beta - \frac{5}{3}\right)}. \tag{5.3.21}$$

A plot of $W(t)$ against time, t, is presented in Figure 5.1.

If we examine volume $V(t)$ given by (5.3.8) and (5.3.18), then when $\beta = 0$, the volume remains constant as there is no suction or blowing at the base. For $\beta < 0$

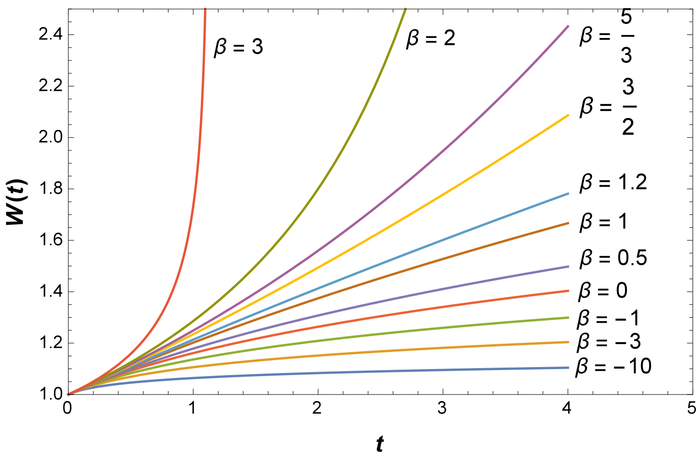

Figure 5.1: $W(t)$ given by (5.3.7) and (5.3.17) plotted against t for a range of β.

which describes suction at the base, $\frac{dV}{dt} < 0$, thus the volume decreases and it takes an infinite amount of time for the thin film to disappear. For $\beta > 0$ describing blowing, $\frac{dV}{dt} > 0$. When $0 < \beta < \frac{5}{3}$, $V(t) \to \infty$ algebraically as $t \to \infty$, for $\beta = \frac{5}{3}$, $V(t) \to \infty$ exponentially as $t \to \infty$ and for $\frac{5}{3} < \beta < \infty$, $V(t) \to \infty$ in a finite time given by (5.3.21). A plot of $V(t)$ against time, t, is presented in Figure 5.2.

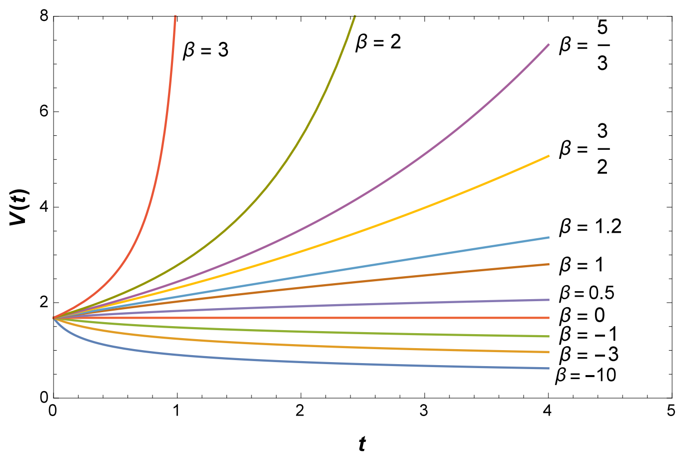

Figure 5.2: Volume $V(t)$ given by (5.3.8) and (5.3.18) plotted against t for a range of β.

If we now take into consideration the thickness of the thin film given by (5.3.10) where ζ is defined by (5.3.12) then

$$\frac{\partial h}{\partial x} = -\frac{2}{3}\, x\, W(t)^{\beta-3} \left(1 - \frac{x^2}{W^2(t)}\right)^{-\frac{2}{3}}. \tag{5.3.22}$$

Thus $\frac{\partial h}{\partial x} \to -\infty$ as $x \to W(t)$ and hence in the vicinity of $x = W(t)$, the thin film approximation is no longer satisfied. The inclusion of blowing or suction did not eliminate the singularity at $x = W(t)$. One may consider including surface tension effects or imposing a slip condition to remove the singularity at $x = W(t)$. Also

$$\frac{\partial h(t,0)}{\partial t} = \frac{2}{9}\,(\beta - 1)\left[1 + \frac{2}{9}\,(5 - 3\beta)\, t\right]^{\frac{2(2\beta-3)}{5-3\beta}}. \tag{5.3.23}$$

For $\beta < 1$, $\frac{\partial h(t,0)}{\partial t} < 0$ and therefore the height of the thin film decreases with time even when there is blowing at the base for $0 < \beta < 1$. The decrease in the height due to spreading is greater than the increase in height due to blowing. The height $h(t,0)$ remains constant for $\beta = 1$. For $\beta > 1$, $\frac{\partial h(t,0)}{\partial t} > 0$ and thus the height of the thin film increases with time. For $1 < \beta < \frac{5}{3}$, $h(t,0) \to \infty$ algebraically as $t \to \infty$ and when $\beta = \frac{5}{3}$, $h(t,0) \to \infty$ exponentially. For $\beta > \frac{5}{3}$, $h(t,0) \to \infty$ in a finite time given by (5.3.21). Graphs of $h(t,0)$ are plotted against time for a range of β in Figure 5.3.

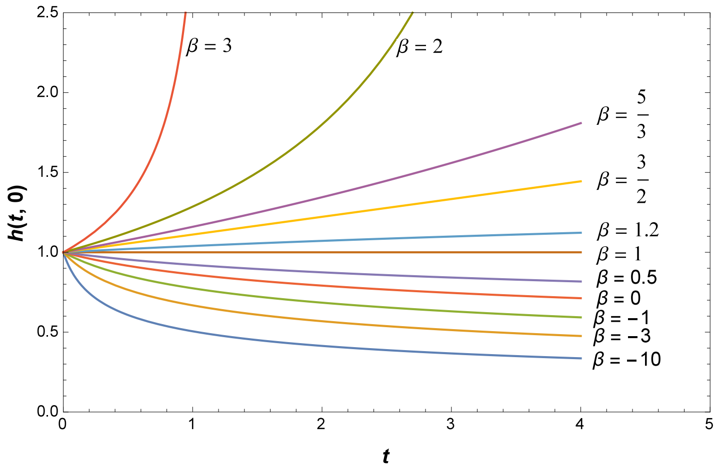

Figure 5.3: Height of the thin film at the centre, $h(t,0)$, given by (5.3.10) and (5.3.19) with $\zeta = 0$, plotted against t for a range of β.

Finally we consider the normal velocity $v_n(t,0)$ given by (5.3.11) and (5.3.20) which describes the suction or blowing at $x = 0$. For $-\infty < \beta < 0$, $v_n(t,0) < 0$ and $v_n(t,0) \to 0$ as $t \to \infty$. In this range, $v_n(t,0)$ describes suction. When $\beta = 0$, $v_n(t,0) = 0$. The base is impermeable and there is no suction or blowing. For $\beta > 0$ there is blowing of fluid at the base into the thin film. For $0 < \beta < \frac{3}{2}$, $v_n(t,0) > 0$ and $v_n(t,0) \to 0$ as $t \to \infty$. For $\beta = \frac{3}{2}$, $v_n(t,0) = \frac{1}{3}$ and the blowing velocity is constant in time. For $\frac{3}{2} < \beta < \frac{5}{3}$, $v_n(t,0) > 0$ and $v_n(t,0) \to \infty$ exponentially as $t \to \infty$. For $\frac{5}{3} < \beta < \infty$, $v_n(t,0) > 0$ and $v_n(t,0) \to \infty$ in a finite time defined by (5.3.21). Graphs of $v_n(t,0)$ are plotted against time for a range of β in Figure 5.4.

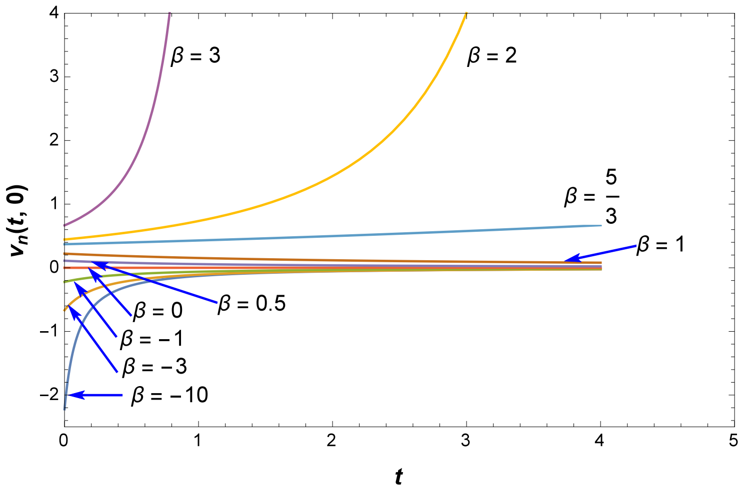

Figure 5.4: Normal velocity $v_n(t,0)$ given by (5.3.11) and (5.3.20) plotted against t for a range of β.

Consider the thin film ratio, in dimensionless variables,

$$\epsilon(t) = \frac{h(t,0)}{W(t)}. \tag{5.3.24}$$

Expressed in dimensionless variables defined in Section 3.2

$$\epsilon(t) = \frac{h(0,0)}{W(0)} \frac{\overline{h}(\overline{t},0)}{\overline{W}(\overline{t})} = \frac{h(0,0)}{W(0)} \overline{\epsilon}(\overline{t}), \tag{5.3.25}$$

$$\overline{\epsilon}(\overline{t}) = \frac{\overline{h}(\overline{t},0)}{\overline{W}(\overline{t})}. \tag{5.3.26}$$

We are assuming that the thin fluid film approximation is satisfied initially so that

$$\frac{h(0,0)}{W(0)} \ll 1. \tag{5.3.27}$$

Hence the thin fluid film approximation will be satisfied throughout the evolution of the thin film if either

$$\bar{\epsilon}(\bar{t}) = \text{constant} = 1 \quad \text{since} \quad \bar{h}(0,0) = 1 \quad \text{and} \quad \overline{W}(0) = 1, \tag{5.3.28}$$

or

$$\bar{\epsilon}(\bar{t}) \to 0 \quad \text{as} \quad \bar{t} \to \bar{t}_1 \quad \text{or} \quad \bar{t} \to \infty. \tag{5.3.29}$$

It will break down at sufficiently large time if

$$\bar{\epsilon}(\bar{t}) \to \infty \quad \text{as} \quad \bar{t} \to \bar{t}_1 \quad \text{or} \quad \bar{t} \to \infty. \tag{5.3.30}$$

Consider now the dimensionless thin film ratio and suppress the overhead bars. From (5.3.7) and (5.3.10) for $\beta \neq \frac{5}{3}$

$$\frac{h(t,0)}{W(t)} = \left(1 + \frac{2(5-3\,\beta)t}{9}\right)^{\frac{\beta-2}{5-3\beta}}, \tag{5.3.31}$$

and from (5.3.17) and (5.3.19) for $\beta = \frac{5}{3}$

$$\frac{h(t,0)}{W(t)} = \exp\left[-\frac{2\,t}{27}\right]. \tag{5.3.32}$$

For $-\infty < \beta < \frac{5}{3}$, $\epsilon \to 0$ algebraically as $t \to \infty$ and for $\beta = \frac{5}{3}$, $\epsilon \to 0$ exponentially as $t \to \infty$ while for $\frac{5}{3} < \beta < 2$, $\epsilon \to 0$ in a finite time given by (5.3.21). For $\beta = 2$, ϵ remains constant. When $2 < \beta < \infty$, $\epsilon \to \infty$ in a finite time given by (5.3.21). Thus the thin film approximation remains valid for $-\infty < \beta < 2$. If the thin film approximation is initially satisfied for $\beta = 2$ then it will remain satisfied for all time. It holds for blowing at the base $0 < \beta \leq 2$ because this is moderate blowing and $h(t,0)$ is not increased too rapidly compared with the width of the base. Graphs of ϵ are plotted against time for a range of β in Figure 5.5.

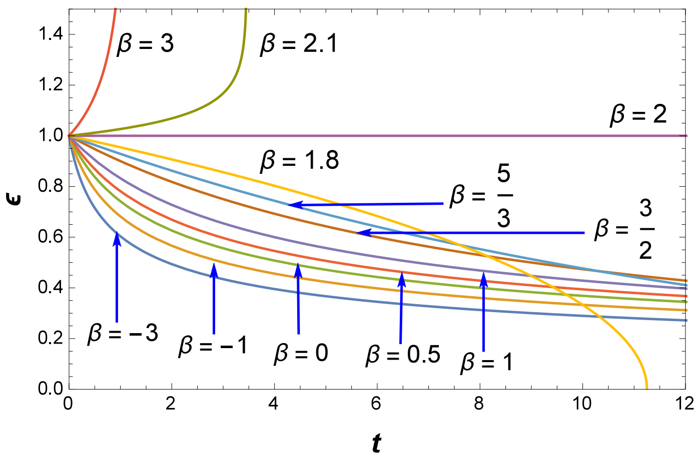

Figure 5.5: Thin film approximation ϵ given by (5.3.31) and (5.3.32) plotted against t for a range of β.

In Figure 5.6, pairs of graphs of $h(t, x)$ and $v_n(t, x)$ have been plotted against x for a range of t values. We observe that as we increase the magnitude of β the suction and injection velocity increases. Thus for $\beta > 0$, increasing β causes a greater increase in $h(t, 0)$ and for $\beta < 0$ increasing $|\beta|$ causes a greater decrease in $h(t, 0)$. The graphs in Figure 5.6(a) also show that the height can decrease with time even when there is injection of fluid. In Figure 5.6(b) it can be seen that the height on the axis remains constant for all time for $\beta = 1$ and in Figure 5.6(c) it can be seen the velocity $v_n(t, x)$ remains constant at $x = 0$ for all time for $\beta = 1.5$. A distinguishing feature of this solution is that the base increases for all time even when there is suction of the fluid as depicted in Figures 5.6(e) and 5.6(f). The suction/injection velocity is stronger at the center of the thin film and weaker near the edge of the thin film.

5.4 Velocity on the centre line $x = 0$

In this section we examine the velocity on the centre line $x = 0$. We look for both a perturbation solution and an exact solution.

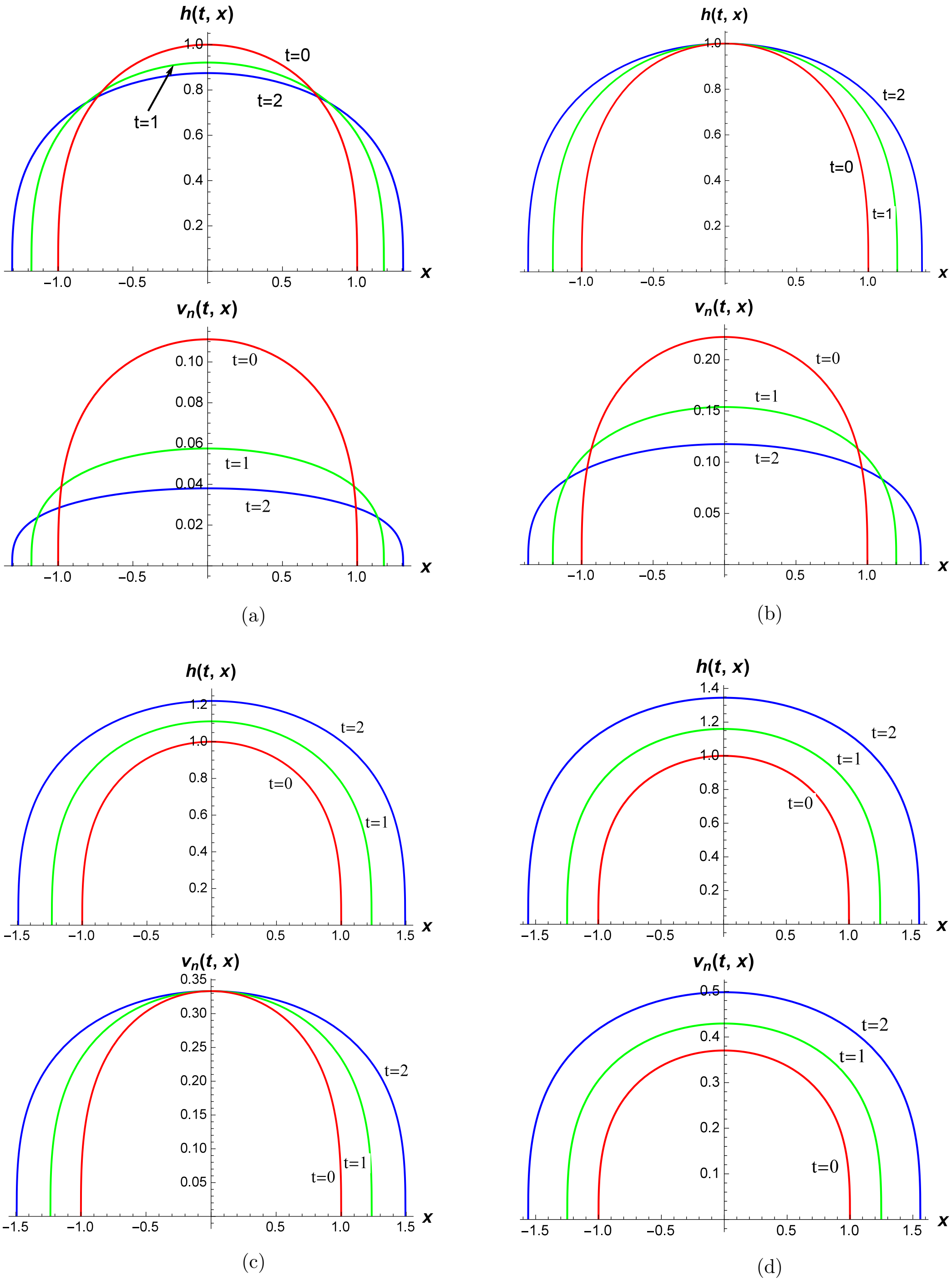

Figure 5.6: Graphs of $h(t, x)$ given by (5.3.10) and the fluid velocity at the base, $v_n(t, x)$, given by (5.3.11) plotted against x for a range of values of t and for: (a) $\beta = 0.5$, (b) $\beta = 1$, (c) $\beta = 1.5$, (d) $\beta = \frac{5}{3}$.

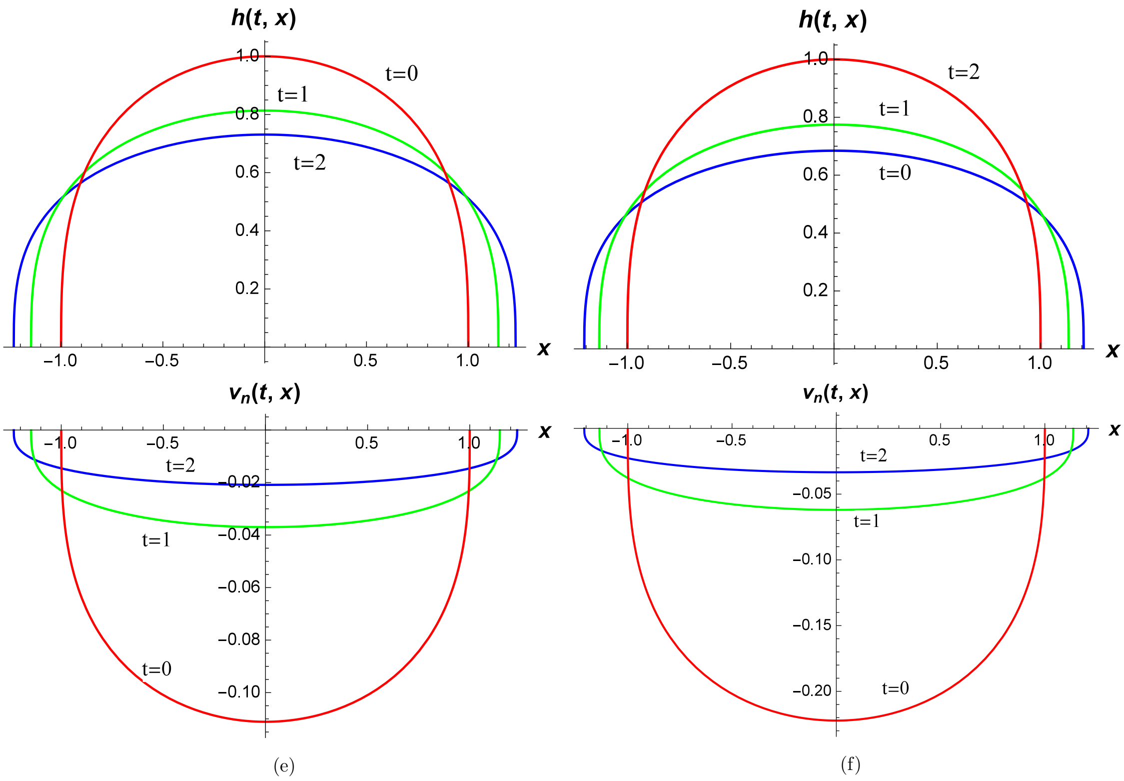

Figure 5.6: Graphs of $h(t,x)$ given by (5.3.10) and the fluid velocity at the base, $v_n(t,x)$, given by (5.3.11) plotted against x for a range of values of t and for: (e) $\beta = -0.5$, (f) $\beta = -1$.

We first express $h(t,x)$ and $v_n(t,x)$ given by (5.3.10) and (5.3.11) respectively in terms of $W(t)$ and then in terms of $h(t,0)$ since we know that $h(0,0) = 1$. Thus

$$h(t,x) = W^{\beta-1}(t)\left(1-\zeta^2\right)^{\frac{1}{3}}, \tag{5.4.1}$$

$$= h(t,0)\left(1-\zeta^2\right)^{\frac{1}{3}}, \tag{5.4.2}$$

where

$$h(t,0) = W^{\beta-1}(t), \tag{5.4.3}$$

and

$$v_n(t,x) = \frac{2\,\beta}{9} W^{4\,\beta-6}(t)\left(1-\zeta^2\right)^{\frac{1}{3}}, \tag{5.4.4}$$

$$= \frac{2\,\beta}{9}\frac{h^4(t,0)}{W^2(t)}\left(1-\zeta^2\right)^{\frac{1}{3}}. \tag{5.4.5}$$

The dimensionless velocity components v_x is given by (3.2.46). To obtain v_z we integrate the continuity equation (3.2.27)from 0 to z. Thus

$$v_x(t,x,z) = \frac{z}{2}\left(z - 2\,h(t,x)\right)\,\frac{\partial h(t,x)}{\partial x}, \tag{5.4.6}$$

$$v_z(t,x,z) = v_n(t,x) - \frac{\partial}{\partial x}\int_0^z v_x(t,x,z)\,dz. \tag{5.4.7}$$

Substituting (5.4.6) into (5.4.7) and integrating with the respect to z and then differentiating partially with respect to x gives

$$v_z(t,x,z) = -\frac{1}{6}\frac{\partial^2 h}{\partial x^2} z^3 + \frac{1}{2}\left[h(t,x)\frac{\partial^2 h}{\partial x^2} + \left(\frac{\partial h}{\partial x}\right)^2\right] z^2 + v_n(t,x). \tag{5.4.8}$$

Now

$$h\frac{\partial^2 h}{\partial x^2} + \left(\frac{\partial h}{\partial x}\right)^2 = \frac{1}{2}\frac{\partial^2}{\partial x^2}\left(h^2\right), \tag{5.4.9}$$

thus by substituting (5.4.9) into (5.4.8)

$$v_z(t,x,z) = -\frac{1}{6}\frac{\partial^2 h}{\partial x^2} z^3 + \frac{1}{4}\frac{\partial^2}{\partial x^2}\left(h^2\right) z^2 + v_n \tag{5.4.10}$$

and therefore the velocity on the axis $x = 0$ is given by

$$v_z(t,0,z) = -\frac{1}{6}\left.\frac{\partial^2 h(t,x)}{\partial x^2}\right|_{x=0} z^3 + \frac{1}{4}\left.\frac{\partial^2}{\partial x^2}\left(h^2(t,x)\right)\right|_{x=0} z^2 + v_n(t,0). \tag{5.4.11}$$

Now using (5.4.2) and (5.3.12) for ζ,

$$\frac{\partial^2 h(t,x)}{\partial x^2} = -\frac{2}{3}\frac{h(t,0)}{W^2(t)}\left(1-\frac{x^2}{W^2(t)}\right)^{-\frac{2}{3}} - \frac{8}{9}x^2\frac{h(t,0)}{W^4(t)}\left(1-\frac{x^2}{W^2(t)}\right)^{-\frac{5}{3}}, \quad (5.4.12)$$

and

$$\frac{\partial^2}{\partial x^2}\left(h^2(t,x)\right) = -\frac{4}{3}\frac{h^2(t,0)}{W^2(t)}\left(1-\frac{x^2}{W^2(t)}\right)^{-\frac{1}{3}} - \frac{8}{9}\frac{h^2(t,0)}{W^2(t)}x^2\left(1-\frac{x^2}{W^2(t)}\right)^{-\frac{4}{3}}. \quad (5.4.13)$$

Thus putting $x = 0$ in (5.4.12), (5.4.13) and (5.4.5) for $v_n(t,x)$ and replacing these terms in (5.4.11) results in

$$v_z(t,0,z) = \frac{1}{9}\frac{h(t,0)}{W^2(t)}\left[z^3 - 3\,h(t,0)z^2 + 2\,\beta\,h^3(t,0)\right]. \quad (5.4.14)$$

The points on the axis at which

$$v_z(t,0,z) = 0 \quad (5.4.15)$$

therefore satisfy the cubic equation

$$z^3 - 3\,h(t,0)z^2 + 2\,\beta\,h^3(t,0) = 0. \quad (5.4.16)$$

We will be concerned with finding the roots of the cubic equation (5.4.16) but before we do that we consider some properties of $v_z(t,0,z)$. The velocity (5.4.14) at $z = h(t,0)$ is the velocity of the point of maximum height of the thin film as depicted in Figure 5.7. Substituting $z = h$ into (5.4.14) gives

$$v_z(t,0,h) = \frac{2}{9}(\beta-1)\frac{h^4(t,0)}{W^2(t)}. \quad (5.4.17)$$

There are two competing effects in the evolution of $h(t,0)$. These are the increase in height due to blowing and the decrease in height due to spreading by gravity. Consider now in more detail the dependence of $v_z(t,0,h)$ on β. Substituting (5.4.3) into (5.4.17) we obtain

$$v_z(t,0,h) = \frac{2}{9}(\beta-1)\,W^{4\left(\beta-\frac{3}{2}\right)}(t), \quad (5.4.18)$$

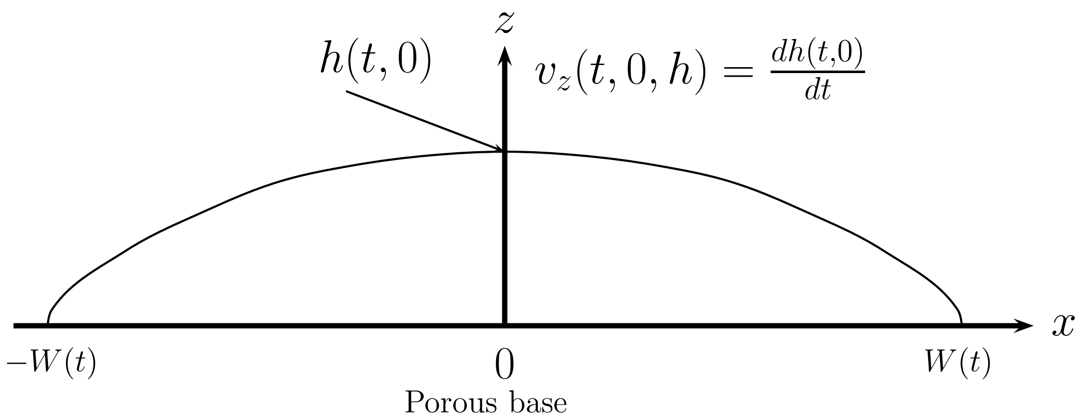

Figure 5.7: Velocity v_z at $z = h$ on the centre line $x = 0$.

thus when

$$\beta \neq \frac{5}{3}: \qquad v_z(t,0,h) = \frac{2}{9}(\beta - 1)\left[1 + \frac{2}{3}\left(\frac{5}{3} - \beta\right)t\right]^{\frac{4\left(\beta - \frac{3}{2}\right)}{3\left(\frac{5}{3} - \beta\right)}}, \tag{5.4.19}$$

$$\beta = \frac{5}{3}: \qquad v_z(t,0,h) = \frac{4}{27}\exp\left(\frac{4}{27}t\right). \tag{5.4.20}$$

The graph of the exponent $\frac{4\left(\beta - \frac{3}{2}\right)}{3\left(\frac{5}{3} - \beta\right)}$ against β is presented in Figure 5.8.

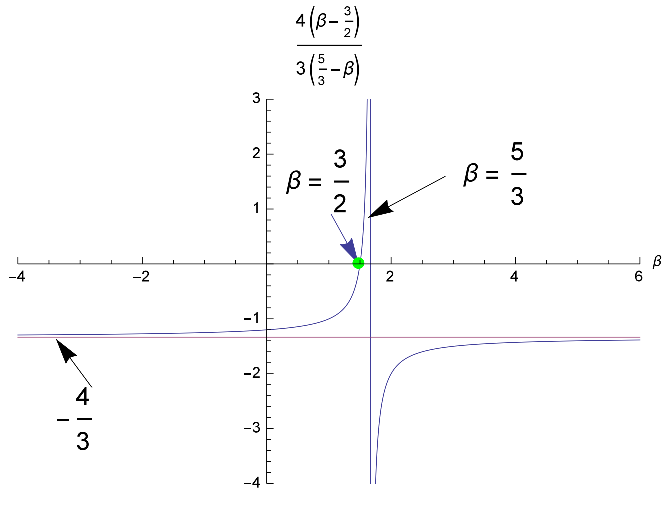

Figure 5.8: Plot of the exponent $\frac{4\left(\beta - \frac{3}{2}\right)}{3\left(\frac{5}{3} - \beta\right)}$ against β.

Physical significance of ranges of β:

$$-\infty < \beta < 1: \qquad v_z(t,0,h) < 0, \tag{5.4.21}$$

$$\mid v_z(t,0,h) \mid \quad \text{decreases with time}, \tag{5.4.22}$$

$$v_z(t,0,h) \to 0 \quad \text{as} \quad t \to \infty. \tag{5.4.23}$$

$$\beta = 1: \qquad v_z(t,0,h) = 0. \tag{5.4.24}$$

$$1 < \beta < \frac{3}{2}: \qquad v_z(t,0,h) > 0, \tag{5.4.25}$$

$$\mid v_z(t,0,h) \mid \quad \text{decreases with time}, \tag{5.4.26}$$

$$v_z(t,0,h) \to 0 \quad \text{as} \quad t \to \infty. \tag{5.4.27}$$

$$\beta = \frac{3}{2}: \qquad v_z(t,0,h) \quad \text{is constant in time}, \tag{5.4.28}$$

$$v_z(t,0,h) = \frac{1}{9}. \tag{5.4.29}$$

$$\frac{3}{2} < \beta < \frac{5}{3}: \qquad v_z(t,0,h) > 0, \tag{5.4.30}$$

$$v_z(t,0,h) \quad \text{increases with time}, \tag{5.4.31}$$

$$v_z(t,0,h) \to \infty \quad \text{as} \quad t \to \infty. \tag{5.4.32}$$

$$\beta = \frac{5}{3}: \qquad v_z(t,0,h) = \frac{4}{27}\exp\left(\frac{4}{27}t\right), \tag{5.4.33}$$

$$v_z(t,0,h) \to \infty \quad \text{exponentially as} \quad t \to \infty. \tag{5.4.34}$$

$$\frac{5}{3} < \beta < \infty: \qquad v_z(t,0,h) > 0, \tag{5.4.35}$$

$$v_z(t,0,h) \quad \text{increases with time}, \tag{5.4.36}$$

$$v_z(t,0,h) \to \infty \quad \text{as} \quad t \to \frac{3}{2\left(\beta - \frac{5}{3}\right)}, \tag{5.4.37}$$

$$\text{that is, in a finite time.} \tag{5.4.38}$$

A plot of $v_z(t, 0, h)$ for a range of β values is presented if Figure 5.9.

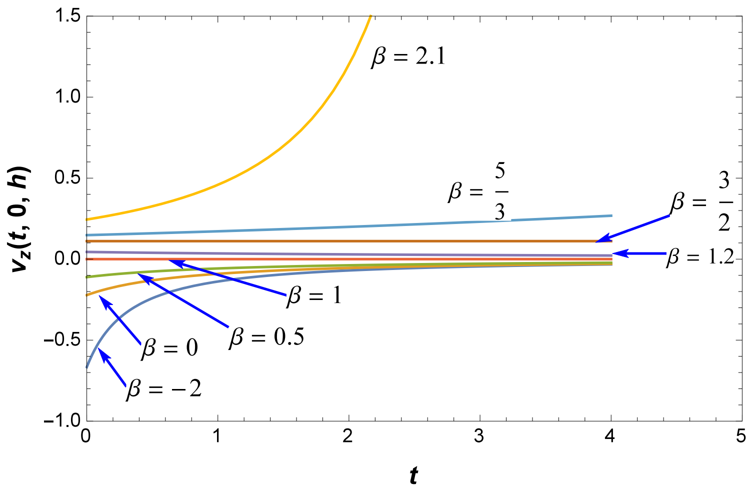

Figure 5.9: Graphs of $v_z(t, 0, h)$ given by (5.4.19) and (5.4.20), plotted against time t for a range of values of β.

5.4.1 Roots of the cubic equation

Consider the values of z for which $v_z(t, 0, z) = 0$:

$$z^3 - 3\,h(t, 0)z^2 + 2\,\beta\,h^3(t, 0) = 0. \tag{5.4.39}$$

When $\beta = 0$,

$$z^2\,(z - 3h(t, 0)) = 0. \tag{5.4.40}$$

Thus $z = 0, z = 0, z = 3h(t, 0)$. The roots are illustrated in Figure 5.10.

When $\beta = 0$, from (5.4.14),

$$v_z(t, 0, z) = \frac{h(t, 0)}{9W^2(t)} z^2\,(z - 3\,h(t, 0))\,. \tag{5.4.41}$$

Thus

$$0 < z < 3h(t, 0) \quad \text{then} \quad v_z(t, 0, z) < 0. \tag{5.4.42}$$

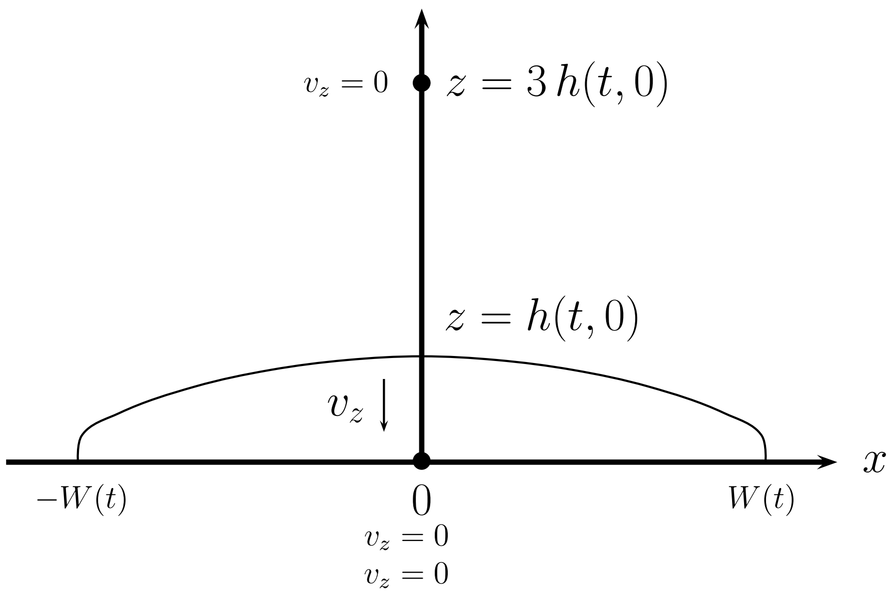

Figure 5.10: Roots of the cubic equation (5.4.39) for $\beta = 0$.

When $\beta = 0$, $v_z(t,0,z)$ is negative for $0 < z < h(t,0)$. There are no zeros on the centre line $x = 0$ inside the thin fluid film.

We now investigate how the roots

$$z = 0, \quad z = 0, \quad z = 3h(t,0) \tag{5.4.43}$$

move for $\beta \neq 0$. This will be done in terms of a perturbation solution and exact solution.

5.4.2 Perturbation solution of the cubic equation

We determine the perturbation solution of the cubic equation (5.4.39). The perturbation parameter is β. We first consider the straightforward perturbation expansion

$$z = z_0 + \beta\, z_1 + \bigcirc(\beta^2). \tag{5.4.44}$$

Substituting (5.4.44) into (5.4.39) and expanding gives

$$z_0^3 + 3\beta\, z_0^2\, z_1 - 3h(t,0)z_0^2 - 6\beta\, h(t,0)z_0\, z_1 + 2\beta\, h^3(t,0) + \bigcirc\left(\beta^2\right) = 0. \qquad (5.4.45)$$

We equate the coefficients of like powers of β

$$\beta^0: \qquad z_0^3 - 3h(t,0)z_0^2 = 0, \qquad (5.4.46)$$

$$\beta^1: \qquad 3z_0^2 z_1 - 6h(t,0)z_0 z_1 + 2h^3(t,0) = 0. \qquad (5.4.47)$$

From (5.4.46), we obtain

$$z_0 = 0, \quad z_0 = 0, \quad z_0 = 3h(t,0). \qquad (5.4.48)$$

If we consider the solution $z_0 = 3h(t,0)$ and substitute into (5.4.47), we obtain

$$z_1 = -\frac{2}{9}\, h(t,0), \qquad (5.4.49)$$

and hence the perturbation expansion is

$$z = 3\left(1 - \frac{2}{27}\,\beta + \bigcirc(\beta^2)\right) h(t,0). \qquad (5.4.50)$$

We see that if $\beta > 0$ (blowing) the root $z = 3h(t,0)$ is decreasing when we include the first order term. If we now consider the solution $z_0 = 0$ and substitute into (5.4.47), we find that

$$z_1 = \frac{-2h^3(t,0)}{z_0(3z_0 + 6h(t,0))} = -\infty. \qquad (5.4.51)$$

The straightforward perturbation expansion (5.4.44) therefore breaks down. The assumed form (5.4.44) for the expansion is wrong. The problem is a singular perturbation problem [29]. For a singular perturbation expansion we consider the following

$$z = z_0 + z_1\, \beta^\nu + z_2\, \beta^{2\nu} + z_3\, \beta^{3\nu} + \bigcirc\left(\beta^{4\nu}\right). \qquad (5.4.52)$$

Substituting (5.4.52) into (5.4.39) and expanding results in

$$z_0^3 - 3h(t,0)\, z_0^2 + 2\beta\, h^3(t,0) + \beta^\nu\left(3z_0^2\, z_1 - 6h(t,0)z_0\, z_1\right)$$
$$+ \beta^{2\nu}\left(3z_0\, z_1^2 + 3z_0^2\, z_2 - 3h(t,0)z_1^2 - 6h(t,0)z_0\, z_2\right)$$

$$+\beta^{3\nu}\left(z_1^3+3\,z_0^2\,z_3+6\,z_0\,z_1\,z_2-6\,h(t,0)\,z_0\,z_3-6\,h(t,0)\,z_1\,z_2\right)+\bigcirc\left(\beta^{4\nu}\right)$$
$$=0. \tag{5.4.53}$$

The zero order perturbation solution remains unchanged and is given in (5.4.48). Hence we consider the roots $z_0=0$ and $z_0=3h(t,0)$ separately when determining the singular perturbation expansion.

(a) $\mathbf{z_0=3h(t,0)}$:

Substituting $z_0=3h(t,0)$ into (5.4.53) results in

$$9h^2(t,0)\,z_1\,\beta^\nu+2\beta\,h^3(t,0)+\bigcirc\left(\beta^{2\nu}\right)=0. \tag{5.4.54}$$

The dominant terms in (5.4.54) will balance provided

$$\nu=1. \tag{5.4.55}$$

Thus we obtain

$$9h^2(t,0)\,z_1\,\beta+2\beta\,h^3(t,0)+\bigcirc\left(\beta^2\right)=0, \tag{5.4.56}$$

and consequently

$$z_1=-\frac{2}{9}h(t,0). \tag{5.4.57}$$

Hence

$$z=3\left(1-\frac{2}{27}\beta+\bigcirc(\beta^2)\right)h(t,0). \tag{5.4.58}$$

This agrees with the result obtained from the straightforward perturbation expansion (5.4.50).

(b) $\mathbf{z_0=0}$:

Substituting $z_0=0$ into (5.4.53) results in

$$-3h(t,0)\,z_1^2\,\beta^{2\nu}+z_1^3\,\beta^{3\nu}-6h(t,0)\,z_1\,z_2\,\beta^{3\nu}+2\beta\,h^3(t,0)+\bigcirc\left(\beta^{4\nu}\right)=0. \tag{5.4.59}$$

The dominant terms are

$$-3h(t,0)\, z_1^2\, \beta^{2\nu} \quad \text{and} \quad 2\beta\, h^3(t,0), \tag{5.4.60}$$

and for the dominant terms to balance we require

$$\nu = \frac{1}{2}. \tag{5.4.61}$$

Thus (5.4.59) becomes

$$-3h(t,0)\, z_1^2\, \beta + z_1^3\, \beta^{\frac{3}{2}} - 6h(t,0)\, z_1\, z_2\, \beta^{\frac{3}{2}} + 2\beta\, h^3(t,0) + \bigcirc\left(\beta^2\right) = 0. \tag{5.4.62}$$

If $\beta < 0$ (suction at the base), $\beta^{\frac{3}{2}}$ will be imaginary. We therefore treat $\beta > 0$ and $\beta < 0$ separately.

(i) $\mathbf{z_0 = 0}$; blowing at the base, $\beta > \mathbf{0}$

We equate the coefficients of like powers of β

$$\beta^1: \qquad -3h(t,0)z_1^2 + 2h^3(t,0) = 0, \tag{5.4.63}$$

$$\beta^{\frac{3}{2}}: \qquad z_1^3 - 6h(t,0)z_1 z_2 = 0. \tag{5.4.64}$$

From (5.4.63), we obtain

$$z_1 = \pm\left(\frac{2}{3}\right)^{\frac{1}{2}} h(t,0), \tag{5.4.65}$$

and substituting (5.4.65) into (5.4.64) gives

$$z_2 = \frac{1}{9} h(t,0). \tag{5.4.66}$$

Hence by substituting (5.4.65) and (5.4.66) into (5.4.52), the two roots are

$$z = \left[\left(\frac{2}{3}\right)^{\frac{1}{2}} \beta^{\frac{1}{2}} + \frac{1}{9}\beta + \bigcirc\left(\beta^{\frac{3}{2}}\right)\right] h(t,0), \tag{5.4.67}$$

$$z = \left[-\left(\frac{2}{3}\right)^{\frac{1}{2}} \beta^{\frac{1}{2}} + \frac{1}{9}\beta + \bigcirc\left(\beta^{\frac{3}{2}}\right)\right] h(t,0), \tag{5.4.68}$$

and we have shown that the third root is given in (5.4.58). The velocity component $v_z(t,0,z)$ therefore has a zero on the z-axis inside the thin film at

$$z = \left[\left(\frac{2}{3}\right)^{\frac{1}{2}} \beta^{\frac{1}{2}} + \frac{1}{9}\beta + \bigcirc\left(\beta^{\frac{3}{2}}\right)\right] h(t,0). \tag{5.4.69}$$

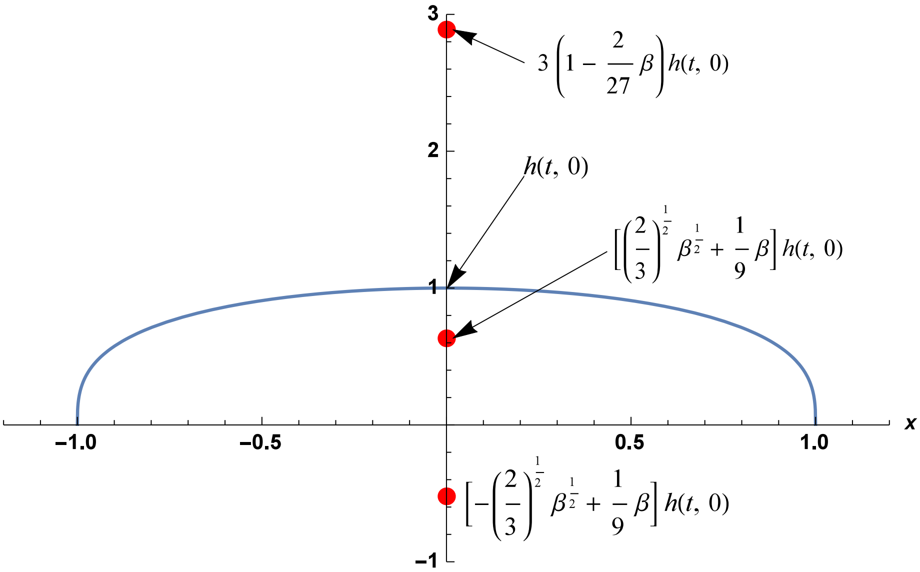

Figure 5.11: Roots of the cubic equation (5.4.39) for $\beta > 0$ correct to order β.

(ii) $\mathbf{z_0 = 0}$; suction at the base, $\beta < 0$

Let

$$\beta = -|\beta|. \tag{5.4.70}$$

We make the expansion

$$z = z_1\,|\beta|^{\nu} + z_2\,|\beta|^{2\nu} + z_3\,|\beta|^{3\nu} + \bigcirc\left(|\beta|^{4\nu}\right). \tag{5.4.71}$$

If ν is a fractional power, for example $\nu = \frac{1}{2}$, then $|\beta|^{\nu}$ is real. Now using (5.4.71)

$$z^2 = z_1^2|\beta|^{2\nu} + 2z_1z_2|\beta|^{3\nu} + \bigcirc\left(|\beta|^{4\nu}\right), \tag{5.4.72}$$

and

$$z^3 = z_1^3|\beta|^{3\nu} + \bigcirc\left(|\beta|\right)^{4\nu}. \tag{5.4.73}$$

Substituting (5.4.72) and (5.4.73) into the cubic equation (5.4.39) results in

$$z_1^3|\beta|^{3\nu} - 3h(t,0)z_1^2|\beta|^{2\nu} - 6h(t,0)z_1z_2|\beta|^{3\nu} - 2h^3(t,0)|\beta| + \bigcirc\left(|\beta|^{4\nu}\right) = 0. \tag{5.4.74}$$

The dominant terms in (5.4.74) are

$$-3h(t,0)\,z_1^2\,|\beta|^{2\nu} \quad \text{and} \quad 2h^3(t,0)\,|\beta|, \tag{5.4.75}$$

and for the dominant terms to balance we require

$$\nu = \frac{1}{2}. \tag{5.4.76}$$

Thus (5.4.74) becomes

$$z_1^3|\beta|^{\frac{3}{2}} - 3h(t,0)z_1^2|\beta| - 6h(t,0)z_1z_2|\beta|^{\frac{3}{2}} - 2h^3(t,0)|\beta| + \bigcirc\left(|\beta|^2\right) = 0. \tag{5.4.77}$$

We equate the coefficients of like powers of $|\beta|$. This gives

$$|\beta| : \qquad -3h(t,0)z_1^2 - 2h^3(t,0) = 0, \tag{5.4.78}$$

$$|\beta|^{\frac{3}{2}} : \qquad z_1^3 - 6h(t,0)z_1z_2 = 0. \tag{5.4.79}$$

From (5.4.78), we obtain

$$z_1 = \pm\, i\left(\frac{2}{3}\right)^{\frac{1}{2}} h(t,0), \tag{5.4.80}$$

and substituting (5.4.80) into (5.4.79) gives

$$z_2 = -\frac{1}{9}h(t,0). \tag{5.4.81}$$

Hence by substituting (5.4.80) and (5.4.81) into (5.4.71), the two roots are

$$z = \left[i\left(\frac{2}{3}\right)^{\frac{1}{2}}|\beta|^{\frac{1}{2}} - \frac{1}{9}|\beta| + \bigcirc\left(|\beta|^{\frac{3}{2}}\right)\right]h(t,0), \tag{5.4.82}$$

$$z = \left[-i\left(\frac{2}{3}\right)^{\frac{1}{2}}|\beta|^{\frac{1}{2}} - \frac{1}{9}|\beta| + \bigcirc\left(|\beta|^{\frac{3}{2}}\right)\right]h(t,0), \tag{5.4.83}$$

and we have shown that the third root is given in (5.4.58):

$$z = 3\left[1 + \frac{2}{27}|\beta| + \bigcirc\left(|\beta|^2\right)\right]h(t,0). \tag{5.4.84}$$

There is one real root and two complex roots. The real root does not lie in the range $0 \leq z \leq h(t,0)$. Hence there is no zero on the z-axis of the velocity $v_z(t,0,z)$:

$$v_z(t,0,z) < 0, \qquad 0 \leq z \leq h(t,0). \tag{5.4.85}$$

5.4.3 Exact solution of the cubic equation

We determine the roots exactly of the cubic equation (5.4.39):

$$z^3 - 3h(t,0)z^2 + 2\beta h^3(t,0) = 0\,.$$

We first investigate the nature of the roots. We do that in two ways. In the first way we sketch the graph of the cubic polynomial with the aid of Descartes' rule of signs. In the second way we transform the cubic polynomial to standard form and calculate the discriminant, Δ, to determine the properties of the roots.

Descartes' rule of signs for a polynomial equation $P(x) = 0$ says that [2, 6]:

$$\begin{aligned}\text{number of positive roots} &\leq \text{number of changes of sign in} \\ &\quad\ \text{the coefficients of } P(x), \\ \text{number of negative roots} &\leq \text{number of changes of sign in} \\ &\quad\ \text{the coefficients of } P(-x).\end{aligned}$$

For the cubic equation (5.4.39), we have

$$P(z) = z^3 - 3h(t,0)z^2 + 2\beta h^3(t,0), \tag{5.4.86}$$

$$P(-z) = -z^3 - 3h(t,0)z^2 + 2\beta h^3(t,0). \tag{5.4.87}$$

We will consider the case for $\beta < 0$ and $\beta > 0$ separately.

(i) Blowing at the base, $\beta > \mathbf{0}$

$$\text{Number of positive roots of P(z)} \leq 2,$$

$$\text{Number of negative roots of P(z)} \leq 1.$$

Special values of $P(z)$:

$$P(0) = 2\beta h^3(t,0), \tag{5.4.88}$$

$$P(h) = 2(\beta - 1)h^3(t,0), \tag{5.4.89}$$

$$P(2h) = 2(\beta - 2)h^3(t, 0), \tag{5.4.90}$$

$$P(3h) = 2\beta h^3(t, 0). \tag{5.4.91}$$

Special values of β.

$\beta = \mathbf{1}$:

$$\begin{aligned} P(z) &= z^3 - 3h(t,0)z^2 + 2h^3(t,0), &(5.4.92)\\ &= (z-h)(z^2 - 2hz - 2h^2). &(5.4.93)\end{aligned}$$

The roots of the quadratic polynomial in (5.4.93) are

$$z = (1 + \sqrt{3})h\,, \qquad z = (1 - \sqrt{3})h\ . \tag{5.4.94}$$

Hence the roots of $P(z) = 0$ are

$$z = -(\sqrt{3} - 1)h\,, \qquad z = h\,, \qquad z = (1 + \sqrt{3})h\ . \tag{5.4.95}$$

$\beta = \mathbf{2}$:

$$\begin{aligned} P(z) &= z^3 - 3h(t,0)z^2 + 4h^3(t,0), &(5.4.96)\\ &= (z+h)(z-2h)^2. &(5.4.97)\end{aligned}$$

The roots of $P(z) = 0$ are therefore

$$z = -h\,, \qquad z = 2h\,, \quad z = 2h\ . \tag{5.4.98}$$

$\beta > \mathbf{2}$:

$$\begin{aligned} P(z) &= z^3 - 3h(t,0)z^2 + 2\beta h^3(t,0), &(5.4.99)\\ &= P(z)\,|_{\beta=2} + 2(\beta-2)h^3(t,0). &(5.4.100)\end{aligned}$$

Thus

$$P(z)\,|_{\beta>2} > P(z)\,|_{\beta=2}. \tag{5.4.101}$$

- $\beta = 0$: $P(z) = z^2(z - 3h)$

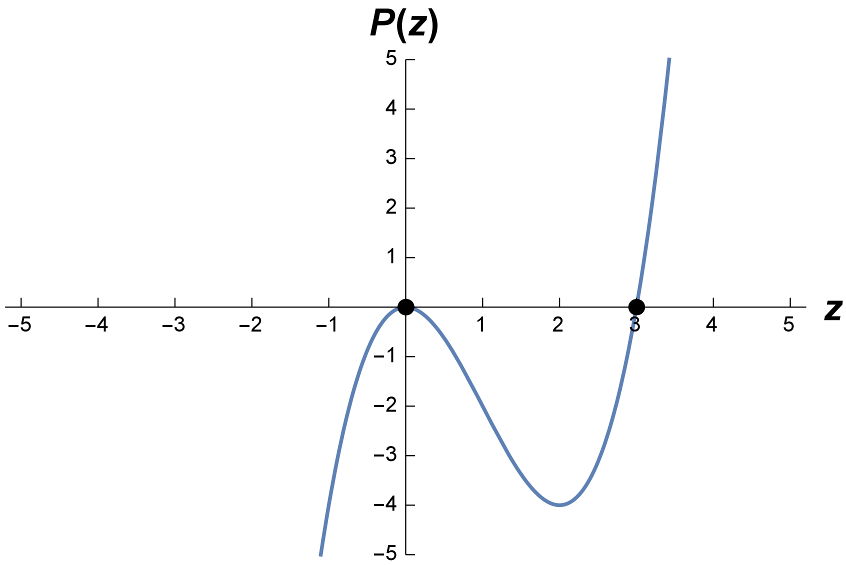

Figure 5.12: Plot of P(z) and its roots for $\beta = 0$ and $h(t, 0) = 1$.

- $0 < \beta < 1$:

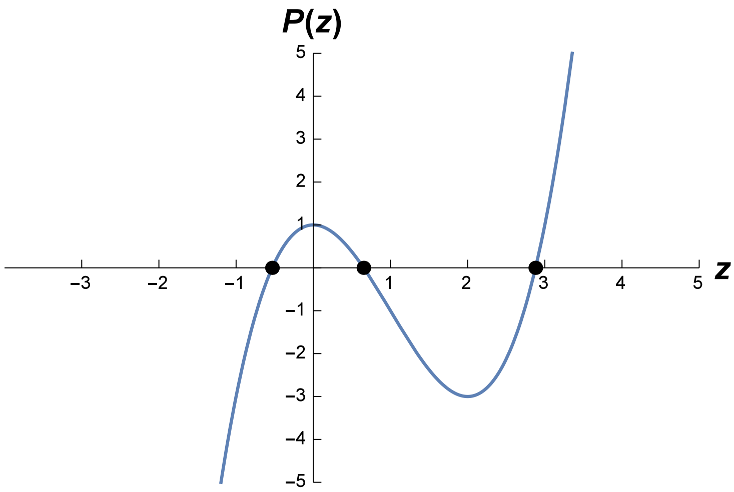

Figure 5.13: Plot of P(z) and its roots for $\beta = 0.5$ and $h(t, 0) = 1$.

- $\beta = 1$:

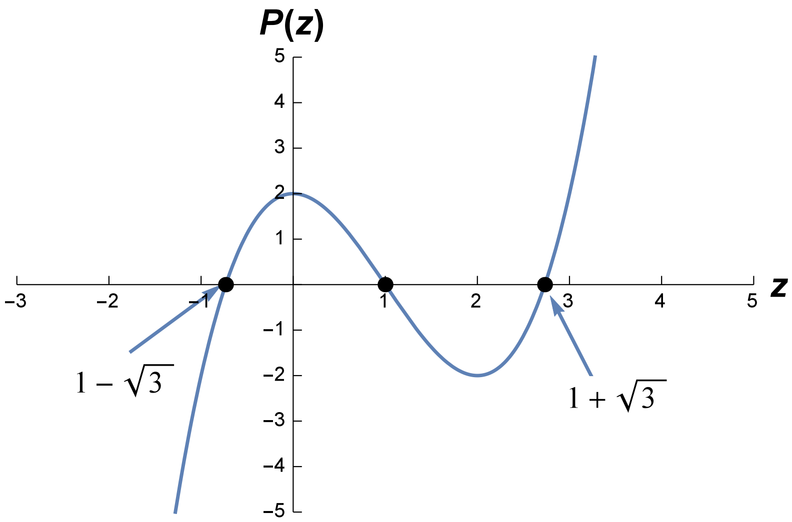

Figure 5.14: Plot of P(z) and its roots for $\beta = 1$ and $h(t, 0) = 1$.

- $1 < \beta < 2$:

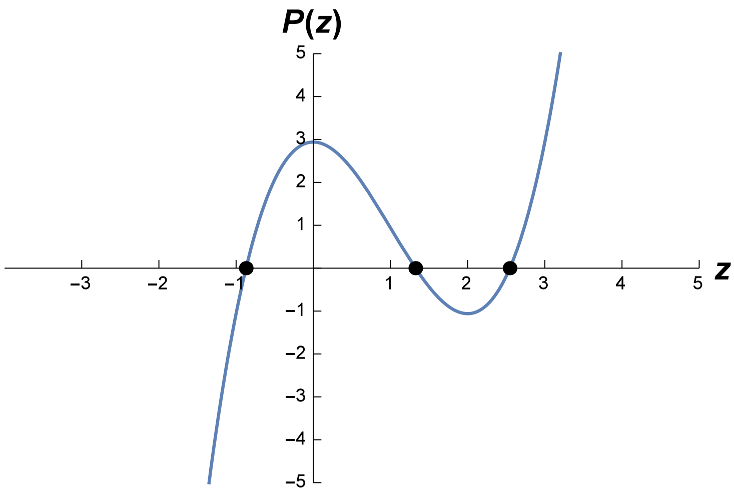

Figure 5.15: Plot of P(z) and its roots for $\beta = 1.47$ and $h(t, 0) = 1$.

- $\beta = 2$:

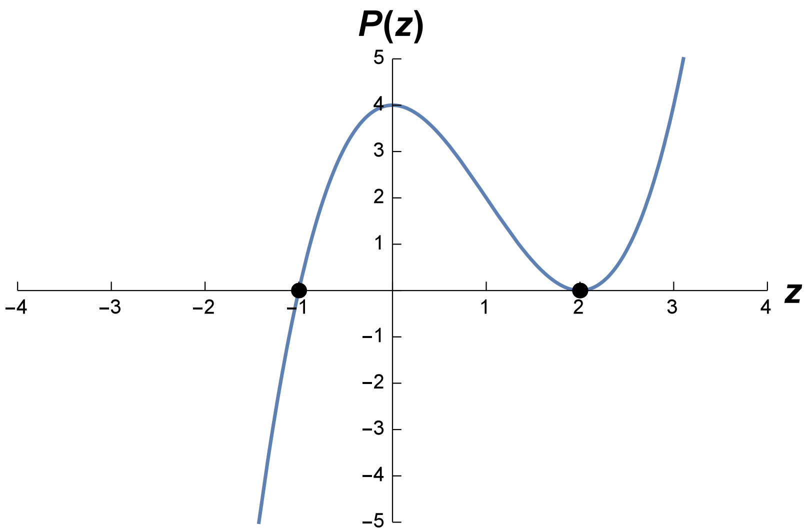

Figure 5.16: Plot of P(z) and its roots for $\beta = 2$ and $h(t, 0) = 1$.

- $\beta > 2$:

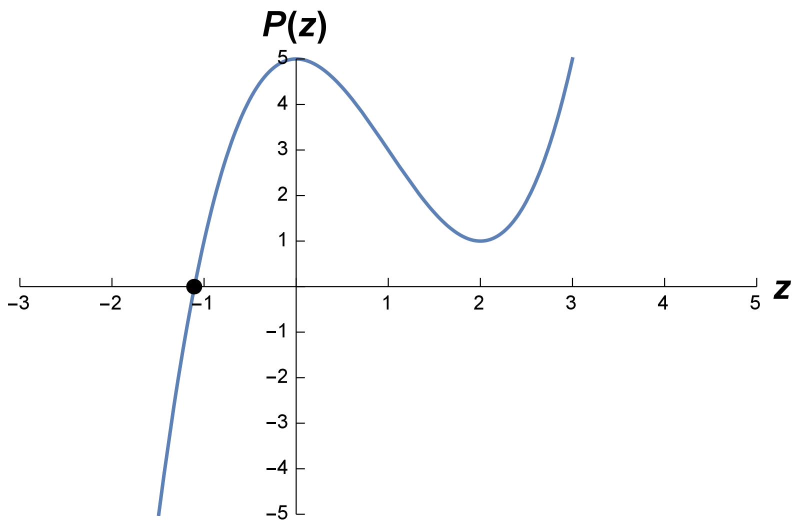

Figure 5.17: Plot of P(z) and its roots for $\beta = 2.5$ and $h(t, 0) = 1$.

Conclusions

- If $\beta = 0$: two coincident real roots at $z = 0$,
  one distinct real root greater than $h(t, 0)$.

- If $0 < \beta < 1$: three distinct real roots,
  one positive real root in the range $0 < z < h(t, 0)$.

- If $\beta = 1$: three distinct real roots,
  one real root $z = h(t, 0)$.
- If $\beta > 1$: there is no positive root in the range $0 < z \leq h(t, 0)$.
- If $\beta = 2$: there is one positive real root at $z = 2h(t, 0)$.
- If $\beta > 2$: there are no positive real roots.
- If $\beta > 0$: there is always exactly one negative root.

(ii) Suction at the base, $\beta < \mathbf{0}$

From Descartes' rule of signs [2, 6], for the polynomial equation $P(z) = 0$ where $P(z)$ is given in (5.4.86),

$$\text{Number of positive roots} \leq 1,$$
$$\text{Number of negative roots} \leq 0.$$

Also

$$P(0) = 2\beta h^3(t, 0) < 0, \tag{5.4.102}$$
$$P(h) = 2(\beta - 1)h^3(t, 0) < 0, \tag{5.4.103}$$
$$P(2h) = 2(\beta - 2)h^3(t, 0) < 0, \tag{5.4.104}$$
$$P(3h) = 2\beta h^3(t, 0) < 0. \tag{5.4.105}$$

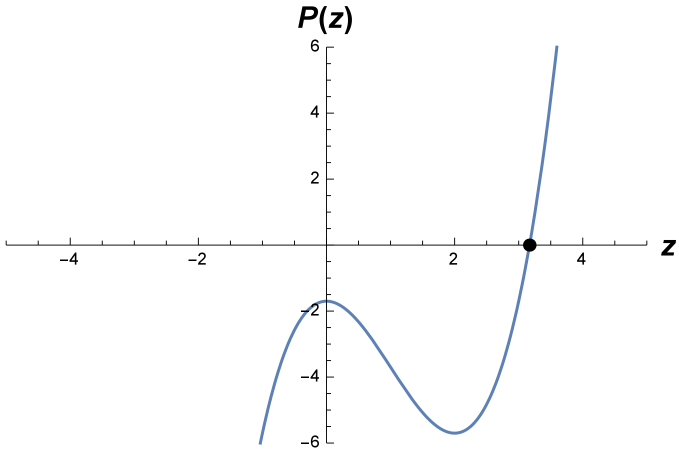

Figure 5.18: Plot of P(z) given by (5.4.86) and its zero for $\beta = -0.85$ and $h(t,0) = 1$.

We see that $P(0) = P(3h)$. There always exists one positive root for $\beta < 0$ and this positive root is greater than $h(t,0)$. It is even greater than $3h(t,0)$. There are no positive roots in the range $0 \le z \le h(t,0)$. There are no negative roots.

From the graphs of $P(z)$ against z for $\beta > 0$ and $\beta < 0$, we see that the range of interest is $0 \le \beta \le 1$ for which there are three real roots. For this range of β, $v_z(t,0,z)$ has a zero in the range $0 \le z \le h(t,0)$. This is a subset of the range for which three real roots exist which is $0 \le \beta \le 2$. For $\beta < 0$ and $\beta > 2$ there are no zeros of $v_z(t,0,z)$ in the range $0 \le z \le h(t,0)$.

We now derive the foregoing results in an alternative way by considering the discriminant of the cubic equation (5.4.39). We first transform the cubic equation to the standard form [2]

$$s^3 + 3Hs + G = 0. \tag{5.4.106}$$

We have, from (5.4.39),

$$z^3 - 3h(t,0)z^2 + 2\beta h^3(t,0) = 0. \tag{5.4.107}$$

Let

$$z = s + a \ , \tag{5.4.108}$$

where a depends at most on time t. Equation (5.4.107) becomes

$$s^3 + 3(a - h(t,0))^2 + 3a(a - 2h(t,0))s + a^3 - 3h(t,0)a^2 + 2\beta\, h^3(t,0) = 0. \quad (5.4.109)$$

In order to transform (5.4.109) to the standard form, (5.4.106), we choose

$$a = h(t,0). \quad (5.4.110)$$

Equation (5.4.109) reduces to

$$s^3 - 3h^2(t,0)s - 2(1-\beta)h^3(t,0) = 0 \quad (5.4.111)$$

where

$$z = s + h(t,0). \quad (5.4.112)$$

We are interested in the roots

$$0 \leq z \leq h(t,0)\ , \quad \text{that is}\ , \qquad -h(t,0) \leq s \leq 0\ .$$

Comparing (5.4.111) with (5.4.106) gives

$$H = -h^2(t,0)\ , \qquad G = -2(1-\beta)h^3(t,0). \quad (5.4.113)$$

The discriminant Δ of the cubic equation in standard form (5.4.106) is defined by

$$\Delta = G^2 + 4H^3. \quad (5.4.114)$$

From (5.4.113) the discriminant of the cubic equation (5.4.111) is

$$\Delta = 4\beta(\beta - 2)h^6(t,0). \quad (5.4.115)$$

General properties of the cubic equation [2]:

(i) $G^2 + 4H^3 < 0$: Three real and distinct roots.

(ii) $G^2 + 4H^3 = 0$: Three real roots, two roots coincident, one root different.
$H \neq 0$ and $G \neq 0$

(iii) $G^2 + 4H^3 = 0$, Three coincident real roots.
$H = 0$ and $G = 0$

(iv) $G^2 + 4H^3 > 0$: One real root and two complex conjugate roots.

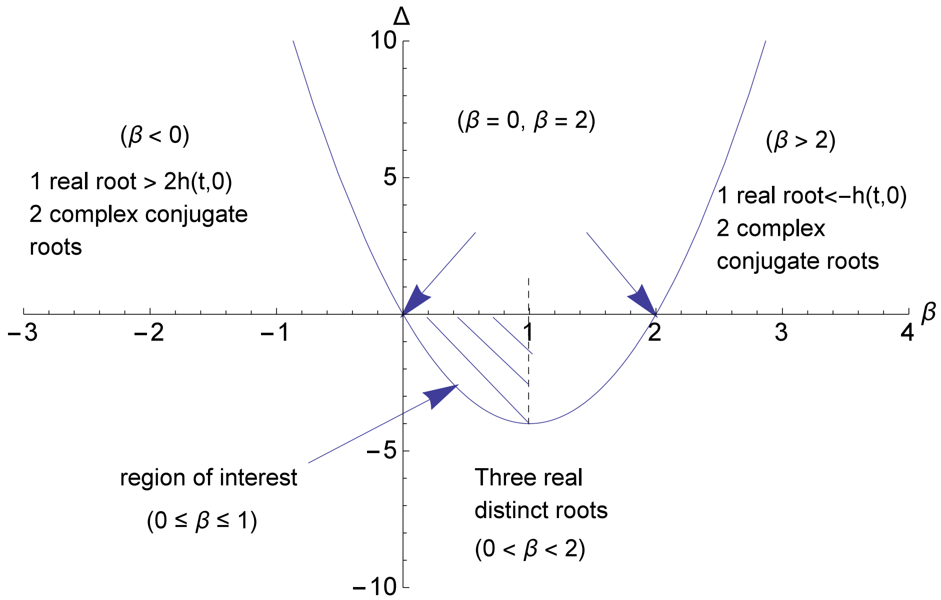

Figure 5.19: Plot of $\Delta = G^2 + 4H^3 = 4\beta(\beta - 2)h^6(t, 0)$ against β.

The discriminant, Δ, given by (5.4.115) is plotted against β in Figure 5.19. The results we deduced from graphs earlier in this section can be deduced from the Properties (i) to (iv) of Δ.

Consider first Property (i). If $\Delta < 0$ then from Figure 5.19, $0 < \beta < 2$ and the cubic equation has three real and distinct roots in agreement with Figures 5.13, 5.14 and 5.15.

Consider next Property (ii). If $\Delta = 2$ then from Figure 5.19, $\beta = 0$ or $\beta = 2$. But when $\beta = 0$ or $\beta = 2$, we see from (5.4.113) that $H \neq 0$ and $G \neq 0$. Hence when $\beta = 0$ or $\beta = 2$ there are three real roots with two roots coincident and the third root different, in agreement with Figures 5.12, 5.16. When $\beta = 0$, (5.4.111) is

$$s^3 - 3h^2(t,0)s - 2h^3(t,0) = 0, \tag{5.4.116}$$

which factorizes as

$$(s + h(t,0))^2(s - 2h(t,0)) = 0. \tag{5.4.117}$$

Thus

$$s = -h(t,0)\ , \quad s = -h(t,0)\ , \quad s = 2h(t,0), \tag{5.4.118}$$

and hence by substituting (5.4.118) into (5.4.112), the roots are

$$z = 0\ , \quad z = 0\ , \quad z = 3h(t,0). \tag{5.4.119}$$

When $\beta = 2$, (5.4.111) is

$$s^3 - 3h^2(t,0)s + 2h^3(t,0) = 0, \tag{5.4.120}$$

and therefore

$$(s - h(t,0))^2(s + h(t,0)) = 0. \tag{5.4.121}$$

Thus

$$s = -2h(t,0)\ , \quad s = h(t,0)\ , \quad s = h(t,0), \tag{5.4.122}$$

and the roots are

$$z = -h(t,0)\ , \quad z = 2h(t,0)\ , \quad z = 2h(t,0). \tag{5.4.123}$$

Consider next Property (iii). Now $\Delta = 0$ when $\beta = 0$ or $\beta = 2$, but $H \neq 0$ and $G \neq 0$ when $\beta = 0$ or $\beta = 2$. Three coincident roots is therefore not possible, in agreement with Figures 5.12 to 5.18.

Finally consider Property (iv). From Figure 5.19, $\Delta > 0$ for $\beta < 0$ and $\beta > 2$ in which case there is one real root and two complex conjugate roots. This is in agreement with Figure 5.18 for $\beta < 0$ and Figure 5.17 for $\beta > 2$.

Consider now the derivation of the three real roots of the cubic equation (5.4.111) when $0 \leq \beta \leq 2$. We observe that $H = -h^2(t,0) < 0$ which ensures that $\Delta = G^2 + 4H^3 \leq 0$ for $0 \leq \beta \leq 2$. Of interest is the real root, $-h(t,0) < s < 0$, which satisfies $\Delta < 0$ when $0 < \beta < 1$. The Cardan solution of the cubic equation is not suitable when $\Delta < 0$ because it gives the solution in complex form even although the roots are real. It is recommended to use a trigonometric solution when $\Delta < 0$ [2].

We work with the cubic equation in standard form,

$$s^3 + 3Hs + G = 0, \qquad (H < 0) \tag{5.4.124}$$

and at the end of the calculation we set

$$H = -h^2(t,0), \qquad G = 2(\beta - 1)h^3(t,0). \tag{5.4.125}$$

We look for a solution of (5.4.124) of the form

$$s = \rho \cos\theta, \qquad \rho > 0. \tag{5.4.126}$$

Substituting (5.4.126) into (5.4.124) we obtain

$$\cos^3\theta + \frac{3H}{\rho^2}\cos\theta + \frac{G}{\rho^3} = 0. \tag{5.4.127}$$

But by the trigonometric identity [17]

$$\cos 3\theta = 4\cos^3\theta - 3\cos\theta, \tag{5.4.128}$$

we have

$$\cos^3\theta - \frac{3}{4}\cos\theta - \frac{1}{4}\cos 3\theta = 0. \tag{5.4.129}$$

Comparing (5.4.127) and (5.4.129) gives

$$\frac{3H}{\rho^2} = -\frac{3}{4}, \qquad \frac{G}{\rho^3} = -\frac{1}{4}\cos 3\theta. \tag{5.4.130}$$

Thus

$$\rho = 2\,(-H)^{\frac{1}{2}}\,, \qquad \cos 3\theta = -\frac{G}{2\,(-H)^{\frac{3}{2}}}\,. \tag{5.4.131}$$

We note that the requirement that $-1 \leq \cos 3\theta \leq 1$ is satisfied since for

$$G^2 + 4H^3 = \frac{\rho^6}{16}\left(\cos^2 3\theta - 1\right) \leq 0, \tag{5.4.132}$$

requires

$$\cos^2 3\theta \leq 1, \tag{5.4.133}$$

and therefore that

$$-1 \leq \cos 3\theta \leq 1. \tag{5.4.134}$$

We let ϕ be the smallest non-negative angle which satisfies

$$\cos 3\phi = -\frac{G}{2\,(-H)^{\frac{3}{2}}} = 1 - \beta, \tag{5.4.135}$$

where

$$0 \leq 3\phi \leq \pi, \qquad 0 \leq \phi \leq \frac{\pi}{3}. \tag{5.4.136}$$

For this range of values of ϕ, $\cos 3\phi$ covers the whole range $[-1, 1]$. The general solution for θ is

$$\theta = \phi + \frac{2n\pi}{3}, \qquad n = 0, 1, 2. \tag{5.4.137}$$

Hence the roots of (5.4.124) are

$$s_n = \rho\cos\theta = 2\,(-H)^{\frac{1}{2}}\cos\left(\phi + \frac{2n\pi}{3}\right), \qquad n = 0, 1, 2. \tag{5.4.138}$$

Thus

$$s_0 = 2\,(-H)^{\frac{1}{2}}\cos\phi, \tag{5.4.139}$$

$$s_1 = 2\,(-H)^{\frac{1}{2}}\cos\left(\phi + \frac{2\pi}{3}\right), \tag{5.4.140}$$

$$s_2 = 2\,(-H)^{\frac{1}{2}}\cos\left(\phi + \frac{4\pi}{3}\right), \tag{5.4.141}$$

and by substituting into (5.4.112) the roots of the cubic (5.4.107) are

$$z_0 = h(t, 0)\left[1 + 2\cos\phi\right], \tag{5.4.142}$$

$$\begin{aligned}
z_1 &= h(t,0)\left[1+2\cos\left(\phi+\frac{2\pi}{3}\right)\right], && (5.4.143)\\
z_2 &= h(t,0)\left[1+2\cos\left(\phi+\frac{4\pi}{3}\right)\right]. && (5.4.144)
\end{aligned}$$

For the roots (5.4.142)-(5.4.144), we will consider the special cases of $\beta = 0$, β small, $\beta = 1$ and $\beta = 2$. Using the trigonometric identities [17]

$$\begin{aligned}
\cos(A+B) &= \cos A\cos B - \sin A\sin B, && (5.4.145)\\
\cos(A-B) &= \cos A\cos B + \sin A\sin B, && (5.4.146)\\
\sin(A+B) &= \sin A\cos B + \cos A\sin B, && (5.4.147)\\
\sin(A-B) &= \sin A\cos B - \cos A\sin B, && (5.4.148)
\end{aligned}$$

and

$$\cos\frac{\pi}{3} = \frac{1}{2}, \qquad \sin\frac{\pi}{3} = \frac{\sqrt{3}}{2}, \tag{5.4.149}$$

we have

$$\begin{aligned}
\cos\frac{2\pi}{3} &= \cos\left(\pi-\frac{\pi}{3}\right) = -\frac{1}{2}, && (5.4.150)\\
\cos\frac{4\pi}{3} &= \cos\left(\pi+\frac{\pi}{3}\right) = -\frac{1}{2}, && (5.4.151)\\
\sin\frac{2\pi}{3} &= \sin\left(\pi-\frac{\pi}{3}\right) = \frac{\sqrt{3}}{2}, && (5.4.152)\\
\sin\frac{4\pi}{3} &= \sin\left(\pi+\frac{\pi}{3}\right) = -\frac{\sqrt{3}}{2}. && (5.4.153)
\end{aligned}$$

Case(i) $\beta = 0$

Substituting $\beta = 0$ into (5.4.135), we have

$$\cos 3\phi = 1, \tag{5.4.154}$$

and therefore since $0 \leq \phi \leq \frac{\pi}{3}$,

$$\phi = 0. \tag{5.4.155}$$

Hence, by substituting (5.4.155) into (5.4.142)-(5.4.144), the roots of the cubic equation (5.4.107) for $\beta = 0$ are

$$z_0 = 3h(t,0), \tag{5.4.156}$$

$$z_1 = 0, \tag{5.4.157}$$

$$z_2 = 0, \tag{5.4.158}$$

where we used (5.4.150) and (5.4.151). We see that it will be either z_1 or z_2 which will evolve into the zero inside the thin fluid film.

Case (ii) Small $\beta > 0$

For a given small $\beta > 0$, we let

$$\phi = \delta. \tag{5.4.159}$$

Equation (5.4.135) then becomes

$$\cos 3\delta = 1 - \beta. \tag{5.4.160}$$

We need to express δ in terms on β. Now using the series expansion for cosine [17],

$$\cos\delta = 1 - \frac{\delta^2}{2} + \frac{\delta^4}{24} + \bigcirc(\delta^6), \tag{5.4.161}$$

equation (5.4.160) becomes

$$\frac{9}{2}\delta^2 - \frac{27}{8}\delta^4 + \bigcirc\left(\delta^6\right) = \beta. \tag{5.4.162}$$

To the lowest order in δ,

$$\delta^2 = \frac{2}{9}\beta \tag{5.4.163}$$

and

$$\delta = \frac{\sqrt{2}}{3}\beta^{\frac{1}{2}}. \tag{5.4.164}$$

To estimate the error in (5.4.164) we note that

$$\delta = \bigcirc\left(\beta^{\frac{1}{2}}\right), \tag{5.4.165}$$

thus (5.4.162) is of the form

$$\delta^2 = \frac{2}{9}\beta + \bigcirc\left(\beta^2\right) = \frac{2}{9}\beta\left[1 + \bigcirc\left(\beta\right)\right], \tag{5.4.166}$$

and consequently

$$\delta = \frac{\sqrt{2}}{3}\,\beta^{\frac{1}{2}}\left[1 + \bigcirc(\beta)\right]^{\frac{1}{2}} = \frac{\sqrt{2}}{3}\,\beta^{\frac{1}{2}} + \bigcirc\left(\beta^{\frac{3}{2}}\right). \tag{5.4.167}$$

This result for δ is sufficiently accurate to re-check the perturbation results obtained in Section 5.4.2.

(a) Perturbation solution for $\mathbf{z_0}$

Substituting (5.4.159) into (5.4.142) for z_0, we obtain

$$z_0 = h(t,0)\left[1 + 2\cos\delta\right]. \tag{5.4.168}$$

But substituting (5.4.167) into (5.4.161) gives

$$\begin{aligned}
\cos\delta &= 1 - \frac{1}{2}\left[\frac{\sqrt{2}}{3}\,\beta^{\frac{1}{2}} + \bigcirc\left(\beta^{\frac{3}{2}}\right)\right]^2 + \frac{1}{24}\left[\frac{\sqrt{2}}{3}\,\beta^{\frac{1}{2}} + \bigcirc\left(\beta^{\frac{3}{2}}\right)\right]^4 \\
&= 1 - \frac{1}{9}\beta\left[1 + \bigcirc(\beta)\right] + \bigcirc\left(\beta^2\right) \\
&= 1 - \frac{1}{9}\beta + \bigcirc\left(\beta^2\right).
\end{aligned} \tag{5.4.169}$$

Hence, substituting (5.4.169) into (5.4.168) we obtain

$$z_0 = 3\left[1 - \frac{2}{27}\beta + \bigcirc\left(\beta^2\right)\right]h(t,0). \tag{5.4.170}$$

This agrees with the perturbation solution given in (5.4.58).

(b) Perturbation solution for $\mathbf{z_1}$

Substituting (5.4.159) into (5.4.143) for z_1 we obtain

$$z_1 = h(t,0)\left[1 + 2\cos\left(\delta + \frac{2\pi}{3}\right)\right]. \tag{5.4.171}$$

But using (5.4.145), (5.4.150) and (5.4.152) we obtain

$$\cos\left(\delta + \frac{2\pi}{3}\right) = -\frac{1}{2}\cos\delta - \frac{\sqrt{3}}{2}\sin\delta. \tag{5.4.172}$$

Substituting (5.4.167) into the series expansion for sine we obtain

$$\sin\delta = \delta - \frac{\delta^3}{6} + \bigcirc\left(\delta^5\right) = \frac{\sqrt{2}}{3}\beta^{\frac{1}{2}} + \bigcirc\left(\beta^{\frac{3}{2}}\right), \tag{5.4.173}$$

Thus substituting (5.4.169) and (5.4.173) into (5.4.172) gives

$$\cos\left(\delta + \frac{2\pi}{3}\right) = -\frac{1}{2}\left[1 + \left(\frac{2}{3}\right)^{\frac{1}{2}}\beta^{\frac{1}{2}} - \frac{1}{9}\beta + \bigcirc\left(\beta^{\frac{3}{2}}\right)\right]. \tag{5.4.174}$$

Hence substituting (5.4.174) into (5.4.171) we obtain

$$z_1 = \left[-\left(\frac{2}{3}\right)^{\frac{1}{2}}\beta^{\frac{1}{2}} + \frac{1}{9}\beta + \bigcirc\left(\beta^{\frac{3}{2}}\right)\right]h(t,0). \tag{5.4.175}$$

This result agrees with the perturbation solution given in (5.4.68). The zero z_1 does not lie inside the thin fluid film.

(c) Perturbation solution for $\mathbf{z_2}$

Substituting (5.4.159) into (5.4.144) for z_2, we obtain

$$z_2 = h(t,0)\left[1 + 2\cos\left(\delta + \frac{4\pi}{3}\right)\right]. \tag{5.4.176}$$

But using (5.4.145), (5.4.151) and (5.4.153)

$$\cos\left(\delta + \frac{4\pi}{3}\right) = -\frac{1}{2}\cos\delta + \frac{\sqrt{3}}{2}\sin\delta. \tag{5.4.177}$$

Thus by substituting (5.4.169) and (5.4.173) into (5.4.177) we obtain

$$\cos\left(\delta + \frac{4\pi}{3}\right) = -\frac{1}{2}\left[1 - \left(\frac{2}{3}\right)^{\frac{1}{2}}\beta^{\frac{1}{2}} - \frac{1}{9}\beta + \bigcirc\left(\beta^{\frac{3}{2}}\right)\right]. \tag{5.4.178}$$

Finally substituting (5.4.178) into (5.4.176) gives

$$z_2 = \left[\left(\frac{2}{3}\right)^{\frac{1}{2}}\beta^{\frac{1}{2}} + \frac{1}{9}\beta + \bigcirc\left(\beta^{\frac{3}{2}}\right)\right]h(t,0). \tag{5.4.179}$$

This result agrees with the perturbation solution given in (5.4.67). The zero z_2 lies inside the thin fluid film. This is the zero in which we are interested. The perturbation expansion of the exact solution helped us to identify where z_0, z_1 and z_2 lie.

Case (iii) $\beta = 1$

Substituting $\beta = 1$ into (5.4.135), we obtain

$$\cos 3\phi = 0, \tag{5.4.180}$$

and thus since $0 \leq \phi \leq \frac{\pi}{3}$,

$$\phi = \frac{\pi}{6}. \tag{5.4.181}$$

Hence, by substituting (5.4.181) into (5.4.142)-(5.4.144), using

$$\cos\frac{\pi}{6} = \frac{\sqrt{3}}{2}, \qquad \sin\frac{\pi}{6} = \frac{1}{2}, \tag{5.4.182}$$

the trigonometric identity (5.4.145) and (5.4.150) to (5.4.153), the roots of the cubic equation (5.4.107) for $\beta = 1$ are found to be

$$z_0 = \left[1 + \sqrt{3}\right] h(t,0), \tag{5.4.183}$$

$$z_1 = -\left[\sqrt{3} - 1\right] h(t,0), \tag{5.4.184}$$

$$z_2 = h(t,0). \tag{5.4.185}$$

This is the limiting case for the existence of the zero z_2 of $v_z(t,z,0)$ inside the thin film. Since

$$v_z(t,0,z)|_{z=h(t,0)} = 0, \tag{5.4.186}$$

it follows that

$$\frac{d}{dt}h(t,0) = 0. \tag{5.4.187}$$

The height of the thin film at the top of the centre line therefore remains constant in time.

Case (iv) $\beta = 2$

This case lies outside the range of physical interest because no roots are inside the thin fluid film. However, it is worth considering because it shows how this form of the solution of the cubic equation gives non-trigonometric results. Substituting $\beta = 2$ into (5.4.135), we obtain

$$\cos 3\phi = -1, \tag{5.4.188}$$

and therefore since $0 \le \phi \le \frac{\pi}{3}$,

$$\phi = \frac{\pi}{3}. \tag{5.4.189}$$

Hence, by substituting (5.4.189) into (5.4.142)-(5.4.144), and using

$$\cos\frac{\pi}{3} = \frac{1}{2}, \qquad \cos\pi = -1, \qquad \cos\frac{5\pi}{3} = \frac{1}{2}, \tag{5.4.190}$$

the roots of the cubic equation (5.4.107) for $\beta = 2$ are obtained:

$$z_0 = 2h(t,0), \tag{5.4.191}$$

$$z_1 = -h(t,0), \tag{5.4.192}$$

$$z_2 = 2h(t,0). \tag{5.4.193}$$

There are no zeros of the cubic polynomial inside the thin film and therefore there are no zeros of $v_z(t,0,z)$ inside the thin film.

5.4.4 Region of flow at the base for fluid injection

The exact and perturbation solution for the zero, z_2, of $v_z(t,0,z)$ on the centre line give an estimate of the thickness of the layer at the base that is affected by fluid injection at the base when $0 < \beta < 1$. For $\beta \ge 1$ the whole of the flow in the thin film is altered by fluid injection at the base. The zero $z = z_2$ is the dividing point between upward flow on the centre line due to fluid injection at the base and downward flow on the centre line due to spreading by gravity. From the exact solution (5.4.144) for $0 \le \beta \le 1$,

$$\frac{z_2}{h(t,0)} = 1 + 2\cos\left(\phi + \frac{4\pi}{3}\right), \tag{5.4.194}$$

where ϕ satisfies

$$\cos 3\phi = 1 - \beta, \qquad 0 \leq \phi \leq \frac{\pi}{3}, \tag{5.4.195}$$

while from the singular perturbation solution (5.4.67) for small $\beta > 0$

$$\frac{z_2}{h(t,0)} = \left(\frac{2}{3}\right)^{\frac{1}{2}} \beta^{\frac{1}{2}} + \frac{1}{9}\beta + \bigcirc\left(\beta^{\frac{3}{2}}\right). \tag{5.4.196}$$

In Table 5.1 the exact and perturbation solutions for $\frac{z_2}{h(t,0)}$ are presented for values of β in the range $0 \leq \beta < 1$. This gives as estimate of the thickness of the layer at the base due to fluid injection at the base. The error in the perturbation solution to order $\beta^{\frac{1}{2}}$ is about 10% for $\beta = 0.4$ while the error in the perturbation solution to order β is less than 7.25% for the whole range $0 \leq \beta \leq 1$. In order to obtain more information about the flow in the thin film we will consider the streamlines in the next section.

β	$\mathbf{1+2}\cos\left(\phi+\frac{\mathbf{4}\pi}{\mathbf{3}}\right)$	$\left(\frac{\mathbf{2}}{\mathbf{3}}\right)^{\frac{\mathbf{1}}{\mathbf{2}}}\beta^{\frac{\mathbf{1}}{\mathbf{2}}}$	Error %	$\left(\frac{\mathbf{2}}{\mathbf{3}}\right)^{\frac{\mathbf{1}}{\mathbf{2}}}\beta^{\frac{\mathbf{1}}{\mathbf{2}}}+\frac{\mathbf{1}}{\mathbf{9}}\beta$	Error %
0	0	0	0	0	0
0.1	0.2707	0.2582	4.62	0.2693	0.52
0.2	0.3916	0.3651	6.77	0.3873	1.10
0.3	0.4888	0.4472	8.51	0.4805	1.7
0.4	0.5743	0.5164	10.08	0.5608	2.35
0.5	0.6527	0.5774	11.54	0.6329	3.03
0.6	0.7265	0.6325	12.94	0.6992	3.76
0.7	0.7972	0.6831	14.31	0.7609	4.55
0.8	0.8659	0.7303	15.66	0.8192	5.39
0.9	0.9332	0.7746	17.00	0.8746	6.28
1	1	0.8165	18.35	0.9276	7.24

Table 5.1: The exact and perturbation solution for the zero, $\frac{z_2}{h(t,0)}$, of $v_z(t,0,z)$ on the centre line .

5.5 Streamlines

The streamlines will be plotted for a range of values of β inside the thin film to investigate how the flow field depends on β.

A streamline is a line in the fluid, the tangent vector to which is everywhere parallel to the velocity vector $\underline{\mathbf{v}}$ instantaneously [3]. In two-dimensional flow the streamlines can be obtained from a stream function. In two-dimensional flow the stream function $\psi(x,z)$ satisfies (in dimensional variables)

$$v_x = \frac{\partial \psi}{\partial z}, \qquad v_z = -\frac{\partial \psi}{\partial x}. \tag{5.5.1}$$

The stream function is constant along a streamline. For

$$(\underline{v} \cdot \underline{\nabla})\psi = v_x \frac{\partial \psi}{\partial x} + v_z \frac{\partial \psi}{\partial z} = \frac{\partial \psi}{\partial z}\frac{\partial \psi}{\partial x} - \frac{\partial \psi}{\partial x}\frac{\partial \psi}{\partial z} = 0. \tag{5.5.2}$$

The streamlines in two-dimensional flow at any instant are therefore obtained by plotting

$$\psi(x,z) = k, \tag{5.5.3}$$

for a range of values of the constant k.

We make (5.5.1) dimensionless by letting

$$\overline{\psi} = \frac{\psi}{\psi_0}, \tag{5.5.4}$$

where ψ_0 is to be determined. Substituting (5.5.4) as well as the dimensionless quantities $\overline{x}, \overline{z}, \overline{v}_x$ and $\overline{v}_z$ defined by (3.2.23) into (5.5.1), we obtain

$$\overline{v}_x = \frac{\psi_0}{H\,U}\frac{\partial \overline{\psi}}{\partial \overline{z}}, \qquad \overline{v}_z = -\frac{\psi_0}{H\,U}\frac{\partial \overline{\psi}}{\partial \overline{x}}. \tag{5.5.5}$$

If we choose

$$\psi_0 = H\,U = \frac{\rho\, g\, H^4}{\mu\, W_0}, \tag{5.5.6}$$

where U was defined in (3.2.22), then (5.5.5) simplifies to

$$\overline{v}_x = \frac{\partial \overline{\psi}}{\partial \overline{z}}, \qquad \overline{v}_z = -\frac{\partial \overline{\psi}}{\partial \overline{x}}. \tag{5.5.7}$$

The overhead bars in (5.5.7) will be suppressed.

We substitute the dimensionless velocity components v_x and v_z given by (3.2.46) and (5.4.8) into (5.5.7) which gives the following two first order partial differential equations for the stream function $\psi(x, z)$:

$$\frac{\partial \psi}{\partial z} = v_x = \left(\frac{z^2}{2} - z\, h(t,x)\right) \frac{\partial h}{\partial x}(t,x), \tag{5.5.8}$$

$$\frac{\partial \psi}{\partial x} = -v_z = -v_n(t,x) + \frac{z^3}{6}\frac{\partial^2 h}{\partial x^2} - \frac{z^2}{2}\left[h(t,x)\frac{\partial^2 h}{\partial x^2} + \left(\frac{\partial h}{\partial x}\right)^2\right]. \tag{5.5.9}$$

We first check the consistency condition

$$\frac{\partial^2 \psi}{\partial x \partial z} = \frac{\partial^2 \psi}{\partial z \partial x}. \tag{5.5.10}$$

Differentiating (5.5.8) partially with respect to x

$$\frac{\partial^2 \psi}{\partial x \partial z} = \frac{z^2}{2}\frac{\partial^2 h}{\partial x^2} - z\left(\frac{\partial h}{\partial x}\right)^2 - z\, h\frac{\partial^2 h}{\partial x^2}, \tag{5.5.11}$$

and (5.5.9) partially with respect to z gives

$$\frac{\partial^2 \psi}{\partial x \partial z} = \frac{\partial^2 \psi}{\partial z \partial x} = \frac{z^2}{2}\frac{\partial^2 h}{\partial x^2} - z\, h\frac{\partial^2 h}{\partial x^2} - z\left(\frac{\partial h}{\partial x}\right)^2. \tag{5.5.12}$$

Thus the compatibility condition (5.5.10) is satisfied. We integrate (5.5.8) with respect to z to obtain

$$\psi(t,z,x) = \frac{z^3}{6}\frac{\partial h}{\partial x} - \frac{z^2}{2}h\frac{\partial h}{\partial x} + M(t,x). \tag{5.5.13}$$

In order to obtain the function of integration $M(t,x)$, substitute (5.5.13) into (5.5.9). Thus

$$\frac{\partial M(t,x)}{\partial x} = -v_n(t,x). \tag{5.5.14}$$

Integrating (5.5.14) from 0 to x gives

$$M(t,x) = -\int_0^x v_n(t,x)\, dx + D(t), \tag{5.5.15}$$

where $D(t) = M(t,0)$. Hence

$$\psi(t,z,x) = A(t,x)\, z^3 + B(t,x)\, z^2 + C(t,x) + D(t), \tag{5.5.16}$$

where

$$A(t,x) = \frac{1}{6}\frac{\partial h}{\partial x}, \qquad B(t,x) = -\frac{1}{2}h\frac{\partial h}{\partial x},$$

$$C(t,x) = -\int_0^x v_n(t,x)\,dx, \qquad D(t) = \text{arbitrary function of t.} \quad (5.5.17)$$

The streamlines in the (x,z) plane at time t satisfy

$$\psi(t,x,z) = k(t), \quad (5.5.18)$$

where $k(t)$ is an arbitrary function of t. The streamlines are obtained by solving the cubic equation

$$A(t,x)z^3 + B(t,x)z^2 + C(t,x) = K(t), \quad (5.5.19)$$

for z where $K(t) = k(t) - D(t)$ is an arbitrary function of t. The streamlines at time t are obtained by giving $K(t)$ a range of values. Along a given streamline at a given time, K is constant. Since $div\, v = 0$, the streamlines either form closed curves or begin and end on a free surface or boundary. Closed curves correspond to values of K that give two real roots of the cubic equation inside the thin film. Lines correspond to values of K that give only one real root inside the thin film.

We calculate the coefficients $A(t,x), B(t,x)$ and $C(t,x)$ in (5.5.17) in terms of the invariant solution obtained in (5.3.7)-(5.3.12). Substituting (5.3.10) into (5.5.17) gives

$$A(t,\zeta) = -\frac{1}{9}W^{\beta-2}(t)\frac{\zeta}{(1-\zeta^2)^{\frac{2}{3}}}, \quad (5.5.20)$$

and

$$B(t,\zeta) = \frac{1}{3}W^{2\beta-3}(t)\frac{\zeta}{(1-\zeta^2)^{\frac{1}{3}}}. \quad (5.5.21)$$

By substituting (5.3.11) for $v_n(t,x)$ into (5.5.17), it can be verified that

$$C(t,\zeta) = -\frac{2\beta}{9}W^{4\beta-5}(t)\int_0^\zeta \left(1-\zeta^{*2}\right)^{\frac{1}{3}} d\zeta^*. \quad (5.5.22)$$

By using (5.3.12), equations (5.5.20) to (5.5.22) may be expressed in terms of t and x as

$$A(t,x) = -\frac{1}{9}W^{\beta-3}(t)\frac{x}{\left(1-\frac{x^2}{W^2(t)}\right)^{\frac{2}{3}}}, \tag{5.5.23}$$

$$B(t,x) = \frac{1}{3}W^{2\beta-4}(t)\frac{x}{\left(1-\frac{x^2}{W^2(t)}\right)^{\frac{1}{3}}}, \tag{5.5.24}$$

$$C(t,x) = -\frac{2\beta}{9}W^{4\beta-6}(t)\int_0^x \left(1-\frac{x^{*2}}{W^2(t)}\right)^{\frac{1}{3}} dx^*. \tag{5.5.25}$$

The solution of the cubic equation will give z as a function of t and x. The streamlines are plotted against x and the range of the base is $W(t) \le x \le W(t)$.

The streamlines will be plotted at $t = 1$ for a range of values of β to investigate the flow within the thin film. The direction of flow is indicated by the arrows. In Figure 5.20 the streamlines are plotted for $\beta = 0$. All streamlines begin and end on the free surface except the streamline $x = 0$ which is the centre line. The two-dimensional thin film spreads by fluid descending as shown by the streamlines. This is a consequence of the spreading due to gravity.

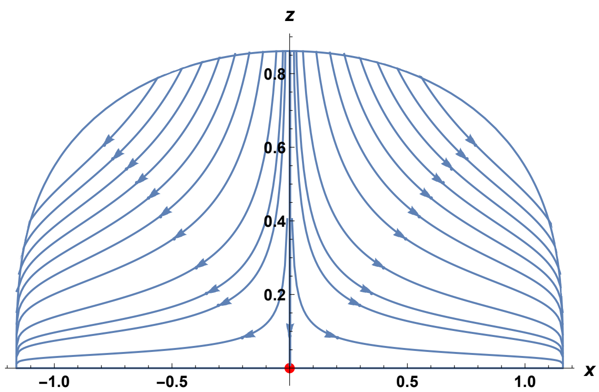

Figure 5.20: Streamlines for $\beta = 0$ plotted against x for $-W(t) \le x \le W(t)$ at $t = 1$.

In Figure 5.21 the streamlines are plotted for negative β values which indicate suction of fluid out of the thin film at the base. The magnitude of suction increases as β becomes more negative. The values of β considered are $\beta = -0.5$, $\beta = -1$ and $\beta = -1.5$. In Figure 5.21 an increase in the magnitude of suction causes a decrease in the height of the surface profile. The streamlines begin on the free surface and end on the free surface and on the boundary. The centre line is a streamline. The arrows along the streamlines point downward indicating that fluid is sucked out of the thin film. The streamlines are perpendicular to the base because there is no slip at the base.

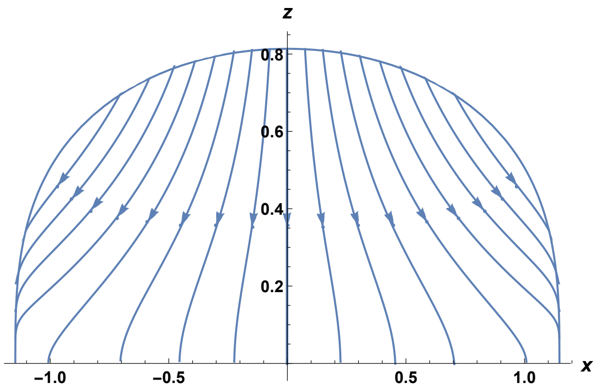

(a) $\beta = -0.5$

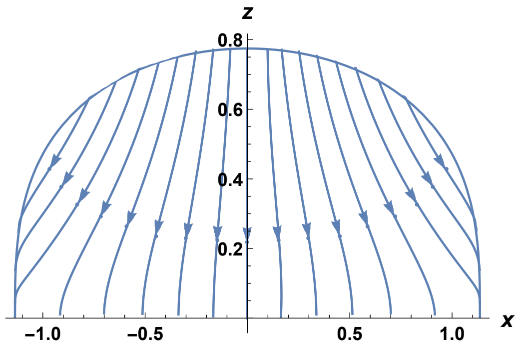

(b) $\beta = -1$

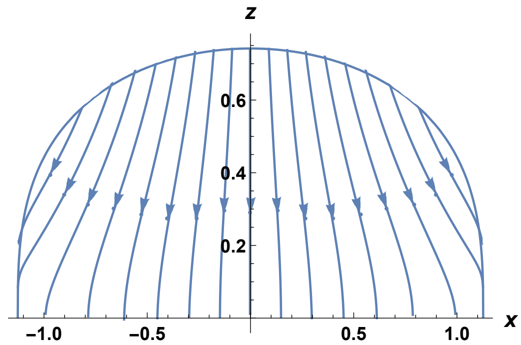

(c) $\beta = -1.5$

Figure 5.21: Streamlines for a range of negative values of β plotted against x for $-W(t) \leq x \leq W(t)$ at $t = 1$.

In Figure 5.22 the streamlines are plotted for positive values of β which describes the injection of fluid into the thin film at the base. The magnitude of fluid injection increases as β increases. The values of β chosen are $\beta = 0.1$, $\beta = 0.2$, $\beta = 0.4$, $\beta = 0.6$, $\beta = 0.8$ and $\beta = 1$. The $\bullet$ indicates the point z_2 on the centre line at which the fluid velocity is zero and is the exact solution (5.4.194) and the perturbation solution (5.4.196). Numerical values of ${}^{z_2}/h(t,0)$ are presented in Table 5.1. A dividing streamline starts at the point $(0, z_2)$ on the centre line and divides the flow into two regions. In the upper region the streamlines begin on the free surface and end on the free surface. In the upper region the fluid descends and spreads due to gravity as indicated by the arrows. It is as if the base on which the spreading occurs has been lifted by an amount z_2 due to blowing. The lower region is due to the injection of fluid into the thin film at the base. The streamlines begin at the base and end on the free surface. The streamlines are perpendicular to the base because there is no slip at the base. They then extend outwards from the centre line because of spreading due to gravity. The thickness of the fluid layer at the base is approximately z_2. As the strength of the blowing, β, increases we see from Figure 5.22 that the thickness of the layer at the base increases. It forms a larger fraction of the thin film in agreement with the numerical values in Table 5.1. For $\beta = 1$ there is no longer two regions. The lower region completely fills the thin film for $\beta \geq 1$. Thus if the blowing is sufficiently strong there is only one fluid region in the thin film and the fluid velocity on the centre line is positive for $0 \leq z \leq h(t,0)$.

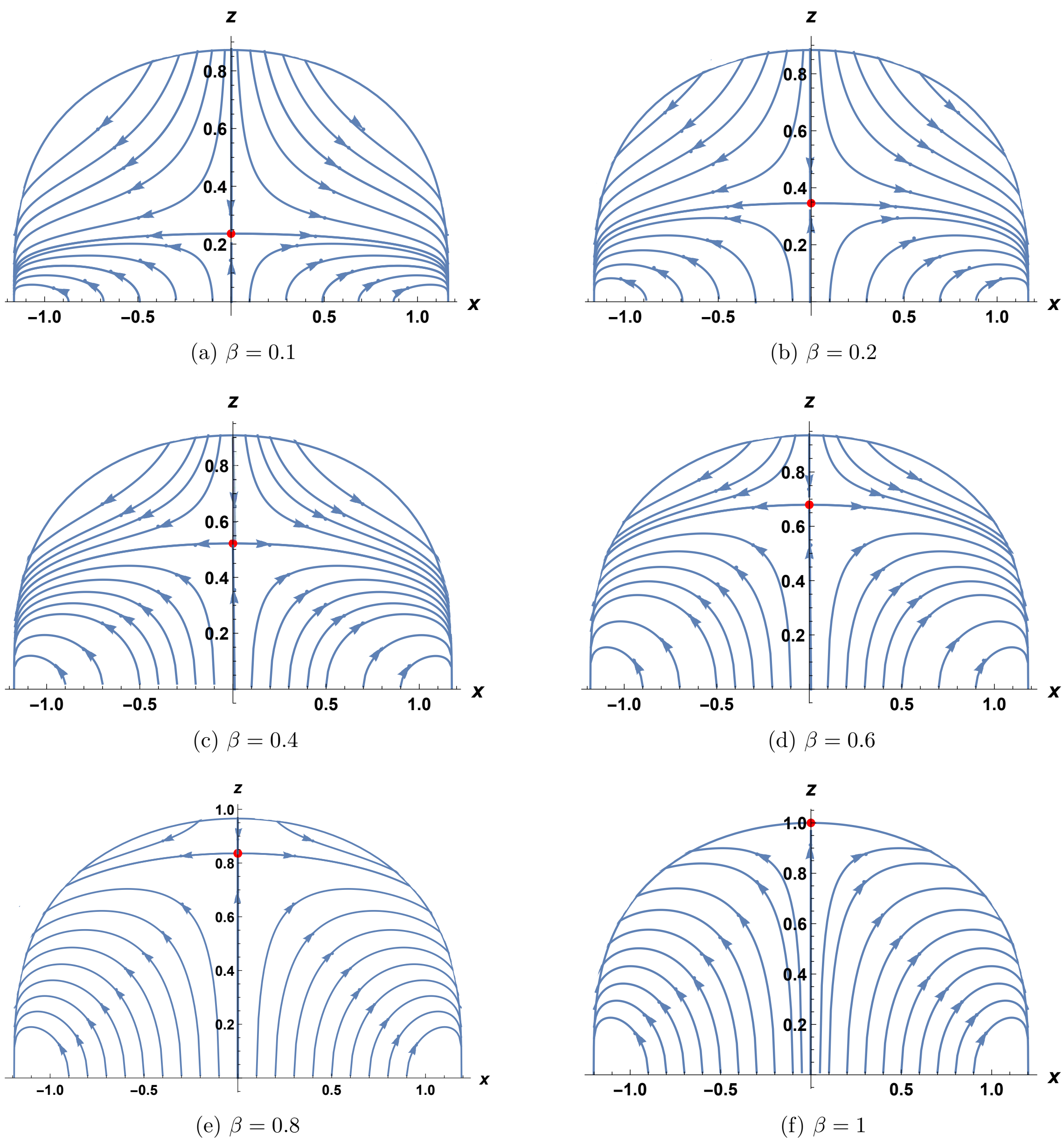

(a) $\beta = 0.1$ (b) $\beta = 0.2$

(c) $\beta = 0.4$ (d) $\beta = 0.6$

(e) $\beta = 0.8$ (f) $\beta = 1$

Figure 5.22: Streamlines for a range of positive values of β plotted against x for $W(t) \leq x \leq W(t)$ at $t = 1$.

In Figure 5.23 the streamlines are plotted for $\beta = 0.4$ at times $t = 1$ and $t = 10$. We see that, z_2 the height above the base of the point of intersection of the dividing streamline with the centre line, decreases with time. The thickness of the fluid layer at the base due to blowing therefore decreases with time as the thin film spreads under gravity.

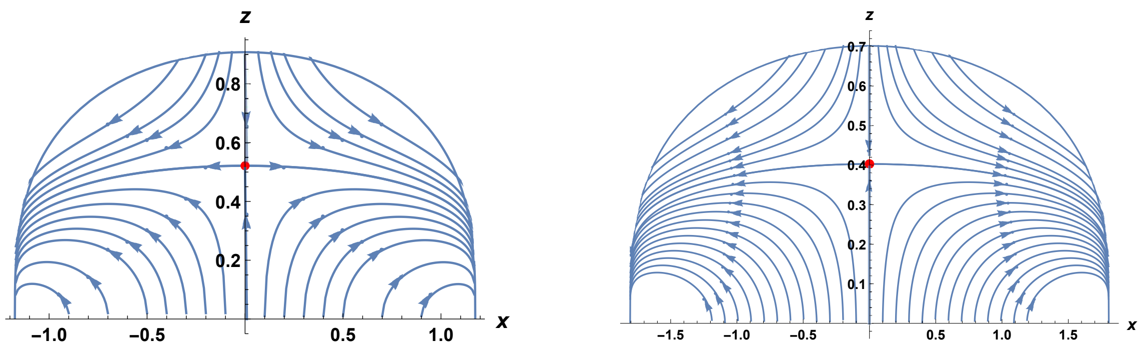

(a) $t = 1$ (b) $t = 10$

Figure 5.23: Streamlines for $\beta = 0.4$ plotted against x for $-W(t) \leq x \leq W(t)$ at $t = 1$ and $t = 10$.

In Figures (5.20) to (5.23), the streamlines are plotted in the (x, z)-plane. The base of the thin film expands and the height increases or decreases. We now investigate the streamlines in the (ζ, z^*)-plane where

$$\zeta = \frac{x}{W(t)}, \qquad -1 \leq \zeta \leq 1, \tag{5.5.26}$$

$$z^* = \frac{z}{h(t,0)}, \qquad 0 \leq z^* \leq 1. \tag{5.5.27}$$

The cubic equation (5.5.19), written in terms of ζ and z^* is

$$A^*(t,\zeta)z^{*3} + B^*(t,\zeta)z^{*2} + C(t,\zeta) = K(t), \tag{5.5.28}$$

where

$$A^*(t,\zeta) = A(t,\zeta)h^3(t,0), \tag{5.5.29}$$

$$B^*(t,\zeta) \quad = \quad B(t,\zeta)h^2(t,0). \tag{5.5.30}$$

But from (5.3.10) and (5.3.7),

$$h(t,0) = W^{\beta-1}(t) \tag{5.5.31}$$

and therefore using (5.5.20) and (5.5.21)

$$A^*(t,\zeta) \quad = \quad -\frac{1}{9}W^{4\beta-5}(t)\frac{\zeta}{(1-\zeta^2)^{\frac{2}{3}}}, \tag{5.5.32}$$

$$B^*(t,\zeta) \quad = \quad \frac{1}{3}W^{4\beta-5}(t)\frac{\zeta}{(1-\zeta^2)^{\frac{1}{3}}}. \tag{5.5.33}$$

Also, $C(t,\zeta)$ is given in (5.5.22). We see that $A^*(t,\zeta)$, $B^*(t,\zeta)$ and $C(t,\zeta)$ depend explicitly on time through the same factor $W^{4\beta-5}(t)$. The cubic equation (5.5.28) becomes

$$-\frac{1}{9}\frac{\zeta}{(1-\zeta^2)^{\frac{2}{3}}}z^{*3} + \frac{1}{3}\frac{\zeta}{(1-\zeta^2)^{\frac{1}{3}}}z^{*2} - \frac{2}{9}\beta\int_0^\zeta \left(1-\zeta^2\right)^{\frac{1}{3}} d\,\zeta = K^*, \tag{5.5.34}$$

where

$$K^* = \frac{K(t)}{W^{4\beta-5}(t)}. \tag{5.5.35}$$

The streamlines at any given instant are obtained by giving K^* a range of values. Since (5.5.34) does not depend on time explicitly the streamline pattern on the (ζ, z^*)-plane is the same for all time and depends only on the parameter β. From (5.4.194) and (5.4.196) the height above the base of the point of intersection of the dividing streamline with the centre line is

$$\begin{aligned} z_2^* = \frac{z_2}{h(t,0)} \quad &= \quad 1 + 2\cos\left(\phi + \frac{4\pi}{3}\right), \\ &= \quad \left(\frac{2}{3}\right)^{\frac{1}{2}}\beta^{\frac{1}{2}} + \frac{1}{9}\beta + \bigcirc\left(\beta^{\frac{3}{2}}\right). \end{aligned} \tag{5.5.36}$$

The centre line is a streamline and the point of the intersection of the dividing streamline with the centre line is a stagnation point of the fluid flow because the fluid velocity is zero at that point. In Figure 5.24 the streamlines are plotted in the

(ζ, z^*)-plane for a range of values of β and for $-1 \leq \zeta \leq 1$ and $0 \leq z^* \leq 1$. The values of z^* on the centre line agrees with the results given in Table 5.1. Figure 5.24 compares with Figure 5.23 plotted in the (x, z)-plane at time $t = 1$.

The representation of the streamlines in Figure 5.24 using coordinates (ζ, z^*) is useful because it illustrates all the properties of the streamlines, except their evolution with time, in one set of graphs.

For Model I for a two-dimensional thin film the thin fluid film approximation is satisfied provided $-\infty < \beta \leq 2$. In all the graphs β was chosen to lie in this range.

5.6 Conclusions

When the fluid velocity at the base is proportional to the height of the thin fluid film a complete analytical solution can be derived and the fluid variables and streamlines can be fully analysed. Provided the blowing is not too strong a layer of fluid forms at the base due to fluid injection. The thickness of this layer was estimated in terms of the strength of the fluid injection velocity. The thin film approximation is satisfied for the whole range of suction but only for weak to moderate blowing.

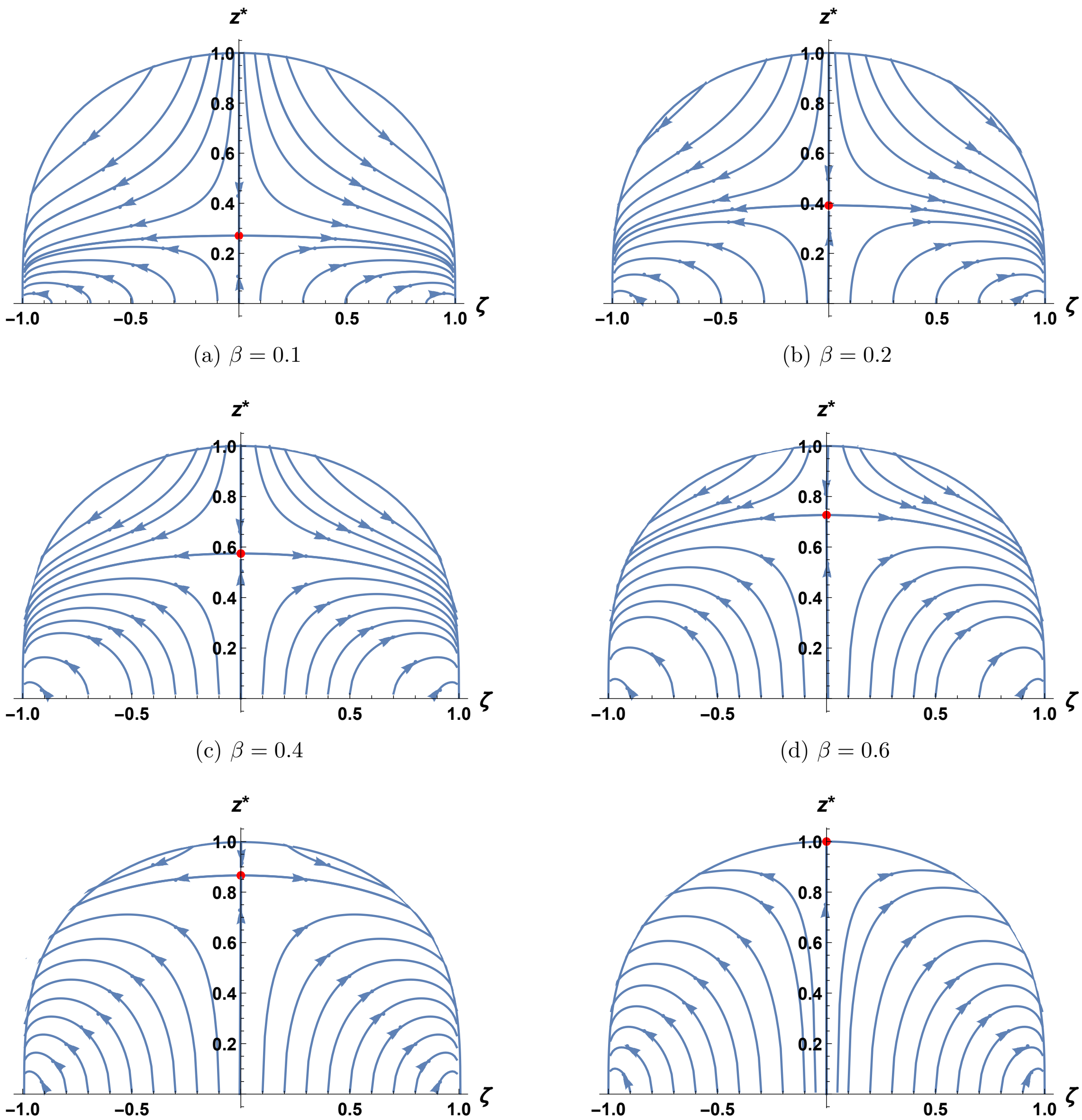

(a) $\beta = 0.1$ (b) $\beta = 0.2$

(c) $\beta = 0.4$ (d) $\beta = 0.6$

(e) $\beta = 0.8$ (f) $\beta = 1$

Figure 5.24: Streamlines for a range of positive values of β ($0 < \beta \leq 1$) plotted in the (ζ, z^*)-plane where $\zeta = x/W(t)$ ($-1 \leq \zeta \leq 1$) and $z^* = z/h(t,0)$ ($0 \leq z^* \leq 1$).

Chapter 6

Leak-off velocity proportional to the spatial gradient of the height of the thin film

6.1 Introduction

In Chapter 5 we made an assumption on $g(\zeta)$ so as to enable us to solve the ordinary differential equation (4.3.69). We assumed that the normal fluid velocity $v_n(t, x)$ at the base was proportional to the height $h(t, x)$. In this chapter we assume that the velocity $v_n(t, x)$ is proportional to the spatial gradient of the height $h(t, x)$. We will also consider the velocity on the centre line $x = 0$ and the streamlines will be plotted to depict the flow within the thin film. We will compare the results obtained in this chapter with those of Chapter 5.

6.2 Relation between $g(\zeta)$ and $\frac{df(\zeta)}{d\zeta}$

We consider

$$g(\zeta) = -\beta\,\zeta\,\frac{df(\zeta)}{d\zeta}, \qquad -\infty < \beta < \infty, \tag{6.2.1}$$

where β is a constant. This form is chosen to give an analytical solution. We can examine the physical significance of the assumption (6.2.1) by examining $h(t,x)$ given in (4.3.75) and $v_n(t,x)$ given in (4.3.76):

$$h(t,x) = \frac{f(\zeta)}{f(0)}\left(1+\frac{t}{\alpha\, f^3(0)}\right)^{\frac{2}{3}\left(\alpha-\frac{1}{2}\right)}, \tag{6.2.2}$$

$$v_n(t,x) = \frac{1}{f^4(0)}\left(1+\frac{t}{\alpha\, f^3(0)}\right)^{\frac{2}{3}(\alpha-2)} g(\zeta). \tag{6.2.3}$$

Differentiating (6.2.2) partially with respect to x, we obtain

$$\frac{\partial h}{\partial x} = \left(1+\frac{t}{\alpha\, f^3(0)}\right)^{-\frac{1}{3}\alpha-\frac{1}{3}} \frac{1}{f(0)}\frac{df}{d\zeta}, \tag{6.2.4}$$

which may be rearranged to give

$$\frac{df}{d\zeta} = f(0)\left(1+\frac{t}{\alpha\, f^3(0)}\right)^{\frac{1}{3}(\alpha+1)} \frac{\partial h}{\partial x}. \tag{6.2.5}$$

Thus by substituting (6.2.1) into (6.2.3) and using (4.3.63) for ζ we obtain

$$v_n(t,x) = -\frac{\beta}{f^4(0)}\left(1+\frac{t}{\alpha\, f^3(0)}\right)^{\frac{2}{3}(\alpha-2)} \frac{x}{W(t)}\frac{df}{d\zeta}, \tag{6.2.6}$$

and by substituting (6.2.5) for ${}^{df}/_{d\zeta}$ results in

$$v_n(t,x) = -\frac{\beta}{f^3(0)\left(1+\frac{t}{\alpha\, f^3(0)}\right)}\, x\,\frac{\partial h}{\partial x}. \tag{6.2.7}$$

Thus $v_n(t,x)$ is proportional to ${}^{\partial h(t,x)}/_{\partial x}$. The velocity $v_n(t,x)=0$ at $x=0$ because both $x=0$ and ${}^{\partial h}/_{\partial x}=0$ and it is small in the neighbourhood of $x=0$ because ${}^{\partial h}/_{\partial x}$ is small in that range. We cannot say more about the behaviour of $v_n(t,x)$ at this stage because the behaviour of ${}^{\partial h}/_{\partial x}$ for $W(t) < x < W(t)$ is only known after the problem has been solved. Also unlike in Chapter 5 where $f(0)$ is independent of β we will find in Chapter 6 that $f(0)$ depends on β.

6.3 Ordinary differential equation and invariant solution

By using the balance law (4.3.71) and (6.2.1) we have

$$-\int_0^1 \beta\,\zeta \frac{df}{d\zeta}\,d\zeta = \frac{1}{3}\left(5-\frac{1}{\alpha}\right)\int_0^1 f(\zeta)\,d\zeta. \tag{6.3.1}$$

But, integrating by parts,

$$\int_0^1 \zeta \frac{df}{d\zeta}\,d\zeta = f(1) - \int_0^1 f(\zeta)\,d\zeta, \tag{6.3.2}$$

and using the boundary conditions, $f(1) = 0$, gives

$$\int_0^1 \zeta \frac{df}{d\zeta}\,d\zeta = -\int_0^1 f(\zeta)\,d\zeta. \tag{6.3.3}$$

Substituting (6.3.3) into (6.3.1) we obtain

$$\left[\beta - \frac{1}{3}\left(5-\frac{1}{\alpha}\right)\right]\int_0^1 f(\zeta)\,d\zeta = 0. \tag{6.3.4}$$

Equation (6.3.4) is satisfied when

$$\beta - \frac{1}{3}\left(5-\frac{1}{\alpha}\right) = 0, \tag{6.3.5}$$

thus

$$\alpha = \frac{1}{5-3\,\beta}, \qquad \beta \neq \frac{5}{3}. \tag{6.3.6}$$

This result for α is the same as derived in Chapter 5.

Using (6.3.6) for α we may solve the ordinary differential equation (4.3.69) for $f(\zeta)$. Substituting (6.3.6) into (4.3.69) results in an integrable ordinary differential equation

$$\frac{d}{d\zeta}\left(f^3\frac{df}{d\zeta}\right) + 3(1-\beta)\frac{d}{d\zeta}(\zeta\, f) = 0. \tag{6.3.7}$$

Unlike the case $g(\zeta) = \beta\, f(\zeta)$, the ordinary differential equation depends on β. Integrating (6.3.7) once with respect to ζ and applying the zero flux boundary condition (5.2.15) at $\zeta = 1$ and also (4.3.57) at $\zeta = 1$ results in a variable separable ordinary differential equation for f

$$f^2 \frac{df}{d\zeta} + 3(1-\beta)\,\zeta = 0, \tag{6.3.8}$$

which when integrated and applying again (4.3.57) at $\zeta = 1$ gives

$$f(\zeta) = \left(\frac{9}{2}(1-\beta)\right)^{\frac{1}{3}} \left(1-\zeta^2\right)^{\frac{1}{3}}. \tag{6.3.9}$$

Thus

$$f(0) = \left(\frac{9}{2}(1-\beta)\right)^{\frac{1}{3}}. \tag{6.3.10}$$

Unlike the case $g(\zeta) = \beta\, f(\zeta)$, both $f(\zeta)$ and $f(0)$ depend on β.

We consider next $v_n(t,x)$ in order to determine the physical significance of β. Using (6.2.1),(6.3.9), (6.3.10) and α given by (6.3.6), equation (6.2.3) becomes for $\beta \neq 1$,

$$v_n(t,x) = \frac{4\,\beta}{27(1-\beta)} \left(1 + \frac{2\,(5-3\,\beta)\,t}{9(1-\beta)}\right)^{\frac{2(2\,\beta-3)}{5-3\,\beta}} \frac{\zeta^2}{(1-\zeta^2)^{\frac{2}{3}}}. \tag{6.3.11}$$

We introduce a new parameter β^* defined by

$$\beta^* = \frac{2}{5}\frac{\beta}{(1-\beta)}, \quad \beta \neq 1. \tag{6.3.12}$$

The factor $\frac{2}{5}$ normalises the critical value of β^* which occurs later as -1. The physical significance of β^* is clear. The velocity $v_n(t,x)$ has the same sign as β^*:

$$\beta^* > 0 \quad \text{then} \quad v_n > 0: \quad \text{blowing of fluid into the thin film,} \tag{6.3.13}$$

$$\beta^* < 0 \quad \text{then} \quad v_n < 0: \quad \text{suction of fluid out of thin film.} \tag{6.3.14}$$

Solving for β from(6.3.12), we obtain

$$\beta = \frac{5\beta^*}{2+5\beta^*}, \tag{6.3.15}$$

where $\beta^* = -\frac{2}{5}$ and substituting (6.3.15) into (6.3.6) and (6.3.10) gives

$$\alpha = \frac{2+5\beta^*}{10(1+\beta^*)}, \tag{6.3.16}$$

$$f(0) = \left(\frac{9}{2+5\beta^*}\right)^{\frac{1}{3}}. \tag{6.3.17}$$

Substituting (6.3.16) and (6.3.17) into (4.3.72), (4.3.73), (4.3.74), (4.3.75) and (6.3.11) gives

$$W(t) = \left(1+\frac{10}{9}(1+\beta^*)t\right)^{\frac{2+5\beta^*}{10(1+\beta^*)}}, \tag{6.3.18}$$

$$V(t) = V_0\left(1+\frac{10}{9}(1+\beta^*)t\right)^{\frac{\beta^*}{2(1+\beta^*)}}, \tag{6.3.19}$$

$$V_0 = 2\int_0^1 \zeta\,\left(1-\zeta^2\right)^{\frac{1}{3}}\,d\zeta = \frac{3}{4}, \tag{6.3.20}$$

$$h(t,x) = \left(1+\frac{10}{9}(1+\beta^*)t\right)^{-\frac{1}{5(1+\beta^*)}}\left(1-\zeta^2\right)^{\frac{1}{3}}, \tag{6.3.21}$$

$$v_n(t,x) = \frac{10}{27}\beta^*\left(1+\frac{10}{9}(1+\beta^*)t\right)^{-\frac{(6+5\beta^*)}{5(1+\beta^*)}}\frac{\zeta^2}{(1-\zeta^2)^{\frac{2}{3}}}, \tag{6.3.22}$$

where

$$\zeta = \frac{x}{W(t)}, \qquad -1 \le \zeta \le 1. \tag{6.3.23}$$

The results (6.3.18)-(6.3.22) are valid for $\beta^* \neq -1$. We consider now the limit as $\beta^* \to -1$ in (6.3.18). We first obtain $W(t)$ for $\beta^* = -1$ and then use the expressions for $V(t), h(t,x)$ and $v_n(t,x)$ in terms of $W(t)$ to obtain these quantities in the limit $\beta^* = -1$. We first rewrite (6.3.18) as

$$W(t) = \exp\left[\frac{2+5\beta^*}{10(1+\beta^*)}\ln\left(1+\frac{10}{9}(1+\beta^*)\,t\right)\right]. \tag{6.3.24}$$

Using the expansion [17]

$$\ln(1+\epsilon) = \epsilon - \frac{\epsilon^2}{2} + \frac{\epsilon^3}{3} - \frac{\epsilon^4}{4} + \dots \tag{6.3.25}$$

equation (6.3.24) becomes

$$W(t) = \exp\left[\frac{2+5\beta^*}{10(1+\beta^*)}\left(\frac{10}{9}(1+\beta^*)t\right) + \bigcirc\left((1+\beta^*)\right)\right], \quad \text{as} \quad \beta^* \to -1, \tag{6.3.26}$$

and therefore

$$\lim_{\beta^* \to -1} W(t) = \exp\left[-\frac{t}{3}\right]. \tag{6.3.27}$$

By substituting (6.3.27) for $W(t)$ when $\beta^* = -1$ in (6.3.19), (6.3.21) and (6.3.22), we obtain

$$V(t) = V_0\, W^{\frac{5\beta^*}{2+5\beta^*}}(t) = V_0 \exp\left(-\frac{5}{9}t\right), \tag{6.3.28}$$

$$h(t,x) = W^{\frac{-2}{2+5\beta^*}}(t)\left(1-\zeta^2\right)^{\frac{1}{3}} = \exp\left(-\frac{2}{9}t\right)\left(1-\zeta^2\right)^{\frac{1}{3}}, \tag{6.3.29}$$

$$\begin{aligned} v_n(t,x) &= \frac{10}{27}\beta^* W^{-2\left(\frac{6+5\beta^*}{2+5\beta^*}\right)}(t)\frac{\zeta^2}{(1-\zeta^2)^{\frac{2}{3}}} \\ &= -\frac{10}{27}\exp\left(-\frac{2}{9}t\right)\frac{\zeta^2}{(1-\zeta^2)^{\frac{2}{3}}}, \end{aligned} \tag{6.3.30}$$

where V_0 is given by (6.3.20). Davis and Hocking [7] have derived for the volume of a two-dimensional thin film a similar exponential decrease as in (6.3.28).

We now investigate the dependence of $v_n(t,x), W(t), V(t), h(t,0)$ and the thin film ratio ${}^{h(t,0)}/{}_{W(t)}$ on β^*. Consider first $v_n(t,x)$. When $\beta^* < -1.2$, the suction is very strong and $v_n(t,x) \to -\infty$ algebraically as $t \to t_2$ where

$$t_2 = -\frac{9}{10(1+\beta^*)}. \tag{6.3.31}$$

When $\beta^* = -1.2$, $v_n(t,x)$ is constant. For $-1.2 < \beta^* < -1$, $v_n(t,x) \to 0$ algebraically as $t \to t_2$. For $\beta^* = -1$, $v_n(t,0) \to 0$ exponentially as $t \to \infty$. When $-1 < \beta^* < 0$, we have moderate to weak suction and $v_n(t,x) \to 0$ algebraically as $t \to \infty$. There is no suction or blowing when $\beta^* = 0$. For $0 < \beta^* < \infty$ there is blowing of fluid into the thin film and $v_n(t,x) \to 0$ algebraically as $t \to \infty$. Since $v_n(t,x) = 0$ when $x = 0$ for all β^*, graphs of $v_n(t,x)$ are plotted against time for a range of β when $\zeta = 0.5$ in Figure 6.1.

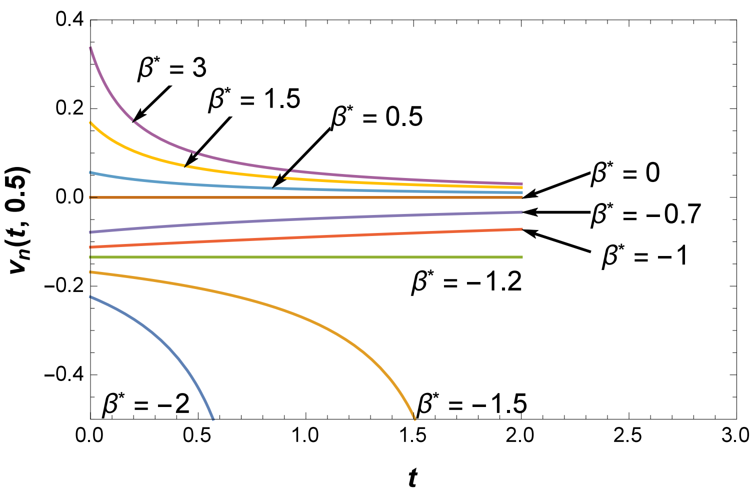

Figure 6.1: Normal velocity v_n given by (6.3.22) for $\beta^* \neq -1$ and (6.3.30) for $\beta^* = -1$ plotted against t at $\zeta = 0.5$ for a range of values of β^*, where $v_n > 0$ describes blowing and $v_n < 0$ describes suction at the base.

Consider next the half-width at the base $W(t)$ given by (6.3.18) for $\beta^* \neq -1$ and by (6.3.27) when $\beta^* = -1$. Now $\frac{dW}{dt} > 0$ when $\beta^* > -0.4$ and $\frac{dW}{dt} < 0$ when $\beta^* < -0.4$. When $\beta^* < -1$ suction is strong and $W(t) \to 0$ in a finite time given by (6.3.31). When $\beta^* = -1$, $W(t) \to 0$ exponentially as $t \to \infty$ and when $-1 < \beta^* < -0.4$, $W(t) \to 0$ algebraically as $t \to \infty$. When $\beta^* = -0.4$, $W(t)$ remains constant since the suction balances the spreading due to gravity. There is weak suction when $-0.4 < \beta^* < 0$, and $W(t) \to \infty$ algebraically as $t \to \infty$. When $\beta^* = 0$ there is no suction or blowing. When $0 < \beta^* < \infty$ there is blowing at the base and $W(t) \to \infty$ as $t \to \infty$. A plot of $W(t)$ against time, t, is presented in Figure 6.2.

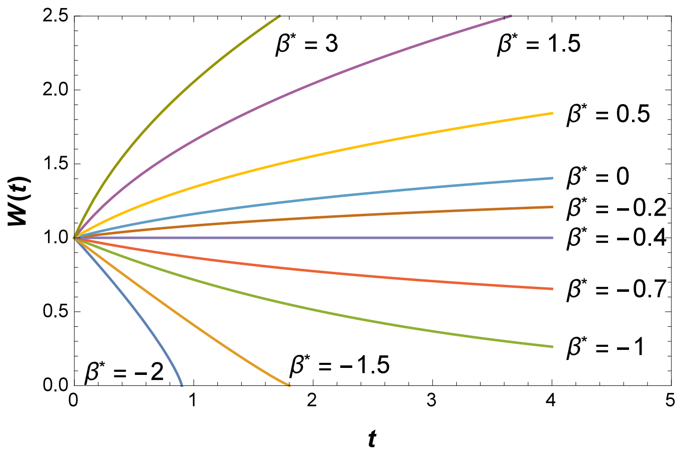

Figure 6.2: $W(t)$ given by (6.3.18) for $\beta^* \neq -1$ and (6.3.27) for $\beta^* = -1$ plotted against t for a range of values of β^*.

Consider next the volume $V(t)$ given by (6.3.19) for $\beta^* \neq -1$ and (6.3.28) for $\beta^* = -1$. For $\beta^* < 0$, $\frac{dV}{dt} < 0$ since there is suction at the base while for $\beta^* > 0$, $\frac{dV}{dt} > 0$ since there is blowing at the base. For $\beta^* < -1$, the suction is strong and $V(t) \to 0$ in the finite time t_2 defined by (6.3.31). When $\beta^* - 2$,

$$\frac{dV}{dt} = \frac{10}{9} V_0 = \text{constant}. \tag{6.3.32}$$

For $\beta^* = -1$, $V(t) \to 0$ exponentially as $t \to \infty$. For $-1 < \beta^* < 0$ the suction is moderate to weak and $V(t) \to 0$ algebraically as $t \to \infty$. For $\beta^* = 0$, $V = V_0$ where the constant V_0 is given by (6.3.20). For $\beta^* > 0$ there is blowing and $V(t) \to \infty$ algebraically as $t \to \infty$. A plot of $V(t)$ against time, t, is presented in Figure 6.3.

Consider now the height on the centre line, $h(t,0)$. Since $\frac{d\,h(t,0)}{dt} < 0$ for $-\infty < \beta^* < \infty$, the height of the thin film decreases for all values of β^* even when there is blowing for $\beta^* > 0$. When $\beta^* < -1$, the height $h(t,0) \to 0$ in the finite time t_2 given by (6.3.31). For $\beta^* = -1$, $h(t,0) \to 0$ exponentially as $t \to \infty$ while for $-1 < \beta^* < 0$, $h(t,0) \to 0$ algebraically as $t \to \infty$. When $\beta^* = 0$, the height decreases due to spreading caused by gravity only and $h(t,0) \to 0$ algebraically as

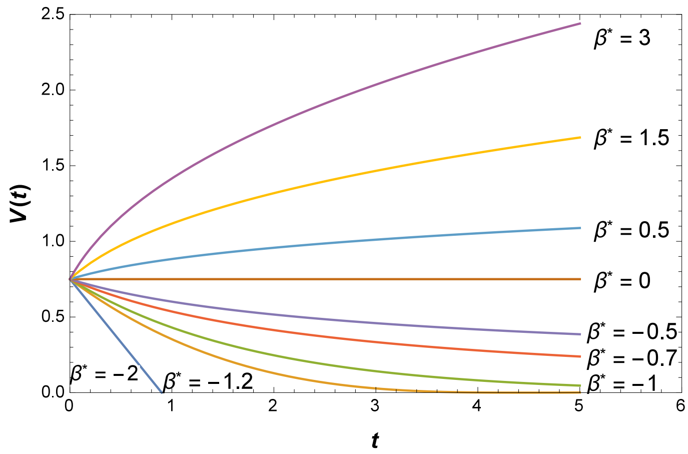

Figure 6.3: Volume $V(t)$ given by (6.3.19) for $\beta^* \neq -1$ and (6.3.28) for $\beta^* = -1$ plotted against t for a range of values of β^*.

$t \to \infty$. When $0 < \beta^* < \infty$, $h(t, 0) \to 0$ algebraically as $t \to \infty$. The decrease in $h(t, 0)$ due to spreading by gravity is stronger than the increase in $h(t, 0)$ due to blowing. Graphs of $h(t, 0)$ are plotted against time for a range of β^* in Figure 6.4.

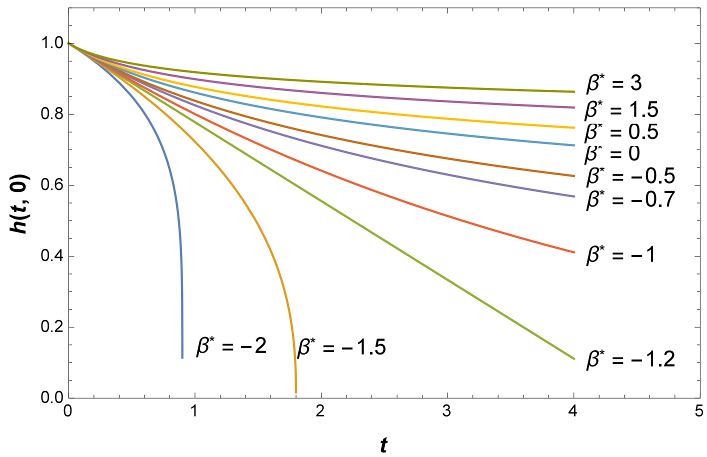

Figure 6.4: Height of the thin film at the centre, $h(t, 0)$ given by (6.3.21) for $\beta^* \neq -1$ and (6.3.29) for $\beta^* = -1$ plotted against t for a range of values of β^*.

Finally, consider the thin film approximation. As explained in Section 5.3, the thin film approximation will be satisfied if either

$$\epsilon(t) = \text{constant} = 1, \tag{6.3.33}$$

or

$$\epsilon(t) \to 0 \quad \text{as} \quad t \to t_2 \quad \text{or} \quad t \to \infty. \tag{6.3.34}$$

The thin approximation will break down at sufficiently large time if

$$\epsilon(t) \to \infty \quad \text{as} \quad t \to t_2 \quad \text{or} \quad t \to \infty. \tag{6.3.35}$$

From (6.3.18) and (6.3.21) for $\beta^* \neq -1$,

$$\frac{h(t,0)}{W(t)} = \left(1 + \frac{10}{9}\left(1+\beta^*\right)t\right)^{-\frac{4+5\beta^*}{10(1+\beta^*)}}, \tag{6.3.36}$$

and from (6.3.27) and (6.3.29) for $\beta^* = -1$,

$$\frac{h(t,0)}{W(t)} = \exp\left[\frac{t}{9}\right]. \tag{6.3.37}$$

For $\beta^* < -1$, $\epsilon \to \infty$ algebraically in the finite time, t_2, given by (6.3.31), for $\beta^* = -1$, $\epsilon \to \infty$ exponentially as $t \to \infty$ while for $-1 < \beta^* < -\frac{4}{5}$, $\epsilon \to \infty$ algebraically as $t \to \infty$. For $\beta^* = -\frac{4}{5}$, ϵ remains constant. When $-\frac{4}{5} < \beta^* \leq \infty$, $\epsilon \to 0$ as $t \to \infty$. Thus since it is assumed that the thin film approximation is satisfied initially it will remain satisfied for all time for $-\frac{4}{5} \leq \beta^* \leq \infty$. For strong suction ($-\infty \leq \beta^* < \frac{4}{5}$), $W(t)$ decreases too rapidly as $t \to \infty$ for the thin film approximation to hold. For blowing ($\beta^* > 0$), $W(t)$ always increases sufficiently rapidly for the thin film approximation to hold for all time. Graphs of ϵ plotted against time for a range of values of β^* are presented in Figure 6.5.

In Figure 6.6, $h(t,x)$ and $v_n(t,x)$ are plotted against x for a range of β^* values and time. A distinguishing feature of this solution is that the height always decreases with time even for values of $\beta^* > 0$ for which there is blowing. For suction the thin film disappears by the base tending to a point for $\beta^* < -0.4$. In Figure 6.6(c) and Figures 6.6(a) and 6.6(b) we see that the height decreases by the base spreading and in Figures 6.6(e) and 6.6(f) we see that the height decreases while the base tends to zero whereas in Figure and 6.6(d) the height decreases and the base remains constant. The suction/blowing velocity $v_n(t,x)$ is stronger at the rim of the thin film and weaker near the centre of the thin film and $v_n(t,0) = 0$.

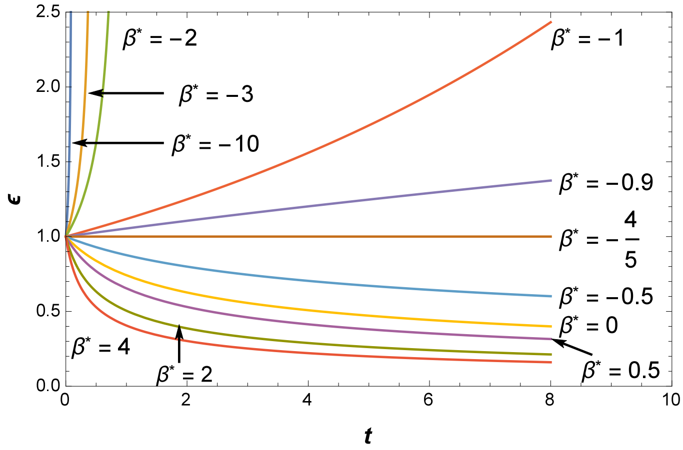

Figure 6.5: Thin film approximation $\epsilon(t)$ given by (6.3.36) for $\beta^* \neq -1$ and (6.3.37) for $\beta^* = -1$ plotted against t for a range of values of β^*.

6.4 Velocity on the centre line

The velocity on the centre line $x = 0$ is given by (5.4.11):

$$v_z(t,0,z) = -\frac{1}{6}\left.\frac{\partial^2 h(t,x)}{\partial x^2}\right|_{x=0} z^3 + \frac{1}{4}\frac{\partial^2}{\partial x^2}\left.\left(h^2(t,x)\right)\right|_{x=0} z^2 + v_n(t,0). \tag{6.4.1}$$

where $h(t,x)$ and $v_n(t,x)$ can be expressed in terms of $h(t,0)$ as

$$h(t,x) = h(t,0)\left(1 - \frac{x^2}{W^2(t)}\right)^{\frac{1}{3}}, \tag{6.4.2}$$

$$v_n(t,x) = \frac{10}{27}\beta^* h^{6+5\beta^*}(t,0)\frac{x^2}{W^2(t)\left(1 - \frac{x^2}{W^2(t)}\right)^{\frac{2}{3}}}, \tag{6.4.3}$$

with $W(t)$ given by (6.3.18) and

$$h(t,0) = W^{-\frac{2}{2+5\beta^*}}(t). \tag{6.4.4}$$

By substituting (6.4.2) and (6.4.3) into (6.4.1) and evaluating at $x = 0$, we obtain

$$v_z(t,0,z) = \frac{1}{9}\frac{h(t,0)}{W^2(t)}\left(z^3 - 3\,h(t,0)z^2\right). \tag{6.4.5}$$

The points on the axis at which $v_z(t,0,z) = 0$ satisfy the cubic equation

$$z^3 - 3\,h(t,0)z^2 = 0. \tag{6.4.6}$$

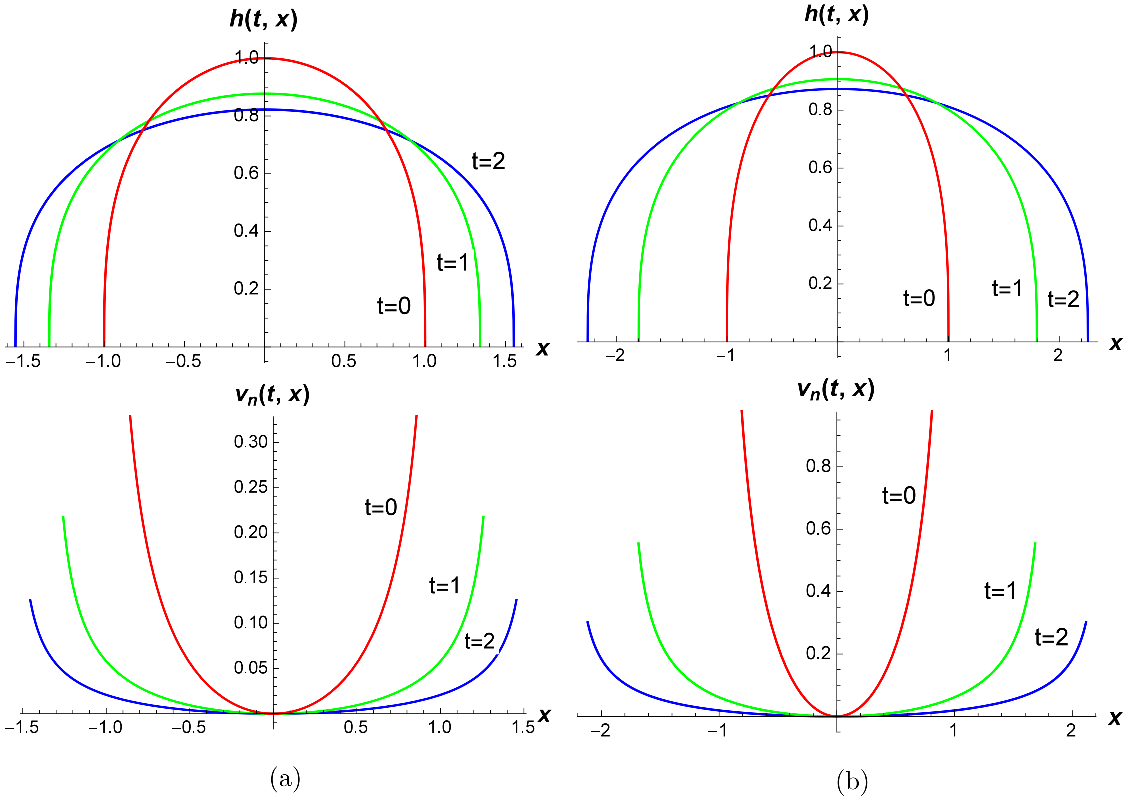

Figure 6.6: Plot of $h(t,x)$ given by (6.3.21) and of the fluid velocity at the base, $v_n(t,x)$ given (6.3.22) against x for a range of values of t and for:(a) $\beta^* = 0.5$, (b) $\beta^* = 2$.

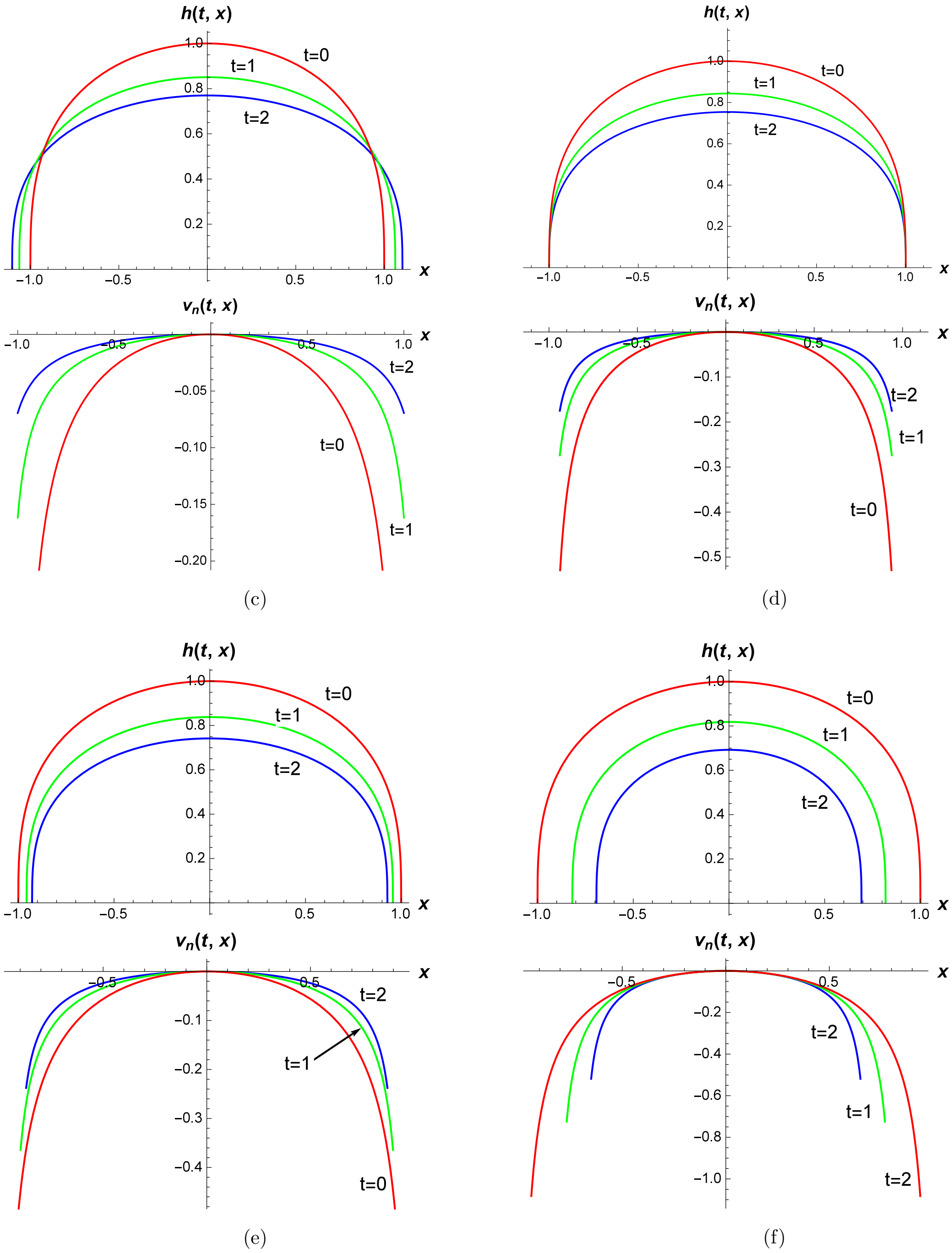

Figure 6.6: Plot of $h(t,x)$ given by (6.3.21) and of the fluid velocity at the base, $v_n(t,x)$ given (6.3.22) against x for a range of values of t and for:(c) $\beta^* = -0.25$, (d) $\beta^* = -0.4$, (e) $\beta^* = -0.5$, (f) $\beta^* = -0.8$.

Thus $v_z = 0$ when $z = 0, z = 0, z = 3h(t,0)$. This corresponds to the case when $\beta = 0$ for the roots of the cubic equation in Section 5.4.1. For $0 \leq z \leq 3h(t,0)$ we have that $v_z(t,0,z) < 0$ thus $v_z(t,0,z)$ is negative for $0 \leq z \leq h(t,0)$. There are no zeros on the centre line $x = 0$ inside the thin film for this model. The only zero is at the point $z = 0$. Thus there is a dividing streamlines inside the thin film which goes through the origin and this will be verified in the next section when the streamlines are plotted for various values of β^*.

From (6.4.5) we may derive some properties of $v_z(t,0,z)$ at $z = h(t,0)$ which is the velocity of the maximum height of the thin film. Substituting $z = h(t,0)$ into (6.4.5) gives

$$\frac{\partial\, h(t,0)}{\partial\, t} = v_z(t,0,h) = -\frac{2}{9}\frac{h^4(t,0)}{W^2(t)} = -\frac{2}{9}W^{\frac{-12-10\beta^*}{2+5\beta^*}}(t). \qquad (6.4.7)$$

We see again that $\partial h(t,0)/\partial t < 0$ for $-\infty < \beta^* < \infty$ and the height of the thin film decreases with time, even for blowing with $0 < \beta < \infty$. Consider now the dependence of $v_z(t,0,h)$ on β^*. From (6.4.7), (6.3.18) and (6.3.27) we have that when

$$\beta^* \neq -1: \qquad v_z(t,0,h) = -\frac{2}{9}\left[1 + \frac{10}{9}(1+\beta^*)t\right]^{\frac{-6-5\beta^*}{5(1+\beta^*)}}, \qquad (6.4.8)$$

$$\beta^* = -1: \qquad v_z(t,0,h) = -\frac{2}{9}\exp\left(\frac{-2}{9}t\right). \qquad (6.4.9)$$

We have also defined for $\beta^* < -1$,

$$t_2 = -\frac{9}{10(1+\beta^*)} > 0. \qquad (6.4.10)$$

Hence when

$$-\infty \leq \beta^* < -\frac{6}{5}: \qquad v_z(t,0,h) \to -\infty \quad \text{as} \quad t \to t_2 \quad \text{in a finite time.} \qquad (6.4.11)$$

$$\beta^* = -\frac{6}{5}: \qquad v_z(t,0,h) = -\frac{2}{9}. \tag{6.4.12}$$

$$-\frac{6}{5} < \beta^* < -1: \qquad v_z(t,0,h) \to 0 \quad \text{as} \quad t \to t_2 \quad \text{in a finite time.} \tag{6.4.13}$$

$$\beta^* = -1: \qquad v_z(t,0,h) \to 0 \quad \text{exponentially as} \quad t \to \infty. \tag{6.4.14}$$

$$-1 < \beta^* \leq \infty: \qquad v_z(t,0,h) \to 0 \quad \text{algebraically, as} \quad t \to \infty. \tag{6.4.15}$$

In Figure 6.7, $v_z(t,0,h)$ is plotted against time for a range of β^* values.

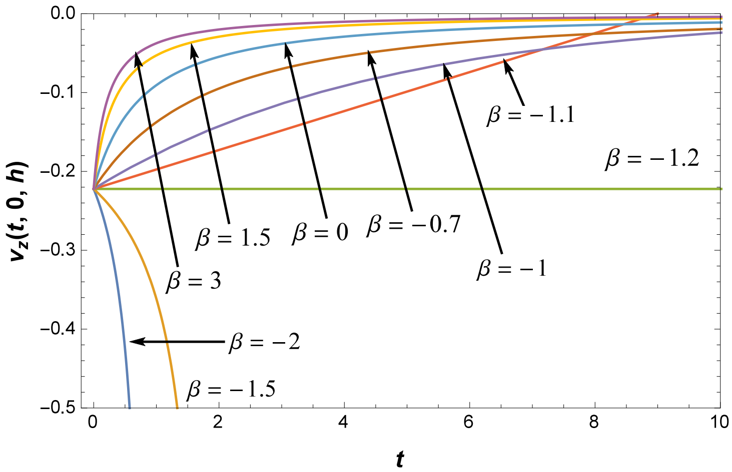

Figure 6.7: Plot of $v_z(t,0,h)$ given in (6.4.7) against time for a range of values of β^*.

6.5 Streamlines

The streamlines inside the thin film will now be investigated. As determined in Section 5.5 the streamlines are obtained by solving the cubic equation (5.5.19)

$$A(t,x)z^3 + B(t,x)z^2 + C(t,x) = K(t), \tag{6.5.1}$$

where $K(t)$ is an arbitrary function of t and from (5.5.17)

$$A(t,x) = \frac{1}{6}\frac{\partial h}{\partial x}, \qquad B(t,x) = -\frac{1}{2}h\frac{\partial h}{\partial x}, \qquad C(t,x) = -\int_0^x v_n(t,x)\,dx. \tag{6.5.2}$$

We calculate the coefficients $A(t,x), B(t,x)$ and $C(t,x)$ in (6.5.2) in terms of the similarity solution obtained in (6.3.18)-(6.3.23). Substituting (6.3.21) into (6.5.2) it can be verified that

$$A(t,\zeta) = -\frac{1}{9}W^{\frac{-4-5\beta^*}{2+5\beta^*}}(t)\frac{\zeta}{(1-\zeta^2)^{\frac{2}{3}}}, \tag{6.5.3}$$

$$B(t,\zeta) = \frac{1}{3}W^{\frac{-6-5\beta^*}{2+5\beta^*}}(t)\frac{\zeta}{(1-\zeta^2)^{\frac{1}{3}}}. \tag{6.5.4}$$

By substituting (6.3.22) for $v_n(t,x)$ into (6.5.2), it can be verified that

$$C(t,\zeta) = -\frac{10}{27}\beta^* W^{-5\left(\frac{2+\beta^*}{2+5\beta^*}\right)}(t)\int_0^\zeta \frac{\zeta^{*2}}{(1-\zeta^{*2})^{\frac{2}{3}}}d\zeta^*. \tag{6.5.5}$$

The base will stay fixed at $-1 \leq \zeta \leq 1$. This may be useful if $W(t)$ becomes very large. By using (6.3.23) which gives the relation between x and ζ, the results may also be expressed in terms of x:

$$A(t,x) = -\frac{1}{9}W^{-2\left(\frac{3+5\beta^*}{2+5\beta^*}\right)}(t)\frac{x}{\left(1-\frac{x^2}{W^2(t)}\right)^{\frac{2}{3}}}, \tag{6.5.6}$$

$$B(t,x) = \frac{1}{3}W^{-2\left(\frac{4+5\beta^*}{2+5\beta^*}\right)}(t)\frac{x}{\left(1-\frac{x^2}{W^2(t)}\right)^{\frac{1}{3}}}, \tag{6.5.7}$$

$$C(t,x) = -\frac{10}{27}\beta^* W^{-4\left(\frac{4+5\beta^*}{2+5\beta^*}\right)}(t)\int_0^x \frac{x^{*2}}{\left(1-\frac{x^{*2}}{W^2(t)}\right)^{\frac{2}{3}}}dx^*. \tag{6.5.8}$$

We first consider the streamlines plotted against x and z where $-W(t) \leq x \leq W(t)$ and $0 \leq z \leq h(t,x)$. The streamline pattern depends on time. We will choose $t = 1$. For a given value of β^* the streamlines are derived by solving the cubic equation (6.5.1) where $A(t,x), B(t,x)$ and $C(t,x)$ are given by (6.5.6) to (6.5.8) and $K(t)$ is given a range of values.

When $\beta^* = 0$, Models I and II reduce to the same model of spreading of a thin film on a base without suction or blowing. The streamlines for $\beta^* = 0$ at $t = 1$ are therefore the same as shown in Figure 5.20.

From (6.3.22) and (6.3.30) for v_n it follows that near the moving contact lines, $x = \pm W(t)$, the suction/injection of fluid is strongest and the magnitude tends to infinity as $x \to \pm W(t)$. Near the centre line the suction/injection of fluid is weakest and the magnitude tends to zero as $x \to 0$.

In Figure 6.8 the streamlines are plotted for negative values of β^*, which describes suction at the base, and for values in the range $-0.8 \leq \beta^* < 0$ for which the thin fluid film approximation is valid. The values chosen are $\beta^* = -0.8, -0.6, -0.5$ for which $W(t) \to 0$ as $t \to \infty$ describing strong suction and $\beta^* = -0.2$ for which $W(t) \to \infty$ as $t \to \infty$ describing weak suction. The streamlines begin on the free surface. The streamlines are perpendicular to the base since there is no slip of fluid at the base. Near the moving contact lines the suction is strongest and the streamlines are less curved because spreading due to gravity is weaker than suction. Near the centre line the streamlines are most curved because the suction is weaker than spreading by gravity. In Figure 6.8 we observe that an increase in the magnitude of suction decreases the height of the surface profile.

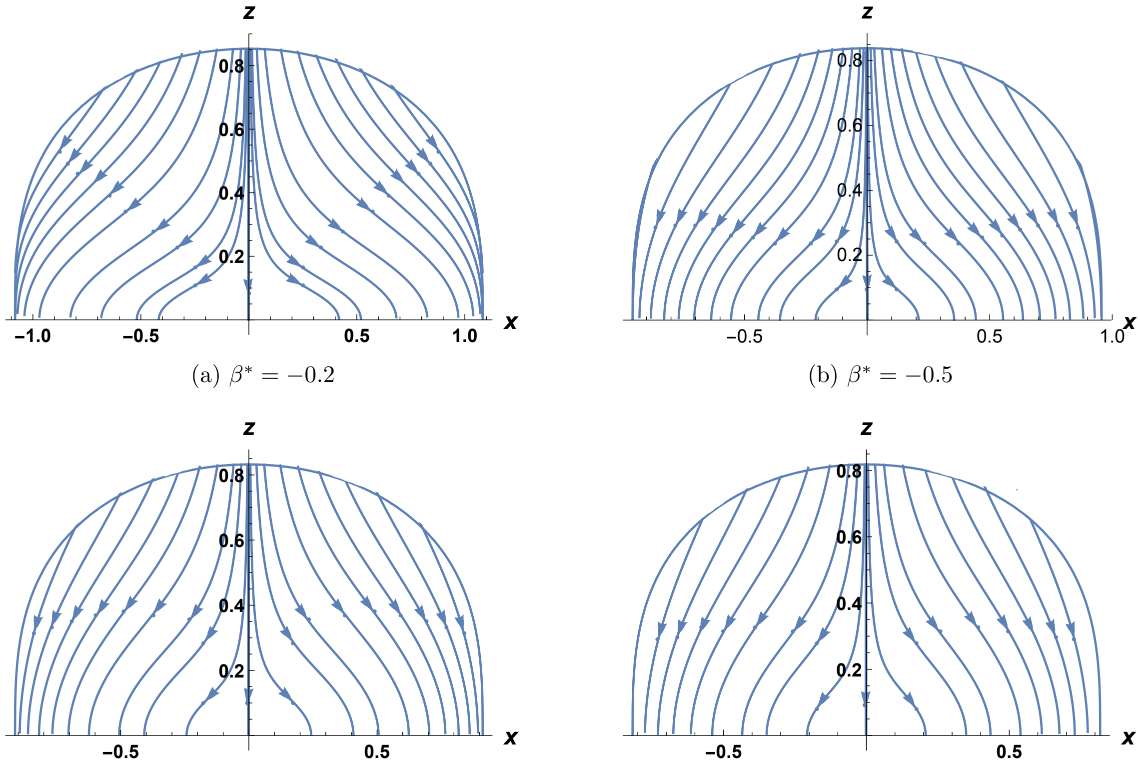

(a) $\beta^* = -0.2$ (b) $\beta^* = -0.5$

(c) $\beta^* = -0.6$ (d) $\beta^* = -0.8$

Figure 6.8: Suction at the base. Streamlines for a range of negative values of β^* plotted against x at $t = 1$.

In Figure 6.9 the streamlines are plotted for positive β^* values which describes the injection of fluid into the thin film. The magnitude of injection velocity v_n is increased by choosing $\beta^* = 0.25$, $\beta^* = 0.5$, $\beta^* = 1$ and $\beta^* = 2$. Since v_n is proportional to $\frac{\partial h}{\partial x}$ and the gradient is zero at $x = 0$, it follows that $v_n(t, 0) = 0$ which can clearly be seen in the plots of the streamlines. A dividing streamline extends from the point $(0, 0)$ and divides the flow into two regions. In the upper region the streamlines begin on the free surface and end on the free surface. The upper region shows fluid descending due to the action of gravity which leads to the spreading of the base. The fluid flow near the centre line is downwards (as indicated by the arrows) but the flow is forced upwards as it approaches the free surface because of the strong injection of fluid at the moving contact lines. The lower region describes the injection of fluid into the thin film as indicated by the arrows pointing upward. In the lower region the streamlines begin at the base and end on the free surface. In comparison with Model I, the thickness of the fluid layer at the base increases approximately linearly from zero at the centre line, reaches a maximum value then decreases rapidly to zero at the moving contact lines. We see from Figure 6.9 that the magnitude of the spatial gradient of the dividing streamline increases as β^*, and therefore v_n, increases. In the next section we will determine an approximate analytical solution for the dividing streamline.

In order to investigate how the streamlines evolve with time they are plotted in

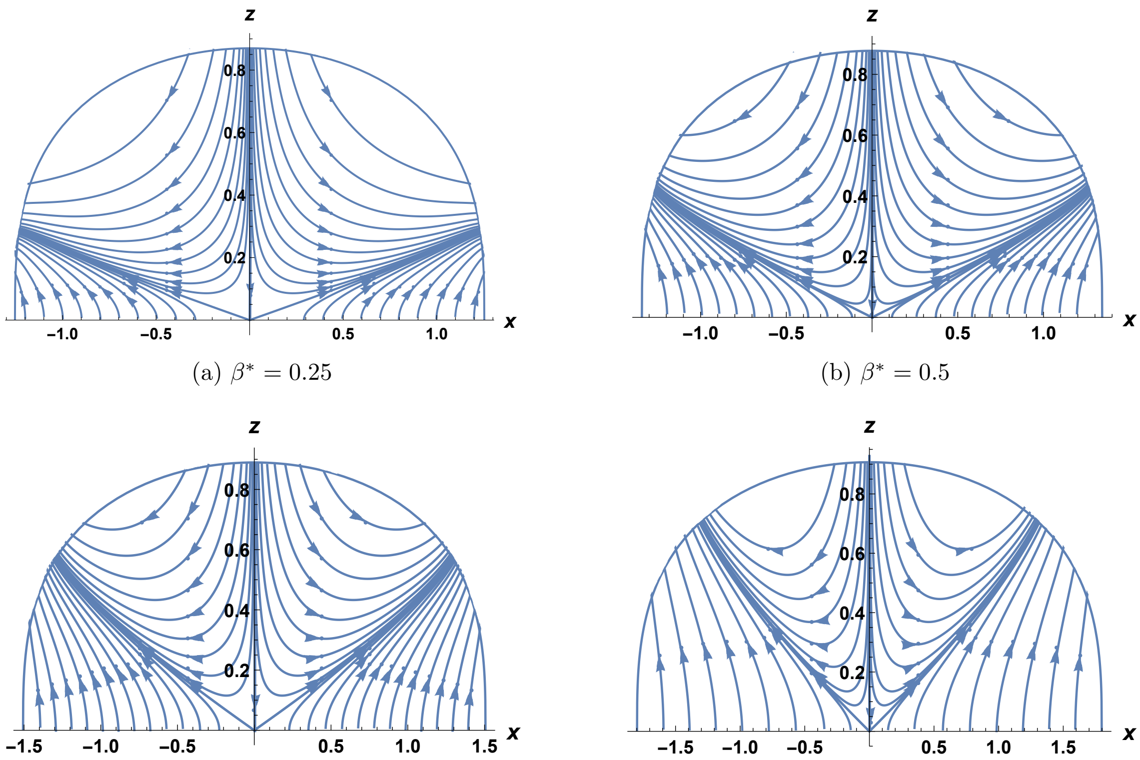

(a) $\beta^* = 0.25$ (b) $\beta^* = 0.5$

(c) $\beta^* = 1$ (d) $\beta^* = 2$

Figure 6.9: Fluid injection at the base. Streamlines for a range of positive values of β^* plotted against x at $t = 1$.

Figure 6.10 for $\beta^* = 1$ at times $t = 1$ and $t = 10$. As time increases the height of the thin film decreases, even with fluid injection at the base, and the width of the base increases. This agrees with the results of Section 6.3. Also, as time increases the angle that the dividing streamline makes with the base decreases. We will derive an approximate analytical solution for the dividing streamline in Section 6.6 and investigate its evolution with time.

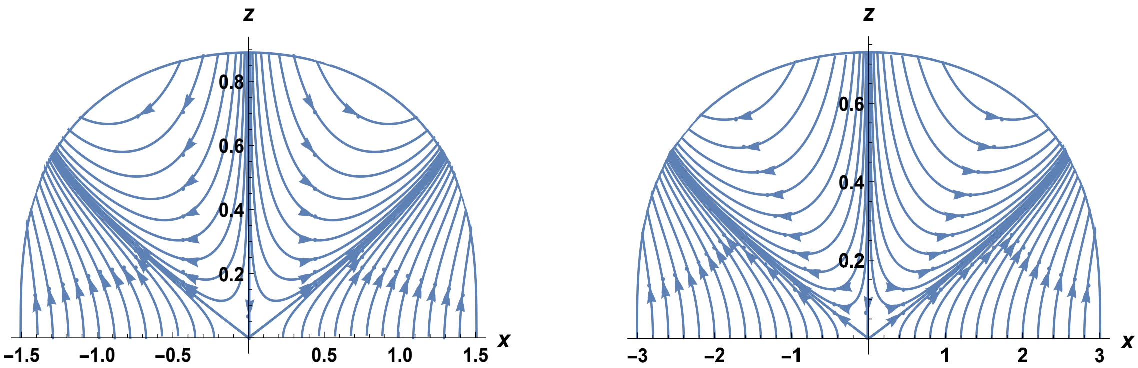

(a) t=1 (b) t=10

Figure 6.10: Streamlines for $\beta^* = 1$ plotted against x for $-W(t) \leq x \leq W(t)$ at $t = 1$ and $t = 10$.

In Figures (6.8) to (6.10) the streamlines were plotted in the (x, z)-plane where $-W(t) \leq x \leq W(t)$ and $0 \leq z \leq h(t, 0)$. The width of the base and the maximum height of the fluid film depend on time and the streamline pattern evolves with time. We now consider the streamlines in the (ζ, z^*)-plane where

$$\zeta = \frac{x}{W(t)}, \qquad -1 \leq \zeta \leq 1, \tag{6.5.9}$$

$$z^* = \frac{z}{h(t,0)}, \qquad 0 \leq z^* \leq 1. \tag{6.5.10}$$

The cubic equation (6.5.1) expressed in terms of ζ and z^* is

$$A^*(t,\zeta)z^{*3} + B^*(t,\zeta)z^{*2} + C(t,\zeta) = K(t), \tag{6.5.11}$$

where

$$A^*(t,\zeta) = A(t,\zeta)\, h^3(t,0), \tag{6.5.12}$$

$$B^*(t,\zeta) \;=\; B(t,\zeta)\, h^2(t,0) \tag{6.5.13}$$

and from (6.3.18) and (6.3.21),

$$h(t,0) = W^{-\frac{2}{2+5\beta^*}}(t). \tag{6.5.14}$$

Thus using (6.5.6) and (6.5.7) for $A(t,\zeta)$ and $B(t,\zeta)$ we obtain

$$A^*(t,\zeta) \;=\; -\frac{1}{9}W^{-5\left(\frac{2+\beta^*}{2+5\beta^*}\right)}(t)\frac{\zeta}{(1-\zeta^2)^{\frac{2}{3}}}, \tag{6.5.15}$$

$$B^*(t,\zeta) \;=\; \frac{1}{3}W^{-5\left(\frac{2+\beta^*}{2+5\beta^*}\right)}(t)\frac{\zeta}{(1-\zeta^2)^{\frac{1}{3}}}. \tag{6.5.16}$$

The coefficients $A^*(t,\zeta)$, $B^*(t,\zeta)$ and $C(t,\zeta)$ given by (6.5.5) depend explicitly on time only through the same power of $W(t)$. The cubic equation (6.5.11) becomes

$$-\frac{1}{9}\frac{\zeta}{(1-\zeta^2)^{\frac{2}{3}}}z^{*3} + \frac{1}{3}\frac{\zeta}{(1-\zeta^2)^{\frac{1}{3}}}z^{*2} - \frac{10}{27}\beta^* \int_0^{\zeta} \frac{\zeta^{*2}}{(1-\zeta^{*2})^{\frac{2}{3}}}d\zeta^* = K^*, \tag{6.5.17}$$

where

$$K^* = K(t) W^{5\left(\frac{2+\beta^*}{2+5\beta^*}\right)}(t). \tag{6.5.18}$$

Since the left hand side of (6.5.17) does not depend explicitly on time it follows that K^* does not depend on time. The results for $A^*(t,\zeta)$, $B^*(t,\zeta)$ and $C(t,\zeta)$ and the cubic equation for z^*, (6.5.17), expressed in terms of $W(t)$ are valid for $\beta^* = -1$ with $W(t)$ given by (6.3.27). The streamlines in the (ζ, z^*)-plane are obtained by giving K^*, which is arbitrary because $K(t)$ was arbitrary, a range of values. The pattern of streamlines in the (ζ, z^*)-plane is independent of time since (6.5.17) does not depend on time. It depends only on the parameter β^* and gives a good way to investigate the dependence of the solution on β^*.

In Figure (6.11) the streamlines are plotted in the (ζ, z^*)-plane for suction with $\beta^* = -0.5$ and for fluid injection $\beta^* = 1, 10$ and 50. As β^* increases and the strength of the blowing increases we see that the angle that the dividing streamline makes with the base at the central line increases.

The origin on the base is a stagnation point of the flow because the fluid velocity is zero from from the no slip boundary condition and since $v_n(t,0) = 0$. In Model II for a two-dimensional thin film the thin film approximation is satisfied provided $-\frac{4}{5} \leq \beta^* < \infty$. In the graphs all values of β^* lie in this range.

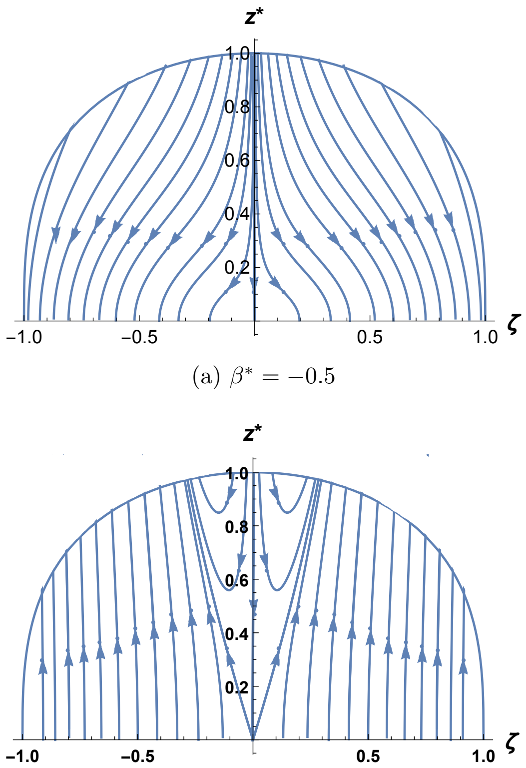

(a) $\beta^* = -0.5$ (b) $\beta^* = 1$ (c) $\beta^* = 20$ (d) $\beta^* = 50$

Figure 6.11: Streamlines for a range of values of β^* plotted in the (ζ, z^*)-plane where $\zeta = x/W(t)$ $(-1 \leq \zeta \leq 1)$ and $z^* = z/h(t,0)$ $(0 \leq z^* \leq 1)$.

6.6 Approximate solution for the dividing streamline

We now derive an approximate solution for the dividing streamline. We will use coordinates (ζ, z^*). After the cubic equation has been solved approximately in these coordinates the solution can be expressed in the coordinates (x, z) if required.

Consider the cubic equation (6.5.17). The dividing streamline passes through the point $\zeta = 0, z^* = 0$. Thus in (6.5.17), $K^* = 0$. The cubic equation for the dividing streamline therefore is

$$z^{*3} - 3\left(1-\zeta^2\right)^{\frac{2}{3}} z^* + \frac{10}{3}\beta^* \frac{(1-\zeta^2)^{\frac{2}{3}}}{\zeta} \int_0^\zeta \frac{\zeta^2\, d\zeta}{(1-\zeta^2)^{\frac{2}{3}}} = 0. \tag{6.6.1}$$

We derive an approximate solution for the cubic equation (6.6.1).

Equation (6.6.1) is first transformed to the standard form [2]

$$s^{*3} + 3Hs^* + G = 0, \tag{6.6.2}$$

as described in Section 5.4.3. Let

$$z^* = s^* + \left(1-\zeta^2\right)^{\frac{1}{3}}. \tag{6.6.3}$$

The cubic equation (6.6.1) becomes

$$s^{*3} - 3\left(1-\zeta^2\right)^{\frac{2}{3}} s^* - 2\left(1-\zeta^2\right) + \frac{10}{3}\beta^* \frac{(1-\zeta^2)^{\frac{2}{3}}}{\zeta} \int_0^\zeta \frac{\zeta^{*2}\, d\zeta^*}{(1-\zeta^{*2})^{\frac{2}{3}}} = 0. \tag{6.6.4}$$

Equation (6.6.4) is in the standard form (6.6.2) with

$$H(\zeta) = -\left(1-\zeta^2\right)^{\frac{2}{3}}, \tag{6.6.5}$$

$$G(\zeta) = -2\left(1-\zeta^2\right) + \frac{10}{3}\beta^* \frac{(1-\zeta^2)^{\frac{2}{3}}}{\zeta} \int_0^\zeta \frac{\zeta^2\, d\zeta}{(1-\zeta^2)^{\frac{2}{3}}}. \tag{6.6.6}$$

On the dividing streamline, $0 \leq |\, \zeta \,| < 1$. We now consider an expansion in powers of ζ^2. No assumption is placed on β^* and time t. The results should be a good approximation for all positive values of $\beta^* > 0$ describing fluid injection and for all time. For large β^* the dividing streamline is closer to the z^*-axis. The approximation should therefore be better for large values of β^* because the maximum value of $|\zeta|$ on the dividing streamline is smaller.

The expansion of $H(\zeta)$ in powers of ζ^2 is

$$H(\zeta) = -\left[1 - \frac{2}{3}\,\zeta^2 - \frac{1}{9}\,\zeta^4 + \bigcirc\left(\zeta^6\right)\right]. \tag{6.6.7}$$

Consider next the expansion of $G(\zeta)$. Using integration by parts twice we obtain

$$\int_0^{\zeta} \frac{\zeta^{*2}\,d\zeta^*}{\left(1-\zeta^{*2}\right)^{\frac{2}{3}}} = \frac{\zeta^3}{3\left(1-\zeta^2\right)^{\frac{2}{3}}} - \frac{4}{45}\frac{\zeta^5}{\left(1-\zeta^2\right)^{\frac{5}{3}}} + \frac{8}{27}\int_0^{\zeta} \frac{\zeta^{*6}\,d\zeta^*}{\left(1-\zeta^{*2}\right)^{\frac{8}{3}}}. \tag{6.6.8}$$

Thus

$$G(\zeta) = -2\left(1-\zeta^2\right) + \frac{10}{3}\beta^*\left[\frac{1}{3}\,\zeta^2 - \frac{4}{45}\,\frac{\zeta^4}{\left(1-\zeta^2\right)} + \bigcirc\left(\zeta^6\right)\right], \tag{6.6.9}$$

and therefore

$$G(\zeta) = -2\left[1 - \left(1 + \frac{5}{9}\beta^*\right)\zeta^2 + \frac{4}{27}\,\beta^*\zeta^4 + \bigcirc\left(\zeta^6\right)\right]. \tag{6.6.10}$$

The expansion of the cubic equation (6.6.4) in powers of ζ^2 is therefore

$$\begin{aligned} s^{*3} &- 3\left[1 - \frac{2}{3}\,\zeta^2 - \frac{1}{9}\,\zeta^4 + \bigcirc\left(\zeta^6\right)\right] s^* \\ &- 2\left[1 - \left(1 + \frac{5}{9}\beta^*\right)\zeta^2 + \frac{4}{27}\beta^*\zeta^4 + \bigcirc\left(\zeta^6\right)\right] = 0, \end{aligned} \tag{6.6.11}$$

where from (6.6.3)

$$z^* = s^* + 1 - \frac{1}{3}\,\zeta^2 - \frac{1}{9}\,\zeta^4 + \bigcirc\left(\zeta^6\right). \tag{6.6.12}$$

We will derive the solution correct to order ζ^2. We find that this gives a sufficiently accurate result. The solution to higher order in ζ^2 can be derived. We have expanded $H(\zeta)$ and $G(\zeta)$ to order ζ^4 which could be used to calculate the solution to order ζ^4.

The discriminant, Δ, of the cubic equation (6.6.11) is

$$\Delta = G^2 + 4H^3 = -\frac{40}{9}\,\beta^*\zeta^2 + \bigcirc\left(\zeta^4\right). \tag{6.6.13}$$

(i) Zero order in ζ^2

To zero order in ζ^2,

$$\Delta = 0, \quad H = -1 \neq 0, \quad G = -2 \neq 0. \tag{6.6.14}$$

The cubic equation has three real roots with two roots coincident, one root different [2]. Equation (6.6.11) reduces to

$$(s^* + 1)^2 (s^* - 2) = 0 \tag{6.6.15}$$

and therefore

$$s^* = -1, \quad s^* = -1, \quad s^* = 2. \tag{6.6.16}$$

From (6.6.12) to zero order in ζ^2,

$$z^* = 0, \quad z^* = 0, \quad z^* = 3. \tag{6.6.17}$$

Since we have imposed the condition $\zeta^* = 0$, the solution is the three points, $(0,0), (0,0)$ and $(0,3)$ on the centre line. The zero order solution for the dividing streamline is the point $(0,0)$ at the base on the centre line.

(ii) Solution correct to first order in ζ^2

Correct to first order in ζ^2, equations (6.6.11), (6.6.7), (6.6.10) and (6.6.12) become

$$s^{*3} - 3\left[1 - \frac{2}{3}\zeta^2 + \bigcirc(\zeta^4)\right] s^* - 2\left[1 - (1 + \frac{5}{9}\beta^*)\zeta^2 + \bigcirc(\zeta^4)\right] = 0, \tag{6.6.18}$$

$$H(\zeta) = -\left[1 - \frac{2}{3}\zeta^2 + \bigcirc\left(\zeta^4\right)\right], \tag{6.6.19}$$

$$G(\zeta) = -2\left[1 - \left(1 + \frac{5}{9}\beta^*\right)\zeta^2 + \bigcirc\left(\zeta^4\right)\right], \tag{6.6.20}$$

$$z^* = s^* + 1 - \frac{1}{3}\zeta^2 + \bigcirc\left(\zeta^4\right). \tag{6.6.21}$$

The discriminant, Δ, of the cubic equation (6.6.18) is given by (6.6.13). Since we are considering $\beta^* > 0$ for blowing, $\Delta < 0$ provided $\zeta \neq 0$. The cubic equation (6.6.18) therefore has three real and distinct roots [2].

Since $\Delta < 0$ we again use the trigonometric method described in Section 5.4.3. The three roots of the cubic equation (6.6.18) are

$$s_n^* = 2\,(-H)^{\frac{1}{2}} \cos\left(\phi + \frac{2n\pi}{3}\right), \qquad n = 0, 1, 2, \tag{6.6.22}$$

where ϕ satisfies

$$\cos 3\phi = -\frac{G}{2\,(-H)^{\frac{3}{2}}} = 1 - \frac{5}{9}\beta^* \zeta^2 + \bigcirc\left(\zeta^4\right). \tag{6.6.23}$$

Thus from (6.6.21),

$$z_0^* = \left[1 - \frac{1}{3}\zeta^2 + \bigcirc\left(\zeta^4\right)\right]\left[1 + 2\cos\phi\right], \tag{6.6.24}$$

$$z_1^* = \left[1 - \frac{1}{3}\zeta^2 + \bigcirc\left(\zeta^4\right)\right]\left[1 + 2\cos\left(\phi + \frac{2\pi}{3}\right)\right], \tag{6.6.25}$$

$$z_2^* = \left[1 - \frac{1}{3}\zeta^2 + \bigcirc\left(\zeta^4\right)\right]\left[1 + 2\cos\left(\phi + \frac{4\pi}{3}\right)\right]. \tag{6.6.26}$$

Consider now ϕ. For $\zeta = 0$, $\cos 3\phi = 1$ and therefore $\phi = 0$ since $0 \leq \phi \leq \frac{\pi}{3}$. Hence for first order in ζ^2, ϕ will be small, We therefore let $\phi = \delta$ where $\delta > 0$ is small. Then from (6.6.23)

$$\cos(3\delta) = 1 - \frac{5}{9}\beta^*\,\zeta^2 + \bigcirc\left(\zeta^4\right). \tag{6.6.27}$$

Using the series expansion (5.4.161) for cosine gives

$$1 - \frac{9}{2}\delta^2 + \bigcirc\left(\delta^4\right) = 1 - \frac{5}{9}\beta^* \zeta^2 + \bigcirc\left(\zeta^4\right) \tag{6.6.28}$$

and therefore since $0 \leq \delta \leq \pi/3$,

$$\delta = \frac{\sqrt{10}}{9}\,\beta^{*\frac{1}{2}}\zeta + \bigcirc\left(\zeta^3\right). \tag{6.6.29}$$

Consider first z_0^*, given by (6.6.24) with $\phi = \delta$. Now

$$\cos\delta = 1 - \frac{1}{2}\delta^2 + \bigcirc\left(\delta^4\right) = 1 - \frac{5}{81}\beta^*\zeta^2 + \bigcirc\left(\zeta^4\right). \tag{6.6.30}$$

Thus

$$z_0^* = \left[1 - \frac{1}{3}\zeta^2 + \bigcirc\left(\zeta^4\right)\right]\left[3 - \frac{10}{81}\beta^*\zeta^2 + \bigcirc\left(\zeta^4\right)\right], \tag{6.6.31}$$

and therefore

$$z_0^* = 3\left[1 - \frac{1}{3}\left(1 + \frac{10}{81}\beta^*\right)\zeta^2 + \bigcirc\left(\zeta^4\right)\right]. \tag{6.6.32}$$

Consider next z_1^* given by (6.6.25) with $\phi = \delta$. From (5.4.172)

$$\cos\left(\delta + \frac{2\pi}{3}\right) = -\frac{1}{2}\left(\cos\delta + \sqrt{3}\sin\delta\right). \tag{6.6.33}$$

Now $\cos\delta$ is given by (6.6.30)and using the series expansion for $\sin\delta$ with δ given by (6.6.29) we obtain

$$\sin\delta = \delta + \bigcirc\left(\delta^3\right) = \frac{\sqrt{10}}{9}\beta^{*\frac{1}{2}}\zeta + \bigcirc\left(\zeta^3\right). \tag{6.6.34}$$

Thus

$$\cos\left(\delta + \frac{2\pi}{3}\right) = -\frac{1}{2}\left[1 + \frac{\sqrt{30}}{9}\beta^{*\frac{1}{2}}\zeta - \frac{5}{81}\beta^*\zeta^2 + \bigcirc\left(\zeta^3\right)\right]. \tag{6.6.35}$$

Hence (6.6.25) becomes

$$z_1^* = \left[1 - \frac{1}{3}\zeta^2 + \bigcirc\left(\zeta^4\right)\right]\left[-\frac{\sqrt{30}}{9}\beta^{*\frac{1}{2}}\zeta + \frac{5}{81}\beta^*\zeta^2 + \bigcirc\left(\zeta^3\right)\right] \tag{6.6.36}$$

and therefore

$$z_1^* = -\frac{\sqrt{30}}{9}\beta^{*\frac{1}{2}}\zeta\left[1 - \frac{\sqrt{30}}{54}\beta^{*\frac{1}{2}}\zeta + \bigcirc\left(\zeta^2\right)\right]. \tag{6.6.37}$$

Finally, consider z_2^* given by (6.6.26) with $\phi = \delta$. From (5.4.177)

$$\cos\left(\delta + \frac{4\pi}{3}\right) = \frac{1}{2}\left(-\cos\delta + \sqrt{3}\sin\delta\right) \tag{6.6.38}$$

and using (6.6.30) for $\cos\delta$ and (6.6.34) for $\sin\delta$ we obtain

$$\cos\left(\delta+\frac{4\pi}{3}\right)=\frac{1}{2}\left[-1+\frac{\sqrt{30}}{9}\beta^{*\frac{1}{2}}\zeta+\frac{5}{81}\beta^{*}\zeta^{2}+\bigcirc\left(\zeta^{3}\right)\right]. \tag{6.6.39}$$

Thus (6.6.26) becomes

$$z_2^*=\left[1-\frac{1}{3}\zeta^2+\bigcirc\left(\zeta^4\right)\right]\left[\frac{\sqrt{30}}{9}\beta^{*\frac{1}{2}}\zeta+\frac{5}{81}\beta^{*}\zeta^{2}+\bigcirc\left(\zeta^{3}\right)\right] \tag{6.6.40}$$

and hence

$$z_2^*=\frac{\sqrt{30}}{9}\beta^{*\frac{1}{2}}\zeta\left[1+\frac{\sqrt{30}}{54}\beta^{*\frac{1}{2}}\zeta+\bigcirc\left(\zeta^2\right)\right]. \tag{6.6.41}$$

The solution $z^*=z_0^*(\zeta)$ is not a dividing streamline because it does not go through the point $\zeta=0, z^*=0$. It passes through the point $\zeta=0, z^*=3$ which lies on the centre line outside the thin film. The root z_2^* is obtained from z_1^* by replacing ζ by $-\zeta$. For $\zeta>0$ we have $z_1^*<0$ and $z_2^*>0$ while for $\zeta<0$ we have $z_1^*>0$ and $z_2^*<0$. The dividing streamline in the (ζ, z^*)-plane is therefore given by

$$\zeta>0 \quad : \qquad z^*=z_2^*(\zeta), \tag{6.6.42}$$

$$\zeta<0 \quad : \qquad z=z_1^*(\zeta). \tag{6.6.43}$$

The equation of the dividing streamline correct to order ζ^2 is

$$\zeta>0 \quad : \qquad z^*=\frac{\sqrt{30}}{9}\beta^{*\frac{1}{2}}\zeta\left[1+\frac{\sqrt{30}}{54}\beta^{*\frac{1}{2}}\zeta+\bigcirc\left(\zeta^2\right)\right], \tag{6.6.44}$$

$$\zeta<0 \quad : \qquad z=-\frac{\sqrt{30}}{9}\beta^{*\frac{1}{2}}\zeta\left[1-\frac{\sqrt{30}}{54}\beta^{*\frac{1}{2}}\zeta+\bigcirc\left(\zeta^2\right)\right]. \tag{6.6.45}$$

The equations of the dividing streamline in the (x,z)-plane, correct to order $(x/W(t))^2$ is

$$x>0 \quad : \qquad z=\frac{\sqrt{30}}{9}\beta^{*\frac{1}{2}}W^{-\frac{2}{2+5\beta^*}}(t)\frac{x}{W(t)}\times$$
$$\left[1+\frac{\sqrt{30}}{54}\beta^{*}\frac{x}{W(t)}+\bigcirc\left(\frac{x^2}{W^2(t)}\right)\right], \tag{6.6.46}$$

$$x < 0 \quad : \qquad z = -\frac{\sqrt{30}}{9}\,\beta^{*\frac{1}{2}}\,W^{-\frac{2}{2+5\beta^*}}(t)\frac{x}{W(t)} \times$$
$$\left[1 - \frac{\sqrt{30}}{54}\beta^* \frac{x}{W(t)} + \bigcirc\left(\frac{x^2}{W^2(t)}\right)\right], \tag{6.6.47}$$

where

$$W(t) = \left[1 + \frac{10}{9}\left(1+\beta^*\right)t\right]^{\frac{2+5\beta^*}{10(1+\beta^*)}} \tag{6.6.48}$$

and we have used

$$h(t,0) = W^{-\frac{2}{2+5\beta^*}}(t). \tag{6.6.49}$$

Let ϑ be the angle that the dividing streamline makes with the positive ζ-axis at the origin $\zeta = 0, z^* = 0$, in the (ζ, z^*)-plane. Then

$$\tan\vartheta = \left.\frac{\partial z_2^*}{\partial \zeta}\right|_{\zeta=0} = \frac{\sqrt{30}}{9}\beta^{*\frac{1}{2}}. \tag{6.6.50}$$

In Figure 6.11 the streamlines are plotted in the (ζ, z^*)-plane for $\beta^* = 1, 20, 50$. From (6.6.50) the corresponding values of $\vartheta = \vartheta(\beta^*)$ are

$$\vartheta(1) = 31.3^\circ, \quad \vartheta(20) = 69.8^\circ, \quad \vartheta(50) = 76.9^\circ, \tag{6.6.51}$$

which agrees well with the slope of the dividing streamlines at the origin in Figure 6.11.

Consider now the (x, z)-plane in which the angle ϑ depends on time. From (6.6.46),

$$\tan\vartheta = \left.\frac{\partial z_2}{\partial x}\right|_{x=0} = \frac{\sqrt{30}}{9}\beta^{*\frac{1}{2}}W^{-\left(\frac{4+5\beta^*}{2+5\beta^*}\right)}(t). \tag{6.6.52}$$

Using (6.6.48) for $W(t)$, (6.6.52) becomes

$$\tan\vartheta = \frac{\sqrt{30}}{9}\beta^{*\frac{1}{2}}\left[1 + \frac{10}{9}\left(1+\beta^*\right)t\right]^{-\left(\frac{4+5\beta^*}{10(1+\beta^*)}\right)}. \tag{6.6.53}$$

The angle ϑ decreases with time in the (x, z)-plane, consistent with Figure (6.10). We now derive two asymptotic results for the time dependence of $\tan\vartheta$ in the (x, z)-plane.

Consider first small values of time such that

$$t < \frac{9}{10\,(1+\beta^*)}. \tag{6.6.54}$$

Then, neglecting terms of order $((1+\beta^*)\,t)^2$,

$$\left[1 + \frac{10}{9}\,(1+\beta^*)\,t\right]^{-\left(\frac{4+5\beta^*}{10(1+\beta^*)}\right)} = \exp\left[-\frac{1}{9}\,(4+5\beta^*)\,t\right] \tag{6.6.55}$$

and therefore for small values of time satisfying (6.6.54) we have approximately,

$$\tan\vartheta = \frac{\sqrt{30}}{9}\beta^{*\frac{1}{2}} \exp\left[-\frac{1}{9}\,(4+5\beta^*)\,t\right]. \tag{6.6.56}$$

Thus the gradient of the dividing streamline at the origin initially decreases exponentially with time.

Consider next the asymptotic value of $\tan\vartheta$ as $\beta^* \to \infty$ at a fixed time t. Keeping only the dominant term in an expansion for large β^*,

$$\left[1 + \frac{10}{9}\,(1+\beta^*)\,t\right]^{-\left(\frac{4+5\beta^*}{10(1+\beta^*)}\right)} \sim \left(\frac{10}{9}\beta^* t\right)^{-\frac{1}{2}}, \tag{6.6.57}$$

and therefore for large β^*,

$$\tan\vartheta \sim \frac{\sqrt{30}}{9}\beta^{*\frac{1}{2}} \left(\frac{10}{9}\beta^* t\right)^{-\frac{1}{2}} = \frac{1}{\sqrt{3}\,t^{\frac{1}{2}}}. \tag{6.6.58}$$

Thus for large β^*, with increasing time the gradient at the origin of the dividing streamline decreases like $1/\sqrt{t}$. This is illustrated in Figure 6.12 where the dividing streamline, given by (6.6.46) and (6.6.47), is plotted against x for $\beta^* = 50$ and a range of values of time. In Figure 6.13, the angle ϑ given by (6.6.53) is plotted against β^* for a range of values of time. We see that as β^* increases, ϑ tends more rapidly to the asymptotic value for large time, (6.6.58).

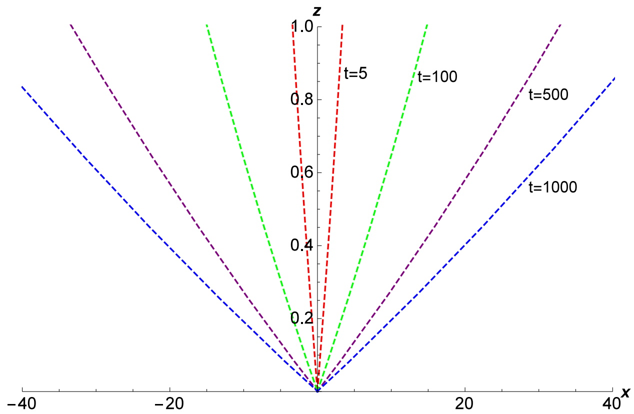

Figure 6.12: Dividing streamline, given by (6.6.46) and (6.6.47), plotted against x for $\beta^* = 50$ at time $t = 5$, $t = 100$, $t = 500$ and $t = 1000$.

Finally consider the point of intersection, P, of the dividing streamline with the surface of the thin film $z = h(t, x)$. Consider the (ζ, z^*)-plane with $\zeta > 0$ and denote the point of intersection by $(\zeta_p\,, z_p^*)$. From (6.3.21) for $h(t, x)$,

$$z_p^* = \left(1 - \zeta_p^2\right)^{\frac{1}{3}}. \tag{6.6.59}$$

Using (6.6.44), the point of intersection satisfies

$$\left(1 - \zeta_p^2\right)^{\frac{1}{3}} = \frac{\sqrt{30}}{9}\beta^{*\frac{1}{2}}\zeta_p\left[1 + \frac{\sqrt{30}}{54}\beta^{*\frac{1}{2}}\zeta_p + \bigcirc(\zeta^2)\right]. \tag{6.6.60}$$

We expand the left hand side and neglect terms of order ζ_p^3. This gives

$$\left(1 + \frac{5}{27}\beta^*\right)\zeta_p^2 + \frac{\sqrt{30}}{3}\beta^{*\frac{1}{2}}\zeta_p - 3 = 0, \tag{6.6.61}$$

which is a quadratic equation for ζ_p.

If terms of order ζ_p^2 are neglected then (6.6.61) and (6.6.59) give

$$\zeta_p = \frac{9}{\sqrt{30}}\frac{1}{\beta^{*\frac{1}{2}}}, \qquad z_p^* = 1. \tag{6.6.62}$$

We see that as β^* increases, ζ_p decreases showing that the expansion in ζ_p is more accurate for large β^*. The combination $\beta^{*\frac{1}{2}}\zeta_p$ occurs in expansions such as in (6.6.35)

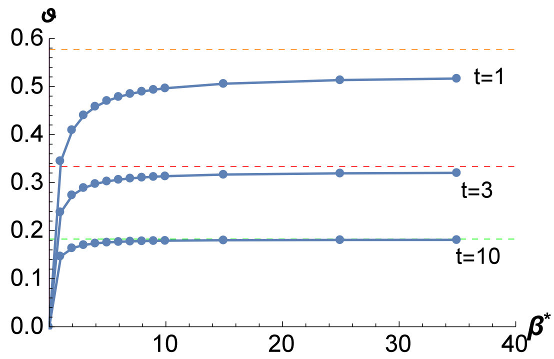

Figure 6.13: The angle ϑ in radians, given by (6.6.53), plotted against β^* for a range of values of time. The asymptotic value of ϑ for large β^*, given by (6.6.58), is shown by a dotted line $(- - -)$.

and (6.6.39). These expansions exist even for large β^* because $\beta^{*\frac{1}{2}}\zeta_p$ is order of magnitude one. In the (x, z)-plane the point of intersection is

$$x_p = \frac{9}{\sqrt{30}}\frac{1}{\beta^{*\frac{1}{2}}}W(t), \qquad z_p = W^{-\frac{2}{2+5\beta^*}}(t), \tag{6.6.63}$$

where we used (6.6.49) for $h(t, 0)$ and $W(t)$ is given by (6.6.48).

The approximation correct to order ζ_p^2 is obtained by solving the quadratic equation (6.6.61). The positive root of (6.6.61) can be expressed as

$$\zeta_p = \frac{\sqrt{3}}{\left(1+\frac{5}{27}\beta^*\right)}\left[\left(1+\frac{25}{54}\beta^*\right)^{\frac{1}{2}} - \frac{\sqrt{10}}{6}\beta^*\right]. \tag{6.6.64}$$

and (6.6.59) expanded correct to order ζ_p^2 is

$$z_p^* = 1 - \frac{1}{3}\zeta_p^2. \tag{6.6.65}$$

In the (x, z)-plane with $x > 0$ the point of intersection is

$$x_p = \zeta_p W(t), \qquad z_p = \left(1 - \frac{1}{3}\left(\frac{x_p}{W(t)}\right)^2\right)W^{-\frac{2}{2+5\beta^*}}(t). \tag{6.6.66}$$

In Figure 6.14 the approximate solutions for the dividing streamlines given by (6.6.46) and (6.6.47) are plotted with the numerical solution of (6.6.1) for the dividing streamline at time $t = 5$ for $\beta^* = 5$, $\beta^* = 10$, $\beta^* = 15$ and $\beta^* = 50$. From the graphs we see that the approximate solution is quite close to the numerical solution and as the value of β^* is increased the approximation moves even closer to the numerical solution and is almost indistinguishable. From the graphs it is also clear that as the magnitude of β^* is increased, the gradient of the dividing streamline

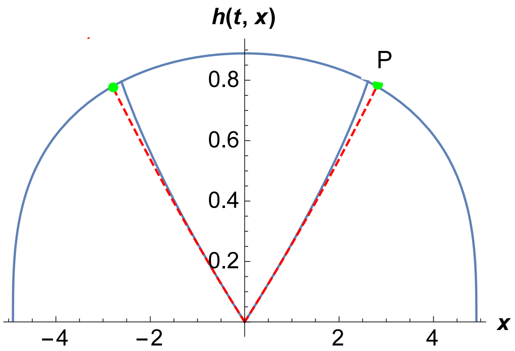

(a) $\beta^* = 5$

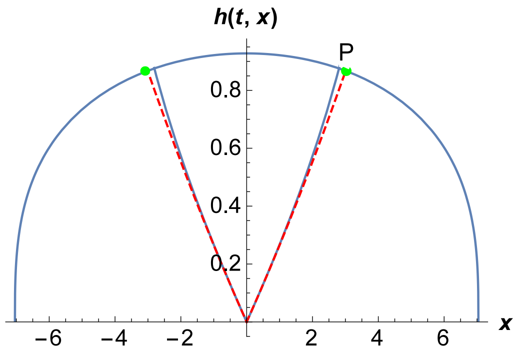

(b) $\beta^* = 10$

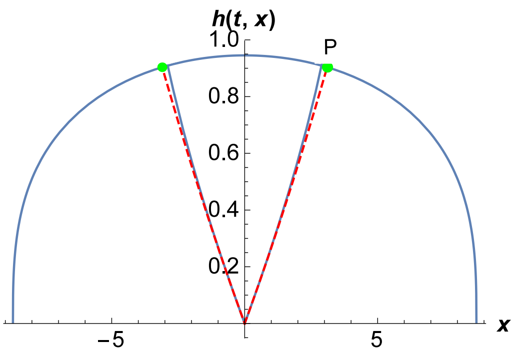

(c) $\beta^* = 15$

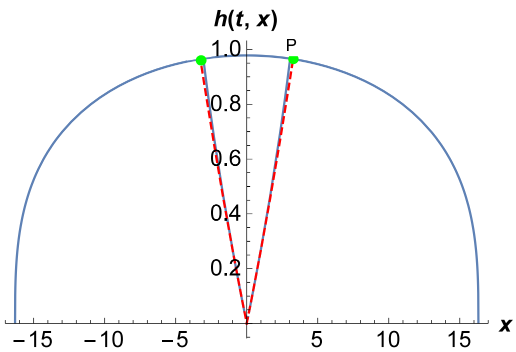

(d) $\beta^* = 50$

Figure 6.14: Approximate solution for the dividing streamlines $(- - -)$ given by (6.6.46) and (6.6.47) plotted with the dividing streamline (—) derived from the numerical solution of (6.6.1) for a range of β^* at a fixed time $t = 5$. The point of intersection of the dividing streamline with the surface $z = h(t, x)$ given by (6.6.66) is depicted on the graphs by $\bullet$.

increases because the velocity of fluid injection at the base increases. The injection velocity increases with x which forces the dividing streamline to moves towards the centre line.

6.7 Conclusions

When the fluid velocity at the base is proportional to the spatial gradient of the height a complete analytical solution can be derived. The fluid variables and the streamlines could be fully analysed. The injection velocity is zero at the centre line and infinite at the moving contact line. This resulted in the formation of a dividing streamline which separated fluid descending due to gravity from fluid ascending due to injection at the base. The properties of the dividing streamline could be analysed by using an approximate solution. The thin film approximation is satisfied for the whole range of blowing but only for weak to moderate suction.

Chapter 7

Axisymmetric liquid drop

7.1 Introduction

In this thesis we compare the spreading under gravity of a two-dimensional thin fluid film with an axisymmetric liquid drop, undergoing suction or blowing at the base. The spreading of an axisymmetric liquid drop with suction or blowing has been considered by Mason and Momoniat [20]. These authors derived the group invariant solution and analysed the evolution of the surface profile, the base radius, the total volume and the normal fluid velocity at the base for Model I on which the velocity at the bases is proportional to the height of the drop and for Model II in which it is proportional to the spatial gradient of the height. They did not impose the condition $h(0,0) = 1$ on the initial dimensionless height which meant that the initial velocity V_0 was not determined or make a change of variable similar to that described in Section 4.3.4 to simplify the parameters. They also did not analyse the fluid velocity on the axis of symmetry in Model I or the streamlines in Model I and II.

In this chapter we will outline the derivation of the mathematical model, giving the equations for the fluid velocity necessary to analyse the fluid velocity inside the liquid drop, and also derive the group invariant solution. We will impose the condition $h(0,0) = 1$ and make a transformation of variables similar to that in Section 4.3.4.

In Chapter 8, Model I will be considered with emphasis on the analysis of the fluid velocity on the axis of symmetry and investigation of the streamlines. In Chapter 9, Model II will be considered, with emphasis on the streamlines. In Chapters 8 and 9, the derivation of the other properties of the spreading of the liquid drop will be summarised because they will be required in the comparison between the evolution of the two-dimensional thin film and the axisymmetric liquid drop.

7.2 Mathematical model of the axisymmetric spreading of a liquid drop with suction/injection

Consider the axisymmetric spreading of an incompressible liquid drop under gravity on a fixed horizontal plane. At the horizontal plane there is suction of fluid from the thin film or blowing of fluid into the thin film. The coordinates and the physical quantities are shown in Figure 7.1

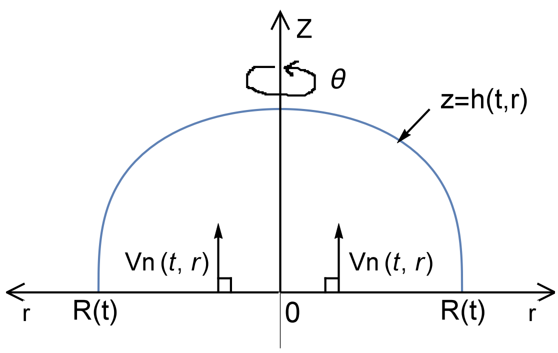

Figure 7.1: Spreading of an axisymmetric liquid drop of radius $R(t)$ under gravity with blowing ($v_n > 0$) or suction ($v_n < 0$) of fluid at the base.

The equation of the free surface of the liquid drop is $z = h(t,r)$.The body force per unit mass is due to gravity and acts in the $-z$ direction:

$$\underline{F} = \underline{g}; \qquad F_x = 0\ , \qquad F_y = 0\ , \qquad F_z = -g. \tag{7.2.1}$$

The dimensional thin film equations are given by equations (2.2.73)-(2.2.76) and the components of the Cauchy stress tensor by (2.2.89). Using (7.2.1), equations (2.2.73)-(2.2.76) become

$$\frac{\partial p}{\partial r} = \mu\,\frac{\partial^2 v_r}{\partial z^2}, \tag{7.2.2}$$

$$\frac{\partial p}{\partial z} = -\rho\, g, \tag{7.2.3}$$

$$\frac{1}{r}\frac{\partial}{\partial r}(r\, v_r) + \frac{\partial v_z}{\partial z} = 0. \tag{7.2.4}$$

The components of the Cauchy stress are

$$\tau_{rr} = -p, \quad \tau_{\theta\theta} = -p, \quad \tau_{zz} = -p, \quad \tau_{r\theta} = 0, \quad \tau_{rz} = \mu\frac{\partial v_r}{\partial z}, \quad \tau_{\theta z} = 0. \tag{7.2.5}$$

Consider now the boundary conditions.

$z = 0$: No slip boundary condition for a viscous fluid at a solid boundary

$$v_r(t,r,0) = 0. \tag{7.2.6}$$

$z = 0$: A normal velocity is induced by the fluid injection/suction

$$v_z(t,r,0) = v_n(t,r), \tag{7.2.7}$$

where if

$$\begin{aligned} v_n(t,r) &> 0 \quad \text{blowing/injection,} \\ v_n(t,r) &< 0 \quad \text{suction.} \end{aligned}$$

$z = h(t,r)$:

$$p(t,r,0) = p_0, \tag{7.2.8}$$

where p_0 is the atmospheric pressure.

$z = h(t, r)$: No tangential stress on the free surface

$$\tau_{zr} = \mu \frac{\partial v_r}{\partial z}(t, r, h) = 0. \tag{7.2.9}$$

$z = h(t, r)$: A fluid particle on a free surface remains on the free surface.

$$v_z(t, r, h) = \frac{\partial h}{\partial t} + v_r(t, r, h) \frac{\partial h}{\partial r}. \tag{7.2.10}$$

We now write the equations and boundary conditions in dimensionless form. We list the characteristic quantities .

Characteristic length in r-direction: $R_0 = R(0)$, initial radius of the liquid drop.

Characteristic length in z-direction: $H = h(0, 0)$, initial height of the liquid drop at the center of the liquid drop.

Characteristic pressure:

$$P = \frac{\mu\, U R_0}{H^2} = \rho\, g\, H.$$

Characteristic velocity in the r-direction:

$$U = \frac{g\, H^3}{\nu\, R_0}.$$

Characteristic velocity in the z-direction:

$$\frac{H\, U}{R_0}.$$

Characteristic time:

$$T = \frac{R_0}{U}.$$

The characteristic velocity U was obtained by equating the two expressions for the characteristic pressure P.

We define the following dimensionless variables:

$$\overline{R} = \frac{R}{R_0}, \qquad \overline{z} = \frac{z}{H}, \qquad \overline{v}_r = \frac{v_r}{U}, \qquad \overline{v}_z = \frac{R_0\, v_z}{H\, U},$$

$$\overline{v}_n = \frac{R_0\, v_n}{H\, U}, \qquad \overline{t} = \frac{t}{T}, \qquad \overline{h} = \frac{h}{H}, \qquad \overline{p} = \frac{p}{P}, \qquad \overline{\tau}_{ik} = \frac{\tau_{ik}}{P}. \tag{7.2.11}$$

Expressed in dimensionless form equations (3.2.5)-(3.2.7) become

$$\begin{aligned} \frac{\partial \overline{p}}{\partial \overline{r}} &= \frac{\partial^2 \overline{v}_r}{\partial \overline{z}^2}, && (7.2.12)\\ \frac{\partial \overline{p}}{\partial \overline{z}} &= -1, && (7.2.13)\\ \frac{1}{\overline{r}}\frac{\partial}{\partial \overline{r}}\left(\overline{r}\overline{v}_r\right) + \frac{\partial \overline{v}_z}{\partial \overline{z}} &= 0. && (7.2.14) \end{aligned}$$

The boundary conditions are:

$$\begin{aligned} \bar{z} &= 0: && \bar{v}_r(\bar{t},\bar{r},0) = 0, && (7.2.15)\\ \bar{z} &= 0: && \bar{v}_z(\bar{t},\bar{r},0) = \bar{v}_n(\bar{r},t), && (7.2.16)\\ \bar{z} &= \bar{h}(\bar{t},\bar{r}): && \bar{p}(\bar{t},\bar{r},\bar{h}) = \bar{p}_0, && (7.2.17)\\ \bar{z} &= \bar{h}(\bar{t},\bar{r}): && \bar{\tau}_{zr}(\bar{t},\bar{r},\bar{h}) = \frac{H}{L}\frac{\partial \bar{v}_r}{\partial \bar{z}}(\bar{t},\bar{r},\bar{h}) = 0, && (7.2.18)\\ \bar{z} &= \bar{h}(\bar{t},\bar{r}): && \frac{\partial \bar{h}}{\partial \bar{t}} + \bar{v}_r(\bar{t},\bar{r},\bar{h})\,\frac{\partial \bar{h}}{\partial \bar{r}} = \bar{v}_z(\bar{t},\bar{r},\bar{h}). && (7.2.19) \end{aligned}$$

Initial conditions:

Since

$$\bar{R}(t) = \frac{R(t)}{R(0)}, \tag{7.2.20}$$

it follows that

$$\bar{R}(0) = 1. \tag{7.2.21}$$

The overhead bars will be suppressed in equations (7.2.12)-(7.2.21).

We now derive the partial differential equation for $h(t,r)$. We first obtain an expression for $v_z(t,r,h)$. Integrate the continuity equation (7.2.14) with respect to z from $z = 0$ to $z = h(t,r)$:

$$\int_0^{h(t,r)} \frac{\partial}{\partial r}(r\, v_r(t,r,z))dz + r\int_0^{h(t,r)} \frac{\partial v_z(t,r,z)}{\partial z}dz = 0. \tag{7.2.22}$$

But from the formula for differentiation under the integral sign [10]

$$\int_0^{h(t,r)} \frac{\partial}{\partial r}(r\, v_r(t,r,z))dz = \frac{\partial}{\partial r}\int_0^{h(t,r)} r\, v_r(t,r,z)dz - r\, v_r(t,r,h)\frac{\partial h}{\partial r}, \qquad (7.2.23)$$

and

$$\int_0^{h(t,r)} \frac{\partial v_z(t,r,z)}{\partial z}dz = v_z(t,r,h) - v_n(t,r), \qquad (7.2.24)$$

where the boundary condition (7.2.16) at $z = 0$ has been applied. Substituting (7.2.23) and (7.2.24) into (7.2.22) and solving for $v_z(t,r,h)$ gives

$$v_z(t,r,h) = -\frac{1}{r}\frac{\partial}{\partial r}\left(r\int_0^{h(t,r)} v_r(t,r,z)dz\right) + v_r(t,r,h)\frac{\partial h}{\partial r} + v_n(t,r). \qquad (7.2.25)$$

Substituting (7.2.25) into (7.2.19) we obtain

$$\frac{\partial h}{\partial t} + \frac{1}{r}\frac{\partial}{\partial r}\left(r\int_0^{h(t,r)} v_r(t,r,z)dz\right) = v_n(t,r). \qquad (7.2.26)$$

We now need to obtain an expression for $v_r(t,r,z)$. From (7.2.13)

$$p(t,r,z) = -z + N(t,r), \qquad (7.2.27)$$

where $N(t,r)$ is an arbitrary function of integration. But imposing the boundary condition (7.2.17) at $z = h(t,r)$ gives

$$N(t,r) = p_0 + h(t,r), \qquad (7.2.28)$$

and therefore

$$p(t,r,z) = p_0 + h(t,r) - z. \qquad (7.2.29)$$

Also from (7.2.12) and (7.2.29)

$$\frac{\partial^2 v_r(t,r,z)}{\partial z^2} = \frac{\partial h(t,r)}{\partial r}. \qquad (7.2.30)$$

Integrating with respect with z gives

$$\frac{\partial v_r(t,r,z)}{\partial z} = z\frac{\partial h(t,r)}{\partial r} + B(t,r), \qquad (7.2.31)$$

where $B(t,r)$ is the arbitrary function of integration and applying the boundary condition (7.2.18) results in

$$B(t,r) = -h(t,r)\frac{\partial h(t,r)}{\partial r}. \tag{7.2.32}$$

Thus

$$\frac{\partial v_r}{\partial z}(t,r,z) = (z - h(t,r))\,\frac{\partial h}{\partial r}(t,r). \tag{7.2.33}$$

and integrating again with respect to z gives

$$v_r(t,r,z) = \left(\frac{1}{2}z^2 - z\,h(t,r)\right)\frac{\partial h}{\partial r}(t,r) + C(t,r), \tag{7.2.34}$$

where $C(t,r)$ is an arbitrary function of integration. Applying the no slip boundary condition (7.2.15) results in $C(t,r) = 0$, hence

$$v_r(t,r,z) = \left(\frac{z^2}{2} - z\,h(t,r)\right)\frac{\partial h}{\partial r}(t,r) \tag{7.2.35}$$

and therefore

$$\int_0^{h(t,r)} v_r(t,r,z)dz = -\frac{1}{3}h^3\frac{\partial h}{\partial r}. \tag{7.2.36}$$

Finally substituting (7.2.36) into (7.2.26) we obtain

$$\frac{\partial h}{\partial t} = \frac{1}{3r}\frac{\partial}{\partial r}\left(r\,h^3\,\frac{\partial h}{\partial r}\right) + v_n(t,r). \tag{7.2.37}$$

Equation (7.2.37) is a nonlinear diffusion equation, with a source or sink term, for the height $h(t,r)$ of the liquid drop.

7.3 Constraint equation

Since the fluid is incompressible the total volume of the liquid drop can change only due to fluid leaking off at the base or being blown into the liquid drop at the base.

We first use dimensional variables. Now the element of volume at distance r from the axis is

$$\delta V = h(t,r)\,2\pi r\delta r, \tag{7.3.1}$$

and therefore the total volume of the liquid drop is

$$V(t) = 2\pi \int_0^{R(t)} r\, h(t, r)\, dr. \tag{7.3.2}$$

Let us now consider the rate of inflow into the liquid drop at the base. The element of area at distance r from the axis is $\delta\, A = 2\pi r\, \delta r$ and therefore if δV now denotes the volume of fluid blown into the liquid drop through area δA in time δt,

$$\delta V = 2\pi r\, \delta r\, v_n(t, r)\, \delta t. \tag{7.3.3}$$

Thus

$$\frac{\delta V}{\delta t} = 2\pi r\, v_n(t, r) \delta r, \tag{7.3.4}$$

hence

$$\frac{dV}{dt} = 2\pi \int_0^{R(t)} r\, v_n(t, r)\, dr. \tag{7.3.5}$$

Equations (7.3.2) and (7.3.5) are made dimensionless using the dimensionless variables (7.2.11). The characteristic volume is $\pi\, R_0^2\, H$ and the dimensionless total volume is

$$\overline{V}(\overline{t}) = \frac{V(t)}{\pi\, R_0^2\, H}. \tag{7.3.6}$$

Expressed in dimensionless variables, (7.3.2) is

$$\overline{V}(\overline{t}) = 2\pi \int_0^{\overline{R}(t)} \overline{r}\, \overline{h}(\overline{t}, \overline{r})\, d\overline{r}, \tag{7.3.7}$$

and the balance law (7.3.5) becomes

$$\frac{d\overline{V}}{d\overline{t}} = 2\pi \int_0^{\overline{R}(t)} \overline{r}\, \overline{v}_n(\overline{t}, \overline{r})\, d\overline{r}. \tag{7.3.8}$$

The overhead bars will be suppressed in (7.3.7) and (7.3.8).

7.4 Group invariant solution

Mason and Momoniat [20] have shown that

$$X = (c_1 + c_2\, t)\frac{\partial}{\partial t} + c_3 r \frac{\partial}{\partial r} + \frac{1}{3}\,(2c_3 - c_2)\, h\, \frac{\partial}{\partial h}, \tag{7.4.1}$$

is the general form of the Lie point symmetry of the partial differential equation (7.2.37) provided that $v_n(t,r)$ satisfies the first order linear partial differential equation

$$(c_1 + c_2\, t)\frac{\partial v_n}{\partial t} + c_3 r\frac{\partial v_n}{\partial r} = \frac{2}{3}\,(c_3 - 2\,c_2)\, v_n, \tag{7.4.2}$$

where c_1, c_2 and c_3 are constants. Equation (7.4.1) can be written as

$$X = c_1 X_1 + c_2 X_2 + c_3 X_3, \tag{7.4.3}$$

where

$$X_1 = \frac{\partial}{\partial t}, \quad X_2 = t\frac{\partial}{\partial t} - \frac{1}{3}h\frac{\partial}{\partial h}, \quad X_3 = r\frac{\partial}{\partial r} + \frac{2}{3}\frac{\partial}{\partial h}. \tag{7.4.4}$$

There are only three Lie point symmetries compared with four for the spreading of a two-dimensional thin film.

Now $h = \Phi(t,r)$ is a group invariant solution of the partial differential equation (7.2.37) on condition that

$$X\,(h - \Phi(t,r))\,|_{h=\Phi} = 0, \tag{7.4.5}$$

where X is given in (7.4.1). Expanding (7.4.5) gives the first order linear partial differential equation

$$(c_1 + c_2\, t)\frac{\partial \Phi}{\partial t} + c_3 r\frac{\partial \Phi}{\partial r} = \frac{1}{3}\,(2c_3 - c_2)\,\Phi. \tag{7.4.6}$$

We consider the general case in which $c_2 \neq 0, c_3 \neq 0$ and $2c_3 \neq c_2$. The differential equations of the characteristic curves of (7.4.6) are

$$\frac{dt}{c_1 + c_2 t} = \frac{dr}{c_3 r} = 3\frac{d\Phi}{(2\,c_3 - c_2)\Phi}. \tag{7.4.7}$$

The first pair of terms gives

$$\frac{r}{(c_1 + c_2 t)^{\frac{c_3}{c_2}}} = a_1, \tag{7.4.8}$$

where a_1 is a constant. The first and third terms give

$$\frac{\Phi}{(c_1 + c_2 t)^{\frac{1}{3}\left(2\frac{c_3}{c_2} - 1\right)}} = a_2, \tag{7.4.9}$$

where a_2 is a constant. The general solution is

$$a_2 = F(a_1), \tag{7.4.10}$$

where F is an arbitrary function. Since $\Phi = h(t,r)$, the general solution is

$$h(t,r) = (c_1 + c_2 t)^{\frac{2}{3}\left(\frac{c_3}{c_2} - \frac{1}{2}\right)} F(\xi), \tag{7.4.11}$$

where

$$\xi = \frac{r}{(c_1 + c_2 t)^{\frac{c_3}{c_2}}}. \tag{7.4.12}$$

Consider now the first order linear partial differential equation (7.4.2) for $v_n(t,r)$. We assume further that $c_3 \neq 2c_2$. The differential equations of the characteristic curves are

$$\frac{dt}{c_1 + c_2 t} = \frac{dr}{c_3\, r} = \frac{dv_n}{\frac{2}{3}(c_3 - 2\, c_2) v_n}. \tag{7.4.13}$$

The first pair of terms again gives

$$\frac{r}{(c_1 + c_2 t)^{\frac{c_3}{c_2}}} = b_1, \tag{7.4.14}$$

where b_1 is a constant and the first and last terms give

$$\frac{v_n}{(c_1 + c_2 t)^{\frac{2}{3}\left(\frac{c_3}{c_2} - 2\right)}} = b_2, \tag{7.4.15}$$

where b_2 is a constant. The general solution is

$$v_n(t,r) = (c_1 + c_2 t)^{\frac{2}{3}\left(\frac{c_3}{c_2} - 2\right)} G(\xi), \tag{7.4.16}$$

where G is an arbitrary function and as before

$$\xi = \frac{r}{(c_1 + c_2 t)^{\frac{c_3}{c_2}}}. \tag{7.4.17}$$

7.4.1 Reduction of nonlinear diffusion equation to an ordinary differential equation

We will reduce the nonlinear diffusion equation

$$\frac{\partial h}{\partial t} = \frac{1}{3\,r}\frac{\partial}{\partial r}\left(r\,h^3\frac{\partial h}{\partial r}\right) + v_n(t,r), \tag{7.4.18}$$

to an ordinary differential equation using the group invariant solution (7.4.11), (7.4.16) and (7.4.17). We work with ξ and t as variables and eliminate r in terms of ξ and t by using (7.4.17). Also

$$\frac{\partial \xi}{\partial r} = \frac{1}{(c_1 + c_2 t)^{\frac{c_3}{c_2}}}, \qquad \frac{\partial \xi}{\partial t} = -\frac{c_3 \xi}{(c_1 + c_2 t)}. \tag{7.4.19}$$

Using (7.4.11) and (7.4.19) we obtain

$$\frac{\partial h}{\partial t} = c_3\,(c_1 + c_2 t)^{\frac{1}{3}\left(\frac{2c_3}{c_2} - 4\right)} \left(\frac{1}{3}\frac{c_2}{c_3}\left(\frac{2\,c_3}{c_2} - 1\right) F(\xi) - \xi\,\frac{dF}{d\xi}\right) \tag{7.4.20}$$

and

$$\frac{1}{3\,r}\frac{\partial}{\partial r}\left(r\,h^3\frac{\partial h}{\partial r}\right) = \frac{1}{3}\,(c_1 + c_2 t)^{\frac{2}{3}\frac{c_3}{c_2} - \frac{4}{3}}\,\frac{1}{\xi}\frac{d}{d\xi}\left(\xi\,F^3(\xi)\frac{dF}{d\xi}\right). \tag{7.4.21}$$

Substituting (7.4.20), (7.4.21) and (7.4.16) into (7.4.18) gives the ordinary differential equation

$$\frac{d}{d\xi}\left(\xi\,F^3\frac{dF}{d\xi}\right) + 3\,c_3\,\xi^2\frac{dF}{d\xi} + (c_2 - 2\,c_3)\,\xi\,F + 3\,\xi\,G(\xi) = 0. \tag{7.4.22}$$

The ordinary differential equation does not depend on the constant c_1.

7.4.2 Boundary condition at the moving contact line

The spreading liquid drop has only one moving contact line at $r = R(t)$ unlike the two-dimensional thin film which had two. Using (7.4.11) we write the boundary condition

$$h(t, R(t)) = 0, \qquad t \geq 0, \tag{7.4.23}$$

in terms of the similarity variable (7.4.17) as

$$F(A(t)) = 0, \tag{7.4.24}$$

where

$$A(t) = \frac{R(t)}{(c_1 + c_2 t)^{\frac{c_3}{c_2}}}. \tag{7.4.25}$$

Differentiating (7.4.24) with respect to t gives

$$\frac{dF}{dA}\frac{dA}{dt} = 0. \tag{7.4.26}$$

But $F(\xi)$ is not a constant function, thus $\frac{dF}{dA} \neq 0$. Hence

$$\frac{dA}{dt} = 0 \tag{7.4.27}$$

and therefore $A(t) = A_0$ where A_0 is a constant. Equation (7.4.25) gives

$$R(t) = A_0 c_1^{\frac{c_3}{c_2}} \left(1 + \frac{c_2}{c_3} t\right)^{\frac{c_3}{c_2}}. \tag{7.4.28}$$

But $R(0) = 1$ because the characteristic length is the initial radius of the liquid drop. Thus

$$A_0 = c_1^{-\frac{c_3}{c_2}} \tag{7.4.29}$$

and

$$R(t) = \left(1 + \frac{c_2}{c_1}\right)^{\frac{c_3}{c_2}}. \tag{7.4.30}$$

The boundary condition (7.4.24) becomes

$$F\left(c_1^{-\frac{c_3}{c_2}}\right) = 0 \tag{7.4.31}$$

and (7.4.17) for ξ can be written as

$$\xi = c_1^{-\frac{c_3}{c_2}} \frac{r}{R(t)}. \tag{7.4.32}$$

The similarity variables for the two-dimensional thin film and the axisymmetric liquid drop are given by (4.3.9) and (7.4.17):

$$\xi = \frac{c_4 + c_3 x}{(c_1 + c_2 t)^{\frac{c_3}{c_2}}}, \qquad \xi = \frac{r}{(c_1 + c_2 t)^{\frac{c_3}{c_2}}}. \tag{7.4.33}$$

For the two-dimensional thin film there is the additional unknown, c_4. The constant c_3 can be removed by redefining c_4, c_1 and c_2. Thus for the thin film there are two unknowns c_4 and $W(t)$, which needed boundary conditions at the two contact lines, $x = \pm W(t)$, to be determined while for the liquid drop there is only one unknown, $R(t)$, which needed a boundary condition at only the one contact line, $r = R(t)$, to be determined.

7.4.3 Balance law for fluid volume

The volume and rate-of-change of volume of the liquid drop are first written in terms of the similarity variable ξ. The two expressions, (7.4.17) and (7.4.32), for ξ are used. The total volume (7.3.7) becomes

$$V(t) = V_0 \left(1 + \frac{c_2}{c_1} t\right)^{\frac{8}{3}\left(\frac{c_3}{c_2} - \frac{1}{8}\right)}, \tag{7.4.34}$$

where

$$V_0 = 2\, c_1^{\frac{8}{3}\left(\frac{c_3}{c_2} - \frac{1}{8}\right)} \int_0^{c_1^{-\frac{c_3}{c_2}}} \xi\, F(\xi)\, d\,\xi. \tag{7.4.35}$$

Using (7.4.16) for v_n, (7.3.8) becomes

$$\frac{dV}{dt} = 2\, c_1^{\frac{8}{3}\left(\frac{c_3}{c_2} - \frac{1}{2}\right)} (c_1 + c_2 t)^{\frac{8}{3}\left(\frac{c_3}{c_2} - \frac{1}{2}\right)} \int_0^{c_1^{-\frac{c_3}{c_2}}} \xi\, G(\xi)\, d\,\xi. \tag{7.4.36}$$

Differentiating (7.4.34) with respect to t and using (7.4.36), we obtain

$$\frac{8}{3} c_2 \left(\frac{c_3}{c_2} - \frac{1}{8}\right) \int_0^{c_1^{-\frac{c_3}{c_2}}} \xi\, F(\xi)\, d\,\xi = \int_0^{c_1^{-\frac{c_3}{c_2}}} \xi\, G(\xi)\, d\,\xi. \tag{7.4.37}$$

Equation (7.4.37) is the balance law for fluid volume expressed in terms of the similarity variable.

7.4.4 Change of variables

In order to reduce the number of parameters in the problem consider the change of variables

$$\xi = A\,\zeta, \qquad F(\xi) = B\,f(\zeta), \qquad G(\xi) = D\,g(\zeta), \tag{7.4.38}$$

where A, B and D have still to be chosen. This change of variable was not considered by Mason and Momoniat [20]. Substituting (7.4.38) into (7.4.22), the ordinary differential equation becomes

$$\frac{1}{c_3}\frac{B^3}{A^2}\frac{d}{d\zeta}\left(\zeta\, f^3(\zeta)\frac{df}{d\zeta}\right)+3\frac{d}{d\zeta}\left(\zeta f(\zeta)\right)+\left(\frac{c_2}{c_3}-8\right)\zeta\, f(\zeta)+\frac{3}{c_3}A\frac{D}{B}\zeta\, g(\zeta)=0. \tag{7.4.39}$$

The boundary condition (7.4.31) now is

$$f\left(\frac{c_1^{-\frac{c_3}{c_2}}}{A}\right)=0 \tag{7.4.40}$$

and the balance law (7.4.37) becomes

$$\frac{B}{D}\frac{8}{3}c_2\left(\frac{c_3}{c_2}-\frac{1}{8}\right)\int_0^{\frac{c_1^{-\frac{c_3}{c_2}}}{A}}\zeta\, f(\zeta)\,d\,\zeta=\int_0^{\frac{c_1^{-\frac{c_3}{c_2}}}{A}}\zeta\, g(\zeta)\,d\,\zeta. \tag{7.4.41}$$

We therefore choose from (7.4.39)

$$\frac{B^3}{c_3A^2}=1, \qquad \frac{D}{c_3B}=1, \tag{7.4.42}$$

and from the boundary condition (7.4.40)

$$\frac{c_1^{-\frac{c_3}{c_2}}}{A}=1. \tag{7.4.43}$$

This gives three equations for the three unknowns A, B, D. Hence

$$A=c_1^{-\frac{c_3}{c_2}}, \qquad B=c_3^{\frac{1}{3}}\,c_1^{-\frac{2}{3}\frac{c_3}{c_2}}, \qquad D=c_3^{\frac{4}{3}}\,c_1^{-\frac{2}{3}\frac{c_3}{c_2}}. \tag{7.4.44}$$

With this choice of A, B and D, the ordinary differential equation simplifies to

$$\frac{d}{d\zeta}\left(\zeta\, f^3(\zeta)\frac{df}{d\zeta}\right)+3\,\frac{d}{d\zeta}\left(\zeta^2\, f(\zeta)\right)+\left(\frac{c_2}{c_3}-8\right)\zeta\, f(\zeta)+3\zeta\, g(\zeta), \tag{7.4.45}$$

with boundary condition

$$f(1) = 0 \tag{7.4.46}$$

and the balance law becomes

$$\frac{1}{3}\left(8 - \frac{c_2}{c_3}\right)\int_0^1 \zeta\, f(\zeta)\, d\,\zeta = \int_0^1 \zeta\, g(\zeta)\, d\,\zeta. \tag{7.4.47}$$

The volume $V(t)$ is given by (7.4.34), however the initial volume simplifies to

$$V_0 = 2\left(\frac{c_3}{c_1}\right)^{\frac{1}{3}}\int_0^1 \zeta\, f(\zeta)\, d\,\zeta. \tag{7.4.48}$$

The equations for the height (7.4.11) and the leak-off velocity (7.4.16) become

$$h(t,r) = \left(\frac{c_3}{c_1}\right)^{\frac{1}{3}}\left(1 + \frac{c_2}{c_1}t\right)^{\frac{2}{3}\left(\frac{c_3}{c_2} - \frac{1}{2}\right)} f(\zeta), \tag{7.4.49}$$

$$v_n(t,r) = \left(\frac{c_3}{c_1}\right)^{\frac{4}{3}}\left(1 + \frac{c_2}{c_1}t\right)^{\frac{2}{3}\left(\frac{c_3}{c_2} - 2\right)} g(\zeta). \tag{7.4.50}$$

where

$$\zeta = \frac{r}{R(t)}. \tag{7.4.51}$$

There remains one condition to impose which is on the initial dimensionless height at the centre of the liquid drop. The dimensionless height satisfies

$$h(0,0) = 1. \tag{7.4.52}$$

This condition was not imposed by Mason and Momoniat [20]. With $h(t,r)$ given by (7.4.49), we obtain

$$\frac{c_3}{c_1} = \frac{1}{f^3(0)}. \tag{7.4.53}$$

Now c_2/c_3 is either given or determined from the balance law and an assumption relating $f(\zeta)$ and $g(\zeta)$. It therefore remains to determine c_2/c_1. We have

$$\frac{c_2}{c_1} = \frac{c_2}{c_3}\frac{c_3}{c_1} = \frac{1}{\alpha\, f^3(0)}. \tag{7.4.54}$$

where

$$\alpha = \frac{c_3}{c_2}. \tag{7.4.55}$$

Expressed in terms of the transformed variables and the parameter α the system of equations takes the form :

$$\frac{d}{d\zeta}\left(\zeta\, f^3(\zeta)\frac{df}{d\zeta}\right) + 3\,\frac{d}{d\zeta}\left(\zeta^2\, f(\zeta)\right) + \left(\frac{1}{\alpha} - 8\right)\zeta\, f(\zeta) + 3\zeta\, g(\zeta) = 0, \tag{7.4.56}$$

$$f(1) = 0, \tag{7.4.57}$$

$$\frac{1}{3}\left(8 - \frac{1}{\alpha}\right)\int_0^1 \zeta\, f(\zeta)\, d\zeta = \int_0^1 \zeta\, g(\zeta)\, d\zeta, \tag{7.4.58}$$

$$R(t) = \left(1 + \frac{t}{\alpha f^3(0)}\right)^{\alpha}, \tag{7.4.59}$$

$$V(t) = V_0\left(1 + \frac{t}{\alpha f^3(0)}\right)^{\frac{8}{3}\left(\alpha - \frac{1}{8}\right)}, \tag{7.4.60}$$

$$V_0 = \frac{2}{f(0)}\int_0^1 f(\zeta)\, d\zeta, \tag{7.4.61}$$

$$h(t,r) = \left(1 + \frac{t}{\alpha f^3(0)}\right)^{\frac{2}{3}\left(\alpha - \frac{1}{2}\right)}\frac{f(\zeta)}{f(0)}, \tag{7.4.62}$$

$$v_n(t,r) = \frac{1}{f^4(0)}\left(1 + \frac{t}{\alpha f^3(0)}\right)^{\frac{2}{3}(\alpha - 2)} g(\zeta), \tag{7.4.63}$$

where

$$\zeta = \frac{r}{R(t)}. \tag{7.4.64}$$

The Lie point symmetry is given in (7.4.1) and when divided by c_1 gives

$$X = \left(1 + \frac{t}{\alpha f^3(0)}\right)\frac{\partial}{\partial t} + \frac{r}{f^3(0)}\frac{\partial}{\partial r} + \frac{1}{3\, f^3(0)}\left(2 - \frac{1}{\alpha}\right) h\frac{\partial}{\partial h}. \tag{7.4.65}$$

There remains an assumption that needs to made on $g(\zeta)$ in order to close the system of equations. We will consider the same two models for axisymmetric spreading as we did for two-dimensional spreading in order to compare the two flows under suction and blowing. In Chapter 8 we will assume that $v_n(t, r)$ is proportional to $h(t, r)$ and in Chapter 9 we will assume that $v_n(t, r)$ is proportional to the spatial gradient of the height, $\partial h(t, r)/\partial r$.

7.5 Conclusions

For the axisymmetric spreading of a liquid drop the nonlinear diffusion equation with a source term admits three Lie point symmetries provided the fluid injection velocity at the base satisfies a first order linear partial differential equation. This compares with the four Lie point symmetries admitted by the nonlinear diffusion equation for the spreading of a two-dimensional thin film. The group invariant solution for the axisymmetric spreading of a liquid drop is given by equations (7.4.56) to (7.4.65). There is only one moving contact line at $r = R(t)$ where the height vanishes compared with two contact lines for the two-dimensional spreading of a thin fluid film. One further condition is required to complete the system of equations. The models we will consider in Chapter 8 and 9 to complete the system will be the same as in Chapters 5 and 6 in order to compare axisymmetric spreading with two-dimensional spreading.

Chapter 8

Fluid injection velocity proportional to the height of the liquid drop

8.1 Introduction

In this chapter we make an assumption on $g(\zeta)$ to close the system so as to enable us to solve the ordinary differential equation (7.4.56). The simplest assumption is to consider the normal fluid velocity $v_n(t, r)$ at the base to be proportional to the height of the liquid drop $h(t, r)$. We will examine the velocity on the axis $r = 0$ and once we have solved for $h(t, r)$ and $v_n(t, r)$ we will calculate the streamlines within the liquid drop.

8.2 Relation between $g(\zeta)$ and $f(\zeta)$

We consider the case

$$g(\zeta) = \beta\, f(\zeta), \tag{8.2.1}$$

where β is a constant. We examine the physical significance of this assumption by expressing $g(\zeta)$ in terms of $h(t,r)$ using (7.4.62) and substituting these expressions into (8.2.1). This gives

$$v_n(t,r) = \frac{\beta h(t,r)}{f^3(0)\left(1 + \frac{t}{\alpha f^3(0)}\right)}. \tag{8.2.2}$$

Thus $v_n(t,r)$ is proportional to $h(t,r)$. The fluid injection velocity $v_n(t,r)$ is greatest at the central region where $h(t,r)$ is greatest and vanishes at the moving contact line $r = R(t)$. We find that $f(0)$ is independent of β. Consequently

$\beta > 0$	then	$v_n > 0$:	blowing of fluid into the liquid drop,	(8.2.3)
$\beta = 0$	then	$v_n = 0$:	no suction or injection, non-porous substrate,	(8.2.4)
$\beta < 0$	then	$v_n < 0$:	suction or leak-off of fluid into porous substrate.	(8.2.5)

8.2.1 Flux boundary condition at $\zeta = 1$

Consider first dimensional variables. There is no flux of fluid across the moving contact line $r = R(t)$. The volume of fluid which flows across the surface element of height δz at radius r in time δt is

$$\delta\, V = 2\, \pi\, r\, \delta\, z\; v_r(t,r,z)\, \delta\, t, \tag{8.2.6}$$

as illustrated in Figure 8.1. Hence the volume flux of fluid across the surface of radius r at time t is

$$Q(t,r) = 2\, \pi\, r \int_0^{h(t,r)} v_r(t,r,z)\; d\, z. \tag{8.2.7}$$

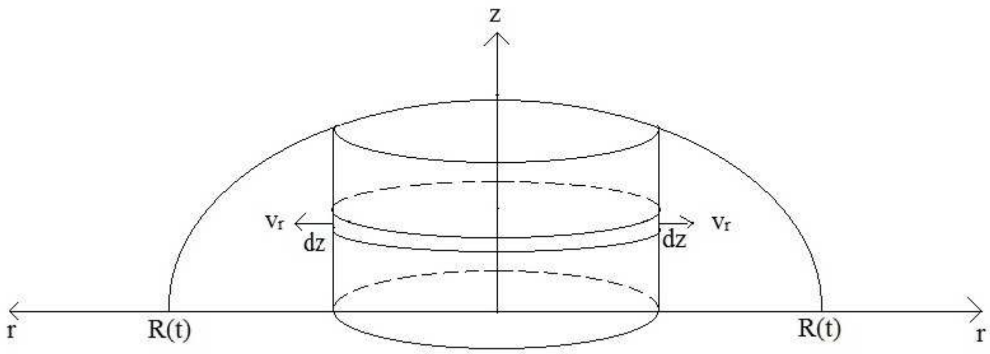

Figure 8.1: Volume $V(t)$

We make (8.2.7) dimensionless using the dimensionless variables (7.2.11). The characteristic volume flux is $\pi\, R_0 H\, U$. Thus

$$\overline{Q}(\overline{t},\overline{r}) = 2\,\overline{r}\int_0^{\overline{h}} \overline{v}_r(\overline{t},\overline{r},\overline{z})\; d\,\overline{z}. \tag{8.2.8}$$

We suppress the overhead bars. Using (7.2.36), (8.2.8) becomes

$$Q(t,r) = -\frac{2}{3} r\, h^3 \frac{\partial h}{\partial r}. \tag{8.2.9}$$

Expressed in terms of the similarity variable ζ using (7.4.62) for $h(t,r)$ we obtain

$$Q(t,r) = -\frac{2}{3}\frac{1}{f^4(0)}\left(1+\frac{t}{\alpha f^3(0)}\right)^{\frac{4}{3}(2\alpha-1)} \zeta f^3(\zeta)\frac{df}{d\zeta}. \tag{8.2.10}$$

There is therefore no flux of fluid across the moving contact line, $r = R(t)$, that is, $\zeta = 1$, provided

$$f^3(1)\frac{df(1)}{d\zeta} = 0. \tag{8.2.11}$$

8.3 Solution of the ordinary differential equation

To obtain α we consider the balance law (7.4.58) and using (8.2.1) we have

$$\frac{1}{3}\left(8-\frac{1}{\alpha}-3\,\beta\right)\int_0^1 \zeta\, f(\zeta)\; d\,\zeta = 0. \tag{8.3.1}$$

But since $f(\zeta) > 0$ for $0 \leq \zeta < 1$,

$$\int_0^1 \zeta\, f(\zeta)\, d\zeta \neq 0, \tag{8.3.2}$$

thus

$$8 - \frac{1}{\alpha} - 3\,\beta = 0, \tag{8.3.3}$$

and subsequently

$$\alpha = \frac{1}{8 - 3\,\beta}, \qquad \beta \neq \frac{8}{3}. \tag{8.3.4}$$

Using this result for α we may solve the ordinary differential equation (7.4.56) for $f(\zeta)$.

Substituting (8.3.4) into (7.4.56) reduces it to the integrable ordinary differential equation

$$\frac{d}{d\zeta}\left(f^3(\zeta)\,\frac{df}{d\zeta}\right) + 3\,\frac{d}{d\zeta}\left(\zeta^2\, f\right) = 0. \tag{8.3.5}$$

Equation (8.3.5) is exactly the same as the ordinary differential equation (5.3.4) for the spreading of a two-dimensional thin film. The boundary conditions (4.3.70) and (5.2.15) and (7.4.57) and (8.2.11) at $\zeta = 1$ are the same for both problems. (For the two-dimensional thin film the boundary conditions can be applied at either $\zeta = -1$ or $\zeta = 1$ since it is symmetrical about the centre line). The solution (5.3.6) is again obtained:

$$f(\zeta) = \left(\frac{9}{2}\right)^{\frac{1}{3}} \left(1 - \zeta^2\right)^{\frac{1}{3}}. \tag{8.3.6}$$

Substituting (8.3.6) and α given by (8.3.4) into (7.4.59) to (7.4.64) gives

$$R(t) = \left(1 + \frac{2}{9}(8 - 3\,\beta)\,t\right)^{\frac{1}{8-3\,\beta}}, \tag{8.3.7}$$

$$V(t) = V_0 \left(1 + \frac{2}{9}(8 - 3\,\beta)\,t\right)^{\frac{\beta}{8-3\,\beta}}, \tag{8.3.8}$$

$$V_0 = 2\int_0^1 \zeta\,\left(1 - \zeta^2\right)^{\frac{1}{3}}\, d\zeta = \frac{3}{4}, \tag{8.3.9}$$

$$h(t,r) = \left(1 + \frac{2}{9}(8 - 3\,\beta)\,t\right)^{\frac{\beta-2}{8-3\,\beta}} \left(1 - \zeta^2\right)^{\frac{1}{3}}, \tag{8.3.10}$$

$$v_n(t,r) = \frac{2}{9}\beta\left(1+\frac{2}{9}(8-3\,\beta)\,t\right)^{2\left(\frac{2\,\beta-5}{8-3\,\beta}\right)}\left(1-\zeta^2\right)^{\frac{1}{3}}, \qquad (8.3.11)$$

where

$$\zeta = \frac{r}{R(t)}, \qquad 0 \le \zeta \le 1. \qquad (8.3.12)$$

The Lie point symmetry (7.4.65) when multiplied by $\frac{9}{2}$ is

$$X = \left(\frac{9}{2}+(8-3\,\beta)\,t\right)\frac{\partial}{\partial t}+r\,\frac{\partial}{\partial r}+(\beta-2)\,h\,\frac{\partial}{\partial h}. \qquad (8.3.13)$$

For the results (8.3.7)-(8.3.12), $\beta \neq \frac{8}{3}$.

The limit $\beta \to \frac{8}{3}$ is obtained as in Section 5.3 by first considering $R(t)$ and rewriting (8.3.7) as

$$R(t) = \exp\left[\frac{1}{\left(\frac{8}{3}-\beta\right)}\ln\left(1+\frac{2}{9}\left(\frac{8}{3}-\beta\right)\,t\right)\right]. \qquad (8.3.14)$$

and by using (5.3.14) to expand $\ln(1+\epsilon)$ for small ϵ. We obtain

$$\lim_{\beta\to\frac{8}{3}} R(t) = \exp\left[\frac{2\,t}{9}\right]. \qquad (8.3.15)$$

As $\beta \to \frac{8}{3}$, (8.3.8), (8.3.10) and (8.3.11) tend to

$$V(t) = V_0 \exp\left[\frac{16\,t}{27}\right], \qquad (8.3.16)$$

$$h(t,r) = \exp\left[\frac{4\,t}{27}\right]\left(1-\zeta^2\right)^{\frac{1}{3}}, \qquad (8.3.17)$$

$$v_n(t,r) = \frac{16}{27}\exp\left[\frac{4\,t}{27}\right]\left(1-\zeta^2\right)^{\frac{1}{3}}, \qquad (8.3.18)$$

where V_0 is given by (8.3.9) and ζ is given by (8.3.12).

The dependence of $R(t), V(t), h(t,0), v_n(t,0)$ and the thin film ratio

$$\epsilon(t) = \frac{h(t,0)}{R(t)} \qquad (8.3.19)$$

on β for $-\infty \le \beta \le \infty$ is similar to the dependence of $W(t), V(t), h(t,0), v_n(t,0)$ and $\epsilon(t)$ on β for a two-dimensional thin film analysed in Chapter 5. Some of the critical values of β are different, for example, exponential behaviour for a liquid drop occurs for $\beta = \frac{8}{3}$ while it occurred for $\beta = \frac{5}{3}$ for a two-dimensional thin film. Some limits occur in the finite time

$$t_3 = \frac{3}{2\left(\beta - \frac{8}{3}\right)} \tag{8.3.20}$$

for a liquid drop while they occurred in the time t_1 defined by (5.3.21) for a two-dimensional thin film. The results for the axisymmetric spreading of a liquid drop are summarised in Tables 8.1 to 8.5 and illustrated in Figures 8.2 to 8.6. Figures 8.2 to 8.5 are similar to Figures presented in [20] and are included for completeness.

We now comment briefly on some of the main deductions from Tables 8.1 to 8.5. Since $\frac{dR}{dt} > 0$ for $-\infty \leq \beta \leq \infty$ the base always expands even when there is suction for $-\infty \leq \beta < 0$. For the height

$$\frac{\partial h}{\partial r}(t,r) = -\frac{2}{3}\, r\, R^{\beta-4}(t)\left(1 - \frac{r^2}{R^2(t)}\right)^{-\frac{2}{3}} \tag{8.3.21}$$

and therefore $\frac{\partial h}{\partial r} \to -\infty$ as $r \to R(t)$. In the vicinity of the moving contact line, $r = R(t)$, the thin film approximation breaks down. Blowing or suction did not remove the singularity at $r = R(t)$ or reduce the power of the singularity in the spatial derivative which remains at $-\frac{2}{3}$. Also

$$\frac{\partial h}{\partial t}(t,0) = \frac{2}{9}(\beta - 2)\left[1 + \frac{2}{9}\,(8 - 3\beta)\,t\right]^{\frac{2(2\beta-5)}{(8-3\beta)}}. \tag{8.3.22}$$

For $-\infty \leq \beta < 2$, $\frac{\partial h}{\partial t}(t,0) < 0$ and therefore the maximum height of the liquid drop decreases with time even when there is blowing at the base for $0 < \beta < 2$. For this range of β the blowing is weak and the decrease in height due to spreading under gravity is greater than the increase in height due to blowing. We see that for $\beta > \frac{5}{2}$, the fluid injection velocity $v_n(t,0)$ increases with time and eventually tends to infinity. For $\frac{5}{2} < \beta \leq \frac{8}{3}$, $v_n(t,0) \to \infty$ in an infinite time and the blowing can be considered as strong, while for $\frac{8}{3} < \beta \leq \infty$, $v_n(t,0) \to \infty$ in the finite time t_3 and the blowing can be regarded as very strong. The thin film approximation is valid if $\epsilon(t) \ll 1$ where $\epsilon(t)$ is given by (8.3.19). From (8.3.7) and (8.3.10) for $\beta \neq \frac{8}{3}$,

$$\epsilon(t) = \left(1 + \frac{2}{9}(8 - 3\,\beta)t\right)^{\frac{\beta-3}{8-3\beta}}, \tag{8.3.23}$$

and from (8.3.15) and (8.3.17) for $\beta = \frac{8}{3}$,

$$\epsilon(t) = \exp\left[-\frac{2}{27}t\right]. \tag{8.3.24}$$

For $-\infty \leq \beta \leq 3$ the thin film approximation is valid for all $t \geq 0$.

β	$R(t)$	$\frac{dR}{dt}$
$-\infty < \beta < \frac{8}{3}$	$R(t) \to \infty$ as $t \to \infty$ algebraically	> 0
$\beta = \frac{8}{3}$	$R(t) \to \infty$ as $t \to \infty$ exponentially	> 0
$\frac{8}{3} < \beta \leq \infty$	$R(t) \to \infty$ as $t \to t_3$ $t_3 = \frac{3}{2\left(\beta - \frac{8}{3}\right)}$	> 0

Table 8.1: Behaviour of the radius of the liquid drop, $R(t)$, for $-\infty \leq \beta \leq \infty$.

The radius $R(t)$ is plotted against time, t, in Figure 8.2.

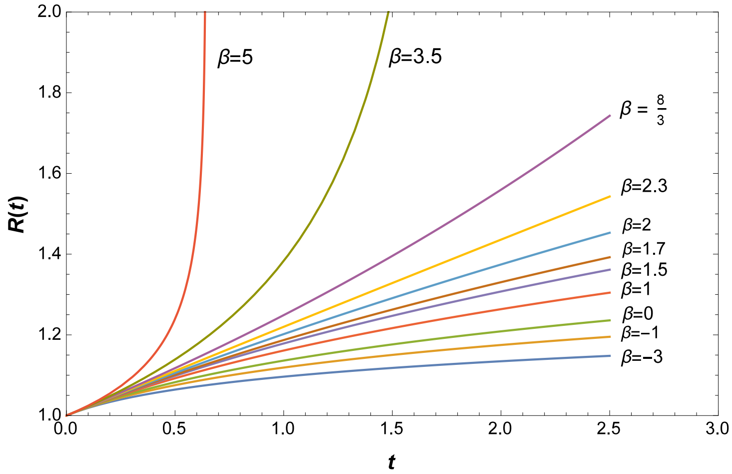

Figure 8.2: Radius $R(t)$ given by (8.3.7) and (8.3.15) plotted against t for a range of values of β.

β	$V(t)$	$\frac{dV}{dt}$
$-\infty \leq \beta < 0$	$V(t) \to 0$ as $t \to \infty$ algebraically	< 0
$\beta = 0$	$V(t) = V_0$	0
$0 < \beta < \frac{8}{3}$	$V(t) \to \infty$ as $t \to \infty$ algebraically	> 0
$\beta = \frac{8}{3}$	$V(t) \to \infty$ as $t \to \infty$ exponentially	> 0
$\frac{8}{3} < \beta \leq \infty$	$V(t) \to \infty$ as $t \to t_3$ $t_3 = \frac{3}{2\left(\beta - \frac{8}{3}\right)}$	> 0

Table 8.2: Behaviour of the total volume of the liquid drop, $V(t)$, for $-\infty \leq \beta \leq \infty$.

The volume $V(t)$ is plotted against time, t, in Figure 8.3.

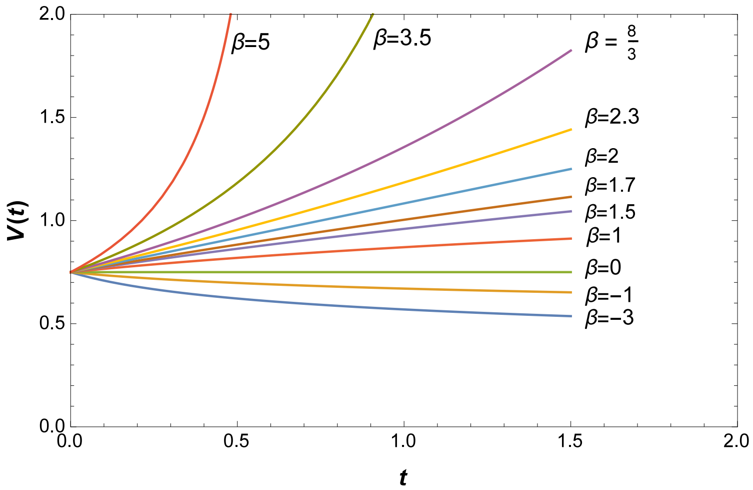

Figure 8.3: Volume $V(t)$ given by (8.3.8) and (8.3.16) plotted against time, t, for a range of values of β.

β	$h(t,0)$	$\frac{\partial h(t,0)}{\partial t}$
$-\infty \leq \beta < 2$	$h(t,0) \to 0$ as $t \to \infty$ algebraically	< 0
$\beta = 2$	$h(t,0) = 1$	$= 0$
$2 < \beta < \frac{8}{3}$	$h(t,0) \to \infty$ as $t \to \infty$ algebraically	> 0
$\beta = \frac{8}{3}$	$h(t,0) \to \infty$ as $t \to \infty$ exponentially	> 0
$\frac{8}{3} < \beta \leq \infty$	$h(t,0) \to \infty$ as $t \to t_3$ $t_3 = \frac{3}{2\left(\beta - \frac{8}{3}\right)}$	> 0

Table 8.3: Behaviour of the height of the liquid drop on the axis, $h(t,0)$, for $-\infty \leq \beta \leq \infty$.

In Figure 8.4, $h(t,0)$ is plotted against time, t, for a range of values of β.

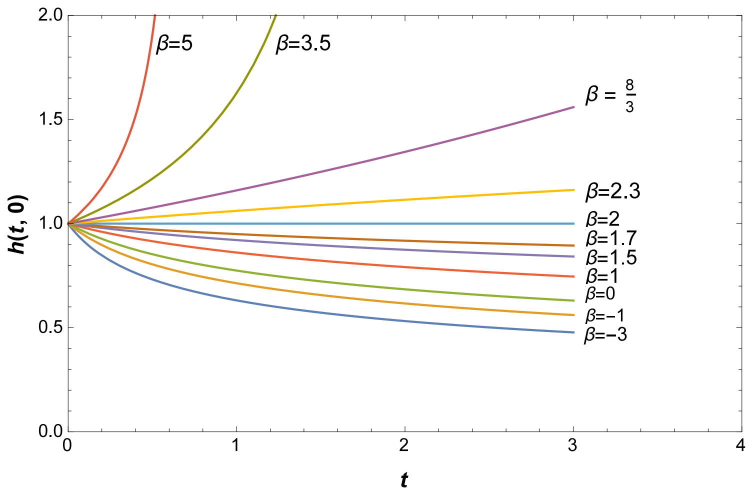

Figure 8.4: Height of the liquid drop, $h(t,0)$, given by (8.3.10) and (8.3.17) with $\zeta = 0$, plotted against t for a range of values of β.

β	$v_n(t,0)$	$\frac{\partial v_n(t,0)}{\partial t}$
$-\infty \leq \beta < 0$	$v_n(t,0) < 0$ $v_n(t,0) \to 0$ as $t \to \infty$ algebraically	> 0
$\beta = 0$	$v_n(t,0) = 0$	0
$0 < \beta < \frac{5}{2}$	$v_n(t,0) > 0$ $v_n(t,0) \to 0$ as $t \to \infty$ algebraically	< 0
$\beta = \frac{5}{2}$	$v_n(t,0) = \frac{5}{9}$	0
$\frac{5}{2} < \beta < \frac{8}{3}$	$v_n(t,0) > 0$ $v_n(t,0) \to \infty$ as $t \to \infty$ algebraically	> 0
$\beta = \frac{8}{3}$	$v_n(t,0) > 0$ $v_n(t,0) \to \infty$ as $t \to \infty$ exponentially	> 0
$\frac{8}{3} < \beta \leq \infty$	$v_n(t,0) > 0$ $v_n(t,0) \to 0$ as $t \to t_3$ $t_3 = \frac{3}{2\left(\beta - \frac{8}{3}\right)}$	> 0

Table 8.4: Behaviour of the fluid injection velocity on the axis, $v_n(t,0)$, for $-\infty \leq \beta \leq \infty$.

In Figure 8.5, $v_n(t,0)$ is plotted against time, t, for a range of values of β.

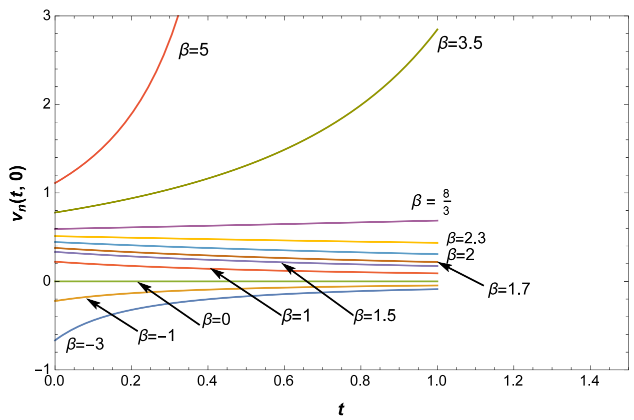

Figure 8.5: Normal velocity $v_n(t,0)$ given by (8.3.11) and (8.3.18) plotted against t for a range of values of β.

β	$\epsilon(t) = \frac{h(t,0)}{R(t)}$	$\frac{\partial \epsilon(t)}{\partial t}$
$-\infty \leq \beta < \frac{8}{3}$	$\epsilon(t) \to 0$ as $t \to \infty$ algebraically	< 0
$\beta = \frac{8}{3}$	$\epsilon(t) \to 0$ as $t \to \infty$ exponentially	< 0
$\frac{8}{3} < \beta < 3$	$\epsilon(t) \to 0$ as $t \to t_3$ $t_3 = \frac{3}{2\left(\beta - \frac{8}{3}\right)}$	< 0
$\beta = 3$	$\epsilon(t) = 1$	0
$3 < \beta \leq \infty$	$\epsilon(t) \to \infty$ as $t \to t_3$	> 0

Table 8.5: Behaviour of the thin fluid film ratio on the axis of the liquid drop, $\epsilon(t)$, for $-\infty \leq \beta \leq \infty$.

In Figure 8.6, $\epsilon(t)$ is plotted against time, t, for a range of values of β.

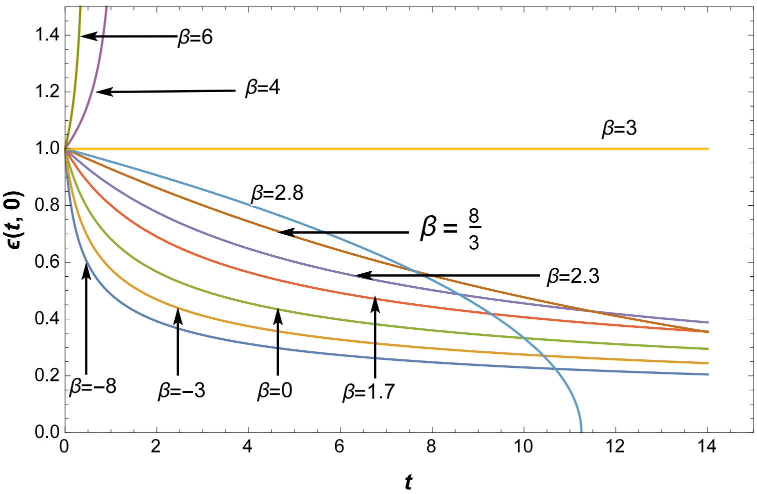

Figure 8.6: Thin fluid film ratio, $\epsilon(t)$, given by (8.3.23) and (8.3.24), plotted against t for a range of values of β.

The dependence of $h(t,r)$ and $v_n(t,r)$ on β for $0 \leq r \leq R(t)$ is illustrated in Figure 8.7. The graphs in Figure 8.7(c) and (d) illustrate that for $0 < \beta < 2$ the height $h(t,0)$ decreases with time even when there is injection of fluid. In Figure 8.7(e) it can be seen that the height on the axis remains constant for all time for $\beta = 2$. A distinguishing feature of this solution is that the base increases for all time even when there is suction of the fluid for $\infty \leq \beta < 0$ as depicted in Figures 8.7(a) and 8.7(b). A similar Figure was presented in [20].

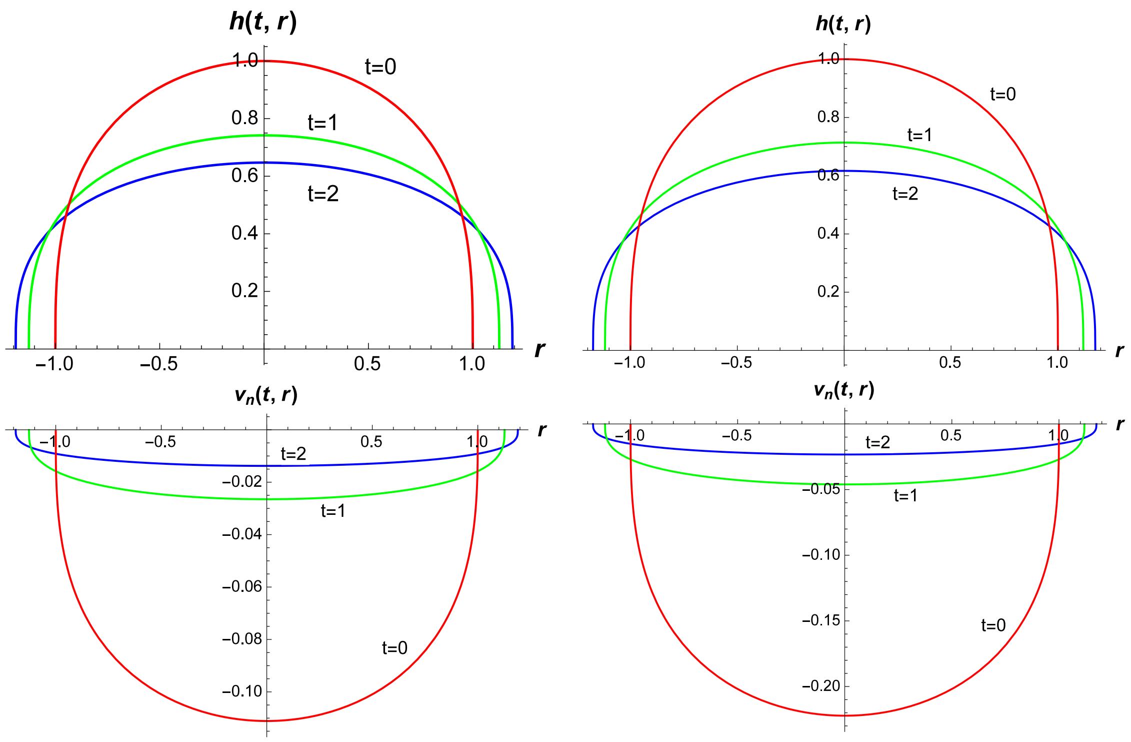

(a) (b)

Figure 8.7: Graphs of $h(t,r)$ given by (8.3.10) and the fluid velocity at the base, $v_n(t,r)$, given by (8.3.11) plotted against r for a range of values of t and for: (a) $\beta = -0.5$, (b) $\beta = -1$.

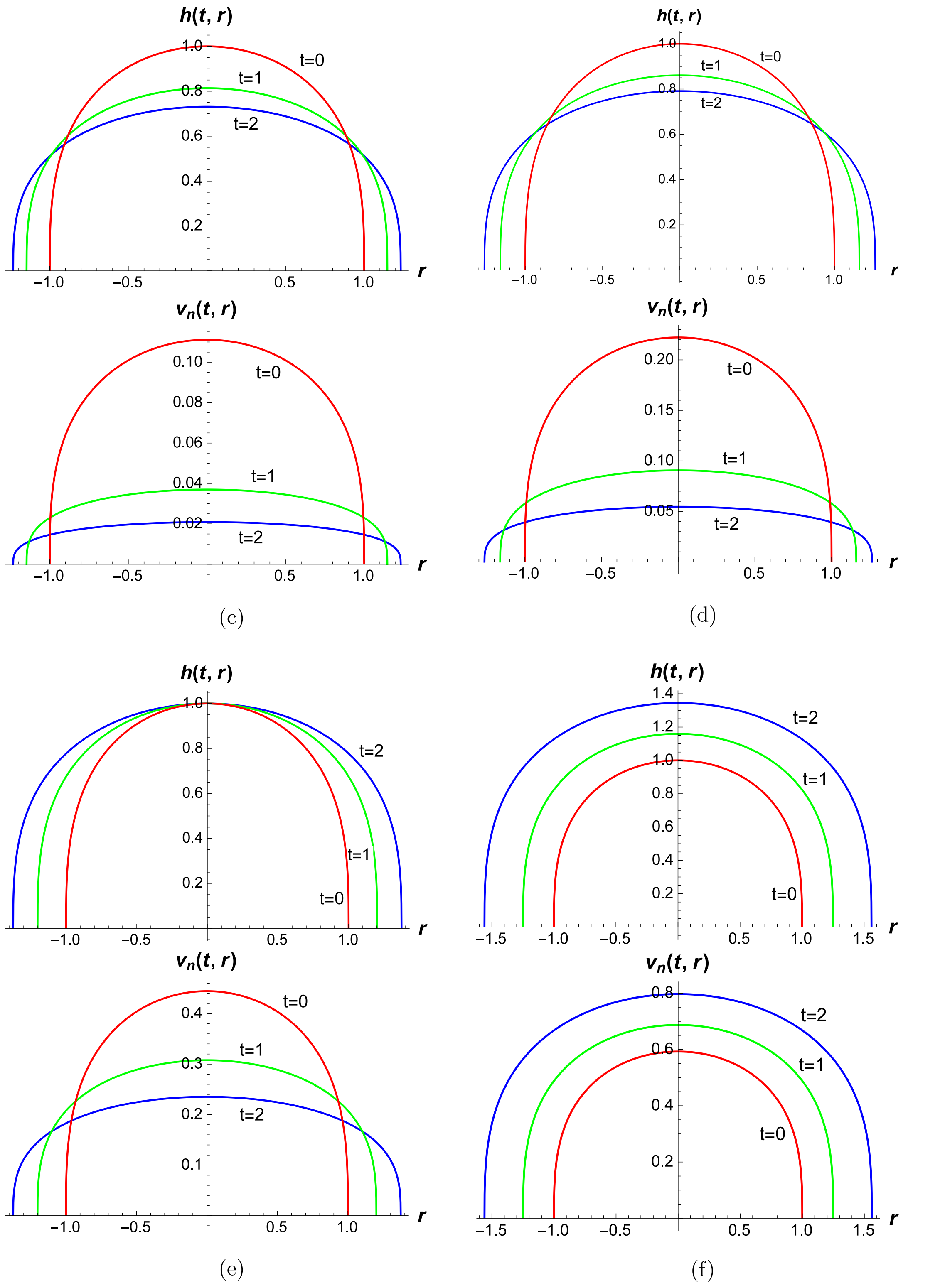

Figure 8.7: Graphs of $h(t,r)$ given by (8.3.10) and the fluid velocity at the base, $v_n(t,r)$, given by (8.3.11) plotted against r for a range of values of t and for: (c) $\beta = 0.5$, (d) $\beta = 1$, (e) $\beta = 2$, (f) $\beta = \frac{8}{3}$.

8.4 Velocity on the axis $r = 0$

We give the details in the derivation of $v_z(t, 0, z)$ to show how the limit $r \to 0$ is taken. We first express $h(t, r)$ and $v_n(t, r)$, given by (8.3.10) and (8.3.11), in terms of $R(t)$ and then in terms of $h(t, 0)$. Thus

$$h(t,r) = R^{\beta-2}(t)\left(1-\zeta^2\right)^{\frac{1}{3}} = h(t,0)\left(1-\zeta^2\right)^{\frac{1}{3}}, \tag{8.4.1}$$

where

$$h(t,0) = R^{\beta-2}(t), \tag{8.4.2}$$

and

$$v_n(t,r) = \frac{2\,\beta}{9} R^{4\,\beta-10}(t)\left(1-\zeta^2\right)^{\frac{1}{3}} = \frac{2\,\beta}{9}\frac{h^4(t,0)}{R^2(t)}\left(1-\zeta^2\right)^{\frac{1}{3}}. \tag{8.4.3}$$

To obtain $v_z(t, r, z)$ we integrate the continuity equation (7.2.14) from 0 to z. Thus

$$v_z(t,r,z) = v_n(t,r) - \frac{1}{r}\frac{\partial}{\partial r}\left(r\int_0^z \frac{\partial v_r(t,r,z)}{\partial r}\,dz\right), \tag{8.4.4}$$

where $v_z(t, r, 0) = v_n(t, r)$. Substitute (7.2.35) for $v_r(t, r, z)$ in (8.4.4) and integrating with respect to z results in

$$v_z(t,r,z) = P(t,r)\,z^3 + Q(t,r)\,z^2 + v_n(t,r), \tag{8.4.5}$$

where

$$P(t,r) \;=\; -\frac{1}{6\,r}\frac{\partial}{\partial r}\left(r\frac{\partial h}{\partial r}\right), \tag{8.4.6}$$

$$Q(t,r) \;=\; \frac{1}{2\,r}\frac{\partial}{\partial r}\left(r\,h\,\frac{\partial h}{\partial r}\right). \tag{8.4.7}$$

In order to obtain $v_z(t, 0, z)$ we first evaluate $P(t, r)$ and $Q(t, r)$ for $r \neq 0$ and then take the limit $r \to 0$. Now using (8.4.1) and (8.3.12) for ζ, gives

$$\frac{\partial h}{\partial r} = -\frac{2}{3}\frac{h(t,0)}{R^2(t)}\,r\left(1-\frac{r^2}{R^2(t)}\right)^{-\frac{2}{3}}, \tag{8.4.8}$$

and

$$\frac{\partial}{\partial r}\left(r\frac{\partial h}{\partial r}\right) = -\frac{4}{3}\frac{h(t,0)}{R^2(t)}r\left(1-\frac{r^2}{R^2(t)}\right)^{-\frac{2}{3}} - \frac{8}{9}\frac{h(t,0)}{R^4(t)}\,r^3\left(1-\frac{r^2}{R^2(t)}\right)^{-\frac{5}{3}}. \tag{8.4.9}$$

Thus substituting (8.4.9) into (8.4.6) results in

$$P(t,r) = \frac{2}{9}\frac{h(t,0)}{R^2(t)}\left(1 - \frac{r^2}{R^2(t)}\right)^{-\frac{2}{3}} - \frac{4}{27}\frac{h(t,0)}{R^4(t)}\,r^2\left(1 - \frac{r^2}{R^2(t)}\right)^{-\frac{5}{3}}, \qquad (8.4.10)$$

and letting $r \to 0$ we obtain

$$P(t,0) = \frac{2}{9}\frac{h(t,0)}{R^2(t)}. \qquad (8.4.11)$$

Using (8.4.8) for $\partial h/\partial r$ and (8.4.1) gives

$$\frac{\partial}{\partial r}\left(r\,h\,\frac{\partial h}{\partial r}\right) = -\frac{4}{3}\frac{h^2(t,0)}{R^2(t)}r\left(1 - \frac{r^2}{R^2(t)}\right)^{-\frac{1}{3}} - \frac{4}{9}\frac{h^2(t,0)}{R^4(t,0)}\,r^3\left(1 - \frac{r^2}{R^2(t)}\right)^{-\frac{4}{3}} \qquad (8.4.12)$$

and substituting (8.4.12) into (8.4.7) yields

$$Q(t,r) = -\frac{2}{3}\frac{h^2(t,0)}{R^2(t)}\left(1 - \frac{r^2}{R^2(t)}\right)^{-\frac{1}{3}} - \frac{2}{9}\frac{h^2(t,0)}{R^4(t,0)}\,r^2\left(1 - \frac{r^2}{R^2(t)}\right)^{-\frac{4}{3}}, \qquad (8.4.13)$$

which when letting $r \to 0$ results in

$$Q(t,0) = -\frac{2}{3}\frac{h^2(t,0)}{R^2(t)}. \qquad (8.4.14)$$

Lastly, putting $r = 0$ in (8.4.3) gives

$$v_n(t,0) = \frac{2}{9}\,\beta\,\frac{h^4(t,0)}{R^2(t)} \qquad (8.4.15)$$

and therefore letting $r \to 0$ in (8.4.5) we obtain

$$v_z(t,0,z) = \frac{2}{9}\frac{h(t,0)}{R^2(t)}\left[z^3 - 3\,h(t,0)z^2 + \beta\,h^3(t,0)\right]. \qquad (8.4.16)$$

The points on the axis $r = 0$ at which $v_z(t,0,z) = 0$ satisfy the cubic equation

$$z^3 - 3\,h(t,0)z^2 + \beta\,h^3(t,0) = 0. \qquad (8.4.17)$$

Consider now the dependence on β of the velocity at the point of maximum height of the drop, $v_z(t,0,h)$. From (8.4.16)

$$v_z(t,0,h) = \frac{2}{9}\,(\beta - 2)\,\frac{h^4(t,0)}{R^2(t)}. \qquad (8.4.18)$$

and substituting (8.4.2) into (8.4.18) we obtain

$$v_z(t,0,h) = \frac{2}{9}\,(\beta-2)\,R^{4\left(\beta-\frac{5}{2}\right)}(t). \tag{8.4.19}$$

Thus from (8.3.7) and (8.3.15), when

$$\beta \neq \frac{8}{3}: \qquad v_z(t,0,h) = \frac{2}{9}\,(\beta-2)\left[1+\frac{2}{3}\left(\frac{8}{3}-\beta\right)t\right]^{\frac{4\left(\beta-\frac{5}{2}\right)}{3\left(\frac{8}{3}-\beta\right)}}, \tag{8.4.20}$$

$$\beta = \frac{8}{3}: \qquad v_z(t,0,h) = \frac{4}{27}\exp\left(\frac{4}{27}t\right). \tag{8.4.21}$$

For the axisymmetric drop $v_z(t,0,h)$ at $\beta=\frac{8}{3}$ is the same as (5.4.20) for the two-dimensional thin film at $\beta=\frac{5}{3}$. Equations (8.4.20) and (8.4.21) can be obtained by differentiating (8.4.2) with respect to time t because

$$\frac{\partial h}{\partial t}(t,0) = v_z(t,0,h). \tag{8.4.22}$$

The properties of $v_z(t,0,h)$ for $-\infty \leq \beta \leq \infty$ are summarised in Table 8.6. The properties of $v_z(t,0,h)$ can be determined with the help of Figure 8.8 in which the exponent $4(\beta-\frac{5}{2})/3(\frac{8}{3}-\beta)$ is plotted against β.

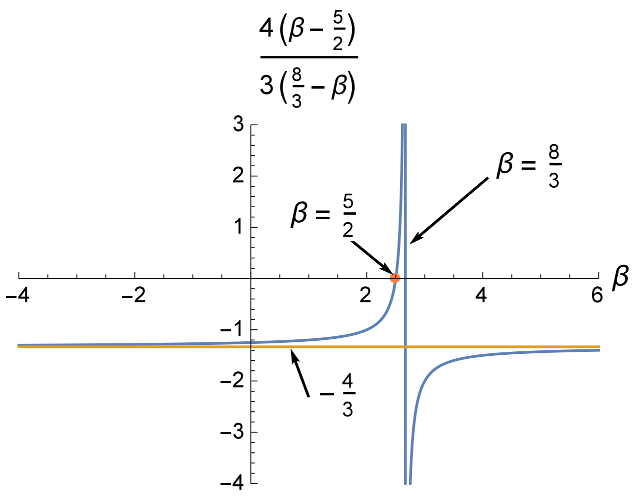

Figure 8.8: Plot of the exponent $\frac{4\left(\beta-\frac{5}{2}\right)}{3\left(\frac{8}{3}-\beta\right)}$ against β.

There are two competing effects in the evolution of $h(t,0)$, the effect of blowing or suction and the spreading effect due to gravity. For $-\infty \leq \beta < 2$ the maximum height of the liquid drop decreases even for blowing with $0 < \beta < 2$. For $0 < \beta < 2$ the effect of spreading due to gravity is stronger than the increase in height due to blowing. For $\beta = 2$, the height of the drop remains constant so that the effects of blowing and spreading exactly balance. From Table 8.3 we know that $h(t, 0) \to \infty$ as $t \to \infty$ for $2 < \beta \leq \infty$ but we see that for $2 < \beta < \frac{5}{2}$, $v_z(t, 0, h) \to 0$ as $t \to \infty$. For $\frac{5}{2} < \beta \leq \frac{8}{3}$, $v_z(t, 0, h) \to \infty$ as $t \to \infty$ and for $\beta > \frac{8}{3}$ the blowing is very strong because $v_z(t, 0, h) \to \infty$ in the finite time t_3. The thin fluid film approximation ceases to be valid for $\beta > 3$. Plots of $v_z(t, 0, h)$ for a range of values of β is presented in Figure 8.9

β	$v_z(t, 0, h)$	$\frac{\partial v_z(t,0)}{\partial t}$
$-\infty \leq \beta < 2$	$v_z(t, 0, h) < 0$ $v_z(t, 0, h) \to 0$ as $t \to \infty$ algebraically	< 0
$\beta = 2$	$v_z(t, 0, h) = 0$	0
$2 < \beta < \frac{5}{2}$	$v_z(t, 0, h) > 0$ $v_z(t, 0, h) \to 0$ as $t \to \infty$ algebraically	> 0
$\beta = \frac{5}{2}$	$v_z(t, 0, h) = \frac{1}{9}$	$\frac{1}{9}$
$\frac{5}{2} < \beta < \frac{8}{3}$	$v_z(t, 0, h) > 0$ $v_z(t, 0, h) \to \infty$ as $t \to \infty$ algebraically	> 0
$\beta = \frac{8}{3}$	$v_z(t, 0, h) > 0$ $v_z(t, 0, h) \to \infty$ as $t \to \infty$ exponentially	> 0
$\frac{8}{3} < \beta \leq \infty$	$v_z(t, 0, h) > 0$ $v_z(t, 0, h) \to \infty$ as $t \to t_3$ $t_3 = \frac{3}{2\left(\beta - \frac{8}{3}\right)}$	> 0

Table 8.6: Behaviour of the fluid velocity at the point of maximum height of the liquid drop, $v_z(t, 0, h)$ for $-\infty \leq \beta \leq \infty$.

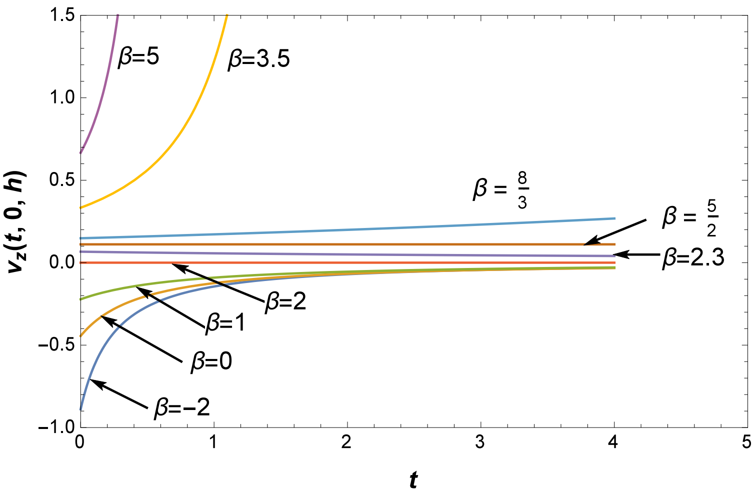

Figure 8.9: Velocity $v_z(t, 0, h)$, given by (8.4.20) and (8.4.21) , plotted against t for a range of values of β

8.4.1 Roots of the cubic polynomial

From (8.4.17) the values of z for which $v_z(t, z, 0) = 0$ satisfy the cubic equation

$$z^3 - 3\,h(t,0)z^2 + \beta\,h^3(t,0) = 0. \tag{8.4.23}$$

When $\beta = 0$ the roots of (8.4.23) are $z = 0, z = 0$ and $z = 3h(t, 0)$ and from (8.4.16),

$$v_z(t,z,0) = -\frac{2}{9}\frac{h(t,0)}{R^2(t)}\,z^2\,(3\,h(t,0) - z)\,. \tag{8.4.24}$$

Thus,

$$\text{if} \quad 0 < z < 3h(t,0) \quad \text{then} \quad v_z(t,0,z) < 0. \tag{8.4.25}$$

When $\beta = 0$, $v_z(t, 0, z)$ is negative for $0 < z < h(t, 0)$. There are no zeros on the axis of symmetry $r = 0$ inside the liquid drop.

In order to investigate how the roots

$$z = 0, \quad z = 0, \quad z = 3h(t,0), \tag{8.4.26}$$

evolve for $\beta \neq 0$ we have to solve the cubic equation (8.4.23). Equation (8.4.23) can be obtained from the cubic equation (5.4.39) by replacing β in (5.4.39) by $\frac{1}{2}\beta$. The perturbation solution in powers of β and the exact solution of (8.4.23) can therefore be obtained from the corresponding solutions of (5.4.39) when expressed in terms of $h(t, 0)$ by replacing β by $\frac{1}{2}\beta$. The expressions for $h(t, 0)$, however, are different and $h(t, 0)$ for the axisymmetric liquid drop cannot be obtained from $h(t, 0)$ for the two-dimensional thin film by replacing β by $\frac{1}{2}\beta$.

We will use the results of Sections 5.4.2 and 5.4.3 to write down the solutions of the cubic equation (8.4.23).

8.4.2 Perturbation solution of the cubic equation

Consider first blowing at the base for with $\beta > 0$. By replacing β by $\frac{1}{2}\beta$ in (5.4.67), (5.4.68) and (5.4.58) we obtain for the three roots of (8.4.23):

$$z = \left[\frac{1}{\sqrt{3}}\beta^{\frac{1}{2}} + \frac{1}{18}\beta + \bigcirc\left(\beta^{\frac{3}{2}}\right)\right] h(t, 0), \tag{8.4.27}$$

$$z = \left[-\frac{1}{\sqrt{3}}\beta^{\frac{1}{2}} + \frac{1}{18}\beta + \bigcirc\left(\beta^{\frac{3}{2}}\right)\right] h(t, 0), \tag{8.4.28}$$

$$z = 3\left[1 - \frac{1}{27}\beta + \bigcirc(\beta^2)\right] h(t, 0). \tag{8.4.29}$$

The root (8.4.29) was obtained from a regular perturbation expansion in powers of β while the roots (8.4.27) and (8.4.28) were obtained from a singular perturbation expansion in powers of $\beta^{\frac{1}{2}}$. The velocity component $v_z(t, 0, z)$ therefore has a zero on the axis of symmetry of the liquid drop at

$$z = \left[\frac{1}{\sqrt{3}}\beta^{\frac{1}{2}} + \frac{1}{18}\beta + \bigcirc\left(\beta^{\frac{3}{2}}\right)\right] h(t, 0). \tag{8.4.30}$$

Consider next suction at the base, $\beta < 0$. Let $\beta = -|\beta|$. By replacing $|\beta|$ by $\frac{1}{2}|\beta|$ in (5.4.82), (5.4.83) and (5.4.84) we obtain the three roots of (8.4.23):

$$z = \left[\frac{i}{\sqrt{3}}|\beta|^{\frac{1}{2}} - \frac{1}{18}|\beta| + \bigcirc\left(|\beta|^{\frac{3}{2}}\right)\right] h(t, 0), \tag{8.4.31}$$

$$z = \left[-\frac{i}{\sqrt{3}}|\beta|^{\frac{1}{2}} - \frac{1}{18}|\beta| + \bigcirc\left(|\beta|^{\frac{3}{2}}\right)\right] h(t, 0), \tag{8.4.32}$$

$$z = 3\left[1 - \frac{1}{27}|\beta| + \bigcirc(\beta^2)\right] h(t,0). \qquad (8.4.33)$$

The root (8.4.33) is the same as (8.4.29) obtained from the regular perturbation expansion in powers of β. The roots (8.4.31) and (8.4.32) were obtained from a singular perturbation expansion in powers of $|\beta|^{\frac{1}{2}}$. There is one real root and two complex conjugate roots. Since the real root does not lie in the range $0 \le z \le h(t,0)$ there is no zero of $v_z(t,0,z)$ on the axis of symmetry of the liquid drop for suction at the base.

8.4.3 Exact solution of the cubic equation

Consider now the exact solution for the roots of the cubic equation

$$z^3 - 3h(t,0)z^2 + \beta h^3(t,0) = 0. \qquad (8.4.34)$$

We determine the nature of the roots of (8.4.34) by replacing β by $\frac{1}{2}\beta$ in the results derived for the cubic equation (5.4.39) in Section 5.4.3. Two approaches were taken in Section 5.4.3. The first approach was to use Descartes' rule of signs and graphs. The second approach was to use the discriminant, Δ, to determine the properties of the roots. A summary of the properties of the roots of (8.4.34) using the first approach is as follows.

- The range of interest is $0 \le \beta \le 2$. For this range of β, $v_z(t,0,z)$ has a zero in the range $0 \le z \le h(t,0)$. For $\beta < 0$ and $\beta > 2$ there are no zeros of $v_z(t,0,z)$ in the range $0 \le z \le h(t,0)$.

- General properties

  $\beta < 0$: There exists two complex conjugate roots and one positive real root greater than $3h(t,0)$.

  $\beta = 0$: There exist three real roots, two coincident.

$\beta > 0:$ There always exists one negative root. For $0 \leq \beta \leq 4$ there exist three real roots, two coincident for $\beta = 4$. For $\beta > 4$ there is one real root and two complex conjugate roots.

- Special exact solutions

$$\beta = 0: \quad z = 0, \qquad z = 0, \qquad z = 3h(t,0). \tag{8.4.35}$$

$$\beta = 2: \quad z = (1-\sqrt{3})h(t,0), \quad z = h(t,0), \quad z = (1+\sqrt{3})h(t,0). \tag{8.4.36}$$

$$\beta = 4: \quad z = -h(t,0), \quad z = 2h(t,0), \quad z = 2h(t,0). \tag{8.4.37}$$

$$\beta > 4: \quad P(z)\,|_{\beta>4} > P(z)\,|_{\beta=4}, \tag{8.4.38}$$

where

$$P(z) = z^3 - 3h(t,0)z^2 + \beta h^3(t,0). \tag{8.4.39}$$

- Figures 5.12 and 8.10 to 8.15 illustrate the roots of $P(z) = 0$ for $\beta = 0$, $0 < \beta < 2$, $\beta = 2$, $2 < \beta < 4$, $\beta = 4$,$\beta > 4$ and $\beta < 0$.

- $0 < \beta < 2$

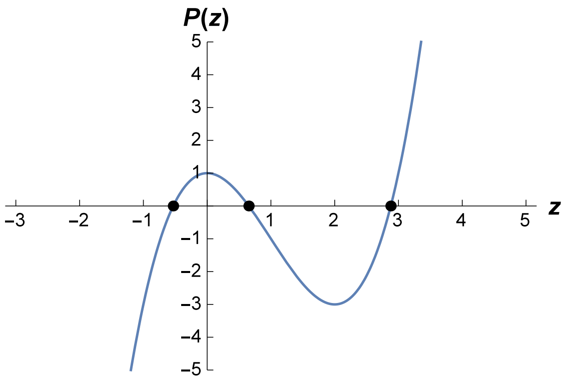

Figure 8.10: Plot of P(z) and its roots for $\beta = 1$ and $h(t,0) = 1$.

- $\beta = 2$:

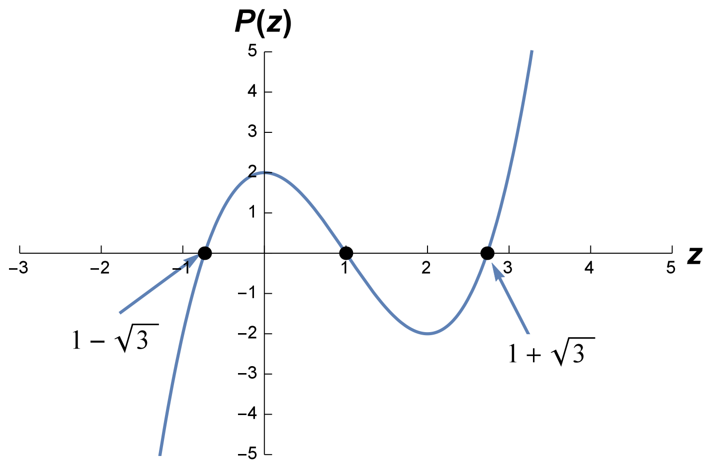

Figure 8.11: Plot of P(z) and its roots for $\beta = 2$ and $h(t, 0) = 1$.

- $2 < \beta < 4$:

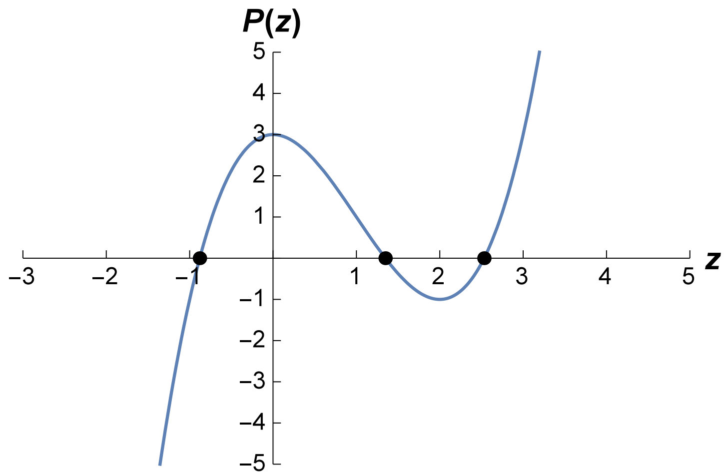

Figure 8.12: Plot of P(z) and its roots for $\beta = 3$ and $h(t, 0) = 1$.

- $\beta = 4$:

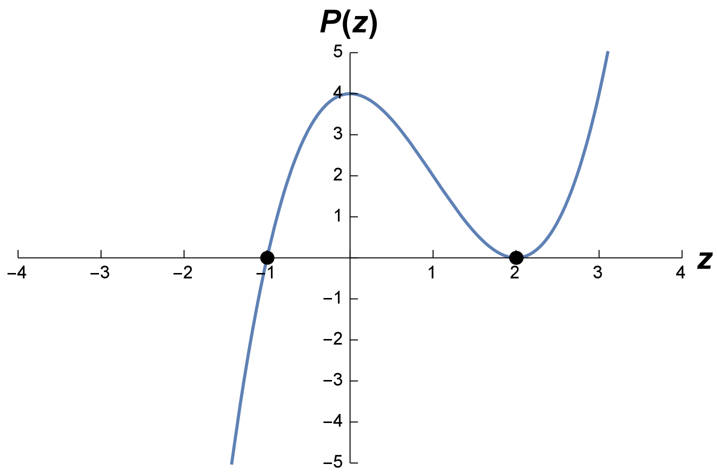

Figure 8.13: Plot of P(z) and its roots for $\beta = 4$ and $h(t, 0) = 1$.

- $\beta > 4$:

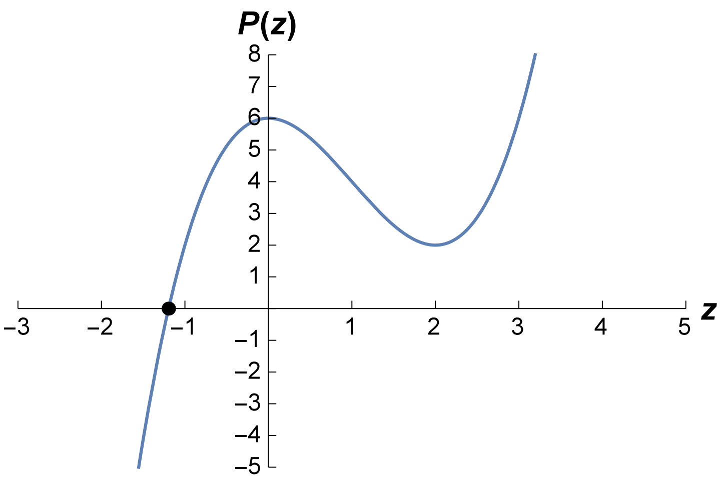

Figure 8.14: Plot of P(z) and its roots for $\beta = 6$ and $h(t, 0) = 1$.

- $\beta < 0$

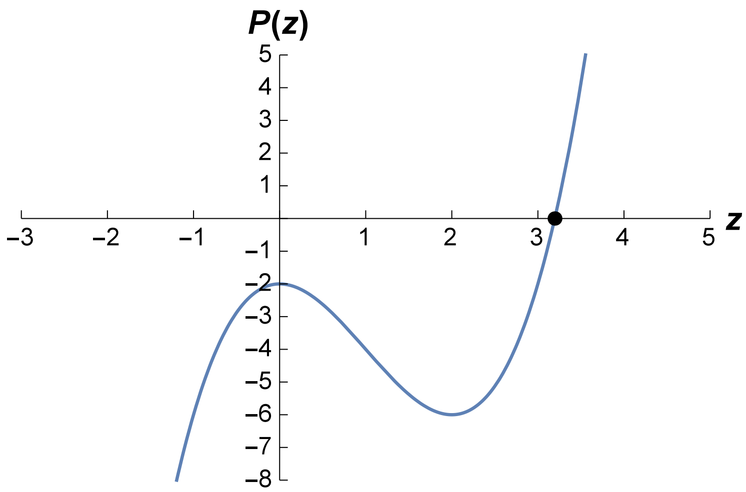

Figure 8.15: Plot of P(z) and its roots for $\beta = -2$ and $h(t,0) = 1$.

Consider now the alternate approach. The cubic equation (8.4.34) is first transformed to standard form

$$s^3 + 3Hs + G = 0 \tag{8.4.40}$$

and the nature of the roots is determined by the discriminant

$$\Delta = G^2 + 4H^3. \tag{8.4.41}$$

We again replace β by $\frac{1}{2}\beta$ in the results of Section 5.4.3. The standard form of (8.4.34) is

$$s^3 - 3h^2(t,0)s - (2-\beta)h^3(t,0) = 0, \tag{8.4.42}$$

where

$$z = s + h(t,0). \tag{8.4.43}$$

Thus

$$H = -h^2(t,0)\ , \qquad G = -2(2-\beta)h^3(t,0) \tag{8.4.44}$$

and the discriminant is

$$\Delta = \beta(\beta - 4)h^6(t,0). \tag{8.4.45}$$

We summarise again the properties of the roots as determined by Δ [2].

(i) $\Delta < 0$: Three real and distinct roots.

(ii) $\Delta = 0$, $H \neq 0$ and $G \neq 0$: Three real roots, two coincident, one root different.

(iii) $\Delta = 0$, $H = 0$ and $G = 0$: Three coincident real roots.

(iv) $\Delta > 0$: One real root, two complex conjugate roots.

A graph of Δ plotted against β is shown in Figure 8.16. The properties of the roots of the cubic equation (8.4.34) are summarised in Table 8.7. They are obtained from the results of Section 5.4.3 by replacing β by $\frac{\beta}{2}$.

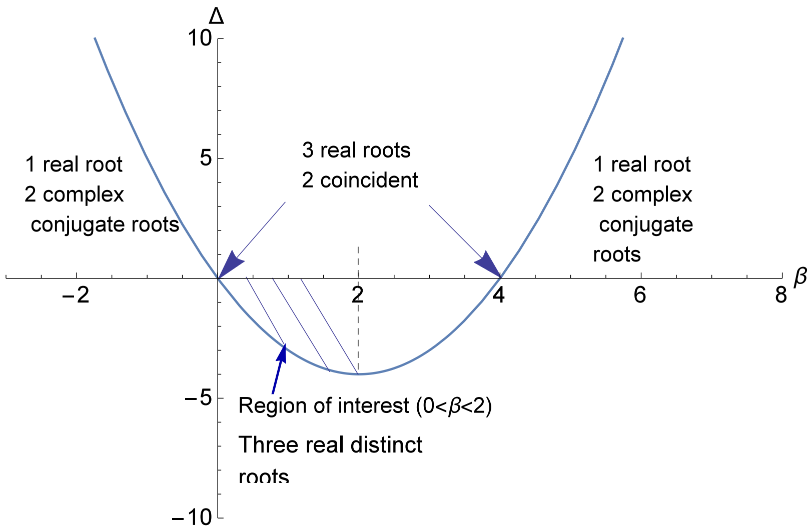

Figure 8.16: Graph of Δ given by (8.4.45) plotted against β.

Consider now the solution for the real roots of the cubic equation (8.4.34) when $0 \leq \beta \leq 4$. We are interested in the real root, $-h(t, 0) < s < 0$, that satisfies $\Delta < 0$ and $0 < \beta < 2$. It gives the root $0 < z < h(t, 0)$. The trigonometric solution described in Section 5.4 will be used. The results can be obtained from those of Section 5.4 by replacing β by $\frac{1}{2}\beta$.

β	Δ	H, G	**Nature of roots**	**Roots**	**Figures**
$\beta < 0$	$\Delta > 0$	$H < 0$ $G < 0$	1 real root 2 complex conjugate roots		Figure 8.15
$\beta = 0$	$\Delta = 0$	$H < 0$ $G < 0$	3 real roots 2 roots coincident 1 root different	$s = -h(t,0)$ $s = -h(t,0)$ $s = 2h(t,0)$ $z = 0$ $z = 0$ $z = 3h(t,0)$	Figure 5.12
$0 < \beta < 4$	$\Delta < 0$	$H < 0$ $G < 0\,(0 < \beta < 2)$ $G = 0\,(\beta = 2)$ $G > 0\,(2 < \beta < 4)$	3 real distinct roots		Figure 8.10 Figure 8.11 Figure 8.12
$\beta = 4$	$\Delta = 0$	$H < 0$ $G > 0$	3 real roots 2 roots coincident 1 root different	$s = -2h(t,0)$ $s = h(t,0)$ $s = h(t,0)$ $z = -h(t,0)$ $z = 2h(t,0)$ $z = 2h(t,0)$	Figure 8.13
$4 < \beta < \infty$	$\Delta > 0$	$H < 0$ $G > 0$	1 real root 2 complex conjugate roots		Figure 8.14

Table 8.7: Classification of the roots of the cubic equation (8.4.34) using the discriminant Δ.

The roots of the cubic equation in standard form, (8.4.42), are

$$s_n = \rho\cos\theta = 2\,(-H)^{\frac{1}{2}}\cos\left(\phi + \frac{2n\pi}{3}\right), \qquad n = 0, 1, 2, \tag{8.4.46}$$

where

$$(-H)^{\frac{1}{2}} = h(t,0) \tag{8.4.47}$$

is independent of β and ϕ is the smallest non-negative angle which satisfies

$$\cos 3\phi = -\frac{G}{2\,(-H)^{\frac{3}{2}}} = 1 - \frac{1}{2}\beta, \tag{8.4.48}$$

where

$$0 \le \phi \le \frac{\pi}{3}. \tag{8.4.49}$$

Using (8.4.43) the roots of the cubic equation (8.4.34) are

$$z_0 = h(t,0)\left[1 + 2\cos\phi\right], \tag{8.4.50}$$

$$z_1 = h(t,0)\left[1 + 2\cos\left(\phi + \frac{2\pi}{3}\right)\right], \tag{8.4.51}$$

$$z_2 = h(t,0)\left[1 + 2\cos\left(\phi + \frac{4\pi}{3}\right)\right]. \tag{8.4.52}$$

The exact solutions for the three roots for $\beta = 0$, $\beta = 2$ and $\beta = 4$ and the perturbation solution for small values of β in the range $0 < \beta < 1$ are listed in Table 8.8. We see from the expansion for small values of β that it is the root z_2 which lies inside the liquid drop for $0 < \beta < 2$ and therefore of physical interest. The results for the expansion for small β agree with the perturbation solution (8.4.27) to (8.4.29). The root $z_2 = h(t,0)$ for $\beta = 2$ is the limiting case for the zero z_2 of the velocity $v_z(t,0,z)$ inside the liquid drop. Since

$$v_z(t,0,z)|_{z=h(t,0)} = 0, \tag{8.4.53}$$

thus

$$\frac{d}{dt}h(t,0) = 0. \tag{8.4.54}$$

Hence the height of the liquid drop at the top of the axis of symmetry remains constant in time. The three roots for $\beta = 4$ lie outside the liquid drop and therefore are not of physical interest. The solutions for $\beta = 0$, $\beta = 2$ and $\beta = 4$ obtained from the general solution, (8.4.50) to (8.4.52), agree with the solutions (8.4.35) to (8.4.37) obtained by factorising (8.4.34).

β	ϕ	Roots z_1, z_2, z_3
$\beta = 0$	$\phi = 0$	$z_0 = 3h(t,0)$ $z_1 = 0$ $z_2 = 0$
$0 < \beta < 1$	$\phi = \frac{1}{3}\beta^{\frac{1}{2}} + \bigcirc\left(\beta^{\frac{3}{2}}\right)$	$z_0 = 3\left[1 - \frac{\beta}{27} + \bigcirc\left(\beta^2\right)\right] h(t,0)$ $z_1 = \left[-\frac{\beta^{\frac{1}{2}}}{\sqrt{3}} + \frac{\beta}{18} + \bigcirc\left(\beta^{\frac{3}{2}}\right)\right] h(t,0).$ $z_2 = \left[\frac{\beta^{\frac{1}{2}}}{\sqrt{3}} + \frac{\beta}{18} + \bigcirc\left(\beta^{\frac{3}{2}}\right)\right] h(t,0).$
$\beta = 2$	$\phi = \frac{\pi}{6}$	$z_0 = \left[1 + \sqrt{3}\right] h(t,0)$ $z_1 = -\left[\sqrt{3} - 1\right] h(t,0)$ $z_2 = h(t,0)$
$\beta = 4$	$\phi = \frac{\pi}{3}$	$z_0 = 2h(t,0)$ $z_1 = -h(t,0)$ $z_2 = 2h(t,0)$

Table 8.8: Exact solution, (8.4.50) to (8.4.52), for the three roots of the cubic equation (8.4.34) for a range of values if β.

8.4.4 Layer at the base due to fluid injection

An estimate of the thickness of the fluid layer at the base of the liquid drop due to injection of fluid is obtained from the zero, z_2, of $v_z(t, 0, z)$ on the axis of symmetry. The exact solution (8.4.52) for z_2 in the range $0 \le \beta \le 2$ is

$$\frac{z_2}{h(t,0)} = 1 + 2\cos\left(\phi + \frac{4\pi}{3}\right), \tag{8.4.55}$$

where

$$\cos 3\phi = 1 - \frac{\beta}{2}, \qquad 0 \le \phi \le \frac{\pi}{3}, \tag{8.4.56}$$

while the singular perturbation solution (8.4.27) for small $\beta > 0$ is

$$\frac{z_2}{h(t,0)} = \frac{\beta^{\frac{1}{2}}}{\sqrt{3}} + \frac{\beta}{18} + \bigcirc\left(\beta^{\frac{3}{2}}\right). \tag{8.4.57}$$

The exact and perturbation solutions for $z_2/h(t,0)$ on the axis of symmetry of the liquid drop for values of β in the range $0 \leq \beta \leq 2$ are given in Table 8.9. The results can be obtained from Table 5.1 for a two-dimensional thin film by replacing β by $\frac{\beta}{2}$. A perturbation expansion in β should normally be applicable only for $0 < \beta < 1$ but we see that it is useful for $1 \leq \beta \leq 2$ because of the numerical factor in the expansion terms. These results of Table 8.9 will be useful and verified when plotting the streamlines in the next section.

β	$\mathbf{1} + \mathbf{2}\cos\left(\phi + \frac{\mathbf{4}\pi}{\mathbf{3}}\right)$	$\frac{\beta^{\frac{1}{2}}}{\sqrt{3}}$	Error %	$\frac{\beta^{\frac{1}{2}}}{\sqrt{3}} + \frac{\beta}{\mathbf{18}}$	Error %
0	0	0	0	0	0
0.2	0.2707	0.2582	4.62	0.2693	0.52
0.4	0.3916	0.3651	6.77	0.3873	1.10
0.6	0.4888	0.4472	8.51	0.4805	1.7
0.8	0.5743	0.5164	10.08	0.5608	2.35
1	0.6527	0.5774	11.54	0.6329	3.03
1.2	0.7265	0.6325	12.94	0.6992	3.76
1.4	0.7972	0.6831	14.31	0.7609	4.55
1.6	0.8659	0.7303	15.66	0.8192	5.39
1.8	0.9332	0.7746	17.00	0.8746	6.28
2	1	0.8165	18.35	0.9276	7.24

Table 8.9: The exact and perturbation solution for the zero, $\frac{z_2}{h(t,0)}$, of $v_z(t,0,z)$ on the axis of the liquid drop.

8.5 Streamlines

As well as in the two-dimensional incompressible flow, in axisymmetric incompressible flow the streamlines can be obtained from a stream function. In axisymmetric incompressible flow the stream function $\psi(t, r, z)$ satisfies (in dimensional variables)

$$v_r = \frac{1}{r}\frac{\partial \psi}{\partial z}, \qquad v_z = -\frac{1}{r}\frac{\partial \psi}{\partial r}. \tag{8.5.1}$$

The continuity equation

$$\frac{\partial}{\partial r}(r\, v_r) + \frac{\partial}{\partial z}(r\, v_z) = 0 \tag{8.5.2}$$

is identically satisfied. The stream function is constant along a streamline in the axisymmetric flow:

$$(\underline{v} \cdot \underline{\nabla})\, \psi = v_r \frac{\partial \psi}{\partial r} + v_z \frac{\partial \psi}{\partial z} = \frac{1}{r}\frac{\partial \psi}{\partial z}\frac{\partial \psi}{\partial r} - \frac{1}{r}\frac{\partial \psi}{\partial r}\frac{\partial \psi}{\partial z} = 0. \tag{8.5.3}$$

Graphs of the streamlines at any instant are therefore obtained by plotting

$$\psi(t, r, z) = k \tag{8.5.4}$$

for a range of values of k. We make (8.5.1) dimensionless using

$$\bar{\psi} = \frac{\psi}{\psi_0}, \tag{8.5.5}$$

where ψ_0 is to be determined. Using the dimensionless variables defined in (7.2.11), (8.5.1) becomes

$$\bar{v}_r = \frac{\psi_0}{R_0\, H\, U}\frac{1}{\bar{r}}\frac{\partial \bar{\psi}}{\partial \bar{z}}, \quad \bar{v}_z = -\frac{\psi_0}{R_0\, H\, U}\frac{1}{\bar{r}}\frac{\partial \bar{\psi}}{\partial \bar{r}}. \tag{8.5.6}$$

We choose

$$\psi_0 = R_0\, H\, U \tag{8.5.7}$$

so that

$$\bar{v}_r = \frac{1}{\bar{r}}\frac{\partial \bar{\psi}}{\partial \bar{z}}, \qquad \bar{v}_z = -\frac{1}{\bar{r}}\frac{\partial \bar{\psi}}{\partial \bar{r}}. \tag{8.5.8}$$

The overhead bars are suppressed.

We now solve the system (8.5.8) for $\psi(t,r,z)$. The dimensionless velocity v_r is given by (7.2.35). To obtain $v_z(t,r,z)$ we integrate the continuity equation (8.5.2) with respect to z from 0 to z:

$$\int_0^z \frac{\partial v_z(t,r,z)}{\partial z}\,dz = -\frac{1}{r}\int_0^z \frac{\partial}{\partial r}\left(r\,v_r(t,r,z^*)\right)\,dz^*. \tag{8.5.9}$$

Thus

$$v_z(t,r,z) = v_n(t,r) - \frac{1}{r}\frac{\partial}{\partial r}\left(r\int_0^z v_r(t,r,z^*)\,dz^*\right) \tag{8.5.10}$$

where $v_z(t,r,0) = v_n(t,r)$. Substituting (7.2.35) for $v_r(t,r,z)$ in (8.5.10) and integrating with respect to z results in

$$v_z(t,r,z) = v_n(t,r) - \frac{1}{r}\frac{\partial}{\partial r}\left[r\frac{\partial h}{\partial r}\left(\frac{z^3}{6} - \frac{z^2}{2}\,h\right)\right]. \tag{8.5.11}$$

We solve the following two equations for the stream function, from (8.5.8),

$$\frac{\partial \psi}{\partial z} = \left(\frac{z^2}{2} - z\,h\right) r\,\frac{\partial h}{\partial r}, \tag{8.5.12}$$

$$\frac{\partial \psi}{\partial r} = -r\,v_n(t,r) + \frac{\partial}{\partial r}\left[r\frac{\partial h}{\partial r}\left(\frac{z^3}{6} - \frac{z^2}{2}\,h\right)\right]. \tag{8.5.13}$$

It is readily verified that the consistency requirement for the system (8.5.12) and (8.5.13),

$$\frac{\partial^2 \psi}{\partial r \partial z} = \frac{\partial^2 \psi}{\partial z \partial r}, \tag{8.5.14}$$

is satisfied. Firstly, we integrate (8.5.12) with respect z which gives

$$\psi(t,r,z) = \left(\frac{z^3}{6} - \frac{z^2}{2}\,h\right) r\,\frac{\partial h}{\partial r} + g(t,r), \tag{8.5.15}$$

where $g(t,r)$ is an arbitrary function of integration. In order to obtain $g(t,r)$ substitute (8.5.15) into (8.5.13). This gives

$$\frac{\partial\, g(t,r)}{\partial r} = -r\,v_n(t,r), \tag{8.5.16}$$

and hence

$$g(t,r) = -\int_0^r r\,v_n(t,r^*)\,dr^* + D(t), \tag{8.5.17}$$

where $D(t) = g(t, 0)$. If we substitute (8.5.17) for $g(t, r)$ into (8.5.15) then we obtain

$$\psi(t, r, z) = A(t, r)\, z^3 + B(t, r)\, z^2 + C(t, r) + D(t), \tag{8.5.18}$$

where

$$\begin{aligned} A(t, r) &= \frac{r}{6}\frac{\partial h}{\partial r}, &(8.5.19)\\ B(t, r) &= -\frac{r}{2}\, h\, \frac{\partial h}{\partial r}, &(8.5.20)\\ C(t, r) &= -\int_0^r r\, v_n(t, r^*)\, dr^*, &(8.5.21)\\ D(t) &= \text{arbitrary function of t.} &(8.5.22) \end{aligned}$$

The streamlines in the $(r, z)-$plane at time t are

$$\psi(t, r, z) = k(t), \tag{8.5.23}$$

where $k(t)$ is an arbitrary function of t. The streamlines at time t are found by solving the cubic equation

$$A(t, r)\, z^3 + B(t, r)\, z^2 + C(t, r) = K(t), \tag{8.5.24}$$

where $K(t) = k(t) - D(t)$ is an arbitrary function of t.

We calculate A, B and C using the invariant solution (8.3.7) to (8.3.12). Using (8.3.7), we can express $h(t, r)$ and $v_n(t, r)$ in terms of $R(t)$ as

$$\begin{aligned} h(t, r) &= R^{\beta-2}(t)\left(1 - \zeta^2\right)^{\frac{1}{3}}, &(8.5.25)\\ v_n(t, r) &= \frac{2\,\beta}{9} R^{2(2\,\beta-5)}(t)\left(1 - \zeta^2\right)^{\frac{1}{3}}. &(8.5.26) \end{aligned}$$

Differentiating (8.5.25) partially with respect to r we obtain

$$A(t, \zeta) = -\frac{1}{9} R^{\beta-2}(t) \frac{\zeta^2}{(1 - \zeta^2)^{\frac{2}{3}}}, \tag{8.5.27}$$

and

$$B(t, \zeta) = \frac{1}{3} R^{2\,\beta-4}(t) \frac{\zeta^2}{(1 - \zeta^2)^{\frac{1}{3}}}. \tag{8.5.28}$$

Substituting (8.5.26) into (8.5.21) results in

$$C(t,\zeta) = -\frac{2\,\beta}{9} R^{4(\beta-2)}(t) \int_0^{\zeta} \zeta^* \left(1-\zeta^{*2}\right)^{\frac{1}{3}} d\zeta^*, \tag{8.5.29}$$

which can be integrated by letting $1-\zeta^2 = w$ to give

$$C(t,\zeta) = \frac{\beta}{12} R^{4(\beta-2)}(t) \left[\left(1-\zeta^2\right)^{\frac{4}{3}} - 1\right]. \tag{8.5.30}$$

We can express A, B and C in terms of t and r using (8.3.12) as

$$A(t,r) = -\frac{1}{9} R^{\beta-4}(t) \frac{r^2}{\left(1-\frac{r^2}{R^2(t)}\right)^{\frac{2}{3}}}, \tag{8.5.31}$$

$$B(t,r) = \frac{1}{3} R^{2\,\beta-6}(t) \frac{r^2}{\left(1-\frac{r^2}{R^2(t)}\right)^{\frac{1}{3}}}, \tag{8.5.32}$$

$$C(t,r) = \frac{\beta}{12} R^{4(\beta-2)}(t) \left[\left(1-\frac{r^2}{R^2(t)}\right)^{\frac{4}{3}} - 1\right]. \tag{8.5.33}$$

The solution of the cubic equation (8.5.24) will give z as a function of t and r. The streamlines are plotted against r for $0 \leq r \leq R(t)$ with $0 \leq \theta \leq 2\pi$.

As with the two-dimensional thin fluid film, the fluid flow inside the liquid drop will be investigated by plotting the streamlines at $t = 1$. They will be compared for a range of values of β with the streamlines in Figure 8.17 for $\beta = 0$. When there is no blowing or suction of fluid at the base the liquid drop spreads only by fluid descending due to gravity. The streamlines begin and end on the free surface except the streamline along the axis of symmetry, $r = 0$.

In Figure 8.18 the streamlines are plotted for $\beta = -0.5$, $\beta = -1.2$ and $\beta = -1.5$ describing suction at the base with increasing magnitude. The streamlines begin on the free surface. Away from the axis of symmetry, which is a streamline, they end on the free surface but if they start sufficiently close to the axis of symmetry they end on the base $0 \leq r \leq R(t)$ and are perpendicular to the base due to the no-slip boundary condition. As the magnitude of the suction increases streamlines which start further from the axis of symmetry end on the base.

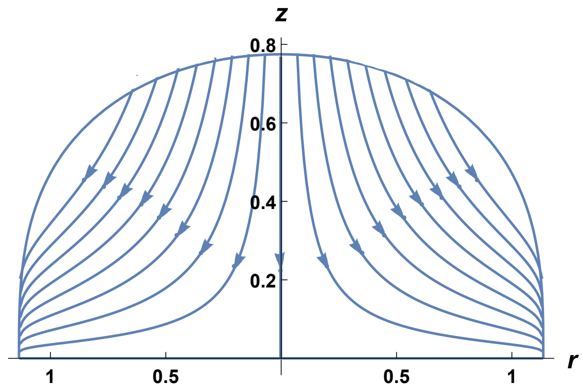

Figure 8.17: Streamlines for $\beta = 0$, plotted against r for $0 \leq r \leq R(t)$ at $t = 1$.

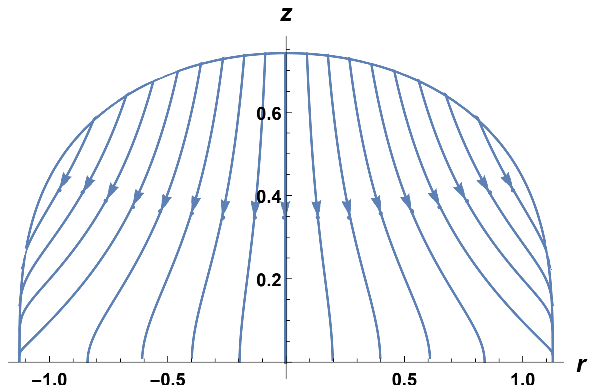

(a) $\beta = -0.5$

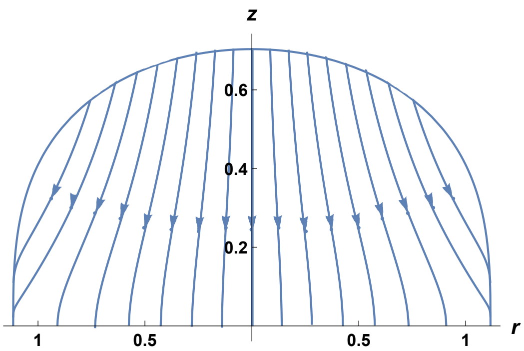

(b) $\beta = -1.2$

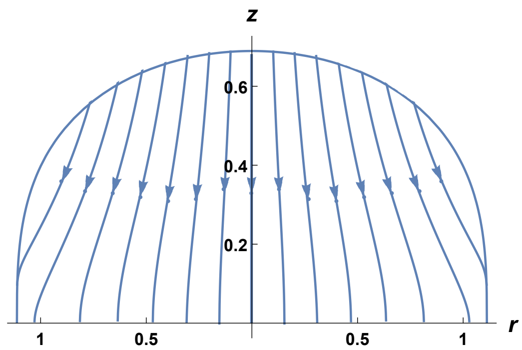

(c) $\beta = -1.5$

Figure 8.18: Streamlines for a range of negative values of β plotted against r for $0 \leq r \leq R(t)$ at $t = 1$.

In Figure 8.19 the streamlines are plotted for $\beta = 0.2$, $\beta = 0.6$, $\beta = 0.8$, $\beta = 1.2$, $\beta = 1.6$ and $\beta = 2$ which describes fluid injection at the base with increasing magnitude. There is a dividing streamline which intersects the axis of symmetry, which is a streamline, at the point $(0, z_2)$ where z_2 is given exactly by (8.4.52) and approximately by (8.4.27). This point on the axis of symmetry is a stagnation point at which the fluid velocity is zero. The dividing streamline separates the flow into two regions. In the upper region the streamlines begin and end on the free surface and show that the flow descends and spreads due to gravity. It appears as if the base on which the spreading occurs has been raised by a distance z_2 due to blowing. In the lower region the streamlines start at the base, leaving it at right angles because there is no slip, spread out due to gravity and end on the free surface. The maximum thickness of the fluid layer at the base is z_2 which is approximately proportional to $\beta^{\frac{1}{2}}$ for small β. As the strength of the blowing increases we see from Figure (8.19) that the fraction of the liquid drop occupied by the lower region increases until $\beta = 2$ for which there are no longer two regions. The lower region completely fills the liquid drop for sufficiently strong blowing with $\beta \geq 2$. The • indicates the stagnation point on the axis of symmetry at which the fluid velocity is zero and is the exact solution given in (8.4.52). In Table 8.9 numerical values of $z_2/h(t, 0)$ are presented.

Consider next the evolution of the streamlines with time. In Figure 8.20 the streamlines are plotted for $\beta = 0.8$ at times $t = 1$ and $t = 10$. Even although there is blowing at the base the maximum height of the liquid drop $h(t, 0)$ and the maximum thickness of the fluid layer at the base, z_2, decreases in time due to spreading of the drop under gravity.

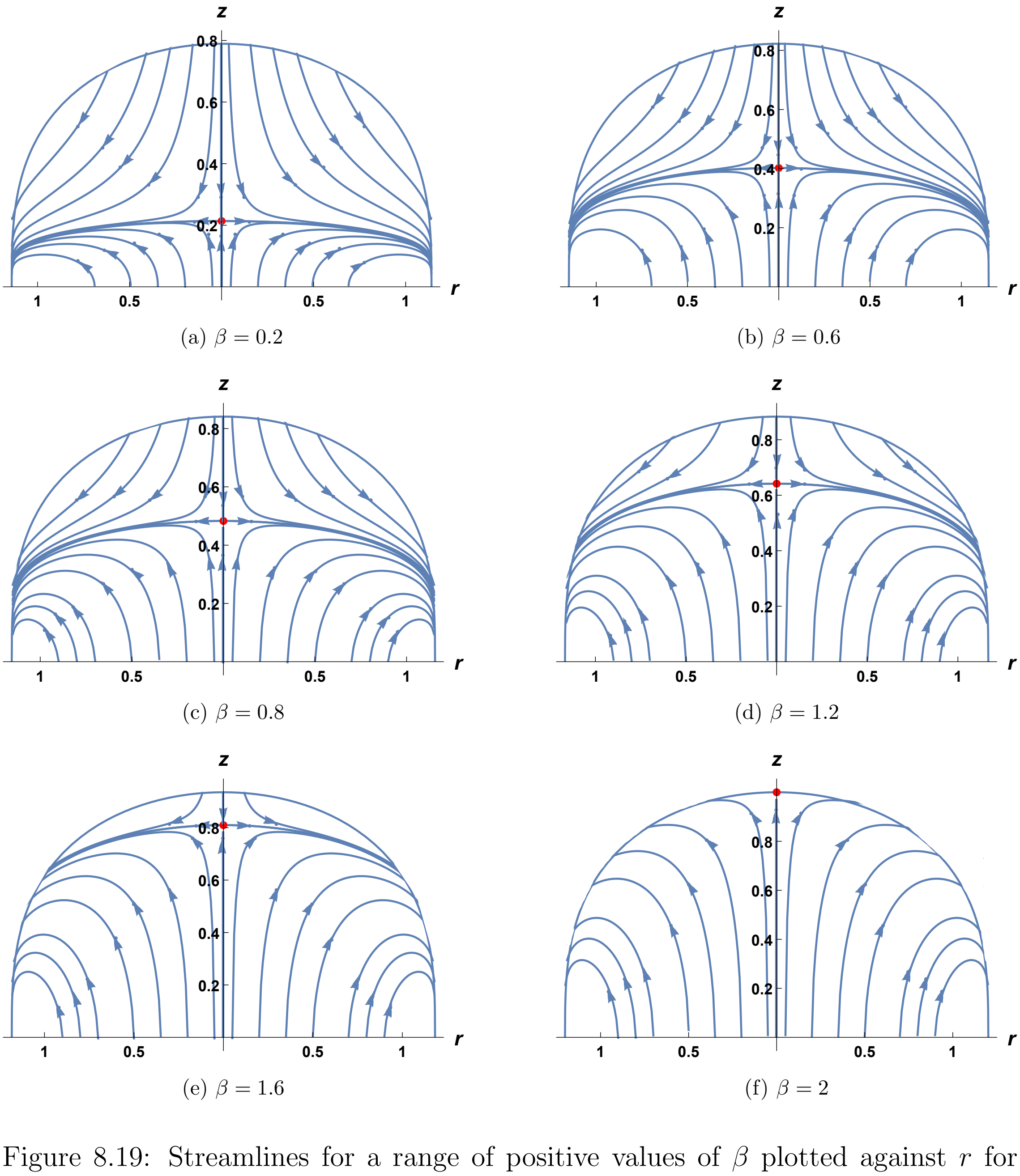

(a) $\beta = 0.2$ (b) $\beta = 0.6$

(c) $\beta = 0.8$ (d) $\beta = 1.2$

(e) $\beta = 1.6$ (f) $\beta = 2$

Figure 8.19: Streamlines for a range of positive values of β plotted against r for $0 \leq r \leq R(t)$ at $t = 1$.

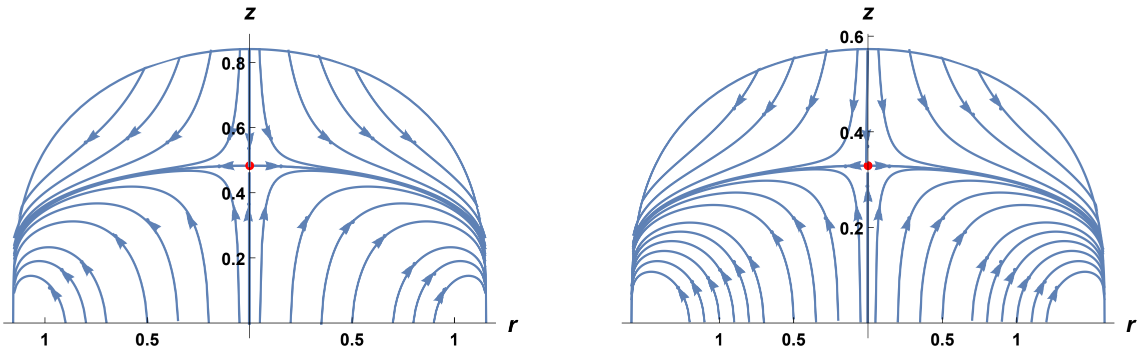

(a) $t = 1$ (b) $t = 10$

Figure 8.20: Streamlines for $\beta = 0.8$ plotted against r for $o \leq r \leq R(t)$ at $t = 1$ and $t = 10$.

In Figures (8.17) to (8.20) the streamlines were plotted in the (r, z)-plane. The base radius and the height of the liquid drop depend on time. Consider now the streamlines in the (ζ, z^*)-plane where

$$\zeta = \frac{r}{R(t)}, \qquad 0 \leq \zeta \leq 1, \tag{8.5.34}$$

$$z^* = \frac{z}{h(t,0)}, \qquad 0 \leq z^* \leq 1. \tag{8.5.35}$$

The cubic equation (8.5.24), expressed in terms of ζ and z^*, is

$$A^*(t,\zeta)z^{*3} + B^*(t,\zeta)z^{*2} + C(t,\zeta) = k(t) \tag{8.5.36}$$

where

$$A^*(t,\zeta) = A(t,\zeta)h^3(t,0), \tag{8.5.37}$$

$$B^*(t,\zeta) = B(t,\zeta)h^2(t,0). \tag{8.5.38}$$

But by (8.3.7) and (8.3.10),

$$h(t,0) = R^{\beta-2}(t) \tag{8.5.39}$$

and hence using (8.5.27) and (8.5.28) we obtain

$$A^*(t,\zeta) = -\frac{1}{9}R^{4\beta-8}(t)\frac{\zeta^2}{(1-\zeta^2)^{\frac{2}{3}}}, \tag{8.5.40}$$

$$B^*(t,\zeta) \quad = \quad \frac{1}{3}R^{4\beta-8}(t)\frac{\zeta^2}{(1-\zeta^2)^{\frac{1}{3}}}. \tag{8.5.41}$$

Unlike for the two-dimensional thin film the integral in the third coefficient C could be evaluated and $C(t,r)$ is given by (8.5.33). The coefficients $A^*(t,r)$, $B^*(t,r)$ and $C(t,r)$ depend explicitly on time through the same factor $R^{4\beta-8}(t)$. The cubic equation (8.5.24) takes the form

$$-\frac{1}{9}\frac{\zeta^2}{(1-\zeta^2)^{\frac{2}{3}}}z^{*3}+\frac{1}{3}\frac{\zeta^2}{(1-\zeta^2)^{\frac{1}{3}}}z^{*2}-\frac{\beta}{12}\left[1-\left(1-\zeta^2\right)^{\frac{4}{3}}\right]=K^*, \tag{8.5.42}$$

where

$$K^*=\frac{K(t)}{R^{4\beta-8}(t)}. \tag{8.5.43}$$

The parameter K^* is independent of time because the left hand side of (8.5.42) does not depend on time explicitly. Also K^* is an arbitrary constant since $K(t)$ was an arbitrary function. The streamlines in the (ζ,z^*)-plane are plotted by giving $k^*(t)$ a range of values. Since (8.5.42) does not depend explicitly on time, the streamline pattern in the (ζ,z^*)-plane is independent of time. It depends only on the parameter β. From (8.4.55) or Table 8.9 and (8.4.57) the point of intersection of the dividing streamline with the axis of symmetry, which is also a streamline, is

$$\begin{aligned} z_2^*=\frac{z_2}{h(t,0)} \quad &= \quad 1+2\cos\left(\phi+\frac{4\pi}{3}\right), \\ &= \quad \frac{\beta^{\frac{1}{2}}}{\sqrt{3}}+\frac{\beta}{18}+\bigcirc\left(\beta^{\frac{3}{2}}\right). \end{aligned} \tag{8.5.44}$$

This point is a stagnation point of the flow. The streamlines in the (ζ,z^*)-plane are plotted in Figure 8.21 for β ranging from 0.2 to 2 and for $0\le\zeta\le1$ and $0\le z^*\le1$. The values of z_2^* on the axis of symmetry agree with Table 8.9. Figure 8.21 can be compared with Figure 8.19 plotted in the (r,z)-plane at time $t=1$.

For model I for an axisymmetric liquid drop the thin film approximation is satisfied for $-\infty\le\beta\le3$. All the values of β used in the graphs in this chapter lie in this range.

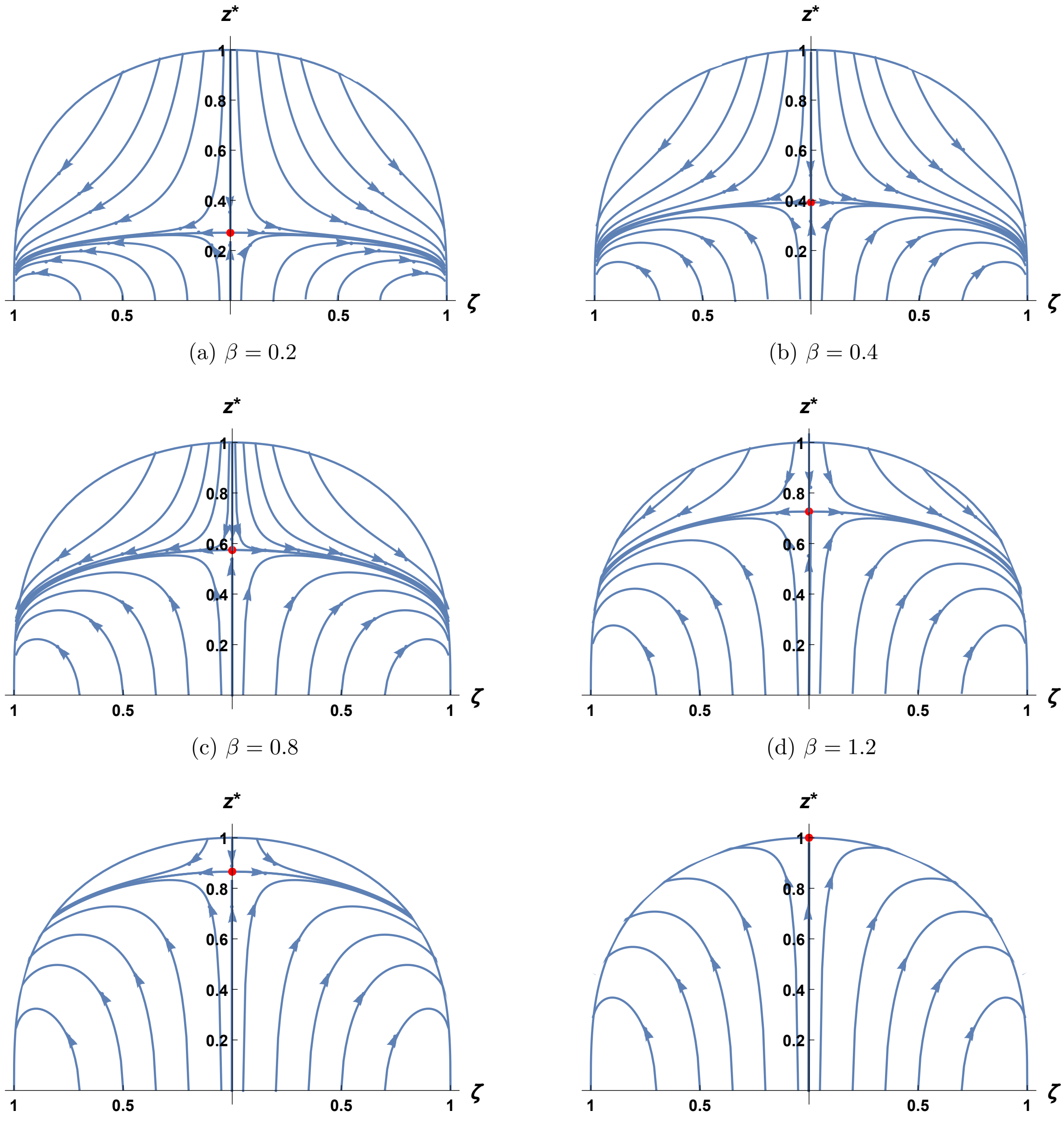

(a) $\beta = 0.2$ (b) $\beta = 0.4$

(c) $\beta = 0.8$ (d) $\beta = 1.2$

(e) $\beta = 1.6$ (f) $\beta = 2$

Figure 8.21: Streamlines for a range of positive values of β $(0 < \beta \leq 2)$ plotted in the $\zeta, z^*)$-plane where $\zeta = r/R(t)$ $(0 \leq \zeta \leq 1)$ and $z^* = z/h(t,0)$ $(0 \leq z^* \leq 1)$.

8.6 Conclusions

The results derived in this Chapter for an axisymmetric liquid drop compare directly with those derived in Chapter 5 for a two-dimensional thin film. Some of the results could be derived from those of Chapter 5 by replacing β by $\frac{\beta}{2}$. The results were displayed in the form of Tables to make the comparison easier. The base radius always spreads to infinity even when there is suction at the base. When there is fluid injection a layer of fluid forms at the base provided the blowing is not too strong. The thin fluid film approximation is satisfied for the whole range of suction but only for weak to moderate blowing.

Chapter 9

Fluid velocity at the base proportional to the spatial gradient of the height of the liquid drop

9.1 Introduction

In Chapter 8 a relation between $g(\zeta)$ and $f(\zeta)$ was assumed in order to close the system of equations and also solve the ordinary differential equation (7.4.56) analytically. In this chapter we consider another relation between $g(\zeta)$ and $f(\zeta)$ for which the differential equation (7.4.56) can be solved analytically. For this relation, $v_n(t,r)$ is proportional to the spatial gradient of $h(t,r)$. The velocity on the axis of symmetry $r = 0$ will be determined and the streamlines will be plotted within the liquid drop. We will compare the results obtained in this chapter with the results of Chapters 6 and 8.

9.2 Relation between $g(\zeta)$ and $\frac{df(\zeta)}{d\zeta}$

We consider the relation

$$g(\zeta) = -\beta\,\zeta\,\frac{df(\zeta)}{d\zeta}, \qquad -\infty < \beta < \infty, \tag{9.2.1}$$

where β is a constant. We can determine the physical significance of (9.2.1) by first differentiating (7.4.62) for $h(t,r)$ with respect to r to obtain

$$\frac{df}{d\zeta} = f(0)\left(1 + \frac{t}{\alpha\, f^3(0)}\right)^{\frac{1}{3}(\alpha+1)}\frac{\partial h}{\partial r}, \tag{9.2.2}$$

and then by substituting (9.2.2) into (7.4.63) for $v_n(t,r)$. This gives

$$v_n(t,r) = -\frac{\beta\, r\,\frac{\partial h}{\partial r}}{f^3(0)\left(1 + \frac{t}{\alpha\, f^3(0)}\right)}. \tag{9.2.3}$$

Thus $v_n(t,r)$ is proportional to $\frac{\partial h(t,r)}{\partial r}$ and $v_n(t,r) = 0$ at $r = 0$ because both $r = 0$ and $\frac{\partial h}{\partial r} = 0$ and it will be small in the neighbourhood of $r = 0$ because $\frac{\partial h}{\partial r}$ will be small in that range.

We cannot determine further properties of $v_n(t,r)$ at this stage because $\frac{\partial h}{\partial r}$ for $0 \le r \le R(t)$ will only be known once the problem has been solved. Also we find later that $f(0)$ depends on β which compares with the solution in Chapter 8 where $f(0)$ is independent of β.

9.3 Solution of the ordinary differential equation

In order to determine α we consider the balance law (7.4.58) and substitute (9.2.1) which gives

$$-\beta\int_0^1 \zeta^2\frac{df}{d\zeta}\,d\zeta = \frac{1}{3}\left(8 - \frac{1}{\alpha}\right)\int_0^1 \zeta\, f(\zeta)\,d\zeta. \tag{9.3.1}$$

But integrating the left hand side by parts and using the boundary condition $f(1) = 0$ we obtain

$$\left(8 - \frac{1}{\alpha} - 6\beta\right) \int_0^1 \zeta \, f(\zeta) \, d\zeta = 0. \tag{9.3.2}$$

Hence since the integral in (9.3.2) is non-zero,

$$\alpha = \frac{1}{2\,(4 - 3\,\beta)}, \qquad \beta \neq \frac{4}{3}. \tag{9.3.3}$$

Using (9.3.3) for α we now solve the ordinary differential equation (7.4.56) for $f(\zeta)$. The boundary conditions are at $\zeta = 1$ and are the no fluid flux condition (8.2.11) and the zero height condition (7.4.46). Substituting (9.3.1) and (9.3.3) into (7.4.56) results in an integrable ordinary differential equation

$$\frac{d}{d\zeta}\left(\zeta \, f^3 \, \frac{df}{d\zeta}\right) + 3(1-\beta)\,\frac{d}{d\zeta}\left(\zeta^2 \, f\right) = 0. \tag{9.3.4}$$

Unlike the case $g(\zeta) = \beta \, f(\zeta)$, the ordinary differential equation (9.3.4) depends on β. Integrating (9.3.4) once with respect to ζ and applying boundary conditions (7.4.46) and (8.2.11) results in a variable separable ordinary differential equation,

$$f^2 \, \frac{df}{d\zeta} = -3(1-\beta)\,\zeta, \tag{9.3.5}$$

which can be integrated subject to the boundary condition, $f(1) = 0$, to give

$$f(\zeta) = \left(\frac{9}{2}(1-\beta)\right)^{\frac{1}{3}} \left(1 - \zeta^2\right)^{\frac{1}{3}}. \tag{9.3.6}$$

Hence

$$f(0) = \left(\frac{9}{2}(1-\beta)\right)^{\frac{1}{3}}. \tag{9.3.7}$$

The solutions (9.3.6) and (6.3.9) for an axisymmetric liquid drop and a two-dimensional thin film are the same even although the differential equations (9.3.4) and (6.3.7) are different. This is because the boundary conditions are the same and both differential equations reduce to (9.3.5) after one integration. Unlike the case $g(\zeta) = \beta \, f(\zeta)$, both $f(\zeta)$ and $f(0)$ depend on β. In order to determine the physical significance of

β first consider $v_n(t,r)$ which is given by (7.4.63). Substituting (9.2.1) for $g(\zeta)$ into (7.4.63) with $f(\zeta)$ given by (9.3.6) and α by (9.3.3) we obtain

$$v_n(t,r) = \frac{4\,\beta}{27(1-\beta)}\left(1+\frac{4\,(4-3\,\beta)\,t}{9(1-\beta)}\right)^{\frac{(4\,\beta-5)}{4-3\,\beta}}\frac{\zeta^2}{(1-\zeta^2)^{\frac{2}{3}}}, \tag{9.3.8}$$

We define a new parameter β^* by

$$\beta^* = \frac{\beta}{4(1-\beta)}. \tag{9.3.9}$$

The factor $\frac{1}{4}$ is to normalise the critical value to $\beta^* = -1$. Then $v_n(t,r)$ has the same sign as β^* which makes physical interpretation easier:

$$\beta^* > 0 \quad \text{then} \quad v_n > 0: \quad \text{blowing of fluid into liquid drop}, \tag{9.3.10}$$

$$\beta^* < 0 \quad \text{then} \quad v_n < 0: \quad \text{suction of fluid out of liquid drop}. \tag{9.3.11}$$

Also from (9.3.9),

$$\beta = \frac{4\beta^*}{1+4\beta^*}, \tag{9.3.12}$$

and by substituting (9.3.12) into (9.3.3) and (9.3.7) we obtain

$$\alpha = \frac{1+4\beta^*}{8(1+\beta^*)}, \tag{9.3.13}$$

$$f(0) = \left(\frac{9}{2(1+4\beta^*)}\right)^{\frac{1}{3}}. \tag{9.3.14}$$

Substituting (9.3.13) and (9.3.14) into (7.4.59) to (7.4.63)and (9.3.8), where $f(\zeta)$ is given by (9.3.6), we obtain

$$R(t) = \left(1+\frac{16}{9}(1+\beta^*)t\right)^{\frac{1+4\beta^*}{8(1+\beta^*)}}, \tag{9.3.15}$$

$$V(t) = \frac{3}{4}\left(1+\frac{16}{9}(1+\beta^*)t\right)^{\frac{\beta^*}{1+\beta^*}}, \tag{9.3.16}$$

$$h(t,r) = \left(1+\frac{16}{9}(1+\beta^*)t\right)^{-\frac{1}{4(1+\beta^*)}}\left(1-\zeta^2\right)^{\frac{1}{3}}, \tag{9.3.17}$$

$$v_n(t,r) = \frac{16}{27}\beta^*\left(1+\frac{16}{9}(1+\beta^*)t\right)^{-\frac{(5+4\beta^*)}{4(1+\beta^*)}}\frac{\zeta^2}{(1-\zeta^2)^{\frac{2}{3}}}, \tag{9.3.18}$$

where

$$\zeta = \frac{r}{R(t)}, \qquad 0 \le \zeta \le 1. \tag{9.3.19}$$

The Lie point symmetry (7.4.65), when multiplied by $\frac{9}{4}$, is

$$X = \left(\frac{9}{4} + 4\,(1+\beta^*)\,t\right)\frac{\partial}{\partial t} + \frac{1}{2}\,(1+\beta^*)\;r\,\frac{\partial}{\partial r} - h\,\frac{\partial}{\partial h}. \tag{9.3.20}$$

Equations (9.3.15) to (9.3.18) are valid for $\beta^* \neq -1$. We now consider the limit as $\beta^* \to -1$. We first obtain $R(t)$ for $\beta^* = -1$ and then express $V(t), h(t,r)$ and $v_n(t,r)$ in terms of $R(t)$ to obtain these quantities in the limit $\beta^* = -1$. Equation (9.3.15) for $R(t)$ can be written as

$$R(t) = \exp\left[\frac{1+4\beta^*}{8(1+\beta^*)}\ln\left(1 + \frac{16}{9}(1+\beta^*)\,t\right)\right]. \tag{9.3.21}$$

Using the expansion (6.3.25) for $\ln(1+\epsilon)$, (9.3.21) becomes

$$R(t) = \exp\left[\frac{1+4\beta^*}{8(1+\beta^*)}\left(\frac{16}{9}(1+\beta^*)t\right) + \bigcirc\,(1+\beta^*)\right] \quad \text{as} \quad \beta^* \to -1, \tag{9.3.22}$$

and therefore

$$\lim_{\beta^* \to -1} R(t) = \exp\left[-\frac{2\,t}{3}\right]. \tag{9.3.23}$$

Thus in the limit $\beta^* = -1$,

$$V(t) = \frac{3}{4}\,R(t)^{\frac{8\beta^*}{1+4\beta^*}} = \frac{3}{4}\,\exp\left(-\frac{16\,t}{9}\right), \tag{9.3.24}$$

$$h(t,r) = R(t)^{\frac{-2}{1+4\beta^*}}\left(1-\zeta^2\right)^{\frac{1}{3}} = \exp\left(-\frac{4\,t}{9}\right)\left(1-\zeta^2\right)^{\frac{1}{3}}, \tag{9.3.25}$$

$$\begin{aligned} v_n(t,r) &= \frac{16}{27}\beta^* R(t)^{-2\left(\frac{5+4\beta^*}{1+4\beta^*}\right)}\frac{\zeta^2}{(1-\zeta^2)^{\frac{2}{3}}} \\ &= -\frac{16}{27}\exp\left(-\frac{4\,t}{9}\right)\frac{\zeta^2}{(1-\zeta^2)^{\frac{2}{3}}}. \end{aligned} \tag{9.3.26}$$

The way that $R(t)$, $V(t)$, $h(t,0)$, $v_n(t,\zeta)$ and the thin fluid film ratio $\epsilon(t)$ defined by (8.3.19) depend on β^* for $-\infty \leq \beta^* \leq \infty$ is similar to the way $W(t)$, $V(t)$, $h(t,0)$, $v_n(t,\zeta)$ and $\epsilon(t)$ depend on β^* for a two-dimensional thin film which was investigated in Chapter 6. The critical value of β^* at which exponential behaviour occurs is $\beta^* = -1$ in both cases. For a liquid drop some limits occur after the finite time

$$t_4 = -\frac{9}{16\,(1+\beta^*)} > 0 \tag{9.3.27}$$

compared with the finite time t_2 given by (6.3.31) for a two-dimensional thin film. The properties of the axisymmetric spreading of a liquid drop are summarised in Tables 9.1 to 9.5 and presented in Figures (9.1) to (9.5).

We now comment briefly on the main conclusions from Tables 9.1 to 9.5. Since $\frac{dR}{dt} > 0$ for $-\frac{1}{4} < \beta^* \leq \infty$, the base expands even when there is suction for $-\frac{1}{4} < \beta^* < 0$. For the height of the drop

$$\frac{\partial h}{\partial r}(t,r) = -\frac{2}{3}R^{-\frac{2}{1+4\beta^*}}(t)\, r\left(1 - \frac{r^2}{R^2(t)}\right)^{-\frac{2}{3}}. \tag{9.3.28}$$

In the vicinity of the moving contact line the thin fluid film approximation breaks down because $\frac{\partial h}{\partial r}(t,r) \to -\infty$ as $r \to R(t)$. Suction and blowing did not remove the singularity in the spatial derivative at the moving contact line $r = R(t)$ or reduce the power of the singularity from $-\frac{2}{3}$. Also

$$\frac{\partial h}{\partial t}(t,0) = -\frac{4}{9}\left[1 + \frac{16}{9}\,(1+\beta^*)\,t\right]^{-\frac{1}{4}\left(\frac{5+4\beta^*}{1+\beta^*}\right)} \tag{9.3.29}$$

which is negative for all values, $-\infty \leq \beta^* \leq \infty$. The maximum height of the drop decreases with time even when there is blowing at the base for $0 < \beta^* \leq \infty$. The decrease in height due to spreading under gravity is greater than the increase in height due to blowing. For $-\infty \leq \beta^* < -\frac{5}{4}$ the suction can be considered as strong because $v_n(t,\zeta) \to -\infty$ in the finite time t_4. For $\beta^* = -\frac{5}{4}$ the suction velocity is constant while for $-\frac{5}{4} < \beta^* < -1$ the suction is still moderate in strength with the suction velocity tending to zero and the suction process being completed in the finite time t_4. The thin fluid film approximation will be valid if

$$\epsilon(t) = \frac{h(t,0)}{R(t)} \leq 1. \tag{9.3.30}$$

From (9.3.15) and (9.3.17) for $\beta^* \neq -1$,

$$\frac{h(t,0)}{R(t)} = \left(1 + \frac{10}{9}\,(1+\beta^*)\,t\right)^{-\frac{3+4\beta^*}{8(1+\beta^*)}}, \tag{9.3.31}$$

while from (9.3.23) and (9.3.25) for $\beta^* = -1$,

$$\frac{h(t,0)}{R(t)} = \exp\left[\frac{2\,t}{9}\right]. \tag{9.3.32}$$

For $-\frac{3}{4} \leq \beta^* \leq \infty$ the thin fluid film approximation is valid for all $t \geq 0$ if it is satisfied initially. It holds for suction at the base with $-\frac{3}{4} \leq \beta^* < 0$. The suction is strong at the rim and weak at the centre of the drop. For sufficiently strong suction ($\beta^* < -\frac{3}{4}$) the radius of the drop decreases too rapidly for the thin fluid film approximation to be valid. The thin film approximation is valid for all blowing ($0 < \beta^* \leq \infty$). Since the blowing at the rim is strong the radius $R(t)$ increases faster than $h(t,0)$.

β^*	$R(t)$	$\frac{dR}{dt}$
$-\infty < \beta^* < -1$	$R(t) \to 0$ as $t \to t_4$ $t_4 = -\frac{9}{16(1+\beta^*)}$	< 0
$\beta^* = -1$	$R(t) \to 0$ as $t \to \infty$ exponentially	< 0
$-1 < \beta^* < -\frac{1}{4}$	$R(t) \to 0$ as $t \to \infty$ algebraically	< 0
$\beta^* = -\frac{1}{4}$	$R(t) = R_0$, $R_0 =$ constant	0
$-\frac{1}{4} < \beta^* < \infty$	$R(t) \to \infty$ as $t \to \infty$ algebraically	> 0

Table 9.1: Behaviour of the radius of the liquid drop, $R(t)$, for $-\infty \leq \beta^* \leq \infty$.

A plot of $R(t)$ against time, t is presented in Figure 9.1.

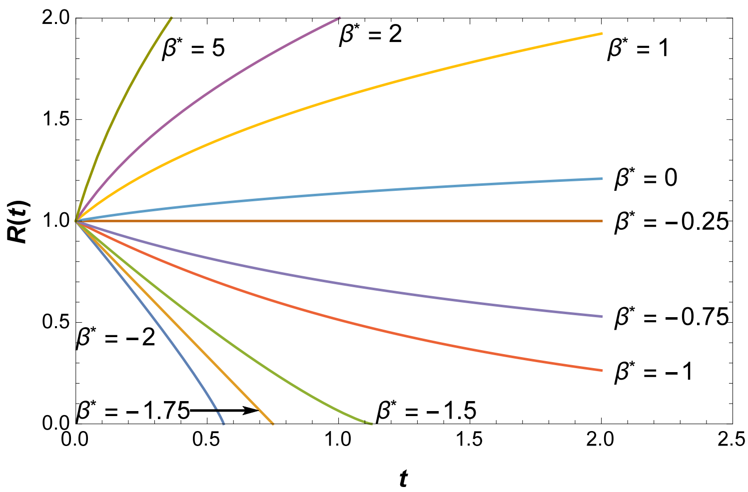

Figure 9.1: Radius $R(t)$ given by (9.3.15) and (9.3.23) plotted against t for a range of values of β^*.

β^*	$V(t)$	$\frac{dV}{dt}$
$-\infty < \beta^* < -1$	$V(t) \to 0$ as $t \to t_4$ $t_4 = -\frac{9}{16(1+\beta^*)}$	< 0
$\beta^* = -1$	$V(t) \to 0$ as $t \to \infty$ exponentially	< 0
$-1 < \beta < 0$	$V(t) \to 0$ as $t \to \infty$ algebraically	< 0
$\beta^* = 0$	$V(t) = V_0 = \frac{3}{4}$	0
$0 < \beta^* < \infty$	$V(t) \to \infty$ as $t \to \infty$ algebraically	> 0

Table 9.2: Behaviour of the total volume of the liquid drop, $V(t)$, for $-\infty < \beta^* < \infty$.

A plot of $V(t)$ against time, t, is presented in Figure 9.2.

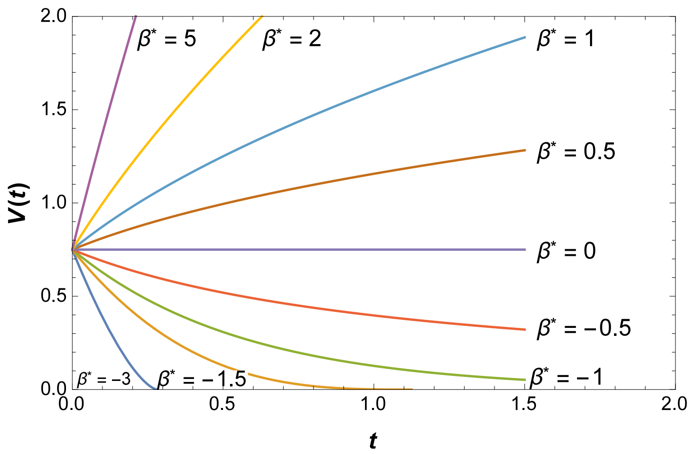

Figure 9.2: Volume $V(t)$ given by (9.3.16) and (9.3.24) plotted against t for a range of values of β^*.

β^*	$h(t,0)$	$\frac{\partial h(t,0)}{\partial t}$
$-\infty \leq \beta^* < -1$	$h(t,0) \to 0$ as $t \to t_4$ $t_4 = -\frac{9}{16(1+\beta^*)}$	< 0
$\beta^* = -1$	$h(t,0) \to 0$ as $t \to \infty$ exponentially	< 0
$-1 < \beta^* \leq \infty$	$h(t,0) \to 0$ as $t \to \infty$ algebraically	< 0

Table 9.3: Behaviour of the height of the liquid drop on the axis, $h(t,0)$, for $-\infty \leq \beta^* \leq \infty$.

Graphs of $h(t,0)$ are plotted against time for a range of β^* in Figure 9.3.

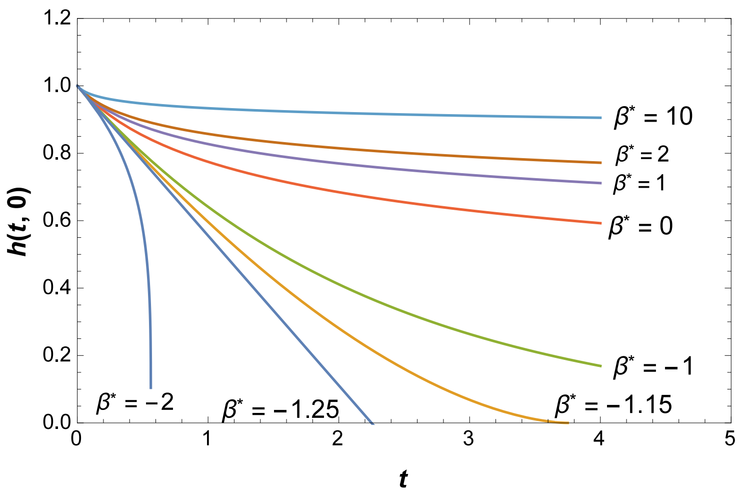

Figure 9.3: Height of the liquid drop at the centre, $h(t,0)$, given by (9.3.17) and (9.3.25) plotted against t for a range of values of β^*.

β^*	$v_n(t,\zeta)$	$\frac{\partial v_n(t,\zeta)}{\partial t}$
$-\infty \leq \beta^* < -\frac{5}{4}$	$v_n(t,\zeta) < 0$ $v_n(t,\zeta) \to -\infty$ as $t \to t_4$ $t_4 = -\frac{9}{16(1+\beta^*)}$	< 0
$\beta^* = -\frac{5}{4}$	$v_n(t,\zeta) = \frac{16}{27}\beta^* \frac{\zeta^2}{(1-\zeta^2)^{\frac{2}{3}}} < 0$	0
$-\frac{5}{4} < \beta^* < -1$	$v_n(t,0) < 0$ $v_n(t,\zeta) \to 0$ as $t \to t_4$ $t_4 = -\frac{9}{16(1+\beta^*)}$	> 0
$\beta^* = -1$	$v_n(t,0) < 0$ $v_n(t,\zeta) \to 0$ as $t \to \infty$ exponentially	> 0
$-1 < \beta^* < 0$	$v_n(t,\zeta) < 0$ $v_n(t,\zeta) \to 0$ as $t \to \infty$ algebraically	> 0
$\beta^* = 0$	$v_n(t,\zeta) = 0$	0
$0 < \beta^* \leq \infty$	$v_n(t,\zeta) > 0$ $v_n(t,\zeta) \to 0$ as $t \to \infty$ algebraically	< 0

Table 9.4: Behaviour of the fluid injection velocity on the axis, $v_n(t,\zeta)$, at a fixed value of ζ $(0 < \zeta < 1)$ for $-\infty \leq \beta^* \leq \infty$.

Since $v_n(t,\zeta) = 0$ when $\zeta = 0$ for all β^*, graphs of $v_n(t,\zeta)$ are plotted against time for a range of β^* at $\zeta = 0.5$ in Figure 9.4.

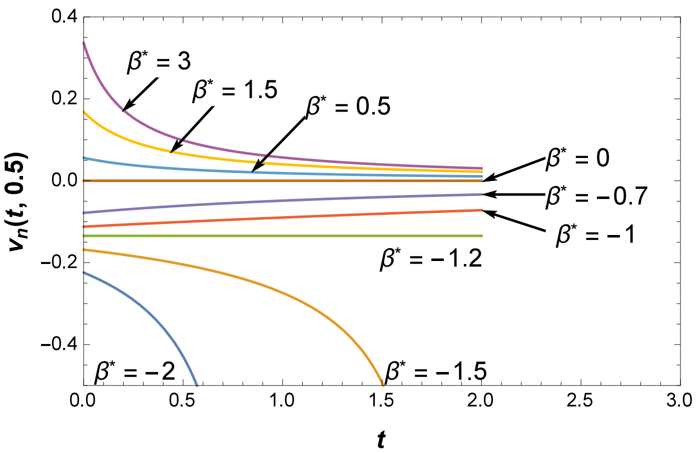

Figure 9.4: Fluid injection velocity at the base, $v_n(t,\zeta)$ given by (9.3.18) and (9.3.26) plotted against t at $\zeta = 0.5$ for a range of values of β^* .

β^*	$\epsilon(t) = \frac{h(t,0)}{R(t)}$	$\frac{\partial \epsilon}{\partial t}$
$-\infty < \beta^* < -1$	$\epsilon(t) \to \infty$ as $t \to t_4$ $t_4 = -\frac{9}{16(1+\beta^*)}$	> 0
$\beta^* = -1$	$\epsilon(t) \to \infty$ as $t \to \infty$ exponentially	> 0
$-1 < \beta^* < -\frac{3}{4}$	$\epsilon(t) \to \infty$ as $t \to \infty$ algebraically	> 0
$\beta^* = -\frac{3}{4}$	$\epsilon(t) = 1$	0
$-\frac{3}{4} < \beta^* \leq \infty$	$\epsilon(t) \to 0$ as $t \to \infty$ algebraically	> 0

Table 9.5: Behaviour of the thin fluid film ratio on the axis of the liquid drop, $\epsilon(t)$, for $-\infty \leq \beta^* \leq \infty$.

Graphs of ϵ are plotted against time for a range of β^* in Figure 9.5.

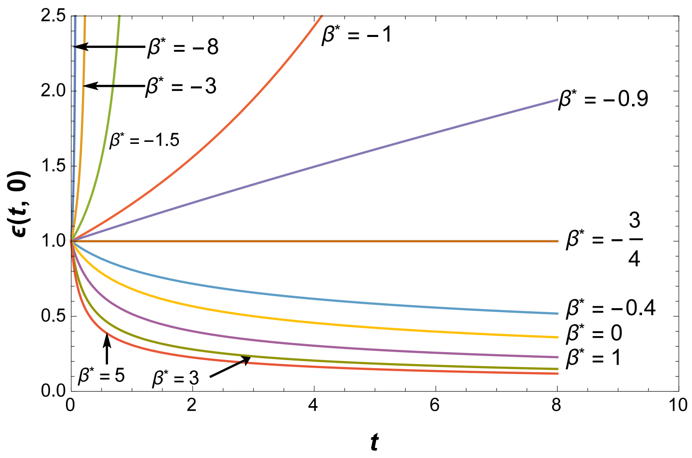

Figure 9.5: Thin fluid film ratio on the axis of the liquid drop, $\epsilon(t)$, given by (9.3.31) and (9.3.32) plotted against t for a range of values of β^*.

In Figure 9.6, $h(t, r)$ and $v_n(t, r)$ are plotted against r for ranges of values of β^* and time. Similar graphs were presented in [20]. The height always decreases with time even for values of β^* for which there is blowing, $\beta^* > 0$. For suction with $\beta^* < -1$ the thin film disappears by the base tending to a point in the finite time t_4 given by (9.3.27). The suction/blowing velocity $v_n(t, r)$ is stronger at the rim of the thin film and weaker near the centre of the thin film and $v_n(t, 0) = 0$.

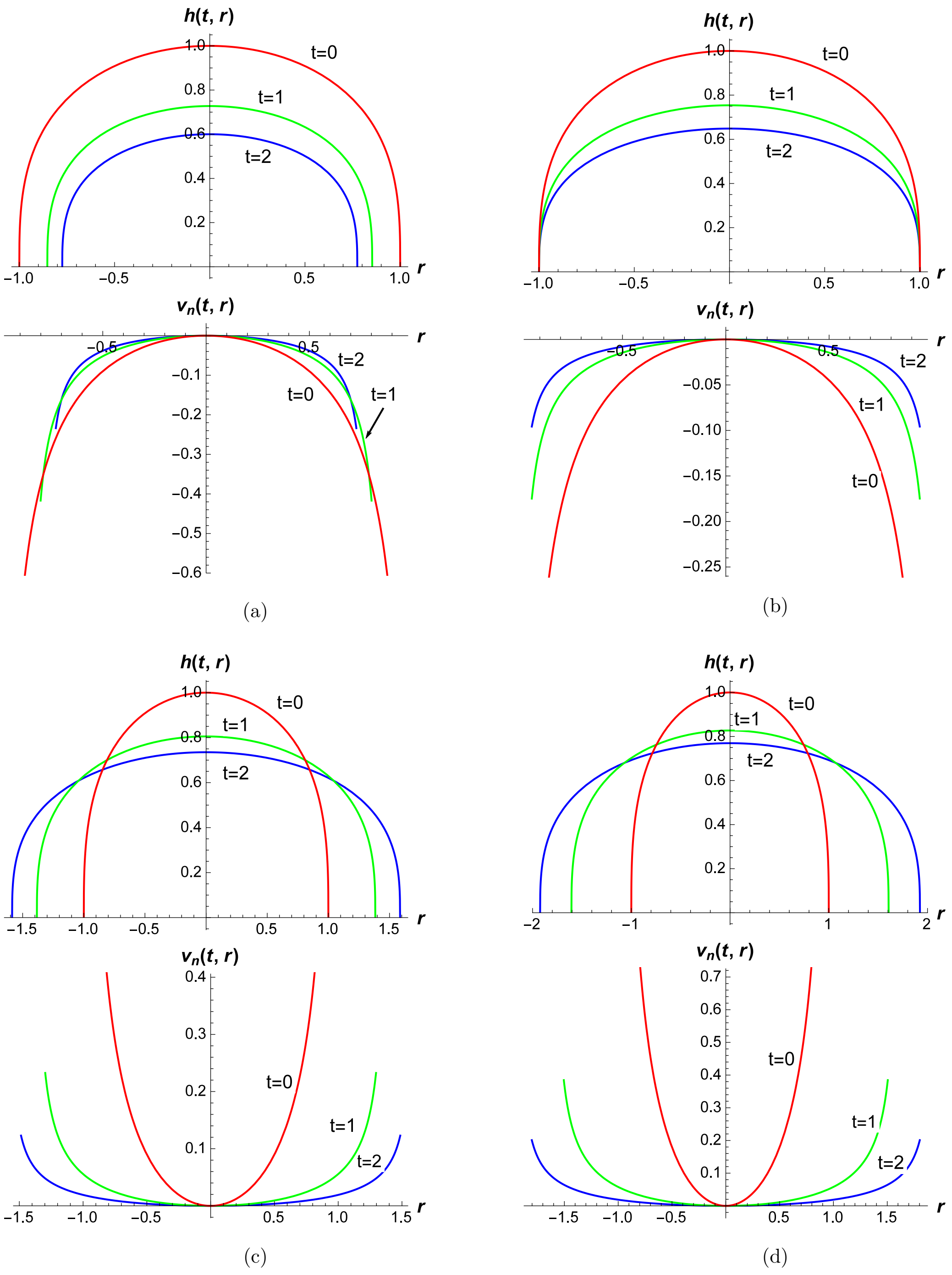

Figure 9.6: Graphs of $h(t,r)$ given by (9.3.17) and (9.3.25) and the fluid velocity at the base, $v_n(t,r)$ given (9.3.18) and (9.3.26) against r for a range of values of t and for:(a) $\beta^* = -0.5$, (b) $\beta^* = -0.25$, (c) $\beta^* = 0.5$, (d) $\beta^* = 1$. The thin fluid film approximation is valid for $-0.75 \leq \beta^* \leq \infty$ if satisfied initially.

9.4 Velocity on the axis of symmetry

The fluid velocity on the axis of symmetry is given by (8.4.5) at $r = 0$ as

$$v_z(t,0,z) = P(t,0)\, z^3 + Q(t,0)\, z^2 + v_n(t,0), \tag{9.4.1}$$

where from (8.4.11), (8.4.14) and (9.3.18),

$$P(t,0) = \frac{2}{9}\frac{h(t,0)}{R^2(t)}, \tag{9.4.2}$$

$$Q(t,0) = -\frac{2}{3}\frac{h^2(t,0)}{R^2(t)}, \tag{9.4.3}$$

$$v_n(t,0) = 0. \tag{9.4.4}$$

Hence

$$v_z(t,0,z) = \frac{2}{9}\frac{h(t,0)}{R^2(t)}\, z^2 \left[z - 3\, h(t,0)\right]. \tag{9.4.5}$$

The points on the axis $r = 0$ at which $v_z(t,0,z) = 0$ satisfy the cubic equation

$$z^2\,(z - 3\, h(t,0)) = 0. \tag{9.4.6}$$

Thus $v_z(t,0,z) = 0$ when $z = 0, z = 0, z = 3h(t,0)$. From (9.4.5)

$$v_z(t,0,z) < 0 \quad \text{for} \quad 0 < z \leq h(t,0). \tag{9.4.7}$$

There are no zeros of $v_z(t,0,z)$ inside the liquid drop although there is a double zero of $v_z(t,0,z)$ on the base $z = 0$. There is therefore no dividing streamline (between descending and ascending fluid) through a point on the axis of symmetry inside the liquid drop. It will be verified in the next section where the streamlines are plotted for a range of values of β^* that, as for the corresponding two-dimensional model in Chapter 6, there is a dividing streamline through the origin, $r = 0, z = 0$.

Consider now the properties of $v_z(t,0,z)$ at the point of maximum height of the drop, $z = h(t,0)$. From (9.4.5)

$$v_z(t,0,h) = -\frac{4}{9}\frac{h^4(t,0)}{R^2(t)} \tag{9.4.8}$$

and using (9.3.15) and (9.3.17) for $\beta^* \neq -1$ and (9.3.23) and (9.3.25) for $\beta^* = -1$ we obtain

$$\beta^* \neq -1: \qquad v_z(t,0,h(t,0)) = -\frac{4}{9}\left[1+\frac{16}{9}(1+\beta^*)t\right]^{-\frac{1}{4}\left(\frac{5+4\beta^*}{1+\beta^*}\right)}, \tag{9.4.9}$$

$$\frac{d\,v_z}{d\,t}(t,0,h(t,0)) = \frac{16}{81}(5+4\beta^*)\left[1+\frac{16}{9}(1+\beta^*)t\right]^{-\frac{1}{4}\left(\frac{9+8\beta^*}{1+\beta^*}\right)} \tag{9.4.10}$$

$$\beta^* = -1: \qquad v_z(t,0,h(t,0)) = -\frac{4}{9}\exp\left(\frac{-4}{9}t\right), \tag{9.4.11}$$

$$\frac{d\,v_z}{d\,t}(t,0,h(t,0)) = \frac{16}{81}\exp\left(\frac{-4}{9}t\right), \tag{9.4.12}$$

The properties of $v_z(t,0,h(t,0))$ for $-\infty \leq \beta^* \leq \infty$ are presented in Table 9.6 and illustrated in Figure 9.7 where $v_z(t,0,h(t,0))$ is plotted against time for a range of values of β^*. The results are in agreement with Table 9.4 for $v_n(t,\zeta)$ where $0 < \zeta < 1$. Since $v_z(t,0,h(t,0)) < 0$ for $-\infty \leq \beta^* \leq \infty$ the height of the liquid drop decreases with time even for blowing for which $0 < \beta^* \leq \infty$. For $-\infty \leq \beta^* < -\frac{5}{4}$ the suction is very strong and $v_z(t,0,h(t,0)) \to -\infty$ in the finite time t_4 while for $-\frac{5}{4} < \beta^* < -1$ the suction is weaker and $v_z(t,0,h(t,0)) \to 0$ in the finite time t_4. In both cases $R(t) \to 0$ and the liquid drop tends to a point in the finite time t_4 (Table 9.1). For $-1 \leq \beta^* \leq \infty$ the velocity $v_z(t,0,h(t,0))$ tends to zero as $t \to \infty$ for both suction, $-1 \leq \beta^* < 0$ and blowing, $0 < \beta^* \leq \infty$.

β^*	$v_z(t,0,h)$	$\frac{d\,v_z\,(t,0,h(t,0))}{d\,t}$
$-\infty \le \beta^* < -\frac{5}{4}$	$v_z(t,0,h(t,0)) \to -\infty$ as $t \to t_4$ $t_4 = -\frac{9}{16(1+\beta^*)}$	< 0
$\beta^* = -\frac{5}{4}$	$v_z(t,0,h(t,0)) = -\frac{4}{9}$	0
$-\frac{5}{4} < \beta^* < -1$	$v_z(t,0,h(t,0)) \to 0$ as $t \to t_4$ $t_4 = -\frac{9}{16(1+\beta^*)}$	> 0
$\beta^* = -1$	$v_z(t,0,h(t,0)) \to 0$ as $t \to \infty$ exponentially	> 0
$-1 < \beta^* \le \infty$	$v_z(t,0,h(t,0)) \to 0$ as $t \to \infty$ algebraically	> 0

Table 9.6: Behaviour of the fluid velocity on the axis of symmetry at the point of maximum height, $v_z(t,0,h(t,0))$ for $-\infty \le \beta \le \infty$.

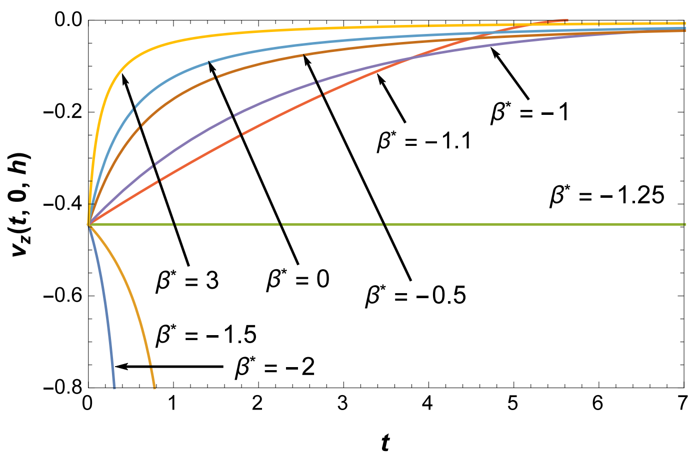

Figure 9.7: Velocity $v_z(t,0,h(t,0))$ given by (9.4.9) for $\beta^* \neq -1$ and by (9.4.11) for $\beta^* = -1$ plotted against time t for a range of values of β^*.

9.5 Streamlines

Consider now the streamlines inside the liquid drop. The streamlines are obtained by solving the cubic equation (8.5.24)

$$A(t,r)z^3 + B(t,r)z^2 + C(t,r) = K(t), \tag{9.5.1}$$

where $K(t)$ is an arbitrary function of t and from (8.5.19) to (8.5.21),

$$A(t,r) = \frac{r}{6}\frac{\partial h}{\partial r}, \qquad B(t,r) = -\frac{r}{2}\,h\,\frac{\partial h}{\partial r}, \qquad C(t,r) = -\int_0^r r\,v_n(t,r)\,dr. \tag{9.5.2}$$

We express $A(t,r), B(t,r)$ and $C(t,r)$ in terms of the invariant solution (9.3.15) to (9.3.19). We first write h and v_n in terms of $R(t)$ as

$$h(t,r) = R^{-\frac{2}{(1+4\beta^*)}}(t)\left(1-\zeta^2\right)^{\frac{1}{3}}, \tag{9.5.3}$$

$$v_n(t,r) = \frac{16}{27}\beta^* R^{-2\left(\frac{5+4\beta^*}{1+4\beta^*}\right)}(t)\frac{\zeta^2}{(1-\zeta^2)^{\frac{2}{3}}} \tag{9.5.4}$$

and therefore

$$A(t,\zeta) = -\frac{1}{9}R^{\frac{-2}{1+4\beta^*}}(t)\,\frac{\zeta^2}{(1-\zeta^2)^{\frac{2}{3}}}, \tag{9.5.5}$$

$$B(t,\zeta) = \frac{1}{3}R^{\frac{-4}{1+4\beta^*}}(t)\,\frac{\zeta^2}{(1-\zeta^2)^{\frac{1}{3}}}, \tag{9.5.6}$$

$$C(t,\zeta) = \frac{2\,\beta^*}{3}R^{\frac{-8}{1+4\beta^*}}(t)\,\left[\frac{1}{3}\left(1-\zeta^2\right)^{\frac{1}{3}}\left(3+\zeta^2\right)-1\right]. \tag{9.5.7}$$

By using (9.3.19) these results may be expressed in terms of r instead of ζ as

$$A(t,r) = -\frac{1}{9}\,R^{-4\left(\frac{1+2\beta^*}{1+4\beta^*}\right)}(t)\frac{r^2}{\left(1-\frac{r^2}{R^2(t)}\right)^{\frac{2}{3}}}, \tag{9.5.8}$$

$$B(t,r) = \frac{1}{3}\,R^{-2\left(\frac{3+4\beta^*}{1+4\beta^*}\right)}(t)\frac{r^2}{\left(1-\frac{r^2}{R^2(t)}\right)^{\frac{1}{3}}}, \tag{9.5.9}$$

$$C(t,r) = \frac{2}{3}\beta^*\,R^{\frac{-8}{1+4\beta^*}}(t)\,\left[\frac{1}{3}\left(1-\frac{r^2}{R^2(t)}\right)^{\frac{1}{3}}\left(3+\frac{r^2}{R^2(t)}\right)-1\right]. \tag{9.5.10}$$

We first consider the streamlines plotted against r and z where $0 \leq r \leq R(t)$, $0 \leq \theta \leq 2\pi$ and $0 \leq z \leq h(t,r)$. The streamlines depend on time. They will be plotted at $t = 1$. The streamlines are obtained by solving the cubic equation (9.5.1) with $A(t,r), B(t,r)$ and $C(t,r)$ given by (9.5.8), (9.5.9) and (9.5.10), for a range of values of $K(t)$.

For $\beta^* = 0$ there is no suction or fluid injection and $v_n = 0$. The streamlines are the same as in Figure 8.17.

From (9.3.18) for v_n we see that near the rim of the liquid drop the suction/blowing is strongest and the magnitude is infinite at the rim, $r = R(t)$. Near the axis of symmetry the suction/blowing is weakest and the magnitude vanishes on the axis of symmetry.

In Figure 9.8 the streamlines are plotted for $\beta^* = -0.15$, $\beta^* - 0.25$, $\beta^* = -0.5$ and $\beta^* = -0.7$. The streamlines start on the free surface and end at the base. They are perpendicular to the base because of the no slip boundary condition at the base. Near the rim the suction is strongest and the streamlines are steeper and less curved since spreading due to gravity is much weaker than suction. Near the axis of symmetry the suction is weakest and the streamlines are most curved because spreading due to gravity is much stronger than suction.

In Figure 9.9 the streamlines are plotted for positive values of β^* which describe the injection of fluid into the liquid drop. The magnitude of the blowing velocity is steadily increased by choosing $\beta^* = 0.25$, $\beta^* = 0.5$, $\beta^* = 1$. The thin fluid film approximation is valid for all positive values of β^*. A dividing streamline extends from the origin $(0,0)$ and separates the flow into two regions. In the upper region the streamlines begin on the free surface and end on the free surface. The fluid descends due to gravity and spreads due to blowing at the base. In the lower region the fluid spreads due to injection of fluid into the liquid drop at the base. The streamlines begin at the base and again they are perpendicular to the base because of the no

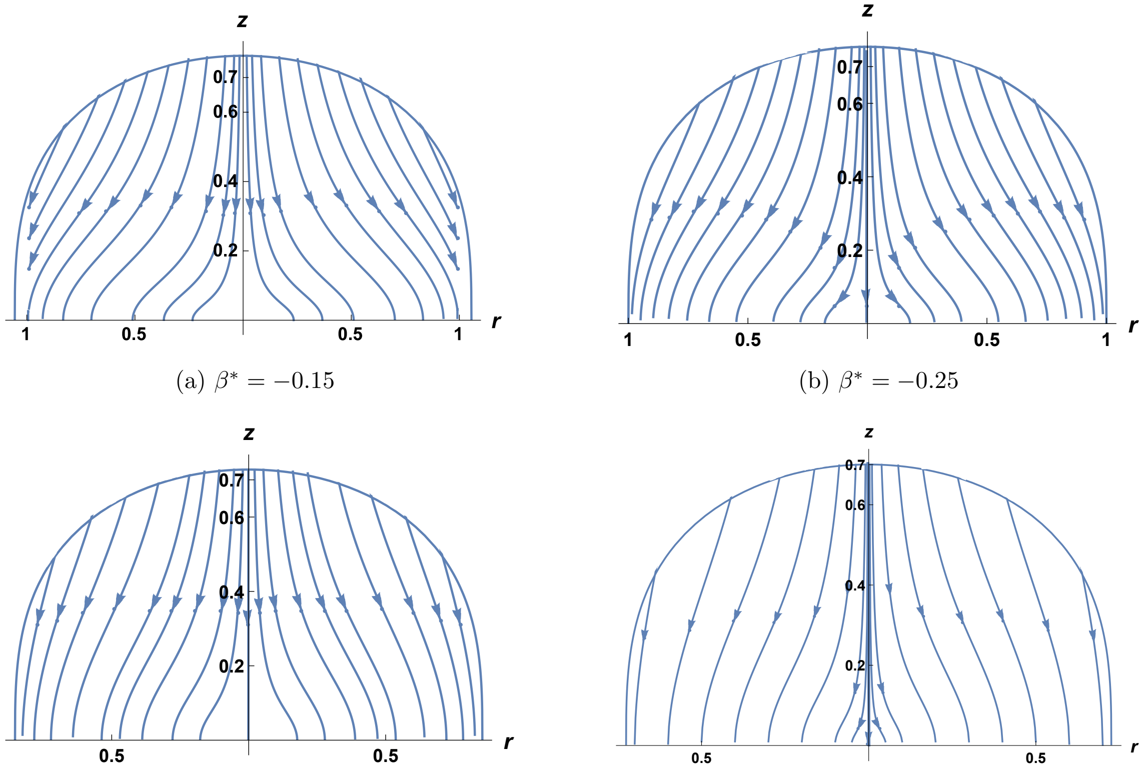

(a) $\beta^* = -0.15$

(b) $\beta^* = -0.25$

(c) $\beta^* = -0.5$

(d) $\beta^* = -0.7$

Figure 9.8: Streamlines for a range of negative β^* plotted against r at $t = 1$.

slip boundary condition. They end on the free surface. We see that as β^* increases and therefore as the magnitude of the injection velocity increases, the angle that the dividing streamline makes with the base increases. The slope of the dividing streamline illustrates clearly the increase in the strength of the fluid injection from the centre of the base to its rim. In the next section we will derive an approximate analytical solution for the dividing streamline.

In Figure 9.10 the streamlines are plotted for $\beta^* = 1$ at times $t = 1$ and $t = 10$ in order to investigate how they evolve with time. The height of the liquid drop decreases, even although there is fluid injection at the base, and the base radius increases, in agreement with the results of Tables 9.1 and 9.3. We also see that as time increases the angle that the dividing streamline makes with the base decreases.

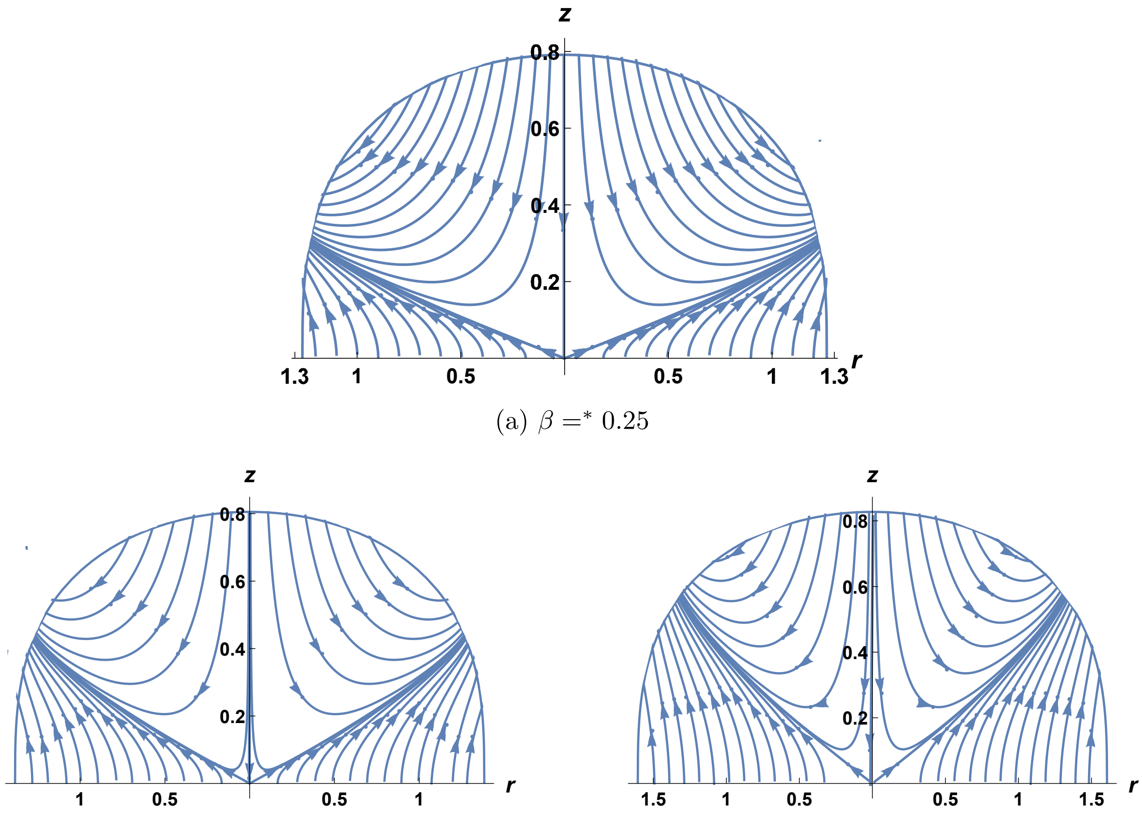

(a) $\beta =^* 0.25$

(b) $\beta^* = 0.5$

(c) $\beta^* = 1$

Figure 9.9: Streamlines for a range of positive β^* plotted against r at $t = 1$.

This will be examined further in the next section using an approximate analytical solution for the dividing streamline.

In Figures 9.8 to 9.10 the streamlines were plotted in the (r, z)-plane where $0 \leq r \leq R(t)$ and $0 \leq z \leq h(t, 0)$. The streamline pattern evolves with time. As in Chapter 8 we now consider the streamlines in the (ζ, z^*)-plane where

$$\zeta = \frac{r}{R(t)}, \qquad 0 \leq \zeta \leq 1, \tag{9.5.11}$$

$$z^* = \frac{z}{h(t,0)}, \qquad 0 \leq z^* \leq 1. \tag{9.5.12}$$

Expressed in terms of ζ and z^* the cubic equation (9.5.1) is

$$A^*(t, \zeta) z^{*3} + B^*(t, \zeta) z^{*2} + C(t, \zeta) = K(t), \tag{9.5.13}$$

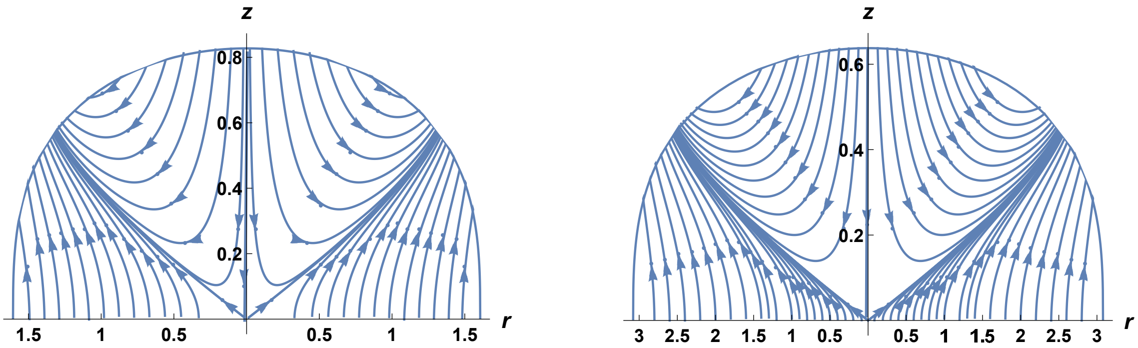

(a) $t = 1$ (b) $t = 10$

Figure 9.10: Streamlines plotted for $\beta^* = 1$ against r at $t = 1$ and $t = 10$.

where

$$A^*(t,\zeta) = A(t,\zeta)\, h^3(t,0), \tag{9.5.14}$$

$$B^*(t,\zeta) = B(t,\zeta)\, h^2(t,0) \tag{9.5.15}$$

and from (9.3.15) and (9.3.17),

$$h(t,0) = R^{-\frac{2}{1+4\beta^*}}(t). \tag{9.5.16}$$

Hence, using (9.5.5) and (9.5.6), we find

$$A^*(t,\zeta) = -\frac{1}{9}R^{-\frac{8}{1+4\beta^*}}(t)\frac{\zeta^2}{(1-\zeta^2)^{\frac{2}{3}}}, \tag{9.5.17}$$

$$B^*(t,\zeta) = \frac{1}{3}R^{-\frac{8}{1+4\beta^*}}(t)\frac{\zeta^2}{(1-\zeta^2)^{\frac{1}{3}}}. \tag{9.5.18}$$

The functions $A^*(t,\zeta)$, $B^*(t,\zeta)$ and $C(t,\zeta)$ defined by (9.5.7) depend explicitly on time through the same factor $R^{\frac{8}{1+4\beta^*}}(t)$. Equation (9.5.13) becomes the cubic equation for z^*,

$$-\frac{1}{9}\frac{\zeta^2}{(1-\zeta^2)^{\frac{2}{3}}}z^{*3} + \frac{1}{3}\frac{\zeta^2}{(1-\zeta^2)^{\frac{1}{3}}}z^{*2} - \frac{2}{3}\beta^*\left[1 - \frac{1}{3}\left(3+\zeta^2\right)\left(1-\zeta^2\right)^{\frac{1}{3}}\right] = K^*, \tag{9.5.19}$$

where

$$K^* = K(t)R^{-\frac{4}{1+4\beta^*}}(t). \tag{9.5.20}$$

Since the left hand side of (9.5.19) does not depend on time t, K^* does not depend on t. The expressions for $A^*(t,\zeta)$, $B^*(t,\zeta)$, $C(t,\zeta)$ and (9.5.19), expressed in terms of $R(t)$, remain valid for $\beta^* = -1$ with $R(t)$ given in (9.3.23). Since $K(t)$ is arbitrary, K^* is also arbitrary and the streamlines in the (ζ, z^*)-plane are plotted by giving the constant K^* a range of values. The streamline pattern in the (ζ, z^*)-plane depends only on the parameter β^* and is independent of time since (9.5.19) does not depend on time.

In Figure 9.11 the streamlines are plotted in the (ζ, z^*)-plane for $\beta^* = -0.5, 0.5, 20, 50$. Figure 9.11 clearly shows that as β^* increases the angle that the dividing streamline makes with the base at the centre increases.

In the graphs of the streamlines the centre of the base is a stagnation point of the flow because of the no slip boundary condition and $v_n(t,0) = 0$. For Model II for an axisymmetric liquid drop the thin film approximation is satisfied provided $-0.75 \leq \beta^* \leq \infty$. In all the graphs the values of β^* chosen lie in this range.

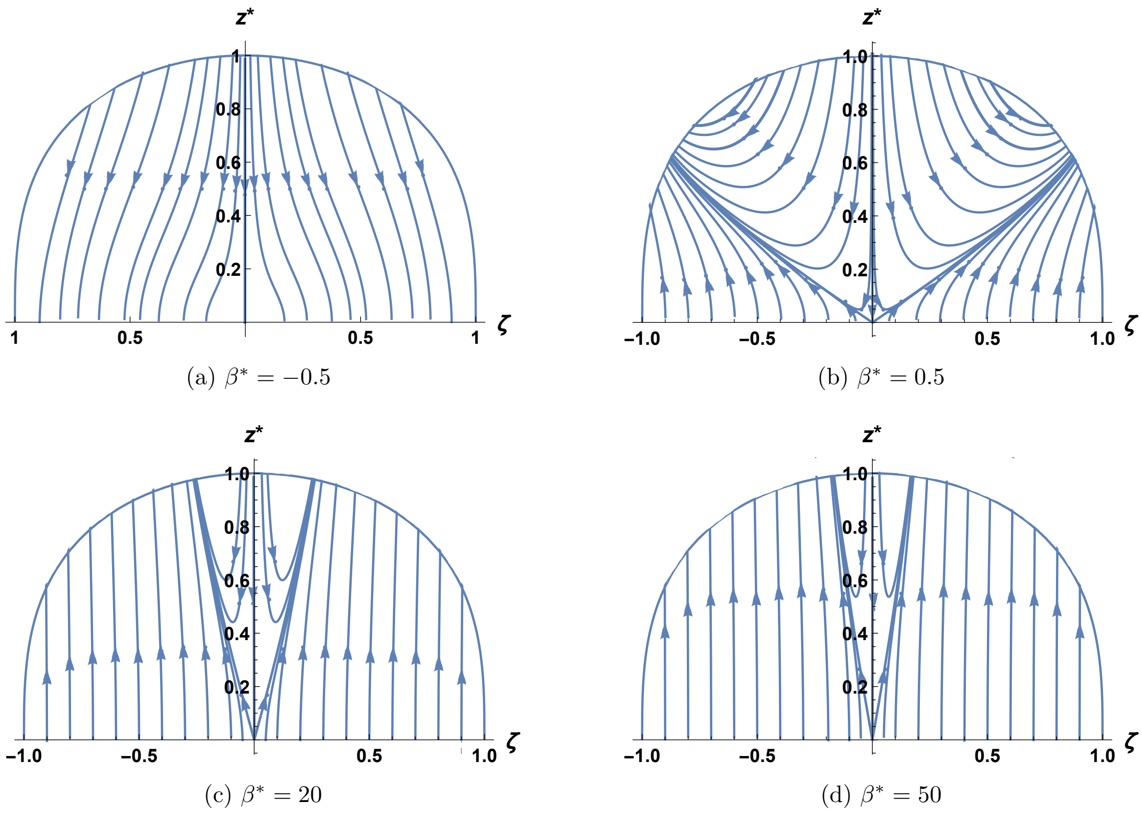

(a) $\beta^* = -0.5$ (b) $\beta^* = 0.5$

(c) $\beta^* = 20$ (d) $\beta^* = 50$

Figure 9.11: Streamlines for a range of values of β^* plotted in the (ζ, z^*)-plane where $\zeta = r/R(t)$ $(0 \leq \zeta \leq 1)$ and $z^* = z/h(t,0)$ $(0 \leq z^* \leq 1)$.

9.6 Approximate solution for the dividing streamline

We derive an approximate solution of the cubic equation (9.5.19) for the special case of the dividing streamline. The approach is the same as in Section 6.6 for the spreading of a two-dimensional thin film.

Since the dividing streamline passes through the origin, $\zeta = 0$ and $z^* = 0$, it follows that $K^* = 0$ in (9.5.19). The cubic equation for the dividing streamline therefore is

$$z^{*3} - 3\left(1-\zeta^2\right)^{\frac{1}{3}} z^{*2} + \frac{6\beta^*}{\zeta^2}\left[\left(1-\zeta^2\right)^{\frac{2}{3}} - \frac{1}{3}\left(3+\zeta^2\right)\left(1-\zeta^2\right)\right] = 0, \qquad (9.6.1)$$

In order to obtain the approximate solution of (9.6.1), we first transform it to standard form

$$s^{*3} + 3Hs^{*} + G = 0, \tag{9.6.2}$$

by letting

$$z^{*} = s^{*} + \left(1-\zeta^{2}\right)^{\frac{1}{3}}. \tag{9.6.3}$$

The cubic equation (9.6.1) becomes

$$s^{*3} - 3\left(1-\zeta^{2}\right)^{\frac{2}{3}} s^{*} - 2\left(1-\zeta^{2}\right) + \frac{6\beta^{*}}{\zeta^{2}}\left[\left(1-\zeta^{2}\right)^{\frac{2}{3}} - \frac{1}{3}\left(3+\zeta^{2}\right)\left(1-\zeta^{2}\right)\right] = 0. \tag{9.6.4}$$

Comparison of (9.6.4) with the standard form (9.6.2) gives

$$\begin{aligned} H(\zeta) &= -\left(1-\zeta^{2}\right)^{\frac{2}{3}}, && (9.6.5)\\ G(\zeta) &= -2\left(1-\zeta^{2}\right) + \frac{6\beta^{*}}{\zeta^{2}}\left[\left(1-\zeta^{2}\right)^{\frac{2}{3}} - \frac{1}{3}\left(3+\zeta^{2}\right)\left(1-\zeta^{2}\right)\right]. && (9.6.6) \end{aligned}$$

On the dividing streamline $0 \leq \zeta < 1$. We make an expansion in powers of ζ^2 which occurs naturally in the cubic equation. No assumption is made on β^* or on time t and the approximation should be valid for all $\beta^* > 0$ and all time. Since the angle between the dividing streamline and the z^*-axis decreases as β^* increases the maximum value of *zeta* on the dividing streamline decreases as β^* increases. The approximation will therefore be more accurate as β^* increases.

The expansion of $H(\zeta)$ and $G(\zeta)$ in powers of ζ^2 is

$$\begin{aligned} H(\zeta) &= -\left[1 - \frac{2}{3}\zeta^{2} - \frac{1}{9}\zeta^{4} + \bigcirc\left(\zeta^{6}\right)\right], && (9.6.7)\\ G(\zeta) &= -2\left[1 - \left(1+\frac{2}{3}\beta^{*}\right)\zeta^{2} + \frac{4}{27}\beta^{*}\zeta^{4} + \bigcirc\left(\zeta^{6}\right)\right]. && (9.6.8) \end{aligned}$$

From (9.6.2) the expansion of the cubic equation in powers of ζ^2 is therefore

$$\begin{aligned} s^{*3} &- 3\left[1 - \frac{2}{3}\zeta^{2} - \frac{1}{9}\zeta^{4} + \bigcirc\left(\zeta^{6}\right)\right] s^{*}\\ &- 2\left[1 - \left(1+\frac{2}{3}\beta^{*}\right)\zeta^{2} + \frac{4}{27}\beta^{*}\zeta^{4} + \bigcirc\left(\zeta^{6}\right)\right] = 0. && (9.6.9) \end{aligned}$$

Also from (9.6.3)

$$z^* = s^* + 1 - \frac{1}{3}\zeta^2 - \frac{1}{9}\zeta^4 + \bigcirc\left(\zeta^6\right). \tag{9.6.10}$$

As with the spreading of a two-dimensional thin film, we will derive the solution for the dividing streamline correct to order ζ^2. We find that this solution is sufficiently accurate. We have expanded $H(\zeta)$ and $G(\zeta)$ to order ζ^4 which would have allowed the solution to be calculated to order ζ^4 if required.

The discriminant, Δ, of the cubic equation (9.6.9) is

$$\Delta = G^2 + 4H^3 = -\frac{16}{3}\beta^*\zeta^2 + \bigcirc\left(\zeta^4\right). \tag{9.6.11}$$

(i) Zero order in ζ^2

To zero order in ζ^2,

$$\begin{aligned} \Delta &= 0, \qquad H = -1 \neq 0, \qquad G = -2 \neq 0, && (9.6.12)\\ z^* &= s^* + 1. && (9.6.13) \end{aligned}$$

As in Section 6.6 for the two-dimensional thin film, the cubic equation has three real roots with two roots coincident and one root different. Equation (9.6.9) becomes

$$\left(s^* + 1\right)^2\left(s^* - 2\right) = 0 \tag{9.6.14}$$

and therefore

$$\begin{aligned} s^* &= -1, \quad s^* = -1, \quad s^* = 2,\\ z^* &= 0, \qquad z^* = 0, \qquad z^* = 3. && (9.6.15) \end{aligned}$$

The solution to zero order in ζ^2 is the three points $(0,0), (0,0)$ and $(0,3)$. The solution for the dividing streamline is therefore the point $(0,0)$ on the axis of symmetry at the base.

(i) Solution correct to first order in ζ^2

Correct to first order in ζ^2, the cubic equation (9.6.9) is

$$s^{*3} - 3\left[1 - \frac{2}{3}\zeta^2 - \bigcirc\left(\zeta^4\right)\right]s^* - 2\left[1 - \left(1 + \frac{2}{3}\beta^*\right)\zeta^2 + \bigcirc\left(\zeta^4\right)\right] = 0. \qquad (9.6.16)$$

and

$$H(\zeta) = -\left[1 - \frac{2}{3}\zeta^2 + \bigcirc\left(\zeta^4\right)\right], \qquad (9.6.17)$$

$$G(\zeta) = -2\left[1 - \left(1 + \frac{2}{3}\beta^*\right)\zeta^2 + \bigcirc\left(\zeta^4\right)\right], \qquad (9.6.18)$$

$$z^* = s^* + 1 - \frac{1}{3}\zeta^2 + \bigcirc\left(\zeta^4\right). \qquad (9.6.19)$$

The discriminant, Δ, of (9.6.16) is given by (9.6.11). Since $\beta^* > 0$ it follows that $\Delta < 0$ for $\zeta \neq 0$. The cubic equation (9.6.16) therefore has three real and distinct roots for $\zeta \neq 0$ [2].

Since $\Delta < 0$ the trigonometric method of solutions described in Section 5.4.3 is again used. The three distinct roots of the cubic equation (9.6.16) are

$$s_n^* = 2\left(-H\right)^{\frac{1}{2}} \cos\left(\phi + \frac{2n\pi}{3}\right), \qquad n = 0, 1, 2, \qquad (9.6.20)$$

where ϕ satisfies

$$\cos 3\phi = -\frac{G}{2\left(-H\right)^{\frac{3}{2}}} = 1 - \frac{2}{3}\beta^*\zeta^2 + \bigcirc\left(\zeta^4\right) \qquad (9.6.21)$$

and therefore from (9.6.19),

$$z_n^* = \left[1 - \frac{1}{3}\zeta^2 + \left(\zeta^4\right)\right]\left[1 + 2\cos\left(\phi + \frac{2n\pi}{3}\right)\right], \quad n = 0, 1, 2. \qquad (9.6.22)$$

Consider first ϕ given by (9.6.21). For $\zeta = 0$, $\cos 3\phi = 1$ and therefore $\phi = 0$ since $0 \leq \phi \leq \frac{\pi}{3}$. For the solution to order ζ^2 we therefore let $\phi = \delta$ where $\delta > 0$ is small. From (9.6.21),

$$\cos 3\delta = 1 - \frac{2}{3}\beta^*\zeta^2 + \bigcirc\left(\zeta^4\right) \qquad (9.6.23)$$

and expanding using (5.4.161) gives

$$1 - \frac{9}{2} + \bigcirc\left(\zeta^4\right) = 1 - \frac{2}{3}\beta^*\zeta^2 + \bigcirc\left(\zeta^4\right). \tag{9.6.24}$$

Thus

$$\delta = \frac{2}{3\sqrt{3}}\,\beta^{*\frac{1}{2}}\zeta + \bigcirc\left(\zeta^3\right). \tag{9.6.25}$$

Consider first z_0^* given by (9.6.22) with $n = 0$ and $\phi = \delta$. We have

$$\cos\delta = 1 - \frac{1}{2}\delta^2 + \bigcirc\left(\delta^4\right) = 1 - \frac{2}{27}\beta^*\zeta^2 + \bigcirc\left(\zeta^4\right). \tag{9.6.26}$$

and hence

$$\delta = \frac{2}{3\sqrt{3}}\,\beta^{*\frac{1}{2}}\zeta + \bigcirc\left(\zeta^3\right). \tag{9.6.27}$$

Thus

$$z_0^* = \left[1 - \frac{1}{3}\zeta^2 + \bigcirc\left(\zeta^4\right)\right]\left[3 - \frac{4}{27}\beta^*\zeta^2 + \bigcirc\left(\zeta^4\right)\right] \tag{9.6.28}$$

and therefore

$$z_0^* = 3\left[1 - \frac{1}{3}\left(1 + \frac{4}{27}\beta^*\right)\zeta^2 + \bigcirc\left(\zeta^4\right)\right]. \tag{9.6.29}$$

Consider next z_1^* given by (9.6.22) with $n = 1$ and $\phi = \delta$. From (5.4.172)

$$\cos\left(\delta + \frac{2\pi}{3}\right) = -\frac{1}{2}\left(\cos\delta + \sqrt{3}\sin\delta\right). \tag{9.6.30}$$

Now

$$\sin\delta = \delta + \bigcirc\left(\delta^3\right) = \frac{2}{\sqrt{27}}\beta^{*\frac{1}{2}}\zeta + \bigcirc\left(\zeta^3\right) \tag{9.6.31}$$

and using (9.6.26) for $\cos\delta$ we obtain

$$\cos\left(\delta + \frac{2\pi}{3}\right) = -\frac{1}{2}\left[1 + \frac{2}{3}\beta^{*\frac{1}{2}}\zeta - \frac{2}{27}\beta^*\zeta^2 + \bigcirc\left(\zeta^3\right)\right]. \tag{9.6.32}$$

Thus from (9.6.22)

$$z_1^* = \left[1 - \frac{1}{3}\zeta^2 + \bigcirc\left(\zeta^4\right)\right]\left[-\frac{2}{3}\beta^{*\frac{1}{2}}\zeta + \frac{2}{27}\beta^*\zeta^2 + \bigcirc\left(\zeta^3\right)\right] \tag{9.6.33}$$

and therefore

$$z_1^* = -\frac{2}{3}\beta^{*\frac{1}{2}}\zeta\left[1 - \frac{1}{9}\beta^{*\frac{1}{2}}\zeta + \bigcirc\left(\zeta^2\right)\right]. \tag{9.6.34}$$

Lastly z_2^* is given by (9.6.22) with $n = 2$ and $\phi = \delta$. From (5.4.177)

$$\cos\left(\delta + \frac{4\pi}{3}\right) = \frac{1}{2}\left[-\cos\delta + \sqrt{3}\sin\delta\right], \tag{9.6.35}$$

and by using (9.6.26) and (9.6.31) for $\cos\delta$ and $\sin\delta$ we obtain

$$\cos\left(\delta + \frac{4\pi}{3}\right) = \frac{1}{2}\left[-1 + \frac{2}{3}\beta^{*\frac{1}{2}}\zeta + \frac{2}{27}\beta^*\zeta^2 + \bigcirc\left(\zeta^3\right)\right]. \tag{9.6.36}$$

Hence from (9.6.22)

$$z_2^* = \left[1 - \frac{1}{3}\zeta^2 + \bigcirc\left(\zeta^4\right)\right]\left[\frac{2}{3}\beta^{*\frac{1}{2}}\zeta + \frac{2}{27}\beta^*\zeta^2 + \bigcirc\left(\zeta^3\right)\right] \tag{9.6.37}$$

which gives

$$z_2^* = \frac{2}{3}\beta^{*\frac{1}{2}}\zeta\left[1 + \frac{1}{9}\beta^{*\frac{1}{2}}\zeta + \bigcirc\left(\zeta^2\right)\right]. \tag{9.6.38}$$

The solution $z^* = z_0^*(\zeta)$ is not a dividing streamline, It does not pass through the origin $\zeta = 0, z^* = 0$. It passes through the point $\zeta = 0, z^* = 3$ on the axis of symmetry and lies outside the liquid drop. The solution $z^* = z_1^*(\zeta)$ does pass through the origin but it is negative and lies outside the liquid drop for $0 < \zeta < 9\beta^{*\frac{1}{2}}$. It is therefore not a dividing streamline. The solution $z^* = z_2^*(\zeta)$ passes through the origin $\zeta = 0, z^* = 0$ and is positive. The equation of the dividing streamline in the (ζ, z^*)-plane correct to order ζ^2 therefore is

$$\zeta \geq 0: \quad z^* = \frac{2}{3}\beta^{*\frac{1}{2}}\zeta\left[1 + \frac{1}{9}\beta^{*\frac{1}{2}}\zeta + \bigcirc\left(\zeta^2\right)\right]. \tag{9.6.39}$$

The equation of the dividing streamline in the (r, z)-plane, correct to order $(r/R(t))^2$, is

$$r \geq 0: \quad z^* = \frac{2}{3}\beta^{*\frac{1}{2}}R^{-\frac{2}{1+4\beta^*}}(t)\frac{r}{R(t)}\left[1 + \frac{1}{9}\beta^{*\frac{1}{2}}\frac{r}{R(t)} + \bigcirc\left(\left(\frac{r}{R(t)}\right)^2\right)\right], \tag{9.6.40}$$

where

$$R(t) = \left(1 + \frac{16}{9}\left(1 + \beta^*\right)t\right)^{\frac{1+4\beta^*}{8(1+\beta^*)}} \tag{9.6.41}$$

and we have used

$$h(t, 0) = R^{-\frac{2}{1+4\beta^*}}(t). \tag{9.6.42}$$

Consider now the angle ϑ that the dividing streamline makes with the ζ-axis at the centre of the base $\zeta = 0, z^* = 0$ in the (ζ, z^*) plane. From (9.6.38)

$$\tan\vartheta = \left.\frac{\partial z_2}{\partial \zeta}\right|_{\zeta=0} = \frac{2}{3}\beta^{*\frac{1}{2}}. \tag{9.6.43}$$

The streamlines are plotted in the (ζ, z^*)-plane in Figure 9.11 for $\beta^* = 0.5, 20$ and 50. Equation (9.6.43) gives for the angle $\vartheta(\beta)$ that the dividing streamline makes with the base

$$\vartheta(0.5) = 25.2°, \qquad \vartheta(20) = 71.4°, \qquad \vartheta(50) = 78°, \tag{9.6.44}$$

which agrees well with Figure 9.11 .

Consider next the (r, z)-plane and on how ϑ depends on time. From (9.6.40)

$$\tan\vartheta = \left.\frac{\partial z_2}{\partial r}\right|_{r=0} = \frac{2}{3}\beta^{*\frac{1}{2}} R^{-\left(\frac{3+4\beta^*}{1+4\beta^*}\right)}(t). \tag{9.6.45}$$

which becomes on using (9.6.41) for $R(t)$,

$$\tan\vartheta = \frac{2}{3}\beta^{*\frac{1}{2}}\left[1 + \frac{16}{9}\left(1+\beta^*\right)t\right]^{-\frac{1}{8}\left(\frac{3+4\beta^*}{1+\beta^*}\right)} \tag{9.6.46}$$

Hence ϑ decreases steadily with time in the (r, z)-plane which agrees with Figure 9.11. We now derive two asymptotic results for ϑ in the (r, z)-plane.

Consider first small values of time satisfying

$$t < \frac{9}{16\left(1+\beta^*\right)}. \tag{9.6.47}$$

Then if terms of order $\left(\left(1+\beta^*\right)t\right)^2$ are neglected

$$\left[1 + \frac{16}{9}\left(1+\beta^*\right)t\right]^{-\frac{1}{8}\left(\frac{3+4\beta^*}{1+\beta^*}\right)} = \exp\left[-\frac{2}{9}\left(3+4\beta^*\right)t\right] \tag{9.6.48}$$

and therefore for small values of time

$$\tan\vartheta = \frac{2}{3}\beta^{*\frac{1}{2}}\exp\left[-\frac{2}{9}\left(3+4\beta^*\right)t\right]. \tag{9.6.49}$$

Hence the gradient of the dividing streamline at the centre of the base initially decreases approximately exponentially with time.

Consider now the asymptotic behaviour of $\tan\vartheta$ as $\beta^* \to \infty$ at a fixed time t. For large β^*

$$\left[1 + \frac{16}{9}\left(1+\beta^*\right)t\right]^{-\frac{1}{8}\left(\frac{3+4\beta^*}{1+\beta^*}\right)} \sim \left(\frac{16}{9}\beta^* t\right)^{-\frac{1}{2}} \tag{9.6.50}$$

and therefore from (9.6.46) for large β^*,

$$\tan\vartheta \sim \frac{2}{3}\beta^{*\frac{1}{2}}\left(\frac{16}{9}\beta^* t\right)^{-\frac{1}{2}} = \frac{1}{2\,t^{\frac{1}{2}}}. \tag{9.6.51}$$

For large values of β^* the gradient of the streamline at the origin decreases as $1/\sqrt{t}$, as with (6.6.58) for the spreading of a two-dimensional thin film, although the constant factor is different. The dominant term in the expansion for large β^* is independent of β^*. In Figure 9.12 the approximate solution (9.6.40) for the dividing streamline is plotted against r for a range of values of time. In Figure 9.13 the approximate solution (9.6.40) and the asymptotic solution (9.6.51) for ϑ are compared. The approximate solution for large β^* more rapidly as time t increases.

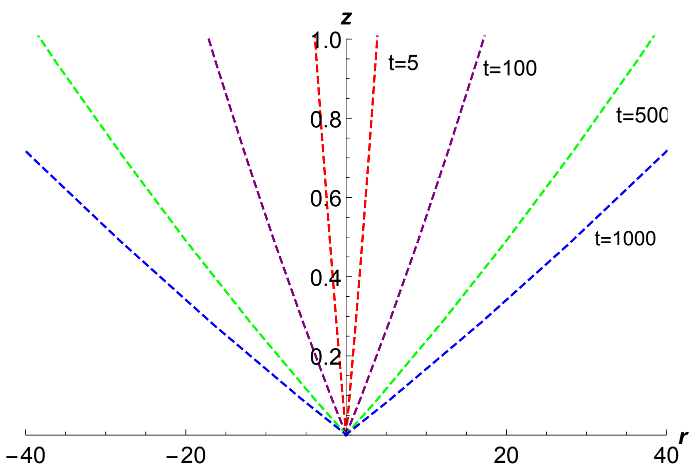

Figure 9.12: Dividing streamline, given by (9.6.10), plotted against r for $\beta^* = 50$ at time $t = 5$, $t = 100$, $t = 500$ and $t = 1000$.

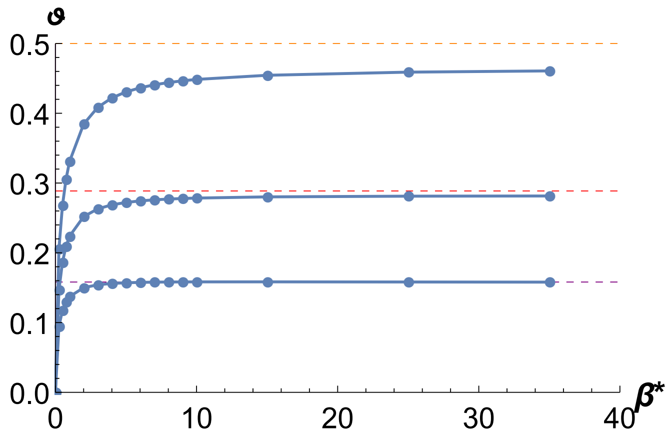

Figure 9.13: The angle ϑ in radians, given by (9.6.45), plotted against β^* for $t = 1, 3$ and $t = 10$. The asymptotic value of ϑ for large β^*, given by (9.6.51), is plotted as a dotted line $(- - -)$.

Consider now the point of intersection, P, of the dividing streamline with the surface of the liquid drop, $z = h(t, r)$.Consider the (ζ, z^*)-plane and let the point of intersection be (ζ_p, z_p^*). From (9.3.17),

$$z_p^* = \frac{h(t,r)}{h(t,0)} = \left(1 - \zeta_p^2\right)^{\frac{1}{3}}. \tag{9.6.52}$$

Using (9.6.38) the point of intersection satisfies

$$\left(1 - \zeta_p^2\right)^{\frac{1}{3}} = \frac{2}{3}\beta^{*\frac{1}{2}}\zeta_p \left[1 + \frac{1}{9}\beta^{*\frac{1}{2}}\zeta_p + \bigcirc\left(\zeta_p^2\right)\right]. \tag{9.6.53}$$

Expanding the left hand side and neglecting terms of order ζ_p^3 gives a quadratic equation for ζ_p:

$$\left(1 + \frac{2}{9}\beta^*\right)\zeta_p^2 + 2\beta^{*\frac{1}{2}}\zeta_p - 3 = 0. \tag{9.6.54}$$

If terms of order ζ_p^2 are neglected then from (9.6.54) and (9.6.52),

$$\zeta_p = \frac{3}{2\beta^{*\frac{1}{2}}}, \qquad z_p^* = 1. \tag{9.6.55}$$

Thus ζ_p decreases as β^* increases showing that neglecting powers of ζ_p becomes more accurate as the blowing becomes stronger. The point of intersection in the

(r, z)-plane is

$$r_p = \frac{2}{3\beta^{*\frac{1}{2}}} R(t), \qquad z_p = R^{-\frac{2}{1+4\beta^*}}(t) \tag{9.6.56}$$

where (9.6.42) was used for $h(t, 0)$ and $R(t)$ is given by (9.6.41).

Consider next the solution correct to order ζ_p^2. The positive root of the quadratic equation (9.6.54) is

$$\zeta_p = \frac{1}{\left(1 + \frac{2}{9}\beta^*\right)} \left[\left(3 + \frac{5}{3}\beta^*\right)^{\frac{1}{2}} - \beta^{*\frac{1}{2}} \right], \tag{9.6.57}$$

and from (9.6.52) expanded to order ζ_p^2,

$$z_p^* = 1 - \frac{1}{3}\zeta_p^2. \tag{9.6.58}$$

The point of the intersection in the (r, z)-plane is

$$r_p = \zeta_p\, R(t), \qquad z_p = \left[1 - \frac{1}{3}\left(\frac{r}{R(t)}\right)^2 \right] R^{-\frac{2}{1+4\beta^*}}(t). \tag{9.6.59}$$

In Figure 9.14 the approximate solution for the dividing streamline (9.6.40) is compared to the numerical solution of (9.6.1) for a range of values of β^* at $t = 5$. We see that the approximate solution slightly underestimates the numerical solution but the approximation improves as β^* increases. Also, as β^* increases the gradient of the dividing streamline increases due to the increase in the strength of the blowing. The fluid injection velocity, v_n is zero at $r = 0$ but increases steadily as r increases which causes the height of the dividing streamline above the base to increase from the centre as r increases.

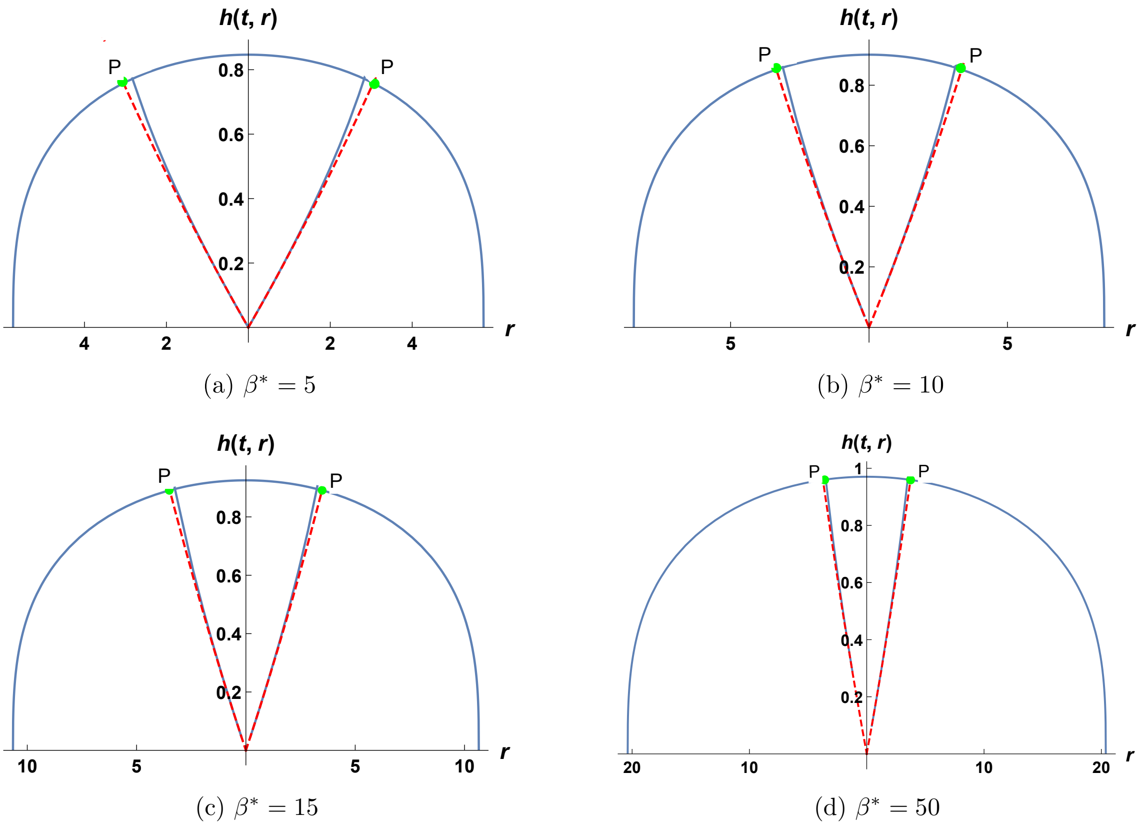

Figure 9.14: Approximate solution for the dividing streamline $(- - -)$ given by (9.6.40) plotted with the streamline (—) derived from the numerical solution of (9.6.1) for a range of β^* at a fixed time $t = 5$. The point of intersection of the dividing streamline with the surface, P, given by the approximate solution (9.6.40) is indicated by the dot $\bullet$.

9.7 Conclusions

The results derived in this Chapter for the spreading of an axisymmetric liquid drop compare directly with those obtained in Chapter 6 for a two-dimensional thin film. As in Chapter 8 the results were displayed in Tables to make the comparison easier. The height of the liquid drop at the centre always decreases to zero even when there is blowing at the base. The angle that the dividing streamline makes with the base as the strength of the blowing tends to infinity tends to a definite limit which depends only on time. The thin film approximation is satisfied for the whole range of blowing but only for weak to moderate suction.

Chapter 10

Comparison of a two-dimensional thin film with a liquid drop and of Model I and Model II

10.1 Introduction

In this chapter we compare the properties of the spreading of a two-dimensional thin film with the spreading of an axisymmetric liquid drop. We first consider the general properties before an assumption on the relation between the normal velocity at the base and the surface profile is made. We next consider a two-dimensional thin film and compare Model I with Model II and then an axisymmetric liquid drop and compare Model I with Model II. Finally we compare Models I and II for a two-dimensional thin film with Models I and II for an axisymmetric liquid drop.

10.2 Comparison of a two-dimensional thin film with an axisymmetric liquid drop: general results

We first compare the general properties of the spreading of a two-dimensional thin film and an axisymmetric liquid drop before an assumption about the leak-off velocity is made. The results therefore apply for both Model I and Model II.

The governing equations and the general form of the group invariant solution for a two-dimensional thin film and an axisymmteric liquid drop are summarised in Table 10.1.

Table 10.1: Comparison between the equations for the two-dimensional thin film and the axisymmetric liquid drop in dimensionless form.

Two-dimensional thin film	**Axisymmetric liquid drop**
Mathematical Formulation	
$\frac{\partial h}{\partial t} = \frac{1}{3}\frac{\partial}{\partial x}\left(h^3\,\frac{\partial h}{\partial x}\right) + v_n(t,x)$	$\frac{\partial h}{\partial t} = \frac{1}{3r}\frac{\partial}{\partial r}\left(r\,h^3\,\frac{\partial h}{\partial r}\right) + v_n(t,r)$
$h(t, \pm W(t)) = 0$	$h(t, R(t)) = 0$
$W(0) = 1$	$R(0) = 1$
$\frac{dV}{dt} = 2\int_0^{W(t)} v_n(t,x)\,dx$	$\frac{dV}{dt} = 2\pi\int_0^{R(t)} r\,v_n(t,r)\,dr$
$V(t) = 2\int_0^{W(t)} h(t,x)\,dx$	$V(t) = 2\pi\int_0^{R(t)} r\,h(t,r)\,dr$
$h(0,0) = 1$	$h(0,0) = 1$

Continued on next page

Table 10.1 – continued from previous page

Two-dimensional thin film	**Axisymmetric liquid drop**
Lie Point Symmetries	
$X_1 = \frac{\partial}{\partial t}, \quad X_2 = t\frac{\partial}{\partial t} - \frac{1}{3}h\frac{\partial}{\partial h}$ $X_3 = x\frac{\partial}{\partial x} + \frac{2}{3}h\frac{\partial}{\partial h}, \quad X_4 = \frac{\partial}{\partial x}$ $(c_1 + c_2\,t)\frac{\partial v_n}{\partial t} + (c_4 + c_3\,x)\,\frac{\partial v_n}{\partial x}$ $= \frac{2}{3}(c_3 - 2c_2)v_n$ $X = \left(1 + \frac{t}{\alpha f^3(0)}\right)\frac{\partial}{\partial t} + \frac{x}{f^3(0)}\frac{\partial}{\partial x}$ $+\frac{1}{3\,f^3(0)}\left(2 - \frac{1}{\alpha}\right)\,h\frac{\partial}{\partial h}$	$X_1 = \frac{\partial}{\partial t}, \quad X_2 = t\frac{\partial}{\partial t} - \frac{1}{3}h\frac{\partial}{\partial h}$ $X_3 = r\frac{\partial}{\partial r} + \frac{2}{3}h\frac{\partial}{\partial h}$ $(c_1 + c_2\,t)\frac{\partial v_n}{\partial t} + (c_3\,r)\,\frac{\partial v_n}{\partial r}$ $= \frac{2}{3}(c_3 - 2c_2)v_n$ $X = \left(1 + \frac{t}{\alpha f^3(0)}\right)\frac{\partial}{\partial t} + \frac{r}{f^3(0)}\frac{\partial}{\partial r}$ $+\frac{1}{3\,f^3(0)}\left(2 - \frac{1}{\alpha}\right)\,h\frac{\partial}{\partial h}$
Group Invariant Solution	
$\frac{d}{d\zeta}\left(f^3\,\frac{df}{d\zeta}\right) + 3\,\frac{d}{d\zeta}\,(\zeta\,f) + \left(\frac{1}{\alpha} - 5\right)f(\zeta)$ $+3\,g(\zeta) = 0$ $W(t) = \left(1 + \frac{t}{\alpha\,f^3(0)}\right)^{\alpha}$ $V(t) = V_0\left(1 + \frac{t}{\alpha\,f^3(0)}\right)^{\frac{5}{3}\,\alpha - \frac{1}{3}}$ $V_0 = \frac{2}{f(0)}\,\int_0^1 f(\zeta)\,d\zeta$ $h(t,x) = \frac{1}{f(0)}\left(1 + \frac{t}{\alpha\,f^3(0)}\right)^{\frac{2}{3}\left(\alpha - \frac{1}{2}\right)} f(\zeta)$ $v_n(t,x) = \frac{1}{f^4(0)}\left(1 + \frac{t}{\alpha\,f^3(0)}\right)^{\frac{2}{3}(\alpha-2)} g(\zeta)$ $\int_0^1 g(\zeta)\,d\zeta = \frac{1}{3}\left(5 - \frac{1}{\alpha}\right)\int_0^1 f(\zeta)\,d\zeta$ $\zeta = \frac{x}{W(t)}, \quad -1 \le \zeta \le 1$	$\frac{d}{d\zeta}\left(\zeta\,f^3(\zeta)\frac{df}{d\zeta}\right) + 3\,\frac{d}{d\zeta}\,(\zeta^2\,f(\zeta))$ $+\left(\frac{1}{\alpha} - 8\right)\zeta\,f(\zeta) + 3\zeta\,g(\zeta) = 0$ $R(t) = \left(1 + \frac{t}{\alpha f^3(0)}\right)^{\alpha}$ $V(t) = V_0\left(1 + \frac{t}{\alpha f^3(0)}\right)^{\frac{8}{3}\alpha - \frac{1}{3}}$ $V_0 = \frac{2}{f(0)}\int_0^1 \zeta f(\zeta)\,d\,\zeta,$ $h(t,r) = \frac{1}{f(0)}\left(1 + \frac{t}{\alpha f^3(0)}\right)^{\frac{2}{3}\left(\alpha - \frac{1}{2}\right)} f(\zeta)$ $v_n(t,r) = \frac{1}{f^4(0)}\left(1 + \frac{t}{\alpha f^3(0)}\right)^{\frac{2}{3}(\alpha-2)} g(\zeta)$ $\int_0^1 \zeta\,g(\zeta)\,d\,\zeta = \frac{1}{3}\left(8 - \frac{1}{\alpha}\right)\int_0^1 \zeta\,f(\zeta)\,d\,\zeta$ $\zeta = \frac{r}{R(t)}, \quad 0 \le \zeta \le 1$

10.2.1 Mathematical formulation

A nonlinear diffusion equation with a sink/source term describes both problems. The normal velocity at the base, v_n describes suction/blowing at the base. When $v_n > 0$ it describes blowing and when $v_n < 0$ it describes suction for both Model I and Model II for the axisymmetric liquid drop and the two-dimensional thin film. For the two-dimensional thin film the nonlinear diffusion equation does not depend explicitly on the spatial coordinate x while for the axisymmetric liquid drop the nonlinear diffusion equation depends on the spatial coordinate r.

In the two-dimensional thin film the boundary condition $h = 0$ is applied at the ends $x = \pm W(t)$, while for the axisymmetric liquid drop it is applied at the rim, $r = R(t)$. In the two-dimensional thin film the characteristic volume per unit length was chosen to be defined in terms of its characteristic length $W_0 H$ and for the axisymmetric liquid drop the characteristic volume was $\pi\, R_0^2\, H$.

10.2.2 Lie point symmetries

The symmetry generators X_1, X_2 and X_3 have the same form for both problems. The main difference is that for the two-dimensional thin film there is an extra generator $X_4 = \frac{\partial}{\partial x}$ because the nonlinear diffusion equation for the two dimensional flow does not contain x explicitly. However we find that X_4 is not required to generate a group invariant solution because it determines only the choice of origin for x.

10.2.3 Group invariant solution

A linear combination of the Lie point symmetries X_1, X_2 and X_3 generated the group invariant solution for both problems. For the two-dimensional thin film the similarity variable ζ where

$$\zeta = \frac{x}{W(t)}, \qquad -1 \leq \zeta \leq 1, \tag{10.2.1}$$

while for the axisymmetric liquid drop

$$\zeta = \frac{r}{R(t)}, \qquad 0 \leq \zeta \leq 1. \tag{10.2.2}$$

A difference in the two problems is the range of definition of ζ.

By considering the volume and its rate of change with time we were able to derive a balance law for the fluid volume. A difference between the two problems is that the axisymmetric problem has the factor $\left(\frac{1}{\alpha} - 8\right)$ appearing in the ordinary equation and the balance law while the two-dimensional problem has the factor $\left(\frac{1}{\alpha} - 5\right)$ appearing in these equations. The form of the equations is however the same for both problems except that for the axisymmetric problem the similarity variable ζ occurs in the ordinary differential equation, balance law and volume V_0 while it is absent in the two-dimensional problem. In one term of the axisymmetric differential equation ζ^2 occurs while only ζ occurs in the two-dimensional differential equation. The difference can be traced to the element of area. For the two-dimensional problem it is $dx\,dy$ while for the axisymmetric problem it is $r\,drd\theta$. For both the axisymmetric liquid drop and the two-dimensional thin film an assumption had to be made on $g(\zeta)$, in the normal velocity at the base, to close the system of equations and solve for $f(\zeta)$. Because two different assumptions were made on $g(\zeta)$ for both problems, we will compare Model I and Model II for the two-dimensional thin film and for the axisymmetric liquid drop. We will then compare the results for the two-dimensional thin film with those for the liquid drop.

10.3 Comparison of Model I and Model II

In this section we first compare Model I with Model II for a two-dimensional thin film and then for an axisymmetric liquid drop.

10.3.1 Two-dimensional thin film

The results for Model I and Model II for the two-dimensional thin film are presented in Table 10.2. In Model I the assumption that is made is that the velocity $v_n(t, x)$ is proportional to the height $h(t, x)$ and in Model II that the velocity $v_n(t, x)$ is proportional to the spatial gradient of the height. Thus in Model I the velocity is greatest in the central region where $h(t, x)$ is greatest and vanishes at the moving contact lines $x = \pm W(t)$ whereas in Model II the velocity $v_n(t, x) = 0$ at $x = 0$ because both $x = 0$ and $\frac{\partial h}{\partial x} = 0$ and it is small in the neighbourhood of $x = 0$ because $\frac{\partial h}{\partial x}$ is small in that region. The magnitude of the normal velocity at the base $|v_n(t, x)|$ increases rapidly as $x \to \pm W(t)$ and $|v_n(t, x)| \to \infty$ as $x \to \pm W(t)$.

Using the balance law for fluid volume for Model I and Model II, the unknown constant α in the group invariant solution was determined in terms of the proportionality constant β. The value for α was the same in both models. In both models the choice of $g(\zeta)$ was made so that the coefficient of $f(\zeta)$ in the ordinary differential equation would vanish, making the ordinary differential equation integrable. In Model II the ordinary differential equation and its solution depended on β because β appeared in the coefficient of $\frac{d}{d\zeta}(\zeta f)$ while in Model I the ordinary differential equation and its solution were independent of β. In Model I, $\beta > 0$ signified injection of fluid into the thin film and $\beta < 0$ signified suction of fluid out of the thin film. We wanted the same interpretation for β in Model II which meant that β was

Model I	**Model II**
Solution to the ODE	
$g(\zeta) = \beta\, f(\zeta)$	$g(\zeta) = -\beta\, \zeta\, \frac{df(\zeta)}{d\zeta}$
$\alpha = \frac{1}{5-3\,\beta}, \qquad \beta \neq \frac{5}{3}$	$\alpha = \frac{1}{5-3\,\beta}, \qquad \beta \neq \frac{5}{3}$
$\frac{d}{d\zeta}\left(f^3\, \frac{df}{d\zeta}\right) + 3\, \frac{d}{d\zeta}\,(\zeta\, f) = 0$	$\frac{d}{d\zeta}\left(f^3\, \frac{df}{d\zeta}\right) + 3(1-\beta)\, \frac{d}{d\zeta}\,(\zeta\, f) = 0$
$f(\zeta) = \left(\frac{9}{2}\right)^{\frac{1}{3}} (1-\zeta^2)^{\frac{1}{3}}$	$f(\zeta) = \left(\frac{9}{2}(1-\beta)\right)^{\frac{1}{3}} (1-\zeta^2)^{\frac{1}{3}}$
Specific Solution	
$t_1 = \frac{3}{2\left(\beta - \frac{5}{3}\right)}$	$t_2 = -\frac{9}{10(1+\beta^*)}$
$W(t) = \left(1 + \frac{2\,(5-3\,\beta)\,t}{9}\right)^{\frac{1}{5-3\,\beta}}$	$W(t) = \left(1 + \frac{10}{9}(1+\beta^*)t\right)^{\frac{2+5\beta^*}{10(1+\beta^*)}}$
$V(t) = V_0 \left(1 + \frac{2\,(5-3\,\beta)\,t}{9}\right)^{\frac{\beta}{5-3\,\beta}}$	$V(t) = V_0 \left(1 + \frac{10}{9}(1+\beta^*)t\right)^{\frac{\beta^*}{2(1+\beta^*)}}$
$V_0 = 2\int_0^1 (1-\zeta^2)^{\frac{1}{3}}\ d\zeta = 1.68262$	$V_0 = 2\int_0^1 \zeta\ (1-\zeta^2)^{\frac{1}{3}}\ d\zeta = \frac{3}{4}$
$h(t,x) = \left(1 + \frac{2\,(5-3\,\beta)\,t}{9}\right)^{\frac{\beta-1}{5-3\,\beta}} (1-\zeta^2)^{\frac{1}{3}}$	$h(t,x) = \left(1 + \frac{10}{9}(1+\beta^*)t\right)^{-\frac{1}{5(1+\beta^*)}} (1-\zeta^2)^{\frac{1}{3}}$
$v_n(t,x) = \frac{2\,\beta}{9}\left(1 + \frac{2\,(5-3\,\beta)\,t}{9}\right)^{\frac{2(2\,\beta-3)}{5-3\,\beta}} (1-\zeta^2)^{\frac{1}{3}}$	$v_n(t,x) = \frac{10}{27}\beta^* \left(1 + \frac{10}{9}(1+\beta^*)t\right)^{-\frac{(6+5\beta^*)}{5(1+\beta^*)}} \frac{\zeta^2}{(1-\zeta^2)^{\frac{2}{3}}}$
Validity of the thin film approximation	
$-\infty < \beta \leq 2$	$-\frac{4}{5} \leq \beta^* < \infty$

Table 10.2: Comparison of Model I and Model II for the two-dimensional thin film

rescaled by defining

$$\beta^* = \frac{2}{5}\frac{\beta}{(1-\beta)}. \tag{10.3.1}$$

In Model I the exponential solution for all the quantities occurred when $\beta = \frac{5}{3}$ which is in the blowing range while in Model II the exponential solution occurred when $\beta^* = -1$ which is in the suction range.

We first compare the half-width of the base $W(t)$. In Model I the base always expands to infinity even for $\beta < 0$ which describes suction whereas in Model II, the base does not always spread to infinity. In Model II, $W(t) \to \infty$ only for $\beta^* > -0.4$. For $\beta^* = -0.4$, $W(t)$ remains constant and for $\beta^* < -0.4$ the half-width of the base tends to zero. In Model I, $W(t) \to \infty$ in a finite time for $\beta > \frac{5}{3}$ whereas in Model II, $W(t) \to 0$ in a finite time for $\beta^* < -1$.

When considering the volume $V(t)$, in both models the volume remains constant for both $\beta = 0$ and $\beta^* = 0$ as there is no suction or injection of fluid. For both models in the suction range the volume decreases to zero. In Model I it takes an infinite time for the thin film to disappear as the base always spreads whereas in Model II for $\beta^* < -1$ the volume tends to zero in a finite time because the base tends to zero in a finite time. For both models in the blowing range the volume always increases to infinity. In Model I for $\beta > \frac{5}{3}$ the volume tends to infinity in a finite time while in Model II it always takes an infinite time.

The height of the thin film in Model I decreases to zero for $\beta^* < 1$, so there is a small range of blowing, $0 < \beta^* < 1$, for which the height decreases and this decrease to zero is in an infinite time. In Model II the height decreases to zero for all values of β^*, $-\infty < \beta^* < \infty$. The decrease in the height due to spreading by gravity is stronger than the increase in the height due to blowing. In Model I the height tends to infinity in a finite time for $\beta > \frac{5}{3}$ whereas in Model II the height tends to zero in a finite time for $\beta^* < -1$. In Model I the height remains constant for $\beta = 1$ whereas in Model II there is no value of β^* for which the height remains constant. There is a small range, $\frac{5}{3} < \beta < 2$, in Model I for which the thin fluid approximation is satisfied even although the height $h(t, 0)$ tends to infinity. In this range $h(t, 0)$ tends to infinity in a finite time but the half-width of the base tends to infinity faster than the height such that the thin fluid film approximation remains valid.

Lastly consider the normal velocity at the base, $v_n(t, x)$, and the thin fluid film approximation ratio, $h(t, 0)/W(t)$. When $\beta = 0$ and $\beta^* = 0$, $v_n(t, x) = 0$ for both models and thus there is no suction or injection of fluid. In Model I the blowing at the center is stronger than at the edges. This causes the height $h(t, 0)$ to increase faster than the base spreads. The thin film approximation is therefore valid only for weak to moderate blowing. The suction is stronger at the center than at the edges. This causes the height $h(t, 0)$ to decrease rapidly which ensures that the thin film approximation remains valid for all values of suction. In comparison for Model II the blowing at the edges is much stronger than at the center. This causes the base to expand faster than the height increases and the thin film approximation is valid for all of blowing. The suction at the edges is stronger than at the center. This causes the base to decrease more rapidly than the height $h(t, 0)$. The thin film approximation is therefore valid only for weak to moderate suction. Consequently Model I is a better for studying suction and Model II is a better for studying injection.

A distinguishing difference between the two models is that all the quantities in Model I tend to infinity in a finite time for $\beta > \frac{5}{3}$ and all the quantities in Model II tend to zero in a finite time for $\beta^* < -1$. From the range for which the thin film approximation is valid we see that Model I is valid for all of suction and a small range of blowing which includes part of the range in which quantities tend to infinity in a finite time and Model II is valid for all of blowing and a small range of suction which does not include the range in which quantities tend to zero in a finite time. In Model I the base increases for all time even when there is suction of fluid and in Model II the height decrease for all time even when there is blowing.

Streamlines

In both Model I and Model II, for the blowing range, $0 < \beta < \infty$ there is a dividing streamline that divides the flow into two regions. The upper region consists of fluid descending due to gravity and the spreading of the base and the lower region consists of fluid rising due to injection of fluid at the base. In Model I the dividing streamline extends approximately horizontally from the point on the centre line at which the fluid velocity is zero, given approximately by

$$z_2 = \left[\left(\frac{2}{3} \right)^{\frac{1}{2}} \beta^{\frac{1}{2}} + \frac{1}{9} \beta + \bigcirc \left(\beta^{\frac{3}{2}} \right) \right] h(t, 0), \tag{10.3.2}$$

obtained by solving the cubic equation (5.4.39),

$$z^3 - 3h(t, 0) z^2 + 2\beta \, h^3(t, 0) = 0, \tag{10.3.3}$$

In Model II the dividing streamline also starts on the centre line but at the origin on the base. In Model I the dividing streamline is approximately horizontal because the fluid injection velocity at the base is proportional to the height and therefore decreases only slowly as the distance from the centre line increases. In Model II the dividing streamlines make an angle with the base because the fluid injection velocity is proportional to the spatial gradient of the surface of the thin film and increases strongly in magnitude from zero to a non-zero value as distance from the centre line increases. In Model II we were able to derive an approximate analytical solution for the dividing streamlines by expanding in powers of $x/W(t)$ because $0 \leq x/W(t) < 1$ and $-1 < x/W(t) \leq 0$ due to the angle it makes with the base. Increasing the injection velocity of fluid at the base meant that in Model I the dividing streamline extended further into the thin film for $0 < \beta < 1$ until the lower region filled the whole film for $\beta \geq 1$. For Model II the gradient of the dividing streamline increased as β^* increased.

In Model II the dividing streamline for the two-dimensional flow is given by

$$z_1 = -\frac{\sqrt{30}}{9}\beta^{*\frac{1}{2}}W^{-\frac{2}{2+5\beta^*}}(t)\frac{x}{W(t)}\left[1 - \frac{\sqrt{30}}{54}\beta^{*\frac{1}{2}}\frac{x}{W(t)} + \bigcirc\left(\left(\frac{x}{W(t)}\right)^2\right)\right], \quad (10.3.4)$$

for $x < 0$ and for $x > 0$

$$z_2 = \frac{\sqrt{30}}{9}\beta^{*\frac{1}{2}}W^{-\frac{2}{2+5\beta^*}}(t)\frac{x}{W(t)}\left[1 + \frac{\sqrt{30}}{54}\beta^{*\frac{1}{2}}\frac{x}{W(t)} + \bigcirc\left(\left(\frac{x}{W(t)}\right)^2\right)\right], \quad (10.3.5)$$

where

$$W(t) = \left[1 + \frac{10}{9}\left(1+\beta^*\right)t\right]^{\frac{2+5\beta^*}{10(1+\beta^*)}}. \quad (10.3.6)$$

The angle ϑ that the dividing streamline for $x > 0$ makes with the x-axis at the origin is given by

$$\tan\vartheta = \frac{\sqrt{30}}{9}\beta^{*\frac{1}{2}}W^{-\left(\frac{4+5\beta^*}{2+5\beta^*}\right)}(t) \quad (10.3.7)$$

and for the limit $\beta^* \to \infty$ at fixed time t, we obtain

$$\tan\vartheta \sim \frac{1}{\sqrt{3}t^{\frac{1}{2}}}. \quad (10.3.8)$$

10.3.2 Axisymmetric liquid drop

The results for Model I and Model II for the axisymmetric liquid drop are presented in Table 10.3. As for the two-dimensional thin film, in Model I the assumption that was made is that the velocity $v_n(t, r)$ is proportional to the height $h(t, r)$ and in Model II that the velocity $v_n(t, r)$ is proportional to the spatial gradient of the height. The results for Model I for the axisymmetric liquid drop are qualitatively the same as those for the two-dimensional thin film. Thus in Model I the velocity $v_n(t, r)$ is greatest in the central region where $h(t, r)$ is greatest and vanishes at the moving contact line $r = R(t)$ whereas in Model II $v_n(t, 0) = 0$ and $v_n(t, r)$ is small in the neighbourhood of $r = 0$ because $\frac{\partial h}{\partial r}$ was small in that region. The magnitude of the normal velocity at the base $|v_n(t, r)|$ increases rapidly as r increases and $|v_n(t, r)| \to \infty$ as $r \to R(t)$.

The unknown constant α in the group invariant solution was determined in terms of the proportionality constant β by using the balance law for fluid volume. The value for α was different in the two Models. However in Model II the ordinary differential equation and its solution were the same as for the two-dimensional thin film. As for the two-dimensional thin film, in Model I, $\beta > 0$ signified injection of fluid into the thin film at the base and $\beta < 0$ signified suction of fluid out of the thin film at the base. In order to give the same interpretation for β in Model II, β was rescaled by defining

$$\beta^* = \frac{\beta}{4(1-\beta)}. \tag{10.3.9}$$

In Model I the exponential solution for all the quantities occurred when $\beta = \frac{8}{3}$ which is in the blowing range while in Model II the exponential solution occurred when $\beta^* = -1$ which is in the suction range.

We first compare the base radius $R(t)$. In Model I the base radius always expands to infinity even for values of $\beta < 0$ which describes suction whereas in Model II, $R(t) \to \infty$ only for $\beta^* > -0.25$. In Model II, R(t) remains constant for $\beta^* = -0.25$ and $R(t) \to 0$ as $t \to \infty$ for $\beta^* < -0.25$. In Model I, $R(t) \to \infty$ in a finite time for $\beta > \frac{8}{3}$ whereas in Model II, $R(t) \to 0$ in a finite time for $\beta^* < -1$. As for the two-dimensional thin film the volume $V(t)$ in both models remains constant for $\beta = 0$ and $\beta^* = 0$ because there is no suction or injection of fluid at the base. The evolution of the volume $V(t)$ in both models is the same as that for the two-dimensional thin film and has been described above.

The height of the thin film $h(t, 0)$ in Model I decreases to zero for $\beta^* < 2$ and therefore there is a small range of blowing, $0 < \beta^* < 2$, for which the height decreases and this decrease to zero is in an infinite time. In Model II the height decreases to zero for all values of β^*, $-\infty \leq \beta^* \leq \infty$. In Model I the height tends to infinity in a finite time for $\frac{8}{3} < \beta \leq \infty$ whereas in Model II the height tends to zero in a finite time for $-\infty \leq \beta^* < -1$. In Model I the height remains constant for

Model I	**Model II**
Solution to the ODE	
$g(\zeta) = \beta\, f(\zeta)$	$g(\zeta) = -\beta\, \zeta\, \frac{df(\zeta)}{d\zeta}$
$\alpha = \frac{1}{8-3\,\beta}, \qquad \beta \neq \frac{8}{3}$	$\alpha = \frac{1}{8-6\,\beta}, \qquad \beta \neq \frac{4}{3}$
$\frac{d}{d\zeta}\left(f^3(\zeta)\,\frac{df}{d\zeta}\right) + 3\,\frac{d}{d\zeta}\,(\zeta^2\, f) = 0$	$\frac{d}{d\zeta}\left(\zeta\, f^3\, \frac{df}{d\zeta}\right) + 3(1-\beta)\,\frac{d}{d\zeta}\,(\zeta\, f) = 0$
$f(\zeta) = \left(\frac{9}{2}\right)^{\frac{1}{3}} (1-\zeta^2)^{\frac{1}{3}}$	$f(\zeta) = \left(\frac{9}{2}(1-\beta)\right)^{\frac{1}{3}} (1-\zeta^2)^{\frac{1}{3}}$
Specific Solution	
$t_3 = \frac{3}{2\left(\beta-\frac{8}{3}\right)}$	$t_4 = -\frac{9}{16(1+\beta^*)}$
$R(t) = \left(1 + \frac{2\,(8-3\,\beta)\,t}{9}\right)^{\frac{1}{8-3\,\beta}}$	$R(t) = \left(1 + \frac{16}{9}(1+\beta^*)t\right)^{\frac{1+4\beta^*}{8(1+\beta^*)}}$
$V(t) = V_0\left(1 + \frac{2\,(8-3\,\beta)\,t}{9}\right)^{\frac{\beta}{8-3\,\beta}}$	$V(t) = \frac{3}{4}\left(1 + \frac{16}{9}(1+\beta^*)t\right)^{\frac{\beta^*}{1+\beta^*}}$
$V_0 = 2\int_0^1 \zeta\,(1-\zeta^2)^{\frac{1}{3}}\; d\zeta = \frac{3}{4}$	$V_0 = 2\int_0^1 \zeta\,(1-\zeta^2)^{\frac{1}{3}}\; d\zeta = \frac{3}{4}$
$h(t,r) = \left(1 + \frac{2\,(8-3\,\beta)\,t}{9}\right)^{\frac{\beta-2}{8-3\,\beta}} (1-\zeta^2)^{\frac{1}{3}}$	$h(t,r) = \left(1 + \frac{16}{9}(1+\beta^*)t\right)^{-\frac{1}{4(1+\beta^*)}} (1-\zeta^2)^{\frac{1}{3}}$
$v_n(t,r) = \frac{2\,\beta}{9}\left(1 + \frac{2\,(8-3\,\beta)\,t}{9}\right)^{2\left(\frac{2\,\beta-5}{8-3\,\beta}\right)} (1-\zeta^2)^{\frac{1}{3}}$	$v_n(t,r) = \frac{16}{27}\beta^*\left(1 + \frac{16}{9}(1+\beta^*)t\right)^{-\frac{(5+4\beta^*)}{4(1+\beta^*)}} \frac{\zeta^2}{(1-\zeta^2)^{\frac{2}{3}}}$
Validity of the thin film approximation	
$-\infty < \beta \leq 3$	$-\frac{3}{4} \leq \beta^* < \infty$

Table 10.3: Comparison of Model I and Model II for the axisymmetric liquid drop.

$\beta = 2$. There is a small range $2 < \beta^* < 3$ for which the thin fluid approximation is valid although the height $h(t, 0)$ tends to infinity. Both the height and the base radius tends to infinity for this range of β^* but the thin fluid film approximation remains valid because the base radius tends to infinity faster than the height. For the subrange $\frac{8}{3} < \beta^* < 3$ both the height and base radius tend to infinity in a finite time.

Consider next the normal velocity at the base, $v_n(t, r)$, and the thin fluid film approximation ratio, $h(t, 0)/R(t)$ for both models. The velocity is zero when $\beta = 0$ and $\beta^* = 0$ and thus there is no suction or injection of fluid. In Model I the blowing at the center is stronger than at the rim. This causes the height $h(t, 0)$ to increase faster than the base spreads. The thin film approximation is therefor valid only for weak to moderate blowing. The suction is stronger at the center than at the rim. This causes the height $h(t, 0)$ to decrease rapidly which ensures that the thin film approximation remains valid for all values of suction. In comparison, for Model II the blowing at the rim is much stronger than at the center. This causes the base to expand faster than the height increases and the thin film approximation is valid for all of blowing. The suction at the rim is stronger than at the center. This causes the base radius to decrease more rapidly than the height $h(t, 0)$ decreases. The thin film approximation is therefore valid only for weak to moderate suction. Consequently Model I is a better for investigating suction and Model II is a better for investigating injection.

A distinguishing difference between the two models is that all the quantities in Model I tend to infinity in a finite time for $\frac{8}{3} < \beta \leq \infty$ and all the quantities in Model II tend to zero in a finite time for $-\infty \leq \beta^* < -1$. From the range for which the thin film approximation is valid we see that Model I is valid for all of suction and a small range of blowing which includes the exponential solution and part of the range in which quantities tend to infinity in a finite time and Model II is valid for all of blowing and a small range of suction which does not include the exponential solution or a part of the range in which quantities tend to zero in a finite time. In Model I the base increases for all time even when there is suction of fluid and in Model II the height decrease for all time even when there is blowing.

Streamlines

In both Model I and Model II, for blowing, there is a dividing streamline that divides the flow into two regions. The upper region shows the descent of fluid caused by gravity and the spreading of the base and the lower region shows the rising of fluid due to the injection of fluid into the liquid drop at the base. In Model I the dividing streamline extends approximately horizontally from the point on the axis of symmetry at which the velocity is zero which is given by

$$z_2 = \left[\frac{\beta^{\frac{1}{2}}}{\sqrt{3}} + \frac{\beta}{18} + \bigcirc\left(\beta^{\frac{3}{2}}\right)\right] h(t,0), \tag{10.3.10}$$

derived by solving the cubic equation

$$z^3 - 3h(t,0)z^2 + \beta\, h^3(t,0) = 0. \tag{10.3.11}$$

In Model II the dividing streamline starts on the axis of symmetry at the base. It is approximately a straight line and generates a cone of revolution about the axis of symmetry. In Model I the dividing streamline is almost horizontal because the fluid injection velocity at the base is proportional to the height which decreases slowly from the axis to the rim. In Model II the dividing streamline meets the base at an angle because the fluid injection velocity is proportional to the spatial gradient of the surface which increases in magnitude from the centre of the base. In Model II we were able to derive an approximate analytical solution for the dividing streamline by expanding in powers of $r/R(t)$ which satisfies $0 \leq r/R(t) < 1$ because the dividing streamline does not extend to the rim $r = R(t)$. Increasing the magnitude of the injection velocity of fluid at the base meant that in Model I the dividing streamline extended further into the thin film for $0 < \beta < 2$ until for $\beta \geq 2$ the lower region filled the whole liquid drop. For Model II the gradient of the dividing streamline increased as β^* increased.

In Model II the dividing streamline for the axisymmetric liquid drop is

$$z_2 = \frac{2}{3}\beta^{*\frac{1}{2}} R^{-\frac{2}{1+4\beta^*}}(t)\frac{r}{R(t)}\left[1 + \frac{1}{9}\beta^{*\frac{1}{2}}\frac{r}{R(t)} + \bigcirc\left(\left(\frac{r}{R(t)}\right)^2\right)\right], \qquad (10.3.12)$$

where

$$R(t) = \left[1 + \frac{16}{9}\left(1+\beta^*\right)t\right]^{\frac{1+4\beta^*}{8(1+\beta^*)}}. \qquad (10.3.13)$$

The angle ϑ that the dividing streamline makes with the r-axis at the origin is

$$\tan\vartheta = \frac{2}{3}\beta^{*\frac{1}{2}} R^{-\left(\frac{3+4\beta^*}{1+4\beta^*}\right)}(t). \qquad (10.3.14)$$

and for the limit $\beta^* \to \infty$ at fixed time t, we obtain

$$\tan\vartheta \sim \frac{1}{2t^{\frac{1}{2}}}. \qquad (10.3.15)$$

10.4 Comparison of Models I and II for a two-dimensional thin film with Models I and II for an axisymmetric liquid drop

We first compare $W(t), R(t), V(t)$ and $h(t,0)$. The solutions for $W(t), R(t), V(t)$ and $h(t,0)$ depend on the parameters β and β^* which have to be prescribed. We choose β and β^* by specifying v_n and therefore the blowing or suction at the base. The results are presented in Table 10.4.

Table 10.4: Comparison of Models I and II for a two-dimensional thin film and an axisymmetric liquid drop

Model	$\boldsymbol{v_n}$	$\boldsymbol{\beta}$ **or** $\boldsymbol{\beta^*}$	$\boldsymbol{W(t)}$ **or** $\boldsymbol{R(t)}$	$\boldsymbol{V(t)}$	$\boldsymbol{h(t,0)}$	$\boldsymbol{\frac{h(t,0)}{W(t)}}$ **or** $\boldsymbol{\frac{h(t,0)}{R(t)}}$
A. No suction or blowing at the base						
Two-dimensional Model I	0	0	$[1+\frac{10}{9}t]^{\frac{1}{5}}$	V_0	$[1+\frac{10}{9}t]^{-\frac{1}{5}}$	$[1+\frac{10}{9}t]^{-\frac{2}{5}}$
Two-dimensional Model II	0	0	$[1+\frac{10}{9}t]^{\frac{1}{5}}$	V_0	$[1+\frac{10}{9}t]^{-\frac{1}{5}}$	$[1+\frac{10}{9}t]^{-\frac{2}{5}}$
Axisymmetric Model I	0	0	$[1+\frac{10}{9}t]^{\frac{1}{8}}$	V_0	$[1+\frac{16}{9}t]^{-\frac{1}{4}}$	$[1+\frac{16}{9}t]^{-\frac{3}{8}}$
Axisymmetric Model II	0	0	$[1+\frac{10}{9}t]^{\frac{1}{8}}$	V_0	$[1+\frac{16}{9}t]^{-\frac{1}{4}}$	$[1+\frac{16}{9}t]^{-\frac{3}{8}}$
B. Normal velocity at the base constant in time						
Two-dimensional Model I	$\frac{1}{3}(1-\zeta^2)^{\frac{1}{3}}$	$\frac{3}{2}$	$[1+\frac{1}{9}t]^2$	$V_0[1+\frac{1}{9}t]^3$	$1+\frac{1}{9}t$	$[1+\frac{1}{9}t]^{-1}$
Two-dimensional Model II	$-\frac{4}{9}\frac{\zeta^2}{(1-\zeta^2)^{\frac{2}{3}}}$	$-\frac{6}{5}$	$[1-\frac{2}{9}t]^2$	$V_0[1-\frac{2}{9}t]^3$	$1-\frac{2}{9}t$	$[1-\frac{2}{9}t]^{-1}$

Continued on next page

Table 10.4 – continued from previous page

Model	v_n	β or β^*	$W(t)$ or $R(t)$	$V(t)$	$h(t,0)$	$\frac{h(t,0)}{W(t)}$ or $\frac{h(t,0)}{R(t)}$
Axisymmetric Model I	$\frac{5}{9}(1-\zeta^2)^{\frac{1}{3}}$	$\frac{5}{2}$	$[1+\frac{1}{9}t]^2$	$V_0[1+\frac{1}{9}t]^5$	$1+\frac{1}{9}t$	$[1+\frac{1}{9}t]^{-1}$
Axisymmetric Model II	$-\frac{20}{27}\frac{\zeta^2}{(1-\zeta^2)^{\frac{2}{3}}}$	$-\frac{5}{4}$	$[1-\frac{4}{9}t]^2$	$V_0[1-\frac{4}{9}t]^5$	$1-\frac{4}{9}t$	$[1-\frac{4}{9}t]^{-1}$
C. Normal velocity at the proportional to time to power -2						
Two-dimensional Model I	$\frac{4}{9}[1-\frac{2}{9}t]^{-2}(1-\zeta^2)^{\frac{1}{3}}$	2	$[1-\frac{2}{9}t]^{-1}$	$V_0[1-\frac{2}{9}t]^{-2}$	$[1-\frac{2}{9}t]^{-1}$	1
Two-dimensional Model II	$-\frac{8}{27}[1+\frac{2}{9}t]^{-2}\frac{\zeta^2}{(1-\zeta^2)^{\frac{2}{3}}}$	$-\frac{4}{5}$	$[1+\frac{2}{9}t]^{-1}$	$V_0[1+\frac{2}{9}t]^{-2}$	$[1+\frac{2}{9}t]^{-1}$	1
Axisymmetric Model I	$\frac{2}{3}[1-\frac{2}{9}t]^{-2}(1-\zeta^2)^{\frac{1}{3}}$	3	$[1-\frac{2}{9}t]^{-1}$	$V_0[1-\frac{2}{9}t]^{-3}$	$[1-\frac{2}{9}t]^{-1}$	1
Axisymmetric Model II	$-\frac{4}{9}[1+\frac{4}{9}t]^{-2}\frac{\zeta^2}{(1-\zeta^2)^{\frac{2}{3}}}$	$-\frac{3}{4}$	$[1+\frac{4}{9}t]^{-1}$	$V_0[1+\frac{4}{9}t]^{-3}$	$[1+\frac{4}{9}t]^{-1}$	1

We first consider $v_n = 0$ which describes an impermeable base with no blowing or suction. Then $\beta = \beta^* = 0$ and the thin fluid film approximation is satisfied for all four cases. We see that $W(t)$ expands more rapidly than $R(t)$ and that $h(t, 0)$ for a thin film descends more slowly for a two-dimensional film than for a liquid drop.

Suppose next that v_n does not depend explicitly on time. Then β and β^* are determined by setting to zero the power of the time dependent factors in v_n in Tables 10.2 and 10.3. The thin film approximation is satisfied for Model I in both cases but not for Model II. For Model I, $W(t)$ and $R(t)$ are the same and $h(t, 0)$ is the same for a thin fluid film and a liquid drop.

From Tables 10.2 and 10.3, for the thin film approximation to be satisfied in each case, β and β^* must be in the following ranges:

two-dimensional thin film	Model I	$-\infty < \beta \leq 2$
	Model II	$-\frac{4}{5} \leq \beta^* < \infty$
axisymmetric liquid drop	Model I	$-\infty < \beta \leq 3$
	Model II	$-\frac{3}{4} \leq \beta^* < \infty$

When the power of the time dependent factor in v_n is -2 it is found from Tables 10.2 and 10.3 that $\beta = 2, \beta^* = -\frac{4}{5}, \beta = 3$ and $\beta^* = -\frac{3}{4}$ which are the finite limits of the ranges for the thin film approximation to be valid. We see from Table 10.1 that for Model 1, $W(t)$ and $h(t, 0)$ are the same for a two-dimensional thin film and a liquid drop while for Model II the exponents are the same although the factor of t is different. The liquid drop contracts faster than the thin film.

Consider now a comparison of the cubic equation for the streamlines for a two-dimensional thin film and an axisymmetric liquid drop. Consider first Model I. For the two-dimensional thin film the cubic equation for the streamlines in the (ζ, z^*)-plane, given by (5.5.34) can be written as

$$P(z^*, \zeta) = K^*, \tag{10.4.1}$$

where

$$P(z^*,\zeta) = -\frac{1}{9}\frac{\zeta}{\left(1-\zeta^2\right)^{\frac{2}{3}}}z^{*3} + \frac{1}{3}\frac{\zeta}{\left(1-\zeta^2\right)^{\frac{1}{3}}}z^{*2} - \frac{2}{9}\beta\int_0^\zeta \left(1-\zeta^2\right)^{\frac{1}{3}}\,d\zeta. \qquad (10.4.2)$$

For the axisymmetric liquid drop the cubic equation for the streamlines is given by (8.5.42) and can be written as

$$\zeta\,Q(z^*,\zeta) = K^*, \qquad (10.4.3)$$

where

$$Q(z^*,\zeta) = -\frac{1}{9}\frac{\zeta}{\left(1-\zeta^2\right)^{\frac{2}{3}}}z^{*3} + \frac{1}{3}\frac{\zeta}{\left(1-\zeta^2\right)^{\frac{1}{3}}}z^{*2} - \frac{\beta}{12}\frac{1}{\zeta}\left[1-\left(1-\zeta^2\right)^{\frac{4}{3}}\right]. \qquad (10.4.4)$$

The first two terms in (10.4.2) and (10.4.4) are the same. Consider the third term and expand in powers of ζ. From (10.4.2),

$$\frac{2}{9}\beta\int_0^\zeta \left(1-\zeta^2\right)^{\frac{1}{3}}\,d\zeta = \frac{2}{9}\beta\left[\zeta - \frac{1}{9}\zeta^3 - \frac{1}{45}\zeta^5 + \bigcirc\left(\zeta^7\right)\right] \qquad (10.4.5)$$

and from (10.4.4),

$$\frac{\beta}{12}\frac{1}{\zeta}\left[1-\left(1-\zeta^2\right)^{\frac{4}{3}}\right] = \frac{\beta}{9}\left[\zeta - \frac{1}{6}\zeta^3 - \frac{1}{27}\zeta^5 + \bigcirc\left(\zeta^7\right)\right]. \qquad (10.4.6)$$

Thus

$$P(z^*,\zeta) = -\frac{1}{9}\frac{\zeta}{\left(1-\zeta^2\right)^{\frac{2}{3}}}z^{*3} + \frac{1}{3}\frac{\zeta}{\left(1-\zeta^2\right)^{\frac{1}{3}}}z^{*2} - \frac{2}{9}\beta\left[\zeta - \frac{1}{9}\zeta^3 - \frac{1}{45}\zeta^5 + \bigcirc\left(\zeta^7\right)\right] \qquad (10.4.7)$$

and

$$Q(z^*,\zeta) = -\frac{1}{9}\frac{\zeta}{\left(1-\zeta^2\right)^{\frac{2}{3}}}z^{*3} + \frac{1}{3}\frac{\zeta}{\left(1-\zeta^2\right)^{\frac{1}{3}}}z^{*2} - \frac{\beta}{9}\left[\zeta - \frac{1}{6}\zeta^3 - \frac{1}{27}\zeta^5 + \bigcirc\left(\zeta^7\right)\right]. \qquad (10.4.8)$$

We see that by rescaling β by 2β in (10.4.8) the coefficients of ζ in (10.4.8) and (10.4.7) are the same with small differences in the coefficients of ζ^3 and ζ^5. We see that the cubic equation (8.4.17) for the zeros of $v_z(t,0,z)$ for axisymmetric flow could be obtained from the cubic equation (5.4.16) for the two-dimensional flow by rescaling β by 2β. However, a significant difference in the streamlines is the factor ζ in (10.4.3) which does not occur in (10.4.1).

Consider next Model II. For the two-dimensional thin film the cubic equation for the streamlines, (6.5.17), can be written as (10.4.1) where

$$P(z^*,\zeta) = -\frac{1}{9}\frac{\zeta}{(1-\zeta^2)^{\frac{2}{3}}}z^{*3} + \frac{1}{3}\frac{\zeta}{(1-\zeta^2)^{\frac{1}{3}}}z^{*2} - \frac{10}{27}\beta^*\int_0^\zeta \frac{\zeta^2\, d\zeta}{(1-\zeta^2)^{\frac{2}{3}}}. \tag{10.4.9}$$

For the axisymmetric liquid drop the cubic equation for the streamlines (9.5.19) can be written as (10.4.3) where

$$Q(z^*,\zeta) = -\frac{1}{9}\frac{\zeta}{(1-\zeta^2)^{\frac{2}{3}}}z^{*3} + \frac{1}{3}\frac{\zeta}{(1-\zeta^2)^{\frac{1}{3}}}z^{*2} - \frac{2}{3}\beta^*\frac{1}{\zeta}\left[1 - \frac{1}{3}\left(3+\zeta^2\right)\left(1-\zeta^2\right)^{\frac{1}{3}}\right]. \tag{10.4.10}$$

Again the first two terms in $P(z^*,\zeta)$ and $Q(z^*,\zeta)$ are the same. We expand the third term in powers of ζ. From (10.4.9),

$$\frac{10}{27}\beta^*\int_0^\zeta \frac{\zeta^2\, d\zeta}{(1-\zeta^2)^{\frac{2}{3}}} = \frac{10}{81}\beta^*\left[\zeta^3 + \frac{2}{5}\zeta^5 + \bigcirc\left(\zeta^7\right)\right] \tag{10.4.11}$$

and from (10.4.10),

$$\frac{2}{3}\beta^*\frac{1}{\zeta}\left[1 - \frac{1}{3}\left(3+\zeta^2\right)\left(1-\zeta^2\right)^{\frac{1}{3}}\right] = \frac{4}{27}\beta^*\left[\zeta^3 + \frac{4}{9}\zeta^5 + \bigcirc\left(\zeta^7\right)\right]. \tag{10.4.12}$$

Thus

$$P(z^*,\zeta) = -\frac{1}{9}\frac{\zeta}{(1-\zeta^2)^{\frac{2}{3}}}z^{*3} + \frac{1}{3}\frac{\zeta}{(1-\zeta^2)^{\frac{1}{3}}}z^{*2} - \frac{10}{81}\beta^*\left[\zeta^3 + \frac{2}{5}\zeta^5 + \bigcirc\left(\zeta^7\right)\right] \tag{10.4.13}$$

and

$$Q(z^*,\zeta) = -\frac{1}{9}\frac{\zeta}{(1-\zeta^2)^{\frac{2}{3}}}z^{*3} + \frac{1}{3}\frac{\zeta}{(1-\zeta^2)^{\frac{1}{3}}}z^{*2} - \frac{4}{27}\beta^*\left[\zeta^3 + \frac{4}{9}\zeta^5 + \bigcirc\left(\zeta^7\right)\right]. \tag{10.4.14}$$

We see that by rescaling β^* in (10.4.14) by $\frac{5}{6}\beta^*$ the coefficients of ζ^3 in (10.4.13) and (10.4.14) are the same and there is a small difference in the coefficients of ζ^5. The factor ζ in (10.4.3) is a significant difference between the two sets of streamlines.

However, since $K^* = 0$ for the dividing streamlines the factor ζ does not contribute to the dividing streamlines.

We next compare the limiting angle ϑ that the dividing streamline makes with the base as $\beta^* \to \infty$ in Model II. We denote this limiting angle by ϑ_1 and ϑ_2 for a two-dimensional thin film and a liquid drop, respectively. Then from (10.3.8) and (10.3.15)

$$\tan\vartheta_1 = \frac{1}{\sqrt{3}t^{\frac{1}{2}}}\,, \qquad \tan\vartheta_2 = \frac{1}{2\,t^{\frac{1}{2}}} \tag{10.4.15}$$

and therefore

$$\frac{\tan\vartheta_1}{\tan\vartheta_2} = \frac{2}{\sqrt{3}} = 1.155. \tag{10.4.16}$$

The angle that the dividing streamline makes with the base as $\beta^* \to \infty$ in a two-dimensional thin film is therefore greater than in a liquid drop.

A stagnation point in the flow exists in the streamline pattern for both Model I and Model II. In Model I the stagnation point is the point of intersection of the dividing streamline with the centre line in a two-dimensional thin film and with the axis of symmetry in a liquid drop. The distance of the stagnation point above the base is given by (10.3.2) for a two-dimensional thin film and by (10.3.10) for a liquid drop. In Model II the stagnation point is on the base at the point where the centre line or axis of symmetry meets the base. It is therefore at the same point for a two-dimensional thin film and axisymmetric liquid drop.

10.5 Conclusions

The properties of Model I and II for a two-dimensional thin film and an axisymmetric liquid drop are qualitatively similar. There are some quantitative differences, for example, in the range of values of the parameters. The angle that the dividing streamline makes with the base as the strength of the blowing tends to infinity is different. Models I and II complement each other. The thin film approximation is satisfied in Model I for the whole range of suction and a small range of blowing while in Model II it is satisfied for the whole range of blowing and a small range of suction.

Chapter 11

Conclusions

The aim of this dissertation was to investigate the properties of the spreading of a thin fluid film under gravity with suction or blowing of fluid at the base. The approach was to analyse the streamlines of the flow inside the thin film in order to understand the effect of the suction or blowing on the thin film and on the spreading.

Two closely related problems were considered and their solutions compared. The first problem was the spreading of a two-dimensional thin film. A nonlinear diffusion equation for the height of the thin film was derived using the thin film approximation. This approximation enabled us to derive the solution analytically. The nonlinear diffusion equation contained the normal fluid velocity at the base, v_n, in the form of a source term. The velocity v_n was not prescribed, other than the requirement that it satisfies the balance law for fluid volume and any conditions for the problem to have an invariant solution. This was in order to investigate the properties of suction and blowing for as general as possible forms of v_n. The Lie point symmetries of the nonlinear diffusion equation were derived and a condition on v_n for the Lie point symmetries to exist was obtained. The general form for the group invariant solution for h and v_n was derived. The balance law for fluid volume was imposed on the solution. However one more assumption had to be made in order to close the model.

In Model I the assumption was made that the normal velocity, v_n, is proportional to the height and in Model II the assumption was that v_n is proportional to the spatial gradient of the height.

The second problem was on the spreading of an axisymmetric liquid drop. All the details were given of the solutions and of the analysis of the two solutions so that the two problems could be compared.

While a lot of the literature is concerned with how the surface profile evolves with time, by investigating the streamlines numerically we were able to see what happens within the two-dimensional thin film and the liquid drop. This applied especially to fluid injection for which the depth of penetration of the injected fluid and its effect on the fluid flow inside the thin film could be investigated.

The streamlines, showed in the blowing ranges for Model I and Model II, the presence of a dividing streamline. Since the two models are quite general we can expect the existence of a dividing streamline in other models for fluid injection at the base. In Model I we were able to determine the dividing streamline, which goes through the axis of symmetry, by determining exactly the stagnation point on the axis of symmetry at which the fluid velocity vanishes. In Model II the dividing streamline starts at the origin which is also a stagnation point for both the two-dimensional and axisymmetric flows. We were able to derive an approximate solution for the dividing streamline which compared favourably with the numerical solution. The form that the dividing streamline takes in Model I, for both the two-dimensional thin film and axisymmetric liquid drop, is almost horizontal near the centre line and axis but dips down near the free surface. It generates an approximately plane surface. In Model II the dividing streamline is approximately a straight line which extends from the origin on the base to a point on the surface. For the two-dimensional thin film the two dividing streamlines generate an approximate V-shape surface which extends along the length of the thin film while for the axisymmetric liquid drop the dividing streamline generates the surface of a cone about the axis of symmetry. The shape and orientation of the dividing streamline depends strongly on the fluid injection velocity at the base, v_n, and on how the velocity depends on distance from the centre line or axis of symmetry. For both the two-dimensional and axisymmetric liquid drop the streamlines did not form vortices, in comparison with spreading of a liquid drop with slip [19]. The dividing streamline separated the fluid flow into two regions, a lower region at the base consisting of rising fluid and an upper region consisting mainly descending fluid. We can expect that this structure will occur in other models of fluid injection. In Model I the two regions with a dividing streamline existed for $0 < \beta < 1$ for a two dimensional thin film and for $0 < \beta < 2$ for an axisymmetric liquid drop. For larger values of β the lower region filled the whole of the thin film. In Model II the two regions with a dividing streamline existed for all values of β^* in the range $0 < \beta^* \leq \infty$ as shown by the asymptotic results as $\beta^* \to \infty$ in (10.3.8) and (10.3.15). The asymptotic results also show that as time t increases the upper region occupies a larger fraction of the thin film and as $t \to \infty$ it will occupy the whole of the thin film.

A distinguishing feature of Model I is that the base half-width and radius increased for all time and for all values of β $(-\infty < \beta < \infty)$ even when there was suction of fluid. In Model II the height decreased for all time and for all values of β^* $(-\infty < \beta^* < \infty)$ even when there is blowing of fluid.

Plotting the streamlines was very useful. It identified that there were dividing streamlines which where then investigated and their approximate solutions derived. The graphs of the streamlines for suction did not show any unexpected features. The streamline pattern for blowing was much richer than for suction.

Further work can be done and extensions considered. The spreading of a thin film with leak-off into a porous substrate could be made more specified by assuming Darcy flow in the substrate. Surface tension was neglected in the two problems considered. The analysis of the streamlines inside a thin fluid film with suction or fluid injection at the base and taking into account the effects of surface tension could be considered. It can be expected that less analytical progress would be made and that more numerical work would be required. The streamlines in an axisymmetric liquid drop spreading with slip at the base were investigated by Mason and Chung [19]. The effect of suction or blowing with slip on the streamlines could be investigated.

Bibliography

[1] Acheson, D. J., Elementary Fluid Dynamics, Clarendon Press, Oxford, 1990.

[2] Barnard, S. and Child, J. M., Higher Algebra, London:Macmillan, 1936.

[3] Batchelor, G. K., An Introduction to Fluid Dynamics, Cambridge University Press, London, 1967, pp. 72,76–79,141–143, 602–603.

[4] Baumann, G., Symmetry Analysis of Differential Equations with Mathematica, Springer-Verlag, Berlin, (2000).

[5] Bluman, G. W. and Kumei, S., Symmetries and Differential Equations, Springer-Verlag, New York, 1989.

[6] Briggs, W. and Bryan, G. H., The Tutorial Algebra, University Tutorial Press, London, 1942, pp. 448–450 and 496–508.

[7] Davis, S. H. and Hocking, L. M., Spreading and imbibitions of viscous liquid on a porous base, Phys. Fluids. **11** (1999), 48–57.

[8] Davis, S. H. and Hocking, L. M., Spreading and imbibitions of viscous liquid on a porous base II, Phys. Fluids. **12** (2000), 1646–1655.

[9] Dussan V, E. B., The moving contact line: the slip boundary condition, J. Fluid Mech. **77** (1976), 665–684.

[10] Gillespie, R. P., Integration, 6th edition. Olivier and Boyd, Edinburgh, 1959, 113–116.

[11] Grotberg, J. B., Pulmonary flow and transport phenomena, Annu. Rev. Fluid Mech. **26** (1994), 529–571.

[12] Head, A.K., Lie: a PC program for Lie analysis of differential equations, Computer Physics Communications **77** (1993), 241–248.

[13] Hill, J. M., Similarity solution for nonlinear diffusion-a new integration procedure, J. Engng. Math **23** (1989) 141–155.

[14] Hill, D. L. and Hill, J. M., Similarity solutions for nonlinear diffusion - further exact solutions, J. Engng. Math **24** (1990) 109–124.

[15] Hocking, L. M., Rival contact-angle models and the spreading of drops, J. Fluid Mech. **239** (1992), 671–681.

[16] Ibragimov, N. H. and Anderson, R. L., Lie theory of differential equations. In Symmetries, Exact Solutions and Conservation Laws, N. H. Ibragimov (ed.). Lie Group Analysis of Differential Equations, **1** CRC Press: Boca Raton, FL, 1994, 7–14.

[17] Larson, R. E., Hostetler, R. P. and Edwards, B. H., Calculus of a Single Variable, Houghton Mifflin Company, 1998.

[18] Mason, D. P., Lecture Notes on Fluid Mechanics, University of the Witwatersrand, Johannesburg.

[19] Mason, D. P. and Chung, M. Y., Group invariant solution for axisymmetric spreading of a thin fluid film with slip at the fluid-base interface, Math. Meth. Appl. Sci. **30** (2007), 2037–2053.

[20] Mason, D. P. and Momoniat, E., Axisymmetric spreading of a thin liquid drop with suction or blowing at the horizontal base, Int. J. Non-Linear Mech. **39** (2004), 1013–1026.

[21] Middleman, S., Modelling Axisymmetric Flows, Academic Press, New York, 1995.

[22] Momoniat, E. and Abelman, S., An investigation into the spreading of a thin liquid drop under gravity on a slowly rotating disk, Int. J. Non-linear Mech. **39** (2004), 265–270.

[23] Momoniat, E. and Mason, D.P., Investigation of the effect of the Cariolis force on a thin liquid film on a rotating disk, Int. J. Non-Linear Mech. **33** (1998), 1069–1088.

[24] Momoniat, E. and Mason, D. P., Spreading of a thin film with suction or blowing including surface tension effects, Comp. Math. Appl. **53** (2007), 198–208.

[25] Momoniat, E., Mason, D. P. and Mahomed, F.M., Non-linear diffusion of an axisymmetric liquid drop: Group invariant solution and conservation law, Int. J. Non-Linear Mech. **36** (2001), 879–885.

[26] Momoniat, E. and Myers, T. G., A new solution for rotation-driven spreading of a thin fluid film, Int. J. Non-Linear Mech. **41** (2006), 192–199.

[27] Momoniat, E., Myers, T. G. and Abelman, S., New solutions for surface tension driven spreading of a thin film, Int. J. Non-linear Mech. **40** (2005), 523–529.

[28] Momoniat, E., Ravindarin, R. and Roy, S., The influence of slot injection/suction on the spreading of a thin film under gravity and surface tension, Acta Mech. **211** (2010), 61–71

[29] Nayfeh, A. H., Introduction to Perturbation Techniques, John Wiley and Sons, New York, 1981, pp. 39–43.

[30] O'Brien, S. B. G. and Schwartz, L. W., Thin Film Flows: Theory and Modeling, Encyclopedia of Surface and Colloid Science (2006), 6304–6317.

[31] Ockendon, H. and Ockendon, J. R., Viscous Flow, Cambridge University Press, 1995.

[32] Oron, A., Davis, S. H. and Bankoff, S. G., Long-scale evolution of thin liquid films, Rev. Modern Phys. **69** (1997), 931–980.

[33] Roy, S., Datta, P., Ravindran, R. and Momoniat, E., Non-uniform multiple slot injection (Suction) on a forced flow over a slender cylinder, Int. J. Heat and Mass Transfer **50** (2007), 3190–3194.

[34] Sherman, F. S., Viscous Flow, McGraw-Hill, New-York, 1990.

[35] Sherring, J., Head, A. K. and Prince, G. E., Dimsym and Lie: symmetry determining packages, Mathematical and Computer Modelling **25** (1997), 153–164.

[36] Van der Berg, J. B., Bowen, M., King, J. R. and El-Sheikh, M. M. A., The self-similar solution for draining in the thin film equation, European J. Applied Mathematics **15** (2004), 329–346.

[37] Wong, H., Fatt, I. and Radke, C. J., Deposition and thinning of the human tear film, J. Colloid Interface Sci. **184** (1996), 44–51.